EPFL

Thèse n° 9108

The S-matrix Bootstrap Reloaded

Présentée le 24 août 2021

Faculté des sciences de base
Laboratoire de théorie des champs et des cordes
Programme doctoral en physique

pour l'obtention du grade de Docteur ès Sciences

par

Aditya HEBBAR

Acceptée sur proposition du jury

Prof. F. Mila, président du jury
Prof. J. M. Augusto Penedones Fernandes, directeur de thèse
Dr B. Bellazzini, rapporteur
Prof. S. Dubovsky, rapporteur
Prof. M. Shaposhnikov, rapporteur

École
polytechnique
fédérale
de Lausanne

2021

The most important step a person can take is always the next one.
— Brandon Sanderson

Acknowledgments

First and foremost, I would like to thank Joao Penedones, my advisor. Joao is a fantastic physicist, whose breadth and depth of knowledge is astonishing. Apart from physics, Joao is also great as a person, always showing concern for his students and being understanding with them.

Next I would like to thank my collaborator Denis Karateev who I worked with for three out of the four years. I learnt a lot of physics from our long discussions. I also saw first-hand how to write clean and logically structured code, hopefully its something I managed to pick up.

Thanks also to Marco Meineri who patiently explained boundary CFTs at length during the project with Robert. I suppose the explanations were for Robert, but I learnt quite a bit as well.

I would also like to thank my other collaborators Joan Elias-Miro, Andrea Guerrieri, Kelian Haring and Pedro Vieira. I gained a lot from all our discussions.

Apart from wonderful collaborators, I was also very lucky to have a big High Energy theory group here at EPFL. I greatly enjoyed the lunch sessions[1] and the seminars. Special thanks to Adrien, Alfredo, Andrea, Dean, Emmanuele, Gabriel, Gil, Jan, Kin, Lorenzo, Marten, Sander and Siyu for many physics (and non-physics) discussions from which I always came away having learnt new things.

I would like to especially thank the three people I shared my office with during my time at EPFL. I enjoyed our numerous discussions in the office, not just about physics but also about everything else. I was glad to have three close friends who could perfectly understand any problems I had professionally and who were always ready to help me out. I especially thank each one of you:

Joao Silva, for the many hikes together, for the Port wine and for enthusiastically taking up gymming. It was great that you pushed me to work out and stay fit during the Covid lockdown.

[1] Particularly when the lunch involved pizza from Antonio.

Acknowledgments

Miguel, for all the jokes and memes, for (reluctantly) sharing Ovomaltine biscuits and Mcflurry shakes, for educating me about obscure S-matrix papers from the 1960s but just as importantly about the intricacies of Portuguese pronunciation.

And Kamran with whom I had the pleasure of supporting Arsenal, appreciating prog music, enjoying road trips among other things. It was especially great that you always pulled me along to parties and events. Indeed my time in Lausanne would have not have been nearly as fun otherwise.

Of course most of these parties and events involved the Silo gang: Amirali, Baran, Deblina and Melanie. Thanks for all the fun times!

Thanks also to Aiswarya, Bhushan, Kartik and Rishabh for the movie sessions. I also thank Bhushan for the numerous hikes and for co-organizing football games with me.

Moving away from Lausanne, I am greatly indebted to Aaditya Salgarkar, Akhil and Rohit for all the enthusiastic discussions on various topics in High Energy Theory.

I have been fortunate to have Athmanathan, Diksha, Janhavi, Namrata, Pranav, Sriram, Sriram[2] and Terrence as friends right from my undergraduate years. All your contrasting ideological and philosophical views definitely helped me grow as a person.

Turning towards family, I would like to thank my cousin Manasa with whom I could talk about anything at any time. Thanks for always being there for me.

I would like to thank my parents for their support throughout my life. I am grateful to you for always letting me make my choices and never putting any pressure on me. Finally, my sister Megha for showering me with love and affection and being a constant source of joy.

Aditya Hebbar

[2]Not a typo.

Abstract

Quantum field theories (QFTs) are the backbone upon which the edifice of modern physics is built. In this thesis we explore the S-matrix bootstrap which is a non-perturbative method that constrains the vast space of QFTs by using consistency conditions that they must satisfy. The thesis is divided into two parts.

In part I of the thesis we study the S-matrix bootstrap for particles with spin in 4 space-time dimensions and apply the formalism to scattering of identical Majorana fermions to estimate bounds on their quartic couplings and their cubic (Yukawa) coupling to scalar particles.

In part II of the thesis, we consider the scattering of massless (Goldstone) excitations on a long flux tube. We use the S-matrix bootstrap to constrain Wilson coefficients of higher dimension operators in the low energy flux tube effective field theory. These constraints naturally translate to bounds on the ground state and excited state energy levels of long flux tubes.

The techniques used in this thesis should be extendable to many other systems, both massive and massless. We conclude by discussing some of these possibilities.

Keywords:

Quantum field theory, S-matrix Bootstrap, Strong coupling, Non-perturbative methods, Flux tubes

Résumé

Les théories Quantiques des Champs (TQC) sont la colonne vertébrale sur laquelle l'édifice de la physique moderne est bâti. Dans cette thèse, nous explorons le bootstrap de la matrice S, qui est une méthode non-perturbative pour contraindre le vaste espace des TQC en utilisant des conditions de cohérence qu'elles doivent satisfaire. Cette thèse est divisée en deux parties.

Dans la partie I de la thèse, nous étudions le bootstrap de la matrice S pour des particules avec spin dans l'espace-temps à 4 dimensions et appliquons le formalisme à la diffusion de fermions de Majorana identiques afin d'estimer des bornes sur leurs couplages quartiques et leur couplage cubique (de Yukawa) avec des particules scalaires.

Dans la partie II de la thèse, nous considérons la diffusion d'excitations sans masse (de Goldstone) sur un long tube de flux. Nous utilisons le bootstrap de la matrice S pour contraindre les coefficients de Wilson d'opérateurs de dimension supérieure dans la théorie des champs effective des tubes de flux à basse énergie. Ces contraintes se traduisent naturellement en bornes sur les niveaux d'énergie de l'état fondamental et de l'état excité des longs tubes de flux.

Les techniques employées dans cette thèse devraient pouvoir être étendues à de nombreux autres systèmes, aussi bien massifs que sans masse. Nous concluons en discutant certaines de ces possibilités.

Mots clés :

Théorie quantique des champs, bootstrap de la matrice S, couplage fort, méthodes non-perturbatives, tubes de flux

Foreword

This thesis is based on the paper

Paper I J. Elias Miró, A. L. Guerrieri, A. Hebbar, J. Penedones and P. Vieira, *Flux Tube S-matrix Bootstrap*, Phys. Rev. Lett. **123** (2019) no.22, 221602 [1906.08098].

And the following preprint:

Paper II A. Hebbar, D. Karateev and J. Penedones, *Spinning S-matrix Bootstrap in 4d*, [2011.11708].

As well as the upcoming works:

Paper III K. Haring, A. Hebbar, D. Karateev, M. Meineri and J. Penedones, *Photon S-matrix Bootstrap in 4d*, to appear.

Paper IV A. Hebbar and J. Penedones, *Glueball-Branon Bootstrap*, to appear.

Chapters 1, 2 and some parts of the overview of Part I are based on **Paper II**. Chapter 3 is based on material that will appear in **Paper III**. Chapter 4 is based on **Paper I**. Finally, chapter 5 is based on **Paper IV**.

Contents

Introduction

Quantum Field Theory (QFT) is an essential tool in modern physics, as it is the framework used to describe a wide range of phenomena in particle physics, cosmology and condensed matter physics. Nevertheless, in spite of extensive research for many decades, solving strongly coupled QFTs remains a herculean task. The standard textbook approach to interacting QFTs involves treating them as a small deformation of a free QFT and then writing observables as a perturbative expansion around the free theory values. Therefore this approach is unsuitable for theories such as Quantum Chromodynamics (QCD), which is the QFT describing strong interactions, where the coupling is large and there is no other obvious small parameter [3] which could act as a handle for perturbative computations.

The S-matrix Bootstrap program of the 1960s [1] was envisaged as a means to non-perturbatively solve strong interactions. The idea was that properties of analyticity, unitarity and crossing symmetry could be used to uniquely pick out the scattering amplitude of strongly interacting particles such as the pion-pion amplitude. Unfortunately, this turned out to be too ambitious and while there were some successful predictions such as mesons lying on Regge trajectories, the program could not make sustained progress and interest declined sharply after the 1970s.

However in the last few years, the S-matrix bootstrap program has undergone a renaissance, thanks to the pioneering work of [2–4], who imposed the constraints of unitarity numerically to bound the cubic and quartic couplings of identical scalars in 2d and 4d. Following their work, the S-matrix bootstrap program has been used in a number of different contexts to find non-perturbative bounds [5–15].

The goal of this thesis is to expand the ambit of the modern S-matrix Bootstrap program. We do this on two fronts. Part I of the thesis deals with the generalization of the numerical S-matrix Bootstrap set-up of [4] to particles of any spin and any mass in four space-time dimensions. On the other hand, in Part II, we will use S-matrix Bootstrap techniques to deduce analytic and numerical bounds on the dynamics of long string-like

[3] For some computations, $N = 3$ is large enough for $\frac{1}{N}$ expansions to work. However note that even the theory with $N = \infty$ remains unsolved.

objects in QFTs. In particular, these bounds will apply to confining flux tubes in Yang Mills and QCD. The rest of the introduction will provide the motivation for the above topics of study.

Quantum field theory

Quantum field theory as the name indicates involves the study of fields. As a quantum mechanical theory, there is a Hilbert space and each vector in this space represents a valid state of the physical system. The quantum fields are operators that act on this Hilbert space of states and their dynamics is governed by a Lagrangian[4]. However neither the fields nor the states themselves are observable, but instead what are observable are the matrix elements of the fields (and their products) in between states, called correlation functions. While correlation functions are important observables especially in statistical physics and in cosmology, in this thesis we will mainly concentrate on the other main observable in QFTs which is the S-matrix.

The scattering matrix (S-matrix)

The S-matrix encodes information about scattering processes in a QFT. The importance of scattering in particle physics of course can not be overstated. For the past century, we have figured out better and better answers to the question “What is everything made up of?" by colliding particles against one other with more energy and observing what happens. The first scattering experiment was by Geiger, Marsden and Rutherford, who in 1909 scattered alpha particles off a thin gold foil and deduced the existence of the nucleus of the atom. Since then there have been numerous scattering experiments that led to the discovery of the various building blocks of nature one by one, culminating with the discovery of the Higgs boson at the Large Hadron Collider in 2012 which completed the last missing piece in the Standard Model [5].

Therefore from the particle physics viewpoint, the S-matrix is “the" observable that one needs to compute in a QFT [6]. Its definition in QFT mimics a typical scattering process - we begin with a state consisting of n particles which are far separated in the far past, called the incoming state. As the state evolves in time, the particles get closer to each other and interact in some complicated manner. In the far future, they separate out again into say m particles, giving rise to the outgoing state.

The S-matrix is the unitary transformation that relates the set of ingoing states to outgo-

[4]This is the typical scenario, there exist QFTs with no Lagrangian description.

[5]While the Standard Model is complete in the sense it accounts for all known elementary particles, there are still phenomena such as neutrino masses, dark matter, dark energy etc. that it does not explain.

[6]In a theory with dynamical gravity, correlation functions are not diffeomorphism invariant and we expect the S-matrix to be the only observable.

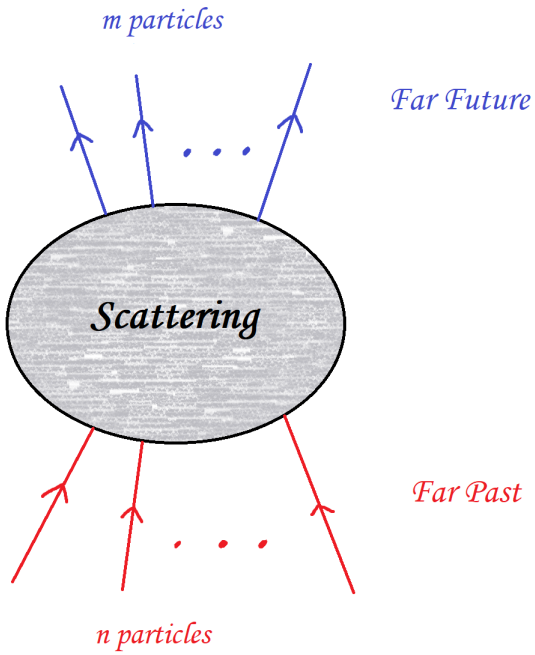

Figure 1: Schematic diagram of an $n \to m$ scattering process

ing states and the matrix element is called the n to m scattering amplitude.

$$\mathcal{S}_{\alpha}^{\beta} \equiv {}_{out}\langle\beta|\alpha\rangle_{in} \tag{1}$$

The unitarity of the S-matrix is the statement that probabilities are conserved in quantum mechanics

$$S^{\dagger}S = SS^{\dagger} = \mathbb{I} \tag{2}$$

In QFT, scattering amplitudes are computed from correlation functions of fields using the LSZ formula [16]. The analyticity of scattering amplitudes follows from the locality of the interactions between the particles and from causality which states that fields at space-like separations (anti)commute

$$[\phi_1(x), \phi_2(y)]_{\pm} = 0 \quad \forall \quad (x^2 - y^2) > 0. \tag{3}$$

Finally crossing symmetry states that the amplitude for a process where a particle is ingoing is the analytic continuation of the amplitude for a process where its anti-particle is outgoing (and vice-versa). It can be understood using the LSZ formula [7].

One way to motivate the formalism of QFT is that it is the natural way to arrive at a

[7] See A.5.3 and B.1 for examples

Lorentz invariant S-matrix in a quantum mechanical theory, while satisfying the cluster decomposition principle which states that experiments at spatially distant locations shouldn't influence each other [17].

The old S-matrix Bootstrap

The S-matrix bootstrap program of the 1960s was a more extreme version of the viewpoint above. To properly understand it, let's take a step back and think about the usual process for how QFTs are used. We begin by conducting a few scattering experiments and observe some spectrum of particles and their associated properties such as scattering cross sections. We then write a Lagrangian for the QFT and use some of the experimental data for example the mass of particles to fix the parameters in the Lagrangian. Using this Lagrangian we make predictions for further scattering experiments. Thus we see that on a practical level, QFTs provide a way to deduce full information about scattering from a partial subset. The proponents of the 1960s S-matrix Bootstrap believed that the properties of crossing, unitarity and analyticity of the S-matrix would be rigid enough that it should be possible to totally bypass fields and directly bootstrap the full scattering amplitude from just basic assumptions such as the mass spectrum. This was the hope (which didn't pan out) for the strongly interacting pion-pion amplitude.

S-matrix Bootstrap Reloaded

Unlike the old S-matrix bootstrap of the 1960s that we just described, the modern S-matrix Bootstrap is meant to be complimentary to usual QFT. The goal is to use the universal properties of analyticity, crossing and unitarity that any good S-matrix should satisfy to chart the space of allowed QFTs. In this sense, the modern S-matrix bootstrap can be thought of as the theory version of performing a new experiment. To elaborate on the analogy, consider a situation where a QFT with a range of parameter values is compatible with existing experimental data. A new experiment that brings more data would generically be incompatible with some of the parameter space and thus reduce the space of "allowed" QFTs. In the case of S-matrix bootstrap, the idea is similar. There may be some range of parameters in a Lagrangian or an S-matrix that at first glance seems reasonable. However, upon studying the aforementioned constraints of analyticity, crossing and unitarity more systematically, we can bound the space of QFTs. This endeavour is inspired by the remarkable success of the modern conformal bootstrap.

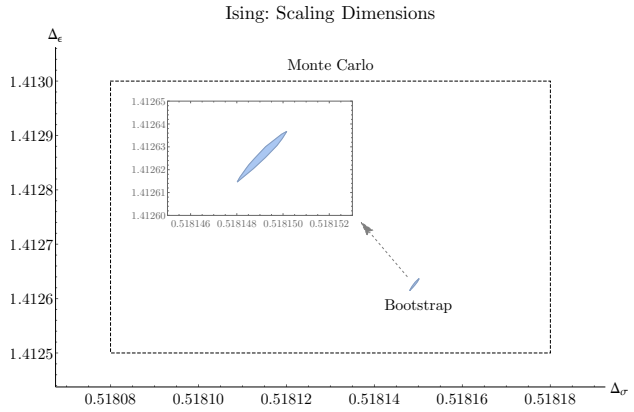

Figure 2: Allowed space in the scaling dimensions of the two relevant operators in the 3d Ising model. Figure from [18]

Conformal Bootstrap

Conformal field theories (CFTs) are special QFTs which are invariant under conformal symmetries. They describe second-order phase transitions in statistical physics systems and are also important due to the AdS/CFT correspondence which states that quantum gravitational theories in $(d+1)$ dimensional Anti-de Sitter space (AdS) are dual to CFTs on the d dimensional boundary. In addition, CFTs are also important conceptually because QFTs can be thought of as renormalization group flows triggered by a UV deformation of some CFT. Moreover, these flows have a CFT at the endpoint as well. The enhanced symmetry in CFTs allows us to prove the convergence of the operator product expansion (OPE) in these theories which allows two operators close to each other to be written as a sum of operators in the theory:

$$\mathcal{O}_i(x)\mathcal{O}_j(0) \sim \sum_k C_{ijk}(x)O_k(0) \tag{4}$$

By applying the OPE repeatedly, all correlation functions can be fully deduced from a set of numbers $\{\Delta_i, \lambda_{ijk}\}$ called CFT data that characterize the CFT [8]. However a generic set of CFT data $\{\Delta_i, \lambda_{ijk}\}$ does not define a CFT. This is because such a set would not satisfy the condition of OPE associativity which is the statement that an n-point correlation function can be computed by applying the OPE in various permutations and all of these should give the same answer. The conformal bootstrap uses this OPE associativity property along with unitarity and analyticity[9] of the correlation functions to tightly constrain putative CFT data. This is exemplified in the famous plot of operator dimensions in the 3d Ising model, see figure 2.

[8] This is true for CFTs in flat space, which is all that we will talk about in this paragraph.

[9] Note that these analyticity properties of correlators in CFT can be proven using OPE convergence.

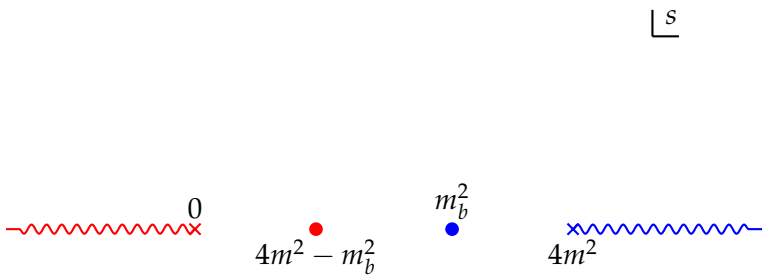

Figure 3: Analytic structure of 2 to 2 amplitude S(s) in 2d

For other examples and a review of the conformal bootstrap, see [19]. While the conformal bootstrap is indeed quite encouraging, how do we know that it is still possible to make progress for general QFTs where we lose the large amount of control afforded by conformal symmetry? The answer is that unitarity and analyticity are still quite powerful. Let's consider a simple example to illustrate this point [3].

What is the maximum cubic coupling of a scalar in a QFT?

Consider the two to two scattering process of identical scalars in 2 space-time dimensions. The scattering amplitude is a function of one variable $s = (p_1 + p_2)^2$, where p_1 and p_2 are the momenta of the incoming particles, satisfying the following property due to crossing symmetry

$$S(s) = S(4m^2 - s). \tag{5}$$

In the complex s plane the amplitude has branch cuts on the real s axis from $s = 4m^2$ to $s = \infty$ and the "crossed" cut from $s = -\infty$ to $s = 0$. In addition we assume that there is a cubic coupling to another stable scalar particle (called a bound state) of mass $m_b \geq m$, which gives rise to a pole at $s = m_b^2$ and the crossed pole at $s = 4 - m_b^2$

$$S(s) \sim \frac{g^2}{s - m_b} \quad \text{near} \quad s = m_b^2 \tag{6}$$

where the residue g^2 is the non-perturbative definition of the cubic coupling of the scalars. The amplitude is otherwise analytic in the rest of the s plane, see figure 3.

Finally, unitarity dictates that the maximum absolute value of the amplitude just on top of the cut $s = 4m^2$ to $s = \infty$ is 1:

$$|S(s)| \leq 1 \quad \forall \quad s \geq 4m^2 \tag{7}$$

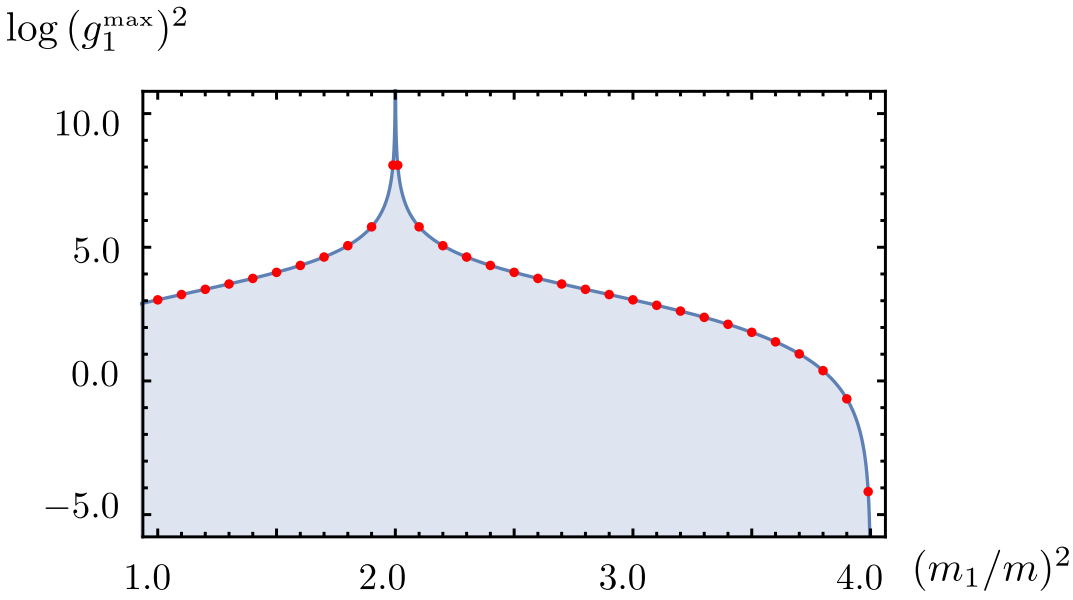

Figure 4: Bound on cubic coupling of scalars in 1+1d. Figure from [3]

The question asked in the title of this paragraph translates mathematically to finding the maximum residue of a function analytic in a domain which is bounded in modulus on the boundary of this domain[10]. This is a straightforward application of the maximum modulus principle as outlined in [4] and we get the following plot for the maximum coupling as a function of the bound state scalar mass m_b^2, see figure 4.

In the four dimensional space-time that we live in, life is not as simple and there are many additional complications, beginning with the fact that the scattering amplitude is a function of two variables s and t and unitarity is an integral equation. It is still possible to apply these constraints numerically and this was the work of [4], resulting in the following bounds on the cubic coupling of scalar particles, this time in 3+1d, see figure 5.

In chapter 1 of this thesis we will establish the formalism to deal with scattering of particles of any spin in $3+1d$. We will then apply the formalism to the special case of scattering of identical Majorana fermions in chapter 2 and obtain bounds on the their quartic couplings as well as their cubic couplings to a scalar particle.

[10]The domain is $\mathbb{C}\backslash\{\text{the cuts}\}$.

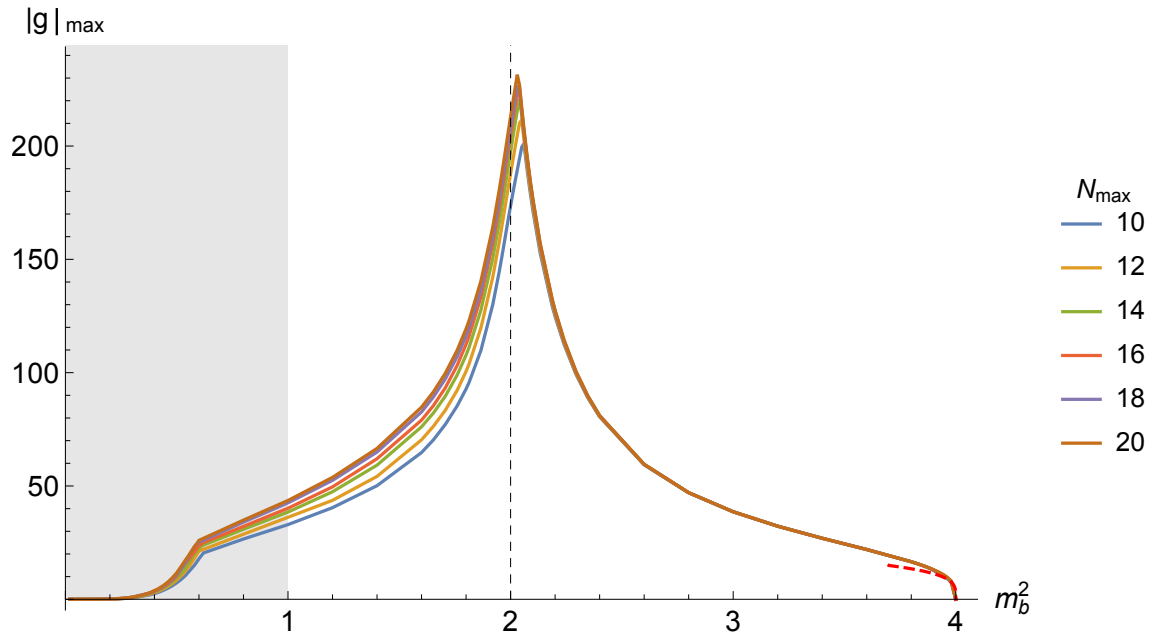

Figure 5: Bound on cubic coupling of scalars in 3+1d

Effective Field Theory applications

Effective field theories (EFTs) are a class of QFTs which are very useful when we need to describe the low energy physics of a particular system. Consider an example where experimentally we only have access to energies less than some scale M. Then it is clear that we would never see particles with energy greater than M as external states in our experiments. Of course, the particles more energetic than the cut-off M would still appear as virtual particles in Feynman diagrams. But is it still possible to describe the low-energy physics using only the low-energy fields? The answer is yes, and effective field theories are the answer. Conceptually, effective field theories can be thought of as derived from the full microscopic theory (a.k.a the UV theory) by integrating out the heavier states above the cut-off M, leaving only the low energy variables. In practice what one does is to consider the symmetry of the system and write all terms in the Lagrangian which are compatible with the given symmetries, including the non-renormalizable ones. Note that if we were writing a fundamental theory, we would naturally require such a theory to be UV complete, which would preclude writing non-renormalizable terms. When writing EFTs, we already know that the theory is not UV complete on its own because we integrated out the heavier particles that are needed to UV complete it, and therefore non-renormalizable terms are fine to include. At this point it seems that we are saying that there are an infinite number of terms in the Lagrangian. What allows EFTs to still be predictive is that at a given order in $\frac{E}{M}$, where E is the energy scale of the process we are interested in, only a finite number of

these infinite terms contribute. The coefficients of these higher dimensional terms in the Lagrangian, called Wilson coefficients, are determined by the UV theory. However it is often the case that either because we do not know the UV theory or because the UV theory is strongly coupled, we can not deduce these coefficients from first principles. It is here that we can use the techniques of the S-matrix Bootstrap to restrict the values that these Wilson coefficients can take. To see this in a example, consider a theory of a massless scalar ϕ, with a mass gap M upto which there are no other particles. At low energies we can write an EFT involving only the field ϕ:

$$\mathcal{L} = \frac{1}{2}\left(\partial_\mu \phi \partial^\mu \phi\right) + c_0 \phi^4 + c_2 (\partial\phi)^4 + \dots \tag{8}$$

A priori, it seems that any value of c_2 should be allowed. However it was shown by [20] that only $c_2 \geq 0$ is allowed by unitarity and analyticity of the scattering amplitude. Similar bounds also apply to higher mass dimension Wilson coefficients and they were recently studied systematically in a series of works [21–33]. In chapter 3 of this thesis will use the spinning S-matrix bootstrap that we set up in chapter 1 to derive bounds on the space of photon EFTs. To be more precise, consider the photon EFT

$$\mathcal{L}_{photon} = -\frac{1}{4} F_{\mu\nu} F^{\mu\nu} + c_1 (F_{\mu\nu} F^{\nu\mu})(F_{\alpha\beta} F^{\beta\alpha}) + c_2 F_{\mu\nu} F^{\nu\rho} F_{\rho\sigma} F^{\sigma\mu} + \dots \tag{9}$$

One of our results is the range of allowed values for the dimensionless ratio $\frac{c_1}{c_2}$. In addition we will also chart the space of allowed values of the coefficients at the next order in the photon EFT.

Confinement, flux tubes and glueballs

The problem of confinement is a long standing problem in QCD. The fundamental fields (i.e the ones that appear in the Lagrangian), the quarks and the gluons, are coloured. The quarks transform in the fundamental representation of the $SU(3)$ colour group while gluons transform in the adjoint representation. However, all observed states are colour neutral. This phenomenon is called confinement and as yet the mechanism as to how this happens is not fully understood. Lattice simulation indicate that upon stretching apart two quarks, a string-like object called “flux tube" develops in between them[11]. The tension of this flux tube leads to a linear potential between the quarks which ensures that quarks are confined to the colour neutral bound state. The long distance corrections to this linear potential in powers of $\frac{1}{R}$ (where R is distance between the quarks) naturally correspond to the low energy dynamics of the excitations of the flux tube[12]. These excitations, which we will call branons, are massless and because QCD develops a mass

[11] Note that the flux tube breaks in the presence of dynamical quarks.
[12] There are contributions from the endpoints as well [34, 35].

gap [13], their low energy dynamics will be described by an EFT consisting only of the branon fields X^μ.

$$\mathcal{L} = \int d^2\sigma \sqrt{-h} \left[\ell_s^{-2} + \ell_s^2 \alpha_3 K^4 + \ell_s^2 \beta_3 K^4 + \ldots \right] \tag{10}$$

where $h = \det h_{\alpha\beta} = det \partial_\alpha X^\mu \partial_\beta X_\mu$ is the induced metric, $K^\mu_{\alpha\beta} = \nabla_\alpha \partial_\beta X^\mu$ is the extrinsic curvature. The two K^4 operators differ in terms of index contractions. Since we know the UV theory which is QCD, in principle it should be possible to derive the Wilson coefficients in the low energy effective Lagrangian. However due to the strong coupling nature of QCD, this is easier said than done and in fact nothing is known about these coefficients. One of the results of this thesis (chapter 4) is that we were able to bound the values of the Wilson coefficients α_3 and β_3 purely from analyticity, crossing and unitarity of the two to two scattering amplitude of these branons.

In chapter 5 we further extend the flux-tube system by also allowing scattering to single glueball states in the bulk. This leads to a rich system of scattering amplitudes: Branon-branon scattering, glueball annihilating into two branons and glueball transmission after interacting with the flux tube. By considering this mixed system, we hope to place bounds on the coupling between glueball and the flux-tube.

[13] Showing the mechanism behind the generation of this mass gap is another outstanding problem in physics.

Spinning S-matrix Bootstrap in 4d Part I

Overview of Part I

This part of the thesis deals with generalizing the work of [4] to scattering of particles with any spin and any mass in four space-time dimensions. Let us therefore begin with a brief summary of their work which dealt with the scattering of identical neutral scalar particles. The fact that the scattered particles are scalar implies that the scattering amplitude is Lorentz invariant and therefore it is a function $T(s,t,u)$ of the three Lorentz invariant variables s, t and u, called Mandelstam variables:

$$s = (p_1 + p_2)^2 \quad , \quad t = (p_1 - p_3)^2 \quad , \quad u = (p_1 - p_4)^2 \tag{11}$$

The Mandelstam variables are not independent and satisfy the following condition:

$$s + t + u = 4m^2 \tag{12}$$

where m is the mass of the scalar particle. The scattering amplitude $T(s,t) \equiv T(s,t,4m^2 - s - t)$ is defined in the physical region:

$$s \geq 4m^2 \quad \text{and} \quad -(s - 4m^2) \leq t \leq 0. \tag{13}$$

where it describes the s channel scattering process $12 \to 34$. However, it is possible to analytically continue the amplitude to the complex s and t planes. One reason to do this is the crossing property which states that the function $T(s,t)$ analytically continued to the t channel physical region given by

$$t \geq 4m^2 \quad \text{and} \quad -(t - 4m^2) \leq s \leq 0. \tag{14}$$

describes the t channel scattering process $1\bar{3} \to \bar{2}4$. An analogous statement holds upon continuing to the u channel physical region

$$u \geq 4m^2 \quad \text{and} \quad -(u - 4m^2) \leq s \leq 0. \tag{15}$$

where the amplitude describes the u channel scattering process $1\bar{4} \to 3\bar{2}$. In the present case of identical neutral scalar scattering, all three processes are the same and hence we

get the following symmetry of the scattering amplitude.

$$T(s,t) = T(t,s) = T(s,4m^2 - t) \tag{16}$$

Another reason to be interested in the analytic continuation of the scattering amplitude is that it allows us to write dispersion relations which express the full amplitude in terms of only its discontinuity $Disc_s(s,t)$ (which coincides with its imaginary part for s,t in the physical region). This discontinuity has positivity properties that follow from unitarity and along with crossing symmetry (16), imposes constraints on the amplitude which can be bootstrapped to obtain non-trivial bounds on the scattering amplitude. We now recap known non-perturbative results on the analyticity of the scattering amplitude. Note that these results are sufficient to prove crossing symmetry for the two to two amplitude [36][14].

Non-perturbative results on the analyticity of the amplitude

- For fixed $t \in [-t_0, 0]$, the amplitude $T(s,t)$ satisfies a subtracted dispersion relation in the s plane. Note that $t_0 = 28m^2$ for scalar scattering [38].
- For fixed $s \in [4m^2, \infty)$, the amplitude $T(s, \cos\theta)$ as a function of the scattering angle $\cos\theta = 1 - \frac{2t}{s-4m^2}$ is analytic in an ellipse (called the Lehmann ellipse) with foci -1 and $+1$ and semi-major axis $\cos\theta_0 > 1$ [39].
- Any point $(s, \cos\theta)$ in the physical region is surrounded by a neighbourhood of analyticity whose precise form is unknown [40].
- For elastic processes, single variable dispersion relations in the three channels implies the following domain of analyticity [41]

$$|st| < 256m^2 \quad s,t \quad \in \quad \mathbb{C}\backslash\{\text{the cuts}\}. \tag{17}$$

- Finally by also using unitarity, it is possible to extend the domain of analyticity which remains the state of the art [42] (to the best of the author's knowledge):

$$|t| < 4m^2 \quad \text{and} \quad s \quad \in \mathbb{C}\backslash\{\text{the cuts}\} \tag{18}$$

In [4], it was assumed that the scattering amplitude is analytic in the entire s and t planes except for poles and branch cuts that are necessarily present due to propagation of intermediate one and multi-particle states. This property, known as Landau analyticity, can be proved to all orders in perturbation theory at least for the scattering of the lightest particles in the theory. In this thesis we will have nothing further to add to the known

[14] For recent progress on proving crossing symmetry for higher particle amplitudes albeit in perturbation theory see [37]

results about the non-perturbative analytic structure of the amplitude. We will continue assuming Landau analyticity for the scattering of particles with spin.

Finally unitarity of the scattering amplitude is easily imposed by decomposing the scattering amplitude into partial waves:

$$S_\ell(s) = 1 + i\frac{\sqrt{s-4m^2}}{32\pi\sqrt{s}}\int_0^\pi d\theta \sin\theta P_\ell(\cos\theta) T(s, t(s,\cos\theta), u(s,\cos\theta)). \tag{19}$$

in terms of which it translates to

$$|S_\ell(s)|^2 \leq 1 \quad \forall \quad s \geq 4m^2 \quad \text{and} \quad \ell \in \mathbb{N} \tag{20}$$

The idea in [4] was to write a linear ansatz for the scattering amplitude

$$T(s,t,u) = \sum_\alpha \alpha_i F_i(s,t,u) \tag{21}$$

where α_i are parameters to be optimized over and $F_i(s,t,u)$ are functions which in the complex s and t planes satisfy assumed (Landau) analyticity properties. Crossing symmetry was then solved as linear constraints on the parameters α_i. This leaves unitarity which can be re-written as the positive semi-definiteness condition

$$\begin{pmatrix} 1 & S_\ell(s) \\ S_\ell(s) & 1 \end{pmatrix} \succeq 0 \quad \forall \quad s \geq 4m^2 \quad \text{and} \quad \ell \in \mathbb{N} \tag{22}$$

which is linear in the parameters α_i and was imposed numerically using SDPB [43].

In the presence of spin, the expressions (16) , (19) and (20) immediately become more complicated. The goal of chapter 1 is to setup the formalism which allows to study crossing and unitarity for amplitudes with generic masses and spins. This chapter is mostly a review of known results [44] in a concise form.

Compared to the scalar case a generic scattering amplitude describing the process $12 \to 34$ has the form

$$T_{12\to 34}{}^{\lambda_3,\lambda_4}_{\lambda_1,\lambda_2}(p_1,p_2,p_3,p_4), \tag{23}$$

where p_i are four-momenta and λ_i are helicities of scattering particles respectively. Given the spins j_i of four particles, helicities take values from the range $\lambda_i = -j_i, \ldots + j_i$ with step one. There are thus

$$N_4 \equiv (2j_1+1)(2j_2+1)(2j_3+1)(2j_4+1) \tag{24}$$

components describing the scattering process $12 \to 34$.[15] We would then like to define

[15] When the scattering process is parity and/or time-reversal invariant, when it contains identical and/or

N_4 scattering amplitudes which depend only on the Mandelstam variables. This can be done in two different ways: using the center of mass frame or using tensor structures. We denote these two options respectively by

$$T_{12\to 34}{}^{\lambda_3,\lambda_4}_{\lambda_1,\lambda_2}(s,t,u) \qquad \text{and} \qquad T^I_{12\to 34}(s,t,u), \tag{25}$$

where $I = 1, \dots N_4$. The two sets of amplitudes in (25) are related by a linear transformation which depends on the Mandelstam variables only. This relation is completely fixed once the basis of tensor structures is chosen. Both options have their advantages and disadvantages. In the center of mass frame one can derive crossing equations once and for all spins and masses as summarized in section 1.3 (see appendix A.5 for details).[16] However, the analyticity properties of the center of mass amplitudes are subtle and one is forced to deal with the issue of kinematic singularities discussed in section 1.7. Analyticity is more straightforward when using tensor structures, however one needs to study crossing case by case due to non-trivial linear relations between covariant tensor structures. As a result we cannot give it a completely general treatment in chapter 1 and instead employ it only in the particular example of identical neutral spin $\frac{1}{2}$ particles in section 2.4. In addition, the construction of general spin tensor structures is discussed to some extent in appendix A.8.

The key element for imposing unitarity constraints are the partial amplitudes (20). In the case of generic spin, (20) remains valid for center of mass amplitudes, if the Legendre polynomial is replaced by the small Wigner d-matrix given in (1.9) in full generality. This is explained in detail in section 1.5. Finally, the unitarity constraints for generic spin are given in section 1.6.

In chapter 2, we specialize to the case of scattering of neutral spin $\frac{1}{2}$ massive fermions, also known as Majorana fermions [45]. This chapter should be seen as the simplest application of the formalism given in section 1. We begin by setting up the optimization problem taking into account the crossing and unitarity constraints. Then in section 2.5 we write an ansatz for the scattering of identical Majorana particles in a parity invariant QFT (assuming this is the lightest particle). Finally, we present our numerical results for the allowed values of the non-perturbative quartic and cubic (Yukawa) couplings defined from the physical scattering amplitude in section 2.3. The universal bounds for the quartic coupling, given in (2.93), and for the cubic couplings, shown in figures 2.5 and 2.6, are our main numerical results.

massless particles, the counting of independent amplitudes becomes much more complicated. We discuss it in section 1.4.

[16] Generically, crossing equations relate physical amplitudes to the analytic continuation of other amplitudes beyond their physical domain. There is no general proof (especially for particles with spin) that this continuation exists and how big is the domain where crossing equations hold. For a review of results for scalar amplitudes, see [38]. In this work we do not address this issue and simply assume that all the amplitudes under consideration are maximally analytic.

In chapter 3 which is work in progress, we turn our attention to the scattering of photons, which from the S-matrix point of view are massless spin-1 particles whose scattering amplitudes have a definite soft ($s \to 0$) behaviour (3.81). Note that this soft behaviour of the amplitude cancels out the usual IR divergences that plague scattering amplitude of massless particles in four spacetime dimensions. We set up the numerical boostrap problem and we will shortly use SDPB to bound the space of photon EFTs.

In the appendix A, we fill in many of the details of the presentation in the main text.

1 Review: spinning S-matrix formalism

In this chapter we study quantum systems invariant under the restricted Poincaré symmetry group. In addition, we consider special situations where parity and/or time-reversal symmetries are also present. Scattering amplitudes are important physical observables in these systems. They are constrained by many non-trivial consistency conditions.

We begin by reviewing its kinematic aspects (the ones fixed by symmetries).[1] Our goal is to provide an updated and easy to use practical summary of the basic ingredients.

1.1 States

We work in Lorentzian metric with the mostly plus signature

$$\eta_{\mu\nu} = \{-+++\}. \tag{1.1}$$

The unitary irreducible representations of the restricted Poincaré group were classified by Wigner.[2] Here we will work with a particular unitary representation which is positive energy time-like. The basis for such a representation is formed by the states

$$|c, \vec{p}; \ell, \lambda; \gamma\rangle \,. \tag{1.2}$$

where the 3-momentum $\vec{p} \in \mathbb{R}^3$ and the helicity $\lambda = -\ell, -\ell+1, \ldots, +\ell$. The other labels are fixed within the irreducible representation and serve to specify a given state. The label $c > 0$ is a continuous real parameter related to the energy $p^0 > 0$ as

$$c^2 = -p_\mu p^\mu = (p^0)^2 - (\vec{p}\,)^2. \tag{1.3}$$

[1] For other sources covering this topic see for example [17].
[2] For a textbook discussion see for example [17, 46].

It is defined as the eigenvalue of the first Casimir of the Poincaré group $c^2 = -P^2$, where P^μ are the generators of translations. Instead of c one can equivalently label the basis of states (1.2) using the energy p^0. We will often use both labels throughout the text interchangeably. The spin label $\ell = 0, \frac{1}{2}, 1, \ldots$ is a non-negative integer or half integer related to the eigenvalue of the second Casimir of the Poincaré group $W^2 = 4c^2\,\ell(\ell+1)$, where W^μ is the Pauli–Lubanski pseudovector.[3] The helicity label λ is the projection of the spin vector along $\vec{p}$. Finally the label γ stands for any other additional (discrete or continuous) labels which might be required to fully specify the state. We will see one particular case of their importance in section 1.1.3.

We will often need to use spherical coordinates in which case the three momentum is parametrized as

$$\vec{p} = (\boldsymbol{p}\sin\theta\cos\phi,\ \boldsymbol{p}\sin\theta\sin\phi,\ \boldsymbol{p}\cos\theta), \quad \boldsymbol{p} \equiv |\vec{p}|, \quad 0 \le \phi < 2\pi, \quad 0 \le \theta \le \pi, \tag{1.4}$$

The helicity basis states (1.2) with non-zero three momentum $\vec{p}$ are defined as follows

$$|c, \vec{p}; \ell, \lambda; \gamma\rangle = e^{-i\phi J_3} e^{-i\theta J_2} e^{+i\phi J_3} e^{-i\eta K_3} |c, \vec{0}; \ell, \lambda; \gamma\rangle, \tag{1.5}$$

where J_a and K_a with $a = 1,2,3$ are the generators of spatial rotations and boosts respectively. The rapidity parameter η is related to the energy and momentum of the states as

$$\cosh\eta = \frac{p^0}{c}, \qquad \sinh\eta = \frac{\boldsymbol{p}}{c}. \tag{1.6}$$

Lastly the helicity λ in the zero three momentum state $|c, \vec{0}; j, \lambda; \gamma\rangle$ is a projection of the spin ℓ onto the z axis. In other words these states are eigenstates of the J_3 generators. Given a generic 3d rotation characterized by the three Euler angles (α, β, γ) (where α and γ parametrize rotations around the z-axis and β parametrizes rotations around the y-axis) we have the following transformation property

$$R(\alpha,\beta,\gamma)|c, \vec{0}; \ell, \lambda; \gamma\rangle = \sum_{\lambda'} \mathscr{D}^{(\ell)}_{\lambda'\lambda}(\alpha,\beta,\gamma)|c, \vec{0}; \ell, \lambda'; \gamma\rangle, \quad R(\vec{a}) \equiv e^{-i\alpha J_3} e^{-i\beta J_2} e^{-i\gamma J_3}. \tag{1.7}$$

The object $\mathscr{D}^{(\ell)}_{\lambda'\lambda}$ is known as the large Wigner D matrix and reads as

$$\mathscr{D}^{(\ell)}_{\lambda'\lambda}(\alpha,\beta,\gamma) = e^{-i\alpha\lambda'} d^{(\ell)}_{\lambda'\lambda}(\beta) e^{-i\gamma\lambda}. \tag{1.8}$$

[3] In our conventions $W_\mu \equiv \epsilon_{\mu\nu\rho\sigma} M^{\nu\rho} P^\sigma$, where $M^{\nu\rho}$ are the generators of the Lorentz group.

Here the object $d^{(\ell)}_{\lambda'\lambda}$ is the small Wigner d matrix, its explicit expression reads[4]

$$d^{(\ell)}_{\lambda'\lambda}(\beta) = \sqrt{(\ell+\lambda)!(\ell-\lambda)!(\ell+\lambda')!(\ell-\lambda')!} \times \sum_{\nu=0}^{2j}(-1)^{\nu}\frac{(\cos(\beta/2))^{2j+\lambda-\lambda'-2\nu}\,(-\sin(\beta/2))^{\lambda'-\lambda+2\nu}}{\nu!(\ell-\lambda'-\nu)!(\ell+\lambda-\nu)!(\nu+\lambda'-\lambda)!}. \tag{1.9}$$

In case both helicities λ and λ' are equal to zero, the small Wigner d matrix reduces to the usual Legendre polynomial

$$d^{(\ell)}_{00}(\beta) = P_{\ell}(\cos\beta). \tag{1.10}$$

The Wigner D matrices satisfy orthogonality relations. They also obey various other useful relations, see for example appendix A.2 in [44].

Consider now a generic Poincaré transformation which consists of a translation fixed by four Lie parameters a^{μ} and the Lorentz transformation $\Lambda^{\mu}{}_{\nu}$ fixed by six Lie parameters $\rho_{[\mu\nu]}$. It transforms the 4-momentum p^{μ} into $p'^{\mu} = \Lambda^{\mu}{}_{\nu}p^{\nu}$. Under the Poincaré transformation (a,ρ) the states (1.2) transform according to

$$U(a,\rho)|c,\vec{p};\ell,\lambda;\gamma\rangle = e^{ia\cdot p'} \times \sum_{\lambda'}\mathscr{D}^{(\ell)}_{\lambda'\lambda}(\alpha,\beta,\gamma)|c,\vec{p}\,';\ell,\lambda';\gamma\rangle, \tag{1.11}$$

where the three Wigner angles (α,β,γ) can be expressed in terms of the six Lie parameters $\rho_{[\mu\nu]}$. We provide an example of a Wigner angles computation in appendix A.1.4. For the special case of pure 3d rotations, the Wigner D matrix reduces to a phase and therefore the helicity of the state remains unchanged[5]

$$R(\vec{a})|c,\vec{p};\ell,\lambda;\gamma\rangle = e^{-i\lambda\,\xi(\vec{a},\phi,\theta)}|c,\vec{p}\,';\ell,\lambda;\gamma\rangle, \tag{1.12}$$

where the phase ξ has a complicated dependence on its arguments.

1.1.1 Particles

So far we discussed states and their properties in a generic Poincaré invariant quantum theory. The related notion of particle does not exist in every QFT. The simplest context where particles are well defined is in free QFTs. A free theory is described by a set of one particle states (describing freely propagating particles with a given mass and spin). Taking tensor products of these states we form a complete basis of states spanning the Hilbert space of the theory. In interacting QFTs, particles can still be defined in the

[4]Note that Mathematica implements the small Wigner d matrices (1.9) with indices λ and λ' flipped. In other words $d^{(\ell)}_{\lambda'\lambda}(\beta)$ is generated by the command WignerD$[\{\ell,\lambda,\lambda'\},\beta]$.

[5]Notice that this is compatible with (1.7) because the limit $\vec{p}\to 0$ of $|c,\vec{p};j,\lambda;\gamma\rangle$ is only equal to $|c,\vec{0};j,\lambda;\gamma\rangle$ if $\vec{p}$ is parallel to the z-axis.

asymptotic far past and future if interactions decay sufficiently fast with distance. This is the case for theories with a mass gap and massless theories with soft interactions like Goldstone bosons or photons (in the absence of charged particles in the asymptotic states). In this paper, we will only consider those theories where particles do exist. Then, one can define two types of asymptotic states: the *in* states (far past) and the *out* states (far future). Both the *in* states and the *out* states span the full Hilbert space of the theory. A natural basis of *in*/*out* states is given by the tensor product of one particle *in*/*out* states.

1.1.2 One particle states (1PS)

One particle states (1PS) are special cases of (1.2) where c takes only discrete values corresponding to the masses of stable particles in the theory. For this reason, we will set $c = m$ from now on. If global symmetries are present, the label γ describes the charge or more generically the representation under the global symmetry group. For simplicity, in this section we ignore global symmetries, thus the 1PS will not carry any extra labels γ.

We introduce a shorthand notation for one particle states

$$|\kappa\rangle \equiv |m, \vec{p}; j, \lambda\rangle. \tag{1.13}$$

For indicating spin we use the label j instead of ℓ here to ease the visual distinction between the 1PS and generic irreps. We normalize 1PS as follows

$$\begin{aligned} \langle m', \vec{p}\,'; j', \lambda' | m, \vec{p}; j, \lambda\rangle &= (2\pi)^3\, 2p^0\, \delta^3(\vec{p}\,' - \vec{p})\, \delta_{m'm}\delta_{j'j}\delta_{\lambda'\lambda} \\ &\equiv \delta(\kappa' - \kappa), \end{aligned} \tag{1.14}$$

where in accordance with (1.3) the energy of the states is

$$p^0 = \sqrt{m^2 + p^2}. \tag{1.15}$$

In the second line of (1.14) we have introduced the shorthand notation $\delta(\kappa' - \kappa)$ for the set of Kronecker and Dirac delta functions. The transformation rule for a one particle state under a Poincare transformation remains the same as in (1.11).

The case of massless particles should be treated separately since $c \neq 0$ in (1.2). Skipping details, the following statement holds: massless particles can be described by the states (1.13) with $m = 0$ and the range of helicities restricted to only two values $\lambda = -j$ and $\lambda = +j$.

Finally we state the transformation properties of 1PS under parity and time-reversal.

For further details see appendix A.2. One has

$$\mathcal{P}|m,\vec{p};j,\lambda\rangle = \eta(-1)^{j-\lambda}\exp(2i\phi\lambda)|m,-\vec{p};j,-\lambda\rangle, \tag{1.16}$$
$$\mathcal{T}|m,\vec{p};j,\lambda\rangle = \varepsilon(-1)^{2j}\exp(-2i\phi\lambda)|m,-\vec{p};j,\lambda\rangle, \tag{1.17}$$

where ϕ is the spherical angle defined in (1.4), see also (1.27), η and ϵ are pure phases. Their values are yet other quantities characterizing the state. Let us briefly discuss the phase η called intrinsic parity. One can argue as in section 3.3 of [17], that one can always define $\mathcal{P}$ in such a way that $\mathcal{P}^2 = +1$ or $\mathcal{P}^2 = -1$. As a result one has

$$\eta = \pm 1 \quad \text{or} \quad \eta = \pm i. \tag{1.18}$$

The imaginary values of intrinsic parities are only possible for fermions, however no such fermions have been discovered so far in the nature.

1.1.3 Two particle states (2PS)

We define the two particle states (2PS) by taking the ordered tensor product of two 1PS

$$|\kappa_1,\kappa_2\rangle \equiv |m_1,\vec{p}_1;j_1,\lambda_1\rangle \otimes |m_2,\vec{p}_2;j_2,\lambda_2\rangle. \tag{1.19}$$

The normalization of the 2PS defined above follows from that of the 1PS:

$$\langle\kappa_1,\kappa_2|\kappa_3,\kappa_4\rangle = \delta(\kappa_1-\kappa_3)\delta(\kappa_2-\kappa_4). \tag{1.20}$$

Two particle states do not form an irreducible representation of the restricted Poincaré group. However, they can be decomposed into a direct sum of states (1.2) transforming in irreducible representations. This is done by injecting the completeness relation into 2PS

$$|\kappa_1,\kappa_2\rangle = \int \frac{d^4p}{(2\pi)^4}\,\theta(p^0)\theta(-p^2)\sum_{\gamma}\sum_{\ell,\lambda}|c,\vec{p};\ell,\lambda;\gamma\rangle\,\langle c,\vec{p};\ell,\lambda;\gamma|\kappa_1,\kappa_2\rangle, \tag{1.21}$$

where we normalize the states (1.2) as follows[6]

$$\langle c',\vec{p}\,';\ell',\lambda';\gamma'|c,\vec{p};\ell,\lambda;\gamma\rangle = (2\pi)^4\delta^4(p'^{\mu}-p^{\mu})\,\delta_{\ell'\ell}\,\delta_{\lambda'\lambda}\,\delta_{\gamma'\gamma}, \tag{1.22}$$

where $p^{\mu} = (p^0,\ \vec{p})$ is the 4-momentum and the symbolic expression $\delta_{\gamma'\gamma}$ will be properly specified when the additional labels γ and γ' are defined. We use the normalization (1.22) for all irreducible Poincaré representations, with the exception of 1PS which are the only states where the label c takes particular discrete values. Looking at the right-hand

[6]The Kronecker deltas follow from the fact that the states here are simultaneous eigenstates of the two Casimirs (A.34) and the helicity operator (A.55).

side of (1.21), we see that the Clebsch-Gordon coefficients of this decomposition (due to translation invariance) obey

$$\langle c, \vec{p}; \ell, \lambda; \gamma | \kappa_1, \kappa_2 \rangle \propto (2\pi)^4 \delta^4(p^\mu - p_1^\mu - p_2^\mu). \tag{1.23}$$

This delta function completely removes the integration over p in (1.21). The label γ is the multiplicity label. In the case of 2PS decomposition the multiplicity label γ consists of only discrete parameters[7] and reads as

$$\gamma = (m_1, j_1, \lambda_1; m_2, j_2, \lambda_2). \tag{1.24}$$

Thus the label γ keeps track of which particles and what helicities were used to make the two particle state. In what follows we will almost always drop the explicit mass and spin labels in order to simplify the formulas. However, when dealing with particles of different masses and spins, the mass and spin labels are important. Finally we choose to normalize the states appearing in (1.21) according to (1.22) with

$$\delta_{\gamma'\gamma} = \delta_{m_1' m_1} \delta_{m_2' m_2} \delta_{j_1' j_1} \delta_{j_2' j_2} \times \delta_{\lambda_1' \lambda_1} \delta_{\lambda_2' \lambda_2}. \tag{1.25}$$

1.1.4 COM two particle states

We can always use Lorentz invariance to go to the frame where the total momentum of the two particles is 0. This frame is called the centre of mass (COM) frame. Therefore, we do not need to know the most general decomposition (1.21), and instead it is enough to focus on the special case of 2PS in the center of mass (COM) frame, namely the states (1.19) obeying the constraint $\vec{p}_1 = -\vec{p}_2$. We give a special label to such two particles states

$$|(\boldsymbol{p}, \theta, \phi); \lambda_1, \lambda_2\rangle \equiv |m_1, +\vec{p}; j_1, \lambda_1\rangle \otimes |m_2, -\vec{p}; j_2, \lambda_2\rangle, \tag{1.26}$$

where the three-momenta have the following spherical coordinates[8]

$$+\vec{p} = (\boldsymbol{p},\, \theta,\, \phi), \quad -\vec{p} = (\boldsymbol{p},\, \pi - \theta,\, \pi + \phi), \quad \theta \in [0, \pi], \quad \phi \in [0, 2\pi]. \tag{1.27}$$

[7] This is no longer the case for the decompositions of three or more particle states. In these cases the multiplicity label γ would also contain continuous parameters associated with the relative momenta of the component particles.

[8] Notice that given the vector $+\vec{p}$ in spherical coordinates, the vector opposite to it is defined as $-\vec{p} = (\boldsymbol{p},\, \pi - \theta,\, \pi + \phi)$ for $\phi \in [0, \pi]$ and $-\vec{p} = (\boldsymbol{p},\, \pi - \theta,\, -\pi + \phi)$ for $\phi \in (\pi, 2\pi]$. In other words in order to describe the vector $-\vec{p}$ in spherical coordinates one needs two different descriptions, one for $\phi \in [0, \pi]$ and one for $\phi \in (\pi, 2\pi]$. We do not indicate it in the main text, since all the consequent formulas remain uniform in the whole range $\phi \in [0, 2\pi]$. The reason for that is the choice of the helicity basis (1.5) and the fact that $R(\phi, \theta, -\phi)$ is 2π periodic, see footnote 3. Notice also that there is a special case when $\theta = \pi$. For this particular point, we choose the spherical angles of the first state to be $+\vec{p} = (\boldsymbol{p},\, \theta = \pi,\, \phi = \pi)$, whereas the spherical angles of the second state are $-\vec{p} = (\boldsymbol{p},\, \theta = 0,\, \phi = 0)$.

The states (1.26) are normalized according to (1.20). By performing a change of variables we can rewrite the normalization in terms of spherical coordinates as

$$\langle(\boldsymbol{p},\theta,\phi);\lambda_1,\lambda_2|(\boldsymbol{p}',0,0);\lambda_1',\lambda_2'\rangle = (2\pi)^4\delta^4(0)\times\frac{16\pi^2\sqrt{s}}{\sqrt{\boldsymbol{p}\boldsymbol{p}'}}\frac{\delta(\theta)\delta(\phi)}{\sin\theta}\times \\ \delta_{m_1'm_1}\delta_{m_2'm_2}\delta_{j_1'j_1}\delta_{j_2'j_2}\times\delta_{\lambda_1\lambda_1'}\delta_{\lambda_2\lambda_2'}, \quad (1.28)$$

where $s=(p_1^0+p_2^0)^2$ is the square of the COM energy. In appendix A.1.2, we compute the Clebsch-Gordon coefficients (1.23) for the COM states (1.26). Here we present only the result which reads as

$$|(\boldsymbol{p},\theta,\phi);\lambda_1,\lambda_2\rangle = \sum_{\ell,\lambda} C_\ell(\boldsymbol{p})\, e^{i\phi(\lambda_1+\lambda_2-\lambda)} d^{(\ell)}_{\lambda\lambda_{12}}(\theta)|c,0;\ell,\lambda;\gamma\rangle, \quad (1.29)$$

where we have

$$\lambda_{12}\equiv\lambda_1-\lambda_2, \quad c=\sqrt{s}=\sqrt{m_1^2+\boldsymbol{p}^2}+\sqrt{m_2^2+\boldsymbol{p}^2}, \quad (1.30)$$

with the multiplicity labels γ given in (1.24) and $d^{(\ell)}_{\lambda\lambda_{12}}(\theta)$ given by (1.9). Using the orthogonality of the small Wigner d matrix and the exponential function, we can invert equation (1.29) as follows

$$|c,0;\ell,\lambda;\gamma\rangle = \frac{2\ell+1}{4\pi C_\ell(\boldsymbol{p})}\int_0^{2\pi}d\phi\int_0^{\pi}d\theta\sin\theta\, e^{-i\phi(\lambda_1+\lambda_2-\lambda)} d^{(\ell)}_{\lambda\lambda_{12}}(\theta)|(\boldsymbol{p},\theta,\phi);\lambda_1,\lambda_2\rangle. \quad (1.31)$$

The coefficient C_ℓ is completely fixed by the consistency requirement that the left-hand side of (1.29) satisfies the normalization condition (1.20) and the state in the right-hand side of (1.29) satisfies the normalization condition (1.22). For non-identical particles it reads as

$$C_\ell(\boldsymbol{p})^2 = 4\pi\,(2\ell+1)\times\frac{c}{\boldsymbol{p}}. \quad (1.32)$$

1.1.5 Identical particles

The discussion presented above should be slightly modified when the two particle state is composed of identical particles. In the latter case it must satisfy

$$|\kappa_1,\kappa_2\rangle_{id} = (-1)^{2j}|\kappa_2,\kappa_1\rangle_{id}. \quad (1.33)$$

We have added the subscript *id* to explicitly indicate that the state describes a system of two identical particles. In order to incorporate (1.33), we have (instead of simply taking an ordered product) to take either symmetrized (in case of bosons) or anti-symmetrized

(in case of fermions) tensor product. Such a state will thus have the following form

$$|\kappa_1,\kappa_2\rangle_{id} \equiv \frac{1}{\sqrt{2}}\left(|m,\vec{p}_1;j,\lambda_1\rangle\otimes|m,\vec{p}_2;j,\lambda_2\rangle + (-1)^{2j}|m,\vec{p}_2;j,\lambda_2\rangle\otimes|m,\vec{p}_1;j,\lambda_1\rangle\right). \tag{1.34}$$

The normalization of the state (1.34) follows from (1.14)

$${}_{id}\langle\kappa_1,\kappa_2|\kappa_3,\kappa_4\rangle_{id} = \delta(\kappa_1-\kappa_3)\delta(\kappa_2-\kappa_4) + (-1)^{2j}\delta(\kappa_1-\kappa_4)\delta(\kappa_2-\kappa_3). \tag{1.35}$$

As before we need to define the identical 2PS in the center of momentum. Adapting (1.26) to the case of identical particles we get

$$|(\boldsymbol{p},\theta,\phi);\lambda_1,\lambda_2\rangle_{\rm id} \equiv \\ \frac{1}{\sqrt{2}}\left(|m,+\vec{p};j,\lambda_1\rangle\otimes|m,-\vec{p};j,\lambda_2\rangle + (-1)^{2j}|m,-\vec{p};j_1,\lambda_2\rangle\otimes|m,\vec{p};j,\lambda_1\rangle\right). \tag{1.36}$$

The normalization of the identical COM states (1.36) is fixed by (1.35). It is still given by (1.22) but with

$$\delta_{\gamma'\gamma} = \frac{1}{2}\left(\delta_{\lambda_1\lambda_1'}\delta_{\lambda_2\lambda_2'} + (-1)^{\ell+\lambda_1-\lambda_2}\delta_{\lambda_1\lambda_2'}\delta_{\lambda_2\lambda_1'}\right). \tag{1.37}$$

We would now like to decompose the identical two particle state (1.36) into irreducible representations

$$|c,0,\ell,\lambda;\lambda_1,\lambda_2\rangle_{id} \equiv \frac{1}{2}\left(|c,0,\ell,\lambda;\lambda_1,\lambda_2\rangle + (-1)^{\ell+\lambda_1-\lambda_2}|c,0,\ell,\lambda;\lambda_2,\lambda_1\rangle\right). \tag{1.38}$$

The decomposition of identical 2PS is obtained straightforwardly by applying (1.29) to both terms in the right-hand side of (1.36) which leads to

$$|(\boldsymbol{p},\theta,\phi);\lambda_1,\lambda_2\rangle_{\rm id} = \sqrt{2}\sum_{\ell,\lambda} C_\ell(\boldsymbol{p})e^{i(\lambda_1+\lambda_2-\lambda)\phi}d^{(\ell)}_{\lambda\lambda_{12}}(\theta)|c,0;\ell,\lambda;\lambda_1,\lambda_2\rangle_{id}, \tag{1.39}$$

where the coefficient C_ℓ is given by (1.32). For the detailed derivation of these equations see appendix A.3.

1.2 S-matrix elements

Given a generic state in the reference frame at $t = 0$, an observer in another reference frame in the far past ($t = -\infty$) or far future ($t = +\infty$) will see the same state as a (linear combination of) tensor product of one particle states which we refer to as *in* or *out* asymptotic states respectively. Asymptotic states have a complicated time evolution. One can however establish a formal one to one map between these states and those of some free theory (which evolve trivially with time) by means of a pair of unitary operators Ω_- and Ω_+ called the Møller operators. See section 2.1 in [13] for a recent

discussion. In their notation

$$|\kappa\rangle_{in} = \Omega_-|\kappa\rangle_{free}, \quad |\kappa\rangle_{out} = \Omega_+|\kappa\rangle_{free}. \tag{1.40}$$

Let us now discuss inner products between asymptotic states. Since the Møller operators are unitary, the inner products of only *in* states or only *out* states are fixed by the normalization conditions (1.22) and (1.14). This means that the only non-trivial matrix elements must include both *in* and *out* states.

Four-particle amplitudes

We start with the most important object for our work

$${}_{out}\langle\kappa_3,\kappa_4|\kappa_1,\kappa_2\rangle_{in} = {}_{free}\langle\kappa_3,\kappa_4|S|\kappa_1,\kappa_2\rangle_{free}, \tag{1.41}$$

where the scattering operator S is defined via (1.40) as

$$S \equiv \Omega_+^\dagger \Omega_-. \tag{1.42}$$

Isometry[9] of Møller operators implies unitarity of the scattering operator

$$S^\dagger S = 1. \tag{1.43}$$

Poincaré invariance implies that[10]

$$U(a,\rho)\, S\, U^{-1}(a,\rho) = S, \tag{1.44}$$

where U represents a generic Poincaré transformation in the Hilbert space. Finally it is convenient to split the scattering operator into the trivial part (identity operator) and the interacting part as

$$S = 1 + iT. \tag{1.45}$$

If $T = 0$ we simply recover the free theory. The matrix element (1.41) describes scattering of two particles. Factoring out the overall delta function due to translation invariance we can define the two to two scattering amplitude as

$$(2\pi)^4\delta^{(4)}(p_1^\mu + p_2^\mu - p_3^\mu - p_4^\mu) \times S_{12\to34}{}^{\lambda_3,\lambda_4}_{\lambda_1,\lambda_2}(p_1,p_2,p_3,p_4) \equiv {}_{free}\langle\kappa_3,\kappa_4|S|\kappa_1,\kappa_2\rangle_{free}. \tag{1.46}$$

Equivalently we define the interacting part of the two to two scattering amplitude

$$(2\pi)^4\delta^{(4)}(p_1^\mu + p_2^\mu - p_3^\mu - p_4^\mu) \times T_{12\to34}{}^{\lambda_3,\lambda_4}_{\lambda_1,\lambda_2}(p_1,p_2,p_3,p_4) \equiv {}_{free}\langle\kappa_3,\kappa_4|T|\kappa_1,\kappa_2\rangle_{free}. \tag{1.47}$$

[9] An isometric operator O on a Hilbert space preserves distances. This implies that $O^\dagger O = \mathbb{1}$, however the operator need not be surjective. A surjective isometric operator is unitary.

[10] See the discussion around (1.11).

Since the (interacting) scattering amplitude is defined via the one particle states, all the 4-momenta are on-shell

$$p_i^2 = -m_i^2. \tag{1.48}$$

We study these amplitudes and their properties in depth in section 1.3. We sometimes drop the subscript $12 \to 34$ when it is clear from the context which scattering process we describe. However, it is necessary to keep this subscript when relating amplitudes describing different processes. Using (1.45) we can relate the scattering amplitude (1.46) with its interacting part (1.47) as

$$S_{12\to34}{}^{\lambda_3,\lambda_4}_{\lambda_1,\lambda_2}(p_1,p_2,p_3,p_4) = \left[\frac{{}_{free}\langle\kappa_3,\kappa_4|\kappa_1,\kappa_2\rangle_{free}}{(2\pi)^4\delta^{(4)}(p_1^\mu+p_2^\mu-p_3^\mu-p_4^\mu)}\right] + iT_{12\to34}{}^{\lambda_3,\lambda_4}_{\lambda_1,\lambda_2}(p_1,p_2,p_3,p_4), \tag{1.49}$$

where the first term $[\ldots]$ is a schematic expression which can be evaluated straightforwardly.[11] This piece is not a function but a distribution. Due to the relation (1.49), in practice we will never need to discuss the full amplitude S and instead we will only need the interacting T amplitude.

1.2.1 Partial amplitudes

The second matrix element we need is between the *in* and *out* states in the irreducible representation

$${}_{out}\langle c',\vec{p}\,';\ell',\lambda';\gamma'|c,\vec{p};\ell,\lambda;\gamma\rangle_{in} = {}_{free}\langle c',\vec{p}\,';\ell',\lambda';\gamma'|S|c,\vec{p};\ell,\lambda;\gamma\rangle_{free}. \tag{1.50}$$

Again factoring out the overall delta function due to translational invariance we can define the partial amplitude with a definite spin ℓ as

$$(2\pi)^4\delta^{(4)}(p^\mu-p'^\mu)\delta_{\ell\ell'}\delta_{\lambda\lambda'}\times S_{\ell\gamma}^{\gamma'}(c) = {}_{free}\langle c',\vec{p}\,';\ell',\lambda';\gamma'|S|c,\vec{p};\ell,\lambda;\gamma\rangle_{free}. \tag{1.51}$$

Equivalently we can define the interacting part of the partial amplitude as

$$(2\pi)^4\delta^{(4)}(p^\mu-p'^\mu)\delta_{\ell\ell'}\delta_{\lambda\lambda'}\times T_{\ell\gamma}^{\gamma'}(c) = {}_{free}\langle c',\vec{p}\,';\ell',\lambda';\gamma'|T|c,\vec{p};\ell,\lambda;\gamma\rangle_{free}. \tag{1.52}$$

[11] For example in the COM frame defined in (3.9) using the normalization condition in spherical coordinates (1.28) it is straightforward to write

$$\left[\frac{{}_{free}\langle\kappa_3,\kappa_4|\kappa_1,\kappa_2\rangle_{free}}{(2\pi)^4\delta^{(4)}(p_1^\mu+p_2^\mu-p_3^\mu-p_4^\mu)}\right]_{com} = \frac{8\pi\sqrt{s}}{\sqrt{\boldsymbol{p}\boldsymbol{p}'}}\times\frac{\delta(\theta)\delta(\phi)}{\sin\theta}\delta_{m_1m_3}\delta_{m_2m_4}\delta_{j_1j_3}\delta_{j_2j_4}\times\delta_{\lambda_1\lambda_3}\delta_{\lambda_2\lambda_4}.$$

Similarly in case of identical particles with mass m and spin j using (A.193) we have

$$\left[\frac{{}_{free}\langle\kappa_3,\kappa_4|\kappa_1,\kappa_2\rangle_{free}}{(2\pi)^4\delta^{(4)}(p_1^\mu+p_2^\mu-p_3^\mu-p_4^\mu)}\right]_{com} = \frac{32\pi^2\sqrt{s}}{\sqrt{s-4m^2}}\times\left(\frac{\delta(\theta)\delta(\phi)}{\sin\theta}\delta_{\lambda_1\lambda_3}\delta_{\lambda_2\lambda_4}+(-1)^{2j}\frac{\delta(\pi-\theta)\delta(\phi+\pi)}{\sin(\pi-\theta)}\delta_{\lambda_1\lambda_4}\delta_{\lambda_2\lambda_3}\right).$$

We prove that the left-hand side of (1.51) and (1.52) must contain $\delta_{\ell\ell'}\delta_{\lambda\lambda'}$ factor in appendix A.4.1. In a generic situation due to (1.22) the two partial amplitudes are simply related as

$$S_{\ell\gamma}^{\gamma'}(c) = \delta_{\gamma'\gamma} + iT_{\ell\gamma}^{\gamma'}(c). \tag{1.53}$$

In practice we will only need to consider partial amplitudes where the irreps come from the decomposition of COM two particle states (1.29). In that case the additional labels γ are multiplicities given by (1.24). The Kronecker delta for distinct particles is given by (1.25) and for identical particles by (1.37). We examine partial amplitudes and their properties in detail in section 1.5. In addition, we also derive the relation between partial and scattering amplitudes.

1.3 Scattering amplitudes and crossing

In this section we carefully study various aspects of the scattering amplitudes (1.46) and its interacting part (1.47).

We start with the transformation property under the Poincaré group. It directly follows from the transformation property of each state given by (1.11). In the most generic case it reads as

$$T^{\lambda_3,\lambda_4}_{\lambda_1,\lambda_2}(p_1,p_2,p_3,p_4) = \sum_{\lambda_i'} \mathscr{D}^{(j_1)}_{\lambda_1'\lambda_1}(\vec{\omega}_1)\mathscr{D}^{(j_2)}_{\lambda_2'\lambda_2}(\vec{\omega}_2)\mathscr{D}^{*(j_3)}_{\lambda_3'\lambda_3}(\vec{\omega}_3)\mathscr{D}^{*(j_4)}_{\lambda_4'\lambda_4}(\vec{\omega}_4)T^{\lambda_3',\lambda_4'}_{\lambda_1',\lambda_2'}(p_1',p_2',p_3',p_4'), \tag{1.54}$$

where $\vec{\omega}_i \equiv (\alpha_i, \beta_i, \gamma_i)$ are the Wigner angles for each one particle state defining the (interacting) scattering amplitude.

Let us now introduce Mandelstam variables which are invariant quantities under Lorentz transformations

$$s \equiv -(p_1+p_2)^2, \quad t \equiv -(p_1-p_3)^2, \quad u \equiv -(p_1-p_4)^2, \quad s+t+u = \sum_{i=1}^{4} m_i^2. \tag{1.55}$$

Using these variables one can split the scattering amplitude (1.47) into parts invariant under Lorentz transformation and parts transforming non-trivially,

$$T^{\lambda_3,\lambda_4}_{\lambda_1,\lambda_2}(p_1,p_2,p_3,p_4) = \sum_{I=1}^{(2j_1+1)\ldots(2j_4+1)} T_I(s,t,u) \times \mathbb{T}_I{}^{\lambda_3,\lambda_4}_{\lambda_1,\lambda_2}(p_1,p_2,p_3,p_4). \tag{1.56}$$

We refer to the quantities $T_I(s,t,u)$ as the scalar components of the scattering amplitudes while $\mathbb{T}_I$ are called tensor structures. The latter ensures the correct transformation property of the amplitude as dictated by (1.54). We abuse notation and call both the full amplitude and its scalar components by the same symbol T. It should be clear which is which by the presence of indices and arguments. We construct tensor structures

explicitly for a particular example in section 2.4.1. For a general approach see appendix A.8.

Instead of defining tensor structures and scalar components of the amplitude as in (1.56) one can evaluate the full amplitude in a particular frame. The standard choice for this frame is the center of mass (COM) defined as

$$\begin{aligned} p_1^{\text{com}} &= (E_1, 0, 0, +\boldsymbol{p}), \\ p_2^{\text{com}} &= (E_2, 0, 0, -\boldsymbol{p}), \\ p_3^{\text{com}} &= (E_3, +\boldsymbol{p}' \sin\theta, 0, +\boldsymbol{p}' \cos\theta), \\ p_4^{\text{com}} &= (E_4, -\boldsymbol{p}' \sin\theta, 0, -\boldsymbol{p}' \cos\theta). \end{aligned} \tag{1.57}$$

Here the angle $\theta \in [0, \pi]$. All the parameters in (1.57) can be expressed in terms of the Mandelstam variables. In the simplest case where all four particles have the same mass m we have

$$E_i = \frac{\sqrt{s}}{2}, \quad \boldsymbol{p} = \boldsymbol{p}' = \sqrt{\frac{s}{4} - m^2}, \quad \sin\theta = \frac{2\sqrt{tu}}{s - 4m^2}, \quad \cos\theta = \frac{t-u}{s-4m^2}. \tag{1.58}$$

Instead of using (s, t, u) variables to characterize the scattering process one can also use (s, θ) by using the relations

$$t = -\frac{s-4m^2}{2}(1 - \cos\theta), \quad u = -\frac{s-4m^2}{2}(1 + \cos\theta). \tag{1.59}$$

From these expressions it is clear that the physical range of the Mandelstam variables is

$$s \geq 4m^2, \quad t \in [4m^2 - s,\, 0], \quad u \in [4m^2 - s,\, 0]. \tag{1.60}$$

For the definition of the center of mass frame for the most generic case see appendix A.4.3.

Using the COM frame we can define the scalar components of the interacting scattering amplitude in either of the two equivalent ways[12]

$$\begin{aligned} T^{\lambda_3,\lambda_4}_{\lambda_1,\lambda_2}(s,t,u) &\equiv T^{\lambda_3,\lambda_4}_{\lambda_1,\lambda_2}(p_1^{\text{com}}, p_2^{\text{com}}, p_3^{\text{com}}, p_4^{\text{com}}), \\ T^{\lambda_3,\lambda_4}_{\lambda_1,\lambda_2}(s,t,u) \times (2\pi)^4 \delta^{(4)}(0) &\equiv {}_{free}\langle(\boldsymbol{p}', \theta, 0); \lambda_3, \lambda_4 | T | (\boldsymbol{p}, 0, 0); \lambda_1, \lambda_2\rangle_{free}, \end{aligned} \tag{1.61}$$

As in (1.56) we abuse notation and call the full (interacting) amplitude in a generic frame and its particular form in the COM frame by the same symbol. The difference should always be clear from the arguments. Given the interacting scattering amplitude in the COM frame one can unambiguously obtain the interacting scattering amplitude in a generic frame by using (1.54). As an example, let us apply a rotation by an angle ϕ

[12] In order to see the equivalence of two definitions simply compare (1.47) evaluated in the COM frame (3.9) with (1.26).

around the z axis to (1.61). One gets the following relation

$$e^{i(\lambda_1-\lambda_2-\lambda_3-\lambda_4)\phi}T^{\lambda_3,\lambda_4}_{\lambda_1,\lambda_2}(s,t,u)\times(2\pi)^4\delta^{(4)}(0)= \\ {}_{free}\langle(\boldsymbol{p}',\theta,\phi);\lambda_3,\lambda_4|T|(\boldsymbol{p},0,0);\lambda_1,\lambda_2\rangle_{free} \quad (1.62)$$

This result will be useful when we compute the partial wave decomposition of the scattering amplitude in section 1.5.

We note that the scalar components of the scattering amplitude defined in (1.56) and the COM frame amplitude defined in (1.61) are simply related by a linear transformation which depends only on s, t and u variables. This relation can be found by evaluating (1.56) in the center of mass frame and comparing with (1.61). We will see an explicit example of this in section 2.4.1.

1.3.1 Parity and time-reversal

Let us now discuss additional constraints which appear if the system is parity or time-reversal invariant. In terms of the S operator (and hence also the T operator), the following must hold

$$\mathcal{P}S\mathcal{P}^\dagger = S, \quad \mathcal{T}S\mathcal{T}^\dagger = S^\dagger. \quad (1.63)$$

At the level of COM amplitudes these translate into the following conditions

$$T_{12\to34}{}^{\lambda_3,\lambda_4}_{\lambda_1,\lambda_2}(s,t,u) = \eta_1\eta_2\eta_3^*\eta_4^*(-1)^{j_1+j_2+j_3+j_4}(-1)^{\lambda_1+\lambda_2+\lambda_3+\lambda_4}T_{12\to34}{}^{-\lambda_3,-\lambda_4}_{-\lambda_1,-\lambda_2}(s,t,u), \quad (1.64)$$

$$T_{12\to34}{}^{\lambda_3,\lambda_4}_{\lambda_1,\lambda_2}(s,t,u) = \varepsilon_1^*\varepsilon_2^*\varepsilon_3\varepsilon_4(-1)^{\lambda_1-\lambda_2-\lambda_3+\lambda_4}T_{34\to12}{}^{\lambda_1,\lambda_2}_{\lambda_3,\lambda_4}(s,t,u). \quad (1.65)$$

We derive them in appendix A.2.

1.3.2 Crossing

Our goal now is to formulate crossing equations. The case of particles with generic spin was first addressed in [47]. It was further discussed in [44,48,49]. For a recent discussion see also [28]. All the results presented below are carefully derived in appendix A.5.

Consider the scattering process of four particles. We denote it schematically by

$$12\to34. \quad (1.66)$$

Each particle is characterized by its mass, spin, helicity and 3-momentum, for instance

$1 = (m_1, j_1, \lambda_1; \vec{p}_1)$. There exist five other related process

$$\begin{aligned} &\bar{4}2 \to 3\bar{1}, \qquad &&\bar{3}2 \to \bar{1}4, \\ &1\bar{3} \to \bar{2}4, \qquad &&1\bar{4} \to 3\bar{2}. \end{aligned} \tag{1.67}$$

together with $\bar{3}\bar{4} \to \bar{1}\bar{2}$. Here if particle i has a charge (or more generally transforms in some representation of a global group) then particle $\bar{i}$ has the opposite charge (transforms in the conjugate representation). In other words $\bar{i}$ is the antiparticle of particle i. The scattering process (1.66) is described by the following interacting part of the amplitude

$$T_{12\to 34}{}^{\lambda_3,\lambda_4}_{\lambda_1,\lambda_2}(p_1, p_2, p_3, p_4), \tag{1.68}$$

whereas the scattering processes in (1.67) are described by

$$\begin{aligned} &T_{\bar{4}2\to 3\bar{1}}{}^{\lambda_3,\lambda_1}_{\lambda_4,\lambda_2}(p_4, p_2, p_3, p_1), \qquad &&T_{\bar{3}2\to \bar{1}4}{}^{\lambda_1,\lambda_4}_{\lambda_3,\lambda_2}(p_3, p_2, p_1, p_4), \\ &T_{1\bar{3}\to \bar{2}4}{}^{\lambda_2,\lambda_4}_{\lambda_1,\lambda_3}(p_1, p_3, p_2, p_4), \qquad &&T_{1\bar{4}\to 3\bar{2}}{}^{\lambda_3,\lambda_2}_{\lambda_1,\lambda_4}(p_1, p_4, p_3, p_2). \end{aligned} \tag{1.69}$$

Here all 4-momenta have positive energies $p_i^0 > 0$ and are on-shell (1.48).

Under the assumption that the amplitudes in (1.68) and (1.69) can be analytically continued in p_i and defined in some common domain of p_i values, one can write a set of crossing equations

$$T_{12\to 34}{}^{\lambda_3,\lambda_4}_{\lambda_1,\lambda_2}(p_1, p_2, p_3, p_4) = T_{\bar{4}2\to 3\bar{1}}{}^{+\lambda_3,-\lambda_1}_{-\lambda_4,+\lambda_2}(-p_4, p_2, p_3, -p_1), \tag{1.70}$$

$$T_{12\to 34}{}^{\lambda_3,\lambda_4}_{\lambda_1,\lambda_2}(p_1, p_2, p_3, p_4) = T_{1\bar{3}\to \bar{2}4}{}^{-\lambda_2,+\lambda_4}_{+\lambda_1,-\lambda_3}(p_1, -p_3, -p_2, p_4). \tag{1.71}$$

which are referred to as the $s-t$ crossing equations and

$$T_{12\to 34}{}^{\lambda_3,\lambda_4}_{\lambda_1,\lambda_2}(p_1, p_2, p_3, p_4) = T_{\bar{3}2\to \bar{1}4}{}^{-\lambda_1,+\lambda_4}_{-\lambda_3,+\lambda_2}(-p_3, p_2, -p_1, p_4), \tag{1.72}$$

$$T_{12\to 34}{}^{\lambda_3,\lambda_4}_{\lambda_1,\lambda_2}(p_1, p_2, p_3, p_4) = T_{1\bar{4}\to 3\bar{2}}{}^{+\lambda_3,-\lambda_2}_{+\lambda_1,-\lambda_4}(p_1, -p_4, p_3, -p_2), \tag{1.73}$$

which are referred to as the $s-u$ crossing equations. Finally the amplitude for the process $\bar{3}\bar{4} \to \bar{1}\bar{2}$ can be related to that of the $12 \to 34$ process by using (1.72) and (1.73) one after the other. There are two distinct paths for the analytic continuation of amplitudes discussed in section A.5.1. In writing (1.70) - (1.73) we have made a particular choice, more precisely the one given by (A.256).

Let us now focus on the 23- and 24-crossing equations given by (1.71) and (1.73) respectively and evaluate them in the standard COM (3.9). We can then use the definition of the center of mass amplitude (1.61) in the left-hand side of (1.71) and (1.73) but not in the right-hand side. The right-hand side is not in the center of mass frame of particles 13 and 14 respectively. In order to bring them to this frame we need to perform a Lorentz

transformation. The 23-crossing equation then reads

$$T_{12\to 34}{}^{\lambda_3,\lambda_4}_{\lambda_1,\lambda_2}(s,t,u) = \epsilon'_{23}\sum_{\lambda'_i} e^{i\pi(\lambda'_1+\lambda'_4)} \times d^{(j_1)}_{\lambda'_1\lambda_1}(\alpha_1) d^{(j_2)}_{\lambda'_2\lambda_2}(\alpha_2) d^{(j_3)}_{\lambda'_3\lambda_3}(\alpha_3) d^{(j_4)}_{\lambda'_4\lambda_4}(\alpha_4) T_{1\bar{3}\to\bar{2}4}{}^{\lambda'_2,\lambda'_4}_{\lambda'_1,\lambda'_3}(t,s,u),. \quad (1.74)$$

where the angles α_i in the equal mass case are given by

$$\begin{aligned} +\cos\alpha_1 = -\cos\alpha_2 = -\cos\alpha_3 = +\cos\alpha_4 &= +\frac{st}{\sqrt{s(s-4m^2)}\sqrt{t(t-4m^2)}}, \\ +\sin\alpha_1 = -\sin\alpha_2 = +\sin\alpha_3 = -\sin\alpha_4 &= -\frac{2m\sqrt{stu}}{\sqrt{s(s-4m^2)}\sqrt{t(t-4m^2)}}. \end{aligned} \quad (1.75)$$

For the most general case see (A.322) and (A.323). Similarly the 24-crossing reads

$$T_{12\to 34}{}^{\lambda_3,\lambda_4}_{\lambda_1,\lambda_2}(s,t,u) = \epsilon'_{24}\sum_{\lambda'_i} e^{i\pi(\lambda'_1+\lambda'_3)} \times d^{(j_1)}_{\lambda'_1\lambda_1}(\beta_1) d^{(j_2)}_{\lambda'_2\lambda_2}(\beta_2) d^{(j_3)}_{\lambda'_3\lambda_3}(\beta_3) d^{(j_4)}_{\lambda'_4\lambda_4}(\beta_4) T_{1\bar{4}\to 3\bar{2}}{}^{\lambda'_3,\lambda'_2}_{\lambda'_1,\lambda'_4}(u,t,s), \quad (1.76)$$

where the angles β_i in the equal mass case are given by

$$\begin{aligned} +\cos\beta_1 = -\cos\beta_2 = +\cos\beta_3 = -\cos\beta_4 &= +\frac{su}{\sqrt{s(s-4m^2)}\sqrt{u(u-4m^2)}}, \\ +\sin\beta_1 = -\sin\beta_2 = -\sin\beta_3 = +\sin\beta_4 &= +\frac{2m\sqrt{stu}}{\sqrt{s(s-4m^2)}\sqrt{u(u-4m^2)}}. \end{aligned} \quad (1.77)$$

For the most general case see (A.337) and (A.338). Notice that small Wigner d-matrices are 4π periodic. As a result the angles α_i and β_i are not completely fixed by the equations (1.75) and (1.77) since sines and cosines are 2π periodic. Any particular choice of α_i and β_i satisfying (1.75) and (1.77) results in different overall phases ϵ'_{23} and ϵ'_{24} in the crossing equations (1.74) and (1.76). In principle by carefully working with $SU(2)$ parametrization of rotation angles instead of $SO(3)$, it should be possible to get the right signs. However, in practice it is much quicker to compute these phases at leading order in perturbation theory and since the phases are purely kinematic in nature, the result can be used non-perturbatively. We also note that the form of crossing equations in a general frame, (1.71) and (1.73), depends on the choice of path for the analytic continuation, however both analytic continuations lead to the same expressions in the center of mass frame (1.74) and (1.76).

It is interesting to consider the case when all four particles are massless. Assuming the physical domain (1.60) of the Mandelstam variables for the process $12 \to 34$ in the limit

$m \to 0$ the expressions (1.75) and (1.77) lead to

$$\alpha_1 = \pi, \quad \alpha_2 = 0, \quad \alpha_3 = 0, \quad \alpha_4 = \pi, \tag{1.78}$$
$$\beta_1 = \pi, \quad \beta_2 = 0, \quad \beta_3 = \pi, \quad \beta_4 = 0. \tag{1.79}$$

Using the following properties of the small Wigner d-matrices

$$d^{(j)}_{\lambda'\lambda}(0) = \delta_{\lambda',\lambda}, \qquad d^{(j)}_{\lambda'\lambda}(\pi) = (-1)^{j-\lambda}\delta_{\lambda',-\lambda} \tag{1.80}$$

we get the following crossing equations

$$T_{12\to34}{}^{\lambda_3,\lambda_4}_{\lambda_1,\lambda_2}(s,t,u) = \epsilon''_{23} T_{1\bar{3}\to\bar{2}4}{}^{+\lambda_2,-\lambda_4}_{-\lambda_1,+\lambda_3}(t,s,u), \tag{1.81}$$
$$T_{12\to34}{}^{\lambda_3,\lambda_4}_{\lambda_1,\lambda_2}(s,t,u) = \epsilon''_{24} T_{1\bar{4}\to3\bar{2}}{}^{-\lambda_3,+\lambda_2}_{-\lambda_1,+\lambda_4}(u,t,s), \tag{1.82}$$

where ϵ''_{23} and ϵ''_{24} are some new phases.

1.3.3 Neutral identical particles

In some practical applications one is required to study scattering processes of identical neutral particles with mass m and spin j. We discuss this case in great detail in appendix A.3. Here we state only the most important results.

We define the scattering amplitude of identical neutral particles in a generic and in the center of mass frames as

$$\begin{aligned} T^{\lambda_3,\lambda_4}_{\lambda_1,\lambda_2}(p_1,p_2,p_3,p_4) \times (2\pi)^4\delta^{(4)}(p_1^\mu + p_2^\mu - p_3^\mu - p_4^\mu) &\equiv {}_{id\ free}\langle\kappa_3,\kappa_4|T|\kappa_1,\kappa_2\rangle_{id\ free}, \\ T^{\lambda_3,\lambda_4}_{\lambda_1,\lambda_2}(s,t,u) \times (2\pi)^4\delta^{(4)}(0) &\equiv {}_{id\ free}\langle(\boldsymbol{p}',\theta,0);\lambda_3,\lambda_4|T|(\boldsymbol{p},0,0);\lambda_1,\lambda_2\rangle_{id\ free}. \end{aligned} \tag{1.83}$$

In comparison with (1.46) we drop the subscript $12 \to 34$ since it does not carry any useful information anymore. The two particle states formed from identical particles were defined in (1.34). According to (1.33) they are (anti)symmetric under the exchange of particles 12 and 34. Due to this condition the following equations hold

$$T^{\lambda_3,\lambda_4}_{\lambda_1,\lambda_2}(s,t,u) = (-1)^{-\lambda_1+\lambda_2-\lambda_3+\lambda_4} T^{\lambda_3,\lambda_4}_{\lambda_2,\lambda_1}(s,u,t), \tag{1.84}$$
$$T^{\lambda_3,\lambda_4}_{\lambda_1,\lambda_2}(s,t,u) = (-1)^{+\lambda_1-\lambda_2-\lambda_3+\lambda_4} T^{\lambda_4,\lambda_3}_{\lambda_1,\lambda_2}(s,u,t). \tag{1.85}$$

See appendix A.3.3 for details. Since the variables t and u are flipped in the left- and right-hand side we refer to them as the t-u crossing equations. Applying them twice we get the following kinematic constraint

$$T^{\lambda_3,\lambda_4}_{\lambda_1,\lambda_2}(s,t,u) = T^{+\lambda_4,+\lambda_3}_{+\lambda_2,+\lambda_1}(s,t,u). \tag{1.86}$$

In the case of distinct particles the crossing equations (1.74) and (1.76) establish relations between different amplitudes. When particles are identical there is only a single amplitude (1.83) and the crossing equations become constraints on this single amplitude.

One can also combine together (1.72), (1.73) and (1.70), (1.71) to obtain

$$T^{\lambda_3,\lambda_4}_{\lambda_1,\lambda_2}(p_1,p_2,p_3,p_4) = T^{-\lambda_1,-\lambda_2}_{-\lambda_3,-\lambda_4}(-p_3,-p_4,-p_1,-p_2), \tag{1.87}$$

$$T^{\lambda_3,\lambda_4}_{\lambda_1,\lambda_2}(p_1,p_2,p_3,p_4) = T^{-\lambda_2,-\lambda_1}_{-\lambda_4,-\lambda_3}(-p_4,-p_3,-p_2,-p_1). \tag{1.88}$$

Using the techniques of appendix A.5.4 one can bring both sides of these two equations to the center of mass frame and show that

$$T^{\lambda_3,\lambda_4}_{\lambda_1,\lambda_2}(s,t,u) = T^{-\lambda_1,-\lambda_2}_{-\lambda_3,-\lambda_4}(s,t,u), \tag{1.89}$$

$$T^{\lambda_3,\lambda_4}_{\lambda_1,\lambda_2}(s,t,u) = T^{-\lambda_2,-\lambda_1}_{-\lambda_4,-\lambda_3}(s,t,u). \tag{1.90}$$

We refer to the conditions (1.86), (1.89) and (1.90) as the kinematic constraints associated with the simultaneous permutation of particles (12)(34), (13)(24) and (14)(23) respectively.

As presented, the transition from (1.87), (1.88) to (1.89), (1.90) is very difficult. Strictly speaking the equations (1.89) and (1.90) might have some overall helicity independent phase which we have little control over. There is a much simpler way of deriving (1.89) however. As discussed in appendix A.2.3 one can use the CPT theorem to obtain (1.89). The constraint (1.90) follows from combining (1.89) with (1.86). This discussion indicates (but not proves) that CPT transformation is equivalent to using crossing twice.

1.4 Counting scattering amplitudes

It is useful to count kinematically independent amplitudes in various cases. Looking at the definition of the center of mass amplitude (1.61) it is obvious that the number of all possible amplitudes N_4 for four different massive particles is

$$N_4 = (2j_1+1)(2j_2+1)(2j_3+1)(2j_4+1), \tag{1.91}$$

since there are no restrictions on the helicity values. Using (1.64) we can further split the amplitudes into parity even and parity odd ones. This is done by taking appropriate linear combinations of

$$T^{\lambda_3,\lambda_4}_{\lambda_1,\lambda_2} \qquad \text{and} \qquad T^{-\lambda_3,-\lambda_4}_{-\lambda_1,-\lambda_2}. \tag{1.92}$$

Since the scattering amplitude must always contain an even number of fermions and due to (1.18) and the comment below, the product of intrinsic parities

$$\eta_1\eta_2\eta_3^*\eta_4^* \tag{1.93}$$

entering (1.64) is either $+1$ or -1[13]. Let us assume for concreteness that the product in (1.93) is $+1$. (In the other case when (1.93) is -1 the role of parity even and odd amplitudes constructed from (1.92) simply flips.) Having constructed the appropriate linear combination from (1.92) the counting follows straightforwardly. In the case when there are two or four fermions we have the same number of parity even N_4^+ and parity odd amplitudes N_4^- which read

$$N_4^{\pm} = \frac{1}{2}(2j_1+1)(2j_2+1)(2j_3+1)(2j_4+1). \tag{1.94}$$

In case all particles are bosons we get

$$N_4^{\pm} = \frac{1}{2}\left((2j_1+1)(2j_2+1)(2j_3+1)(2j_4+1) \pm 1\right). \tag{1.95}$$

The difference between (1.94) and (1.94) arises due to the fact that when all particles are bosons there is always a parity even amplitude with all the zero helicities T_{00}^{00}. The latter is no longer true in the presence of fermions. Clearly, the following is obeyed

$$N_4 = N_4^+ + N_4^-. \tag{1.96}$$

If we impose parity as symmetry of our system only parity even amplitudes will survive.

It is more difficult to perform general counting when particles are identical since we need to take into account the relations (1.86) - (1.90). However it easy to do for any particular case of interest by forming a linear system of all the constraints (due presence of parity, identical and massless particles), solving it and counting the number of independent amplitudes. For example in the case of identical massive Majorana particles and identical massive spin one particles we have

$$\text{identical Majorana fermions:} \quad N_4^+ = 5, \quad N_4^- = 2, \tag{1.97}$$

$$\text{identical spin one bosons:} \quad N_4^+ = 17, \quad N_4^- = 10. \tag{1.98}$$

Time-reversal does not further reduce these numbers. This can be intuitively understood by noticing that P implies T invariance for neutral particles due to the CPT symmetry.

In case a particle with spin j is massless its helicity can only take two values $+j$ and $-j$. As a result if all four particles in the scattering process are massless and carry a non-zero spin we always have, independently of the precise values of spin,

$$\text{four different massless particles:} \quad N_4 = 2^4 = 16. \tag{1.99}$$

[13]Parity invariance implies that $\eta_1\eta_2 = \pm\eta_3\eta_4$.

In the case when all particles are identical, massless and carry a non-zero spin we have

$$\text{identical massless particles:} \quad N_4^+ = 5, \quad N_4^- = 2. \tag{1.100}$$

It was proposed in section 6 of [50] that the number of scattering amplitudes in d dimensions should be equal to the number of tensor structures of four-point functions in $d-1$ conformal field theories, where massless particles correspond to conserved operators. This correspondence got an explanation in [51] where it was noted that the conformal frame analysis of four point function is equivalent group theoretically to the center of mass analysis of scattering amplitudes. When parity is involved or particles are identical or massless the matching of CFT and amplitude counting is more difficult to confirm. Here we explicitly verify this correspondence on some particular examples. For instance (1.94) and (1.95) are in a perfect agreement with the formulas (4.47) and (4.49) in [51], results (1.97) and (1.98) match (2.40) and (4.58) in [51], finally the very special case (1.100) matches (3.24) in [51].[14]

1.5 Partial amplitudes

As we explained in section 1.1.3, the two particle states are in a reducible representation of the Poincaré group and can be expressed as a direct sum of Poincaré irreps according to (1.21) or (1.29) (in the special case of COM states). This leads to a decomposition (often referred to as the partial wave decomposition) of scattering amplitudes into partial amplitudes.

We start from the definition of the center of mass amplitude (1.62) and decompose the two particle states there according to (1.29). As a result we get

$$\begin{aligned} e^{i(\lambda_1-\lambda_2-\lambda_3-\lambda_4)\phi} T^{\lambda_3,\lambda_4}_{\lambda_1,\lambda_2}(s,t,u) \times (2\pi)^4\delta^{(4)}(0) = \sum_{\ell,\ell',\lambda,\lambda'} C_{\ell'}(\boldsymbol{p}')C_{\ell}(\boldsymbol{p}) \\ e^{-i(\lambda_3+\lambda_4-\lambda)\phi} d^{(\ell')}_{\lambda'\lambda_{34}}(\theta)\, d^{(\ell)}_{\lambda\lambda_{12}}(0) \langle c,0,\ell',\lambda';\lambda_3,\lambda_4|T|c,0,\ell,\lambda;\lambda_1,\lambda_2\rangle, \end{aligned} \tag{1.101}$$

where we have defined

$$\lambda_{12} \equiv \lambda_1 - \lambda_2, \quad \lambda_{34} \equiv \lambda_3 - \lambda_4. \tag{1.102}$$

The coefficient $C_\ell(\boldsymbol{p})$ was computed in (1.32). Using it we can write

$$C_\ell(\boldsymbol{p}')C_\ell(\boldsymbol{p}) = 4\pi(2\ell+1)\frac{\sqrt{s}}{\sqrt{\boldsymbol{p}\boldsymbol{p}'}}. \tag{1.103}$$

[14] The number of parity even conserved tensor structures in conformal field theories was first computed in [52], see table 1. In $d=3$ it is 5 as expected.

Due to the standard property of the small Wigner d-matrix

$$d^{(\ell)}_{\lambda\lambda_{12}}(0) = \delta_{\lambda\lambda_{12}} \tag{1.104}$$

the dependence on the azimuthal angle ϕ in (1.101) cancels out on both sides and we obtain

$$T^{\lambda_3,\lambda_4}_{\lambda_1,\lambda_2}(s,t,u) \times (2\pi)^4\delta^{(4)}(0) = \sum_{\ell,\ell',\lambda'} C_{\ell'}(\boldsymbol{p}')C_\ell(\boldsymbol{p})d^{(\ell')}_{\lambda'\lambda_{34}}(\theta)\langle c,0,\ell',\lambda';\lambda_3,\lambda_4|T|c,0,\ell,\lambda_{12};\lambda_1,\lambda_2\rangle.$$

Using the definition of the partial amplitudes (1.52) the above can be written in its final form

$$T^{\lambda_3,\lambda_4}_{\lambda_1,\lambda_2}(s,t,u) = \sum_\ell C_\ell(\boldsymbol{p}')C_\ell(\boldsymbol{p})d^{(\ell)}_{\lambda_{12}\lambda_{34}}(\theta)T_\ell{}^{\lambda_3,\lambda_4}_{\lambda_1,\lambda_2}(s). \tag{1.105}$$

By using orthogonality of the small Wigner d matrix the decomposition (1.105) can be inverted and leads to

$$T_\ell{}^{\lambda_3,\lambda_4}_{\lambda_1,\lambda_2}(s) = \frac{2\ell+1}{2C_\ell(\boldsymbol{p}')C_\ell(\boldsymbol{p})} \times \int_0^\pi d\theta \sin\theta d^{(\ell)}_{\lambda_{12}\lambda_{34}}(\theta)T^{\lambda_3,\lambda_4}_{\lambda_1,\lambda_2}(s,t,u). \tag{1.106}$$

Note that t and u are functions of s and θ. In the equal mass case one has for instance (1.59).

Analogously to (1.106) one can also write the decomposition of the full amplitude

$$S_\ell{}^{\lambda_3,\lambda_4}_{\lambda_1,\lambda_2}(s) = \frac{2\ell+1}{2C_\ell(\boldsymbol{p}')C_\ell(\boldsymbol{p})} \times \int_0^{2\pi}\frac{d\phi}{2\pi}\int_0^\pi d\theta \sin\theta d^{(\ell)}_{\lambda_{12}\lambda_{34}}(\theta)S^{\lambda_3,\lambda_4}_{\lambda_1,\lambda_2}(s,t,u). \tag{1.107}$$

We need to introduce the integration over the azimuthal angle ϕ because the disconnected part of the scattering amplitude depends on it, see (1.49) and footnote 11. A simple relation between (1.106) and (1.107) partial amplitudes follows from (1.53) and (1.25). It reads[15]

$$S_\ell{}^{\lambda_3,\lambda_4}_{\lambda_1,\lambda_2}(s) = \delta_{m_1m_3}\delta_{m_2m_4}\delta_{j_1j_3}\delta_{j_2j_4}\delta_{\lambda_1\lambda_3}\delta_{\lambda_2\lambda_4} + iT_\ell{}^{\lambda_3,\lambda_4}_{\lambda_1,\lambda_2}(s). \tag{1.108}$$

As a consistency check one can obtain this relation in a different way. One can plug (1.49) evaluated in the COM frame together with the very first equation in the footnote 11 into (1.107). The delta functions cancel all the integrals in (1.107) and we simply arrive at (1.108).

[15]Here we have used a simple fact that $\delta_{\lambda_i\lambda_k}\delta_{\lambda_j\lambda_l}\delta_{\lambda_{ij}\lambda_{kl}} = \delta_{\lambda_i\lambda_k}\delta_{\lambda_j\lambda_l}$.

1.5.1 Identical particles

In case either the incoming particles or the outgoing particles are identical we also have relations between the partial amplitudes due to (1.38). If the incoming particles 1 and 2 are identical we get

$$S_{\ell\,\lambda_1,\lambda_2}^{\lambda_3,\lambda_4}(s) = (-1)^{\lambda_2-\lambda_1-\ell} S_{\ell\,\lambda_2,\lambda_1}^{\lambda_3,\lambda_4}(s). \tag{1.109}$$

Similarly if the outgoing particles 3 and 4 are identical we get

$$S_{\ell\,\lambda_1,\lambda_2}^{\lambda_3,\lambda_4}(s) = (-1)^{\lambda_4-\lambda_3-\ell} S_{\ell\,\lambda_1,\lambda_2}^{\lambda_4,\lambda_3}(s). \tag{1.110}$$

For the case of all four particles being identical, we get $\sqrt{\boldsymbol{p}\boldsymbol{p}'} = \sqrt{s/4 - m^2}$ due to (1.58), and thus

$$S_{\ell\,\lambda_1,\lambda_2}^{\lambda_3,\lambda_4}(s) = \frac{\sqrt{s-4m^2}}{32\pi\sqrt{s}} \times \int_0^{2\pi} \frac{d\phi}{2\pi} \int_0^{\pi} d\theta \sin\theta d^{(\ell)}_{\lambda_{12}\lambda_{34}}(\theta) S_{\lambda_1,\lambda_2}^{\lambda_3,\lambda_4}(s,t,u), \tag{1.111}$$

$$T_{\ell\,\lambda_1,\lambda_2}^{\lambda_3,\lambda_4}(s) = \frac{\sqrt{s-4m^2}}{32\pi\sqrt{s}} \times \int_0^{\pi} d\theta \sin\theta d^{(\ell)}_{\lambda_{12}\lambda_{34}}(\theta) T_{\lambda_1,\lambda_2}^{\lambda_3,\lambda_4}(s,t,u). \tag{1.112}$$

Notice that we have used here (1.39) which contains an additional $\sqrt{2}$ factor compared to a non-identical particle case. Analogously to (1.108) there is a simple relation between the S and T partial amplitudes that follows from (1.53) and (1.37). It reads[16]

$$S_{\ell\,\lambda_1,\lambda_2}^{\lambda_3,\lambda_4}(s) = \frac{1}{2}\left(\delta_{\lambda_1\lambda_3}\delta_{\lambda_2\lambda_4} + (-1)^{\ell-\lambda_{34}}\delta_{\lambda_1\lambda_4}\delta_{\lambda_2\lambda_3}\right) + iT_{\ell\,\lambda_1,\lambda_2}^{\lambda_3,\lambda_4}(s). \tag{1.113}$$

This result can also be obtained by plugging (1.49) evaluated in the COM frame together with the second equation in the footnote 11 into (1.111). We also notice that in the case of identical scalar particles we recover the standard result, see for example equation (10) in [4].

Parity and time reversal

As usual parity and time reversal invariance lead to additional constraints. The parity constraint follows directly from (A.145) and reads

$$S_{\ell\,\lambda_1,\lambda_2}^{\lambda_3,\lambda_4}(s) = \eta_1\eta_2\eta_3^*\eta_4^*(-1)^{j_1-j_2+j_3-j_4-2\ell} S_{\ell\,-\lambda_1,-\lambda_2}^{-\lambda_3,-\lambda_4}(s). \tag{1.114}$$

Similarly the time reversal constraint follows from (A.170) and reads

$$S_{12\to34\;\ell\,\lambda_1,\lambda_2}^{\lambda_3,\lambda_4}(s) = \varepsilon_1^*\varepsilon_2^*\varepsilon_3\varepsilon_4 S_{34\to12\;\ell\,\lambda_3,\lambda_4}^{\lambda_1,\lambda_2}(s). \tag{1.115}$$

Note that we reintroduced the subscripts $12 \to 34$ and $34 \to 12$ since Time Reversal is a relation between these two distinct processes.

[16] See footnote 15.

1.6 Unitarity

Unitarity of a quantum theory implies that the norm of any state must be non-negative, *i.e.* $\forall\ |\psi\rangle$ one has $\langle\psi|\psi\rangle \geq 0$. Now suppose we are given some set of N states $|\psi_a\rangle$ with $a = 1, \ldots, N$. Unitarity then requires that the $N \times N$ hermitian matrix with components $\langle\psi_a|\psi_b\rangle$ is positive semi-definite, namely $(\langle\psi_a|\psi_b\rangle) \succeq 0$. This formulation allows us to impose unitarity constraints on the partial amplitudes straightforwardly.

We start by considering the incoming two particles state (formed from particles 1 and 2) together with the outgoing two particle state (formed from particles 3 and 4). We decompose each of these states into irreducible representations according to (1.21). We then have the following $N = N_{\text{in}} + N_{\text{out}}$ independent states transforming in the spin ℓ irreducible representation of the Poincaré group

$$\begin{aligned}
|1\rangle_{\text{in}} &\equiv |c, \vec{p}, \ell, \lambda; j_1, j_2\rangle_{\text{in}}, & |1\rangle_{\text{out}} &\equiv |c, \vec{p}, \ell, \lambda; j_3, j_4\rangle_{\text{out}}, \\
|2\rangle_{\text{in}} &\equiv |c, \vec{p}, \ell, \lambda; j_1, j_2 - 1\rangle_{\text{in}}, & |2\rangle_{\text{out}} &\equiv |c, \vec{p}, \ell, \lambda; j_3, j_4 - 1\rangle_{\text{out}}, \\
&\vdots & &\vdots \\
|N_{\text{in}}\rangle_{\text{in}} &\equiv |c, \vec{p}, \ell, \lambda; -j_1, -j_2\rangle_{\text{in}}, & |N_{\text{out}}\rangle_{\text{out}} &\equiv |c, \vec{p}, \ell, \lambda; -j_3, -j_4\rangle_{\text{out}},
\end{aligned} \tag{1.116}$$

where the number of incoming and outgoing irreducible states is

$$N_{\text{in}} \equiv (2j_1 + 1)(2j_2 + 1), \qquad N_{\text{out}} \equiv (2j_3 + 1)(2j_4 + 1). \tag{1.117}$$

Thus for each spin ℓ we can construct the following hermitian $N \times N$ matrix

$$\mathcal{H}_\ell(s) \times (2\pi)^4 \delta^4(p' - p)\delta_{\ell'\ell}\delta_{\lambda'\lambda} = \begin{pmatrix} {}_{\text{in}}\langle a'|b\rangle_{\text{in}} & {}_{\text{in}}\langle a'|b\rangle_{\text{out}} \\ {}_{\text{out}}\langle a'|b\rangle_{\text{in}} & {}_{\text{out}}\langle a'|b\rangle_{\text{out}}, \end{pmatrix} \tag{1.118}$$

where $s = c^2$ is the square of the COM frame total energy and the primes indicate that the conjugated states to (1.116) have all the labels c, p, ℓ and λ primed. In defining the matrix $\mathcal{H}_\ell(s)$ we have also explicitly factored out the overall delta function appearing due to translation invariance. According to the discussion above, unitarity then implies that

$$\mathcal{H}_\ell(s) \succeq 0, \qquad \forall \ell \quad \text{and} \quad s \geq \max(m_1 + m_2, m_3 + m_4)^2. \tag{1.119}$$

Let us now discuss the components of the matrix (1.118). Since the Møller operators introduced in section 1.2 to define the incoming and outgoing states are isometric, the

elements ${}_{\text{in}}\langle a'|b\rangle_{\text{in}}$ and ${}_{\text{out}}\langle a'|b\rangle_{\text{out}}$ are simply fixed by the normalization condition (1.22)

$$ {}_{\text{in}}\langle c_1', \vec{p}\,'; \ell', \lambda'; \lambda_1', \lambda_2'|c_1, \vec{p}; \ell, \lambda; \lambda_1, \lambda_2\rangle_{\text{in}} = (2\pi)^4\delta^{(4)}(p'^\mu - p^\mu)\,\delta_{\ell'\ell}\,\delta_{\lambda'\lambda}\,\delta_{\lambda_1'\lambda_1}\,\delta_{\lambda_2'\lambda_2}, \tag{1.120} $$

$$ {}_{\text{out}}\langle c_1', \vec{p}\,'; \ell', \lambda'; \lambda_3', \lambda_4'|c_1, \vec{p}; \ell, \lambda; \lambda_3, \lambda_4\rangle_{\text{out}} = (2\pi)^4\delta^{(4)}(p'^\mu - p^\mu)\,\delta_{\ell'\ell}\,\delta_{\lambda'\lambda}\,\delta_{\lambda_3'\lambda_3}\,\delta_{\lambda_4'\lambda_4}. \tag{1.121} $$

On the other hand, the matrix elements ${}_{\text{out}}\langle a'|b\rangle_{\text{in}}$ and ${}_{\text{in}}\langle a'|b\rangle_{\text{out}}$ form partial amplitudes according to (1.51)

$$ {}_{\text{out}}\langle c_1', \vec{p}\,'; \ell', \lambda'; \lambda_3, \lambda_4|c_1, \vec{p}; \ell, \lambda; \lambda_1, \lambda_2\rangle_{\text{in}} = (2\pi)^4\delta^{(4)}(p^\mu - p'^\mu)\delta_{\ell\ell'}\delta_{\lambda\lambda'}\,S_{\ell\,\lambda_1,\lambda_2}^{\lambda_3,\lambda_4}(s), \tag{1.122} $$

$$ {}_{\text{in}}\langle c_1', \vec{p}\,'; \ell', \lambda'; \lambda_1, \lambda_2|c_1, \vec{p}; \ell, \lambda; \lambda_3, \lambda_4\rangle_{\text{out}} = (2\pi)^4\delta^{(4)}(p^\mu - p'^\mu)\delta_{\ell\ell'}\delta_{\lambda\lambda'}\,S_{\ell\,\lambda_1,\lambda_2}^{*\lambda_3,\lambda_4}(s). \tag{1.123} $$

Plugging these to (1.118) we can schematically write the unitarity condition (1.119) as

$$ \begin{pmatrix} \delta_{ab} & S^\dagger_{\ell\,ab} \\ S_{\ell\,ab} & \delta_{ab} \end{pmatrix} \succeq 0. \tag{1.124} $$

1.6.1 Identical particles

In case either the incoming particles 1 and 2 or outgoing particles 3 and 4 are identical there exist relations (1.109) and (1.110) between the partial amplitudes. This introduces redundancies into the condition (1.124). In order to remove these redundancies we restrict our attention to states with $\lambda_1 \geq \lambda_2$ (in case of identical incoming particles) and $\lambda_3 \geq \lambda_4$ (in case of identical outgoing particles).

1.6.2 Parity invariance

In the presence of parity invariance various partial amplitudes entering (1.124) are related according to (1.114). As a consequence the condition (1.124) again becomes redundant. One can reformulate the condition (1.124) in an equivalent but less redundant way by considering parity eigenstates. One then repeats the procedure above taking into account the fact that Parity invariance forbids transitions between parity even and parity odd states. As a result we get two separate positivity conditions for parity even and parity odd states

$$ \mathcal{H}_\ell^+(s) \succeq 0, \qquad \mathcal{H}_\ell^-(s) \succeq 0. \tag{1.125} $$

We will see an explicit example of this in section 2.2.

1.6.3 Time reversal invariance

Time reversal invariance relates the scattering amplitudes for the process $12 \to 34$ to the scattering amplitudes for the process $34 \to 12$. Therefore in general time reversal does not have any implications for the matrix $\mathcal{H}_\ell$ since all its elements are scattering amplitudes for the $12 \to 34$. However in the special case of elastic scattering i.e $12 \to 12$, time reversal invariance (1.115) implies that the sub-matrix S_{ij} is symmetric[17]

$$S_{\ell\,\lambda_1,\lambda_2}^{\lambda_3,\lambda_4}(s) = S_{\ell\,\lambda_3,\lambda_4}^{\lambda_1,\lambda_2}(s) \tag{1.126}$$

1.7 Kinematic non-analyticities and constraints

This section is devoted to the study of the behaviour of COM interacting scattering amplitudes defined in (1.61) at some very particular values of the Mandelstam variables s, t and u. For simplicity we focus on the case of identical particles with mass m and spin j.

Using (1.58) the center of mass frame (3.9) can be written in the following way

$$\begin{aligned}
p_1^{\text{com}} &= \left(\frac{\sqrt{s}}{2}, 0, 0, +\sqrt{\frac{s}{4} - m^2}\right), \\
p_2^{\text{com}} &= \left(\frac{\sqrt{s}}{2}, 0, 0, -\sqrt{\frac{s}{4} - m^2}\right), \\
p_3^{\text{com}} &= \left(\frac{\sqrt{s}}{2}, +\frac{\sqrt{tu}}{\sqrt{s-4m^2}}, 0, +\frac{t-u}{2\sqrt{s-4m^2}}\right), \\
p_4^{\text{com}} &= \left(\frac{\sqrt{s}}{2}, -\frac{\sqrt{tu}}{\sqrt{s-4m^2}}, 0, -\frac{t-u}{2\sqrt{s-4m^2}}\right).
\end{aligned} \tag{1.127}$$

The center of mass amplitude (1.61) is strictly defined in the physical domain of the Mandelstam variables (1.60). If one attempts however to analytically continue the COM frame amplitudes to arbitrary complex values of s, t and u, as can be already expected from (1.127), one will encounter non-analyticities (poles and branch points) at

$$s = 4m^2, \quad s = 0, \quad t = 0, \quad u = 0. \tag{1.128}$$

Some of these non-analyticities have a purely kinematic nature and have nothing to do with the dynamics of the theory. Our goal here is to isolate them. In what follows we will formulate the problem of kinematic non-analyticities precisely and then discuss each of the special points (1.128) in detail. (A concrete example will be presented in section 2.1.) For more details on the subject see chapter 7.3 in [44] and references therein.

[17] Note that $|\varepsilon_1 \varepsilon_2|^2 = 1$

Recall the definition of helicity states (1.5), two particle center of mass states (1.26) and center of mass amplitudes (1.61). Using them we can write explicitly the 1PS describing the center of mass scattering process as

$$\begin{aligned}
|m,+\vec{p}_z;j,\lambda_1\rangle &\equiv e^{-i\eta K_3}|m,\vec{0};j,\lambda_1\rangle,\\
|m,-\vec{p}_z;j,\lambda_2\rangle &\equiv e^{-i\pi J_3}e^{-i(\pi-0)J_2}e^{+i\pi J_3}e^{-i\eta K_3}|m,\vec{0};j,\lambda_2\rangle,\\
|m,+\vec{p}_\theta;j,\lambda_3\rangle &\equiv e^{-i\theta J_2}e^{-i\eta K_3}|m,\vec{0};j,\lambda_3\rangle,\\
|m,-\vec{p}_\theta;j,\lambda_4\rangle &\equiv e^{-i\pi J_3}e^{-i(\pi-\theta)J_2}e^{+i\pi J_3}e^{-i\eta K_3}|m,\vec{0};j,\lambda_4\rangle,
\end{aligned} \tag{1.129}$$

where $\vec{p}_z$ is the 3-momentum in the positive z-direction, $\vec{p}_\theta$ is the 3-momentum in the x-z plane, J_2 is the generator of rotations around the y-axis, K_3 is the boost in the z-direction. In the center of mass frame due to (1.58) the angle θ and the rapidity η defined in (1.6) can be related to the Mandelstam variables as follows

$$\cos\theta = \frac{t-u}{s-4m^2}, \quad \sin\theta = \frac{2\sqrt{tu}}{s-4m^2}, \quad \sinh\eta = \frac{\sqrt{s-4m^2}}{2m}, \quad \cosh\eta = \frac{\sqrt{s}}{2m}. \tag{1.130}$$

The non-analyticities at $s=4m^2$, $s=0$, $t=0$ and $u=0$ of these expressions enter the center of mass amplitude (1.61) via (1.129).

The phenomena of kinematic non-analyticities is closely related to the phenomena of kinematic constraints. When defining the COM scattering amplitudes (1.61) we have used up all of the Lorentz symmetry to bring the scattering particles to the x-z plane. However at the special points (1.128) we get an enhancement of symmetry. For instance at $s=4m^2$ the system is $SO(3)$ symmetric, at $s=0$ the system is $SO(1,1)$ symmetric and at $t=0$ and $u=0$ the system is $SO(2)$ symmetric. This is straightforward to see from (1.127).[18] As a consequence of the enhanced symmetry the amplitudes rearrange themselves into irreducible representations of the enhanced symmetry. Only the amplitudes transforming in the trivial representations are allowed to be present, while the rest must vanish. The latter requirement leads to kinematic constraints.[19]

[18] Notice that for the physical range of Mandelstam values $t=O(s-4m^2)$ and $u=O(s-4m^2)$ which means that $\cos\theta$ and $\sin\theta$ are finite. This is not the case anymore once we promote s and t to independent complex variables during the analytic continuation process.

[19] Kinematic constraints have recently appeared in a similar context in conformal field theories when studying four point correlation functions of local primary operators. They received a proper group theoretic treatment in appendix A of [51] (see also appendix D of [53]).

Special point: $s = 4m^2$

In order to isolate the singular behavior of the COM amplitudes at $s = 4m^2$ we perform a simple rewriting of the states (1.129) as follows[20]

$$\begin{aligned}
|m, +\vec{p}_z; j, \lambda_1\rangle &= e^{-i\frac{\theta}{2}J_2} X_+ e^{+i\frac{\theta}{2}J_2} |m, \vec{0}; j, \lambda_1\rangle, \\
|m, -\vec{p}_z; j, \lambda_2\rangle &= e^{-i\frac{\theta}{2}J_2} e^{+i\pi J_2} X_+ e^{+i\frac{\theta}{2}J_2} |m, \vec{0}; j, \lambda_2\rangle, \\
|m, +\vec{p}_\theta; j, \lambda_3\rangle &= e^{-i\frac{\theta}{2}J_2} X_- e^{-i\frac{\theta}{2}J_2} |m, \vec{0}; j, \lambda_3\rangle, \\
|m, -\vec{p}_\theta; j, \lambda_4\rangle &= e^{-i\frac{\theta}{2}J_2} e^{+i\pi J_2} X_- e^{-i\frac{\theta}{2}J_2} |m, \vec{0}; j, \lambda_4\rangle,
\end{aligned} \tag{1.131}$$

where the operators $X_\pm$ are defined as

$$X_\pm \equiv e^{\pm i\frac{\theta}{2}J_2} e^{-i\eta K_3} e^{\mp i\frac{\theta}{2}J_2} = e^{-i\left(K_3 \cos\frac{\theta}{2} \mp K_1 \sin\frac{\theta}{2}\right)\eta}. \tag{1.132}$$

In (1.132) we have used the commutation properties of the Lorentz generators (A.40). Writing

$$\cos\frac{\theta}{2} = \sqrt{\frac{-u}{s-4m^2}}, \qquad \sin\frac{\theta}{2} = \sqrt{\frac{-t}{s-4m^2}}, \tag{1.133}$$

we notice that the operators $X_\pm$ are completely regular at $s = 4m^2$ since

$$\eta\cos\frac{\theta}{2} = \frac{\sqrt{-u}}{2m} + O(s-4m^2), \qquad \eta\sin\frac{\theta}{2} = \frac{\sqrt{-t}}{2m} + O(s-4m^2). \tag{1.134}$$

Plugging the states (1.131) into the definition of the COM amplitudes (1.61) and using the fact that the scattering operator is invariant under the Poincaré transformations[21] (1.44) and the transformation property (1.7) we can write

$$T^{\lambda_3,\lambda_4}_{\lambda_1,\lambda_2}(s,t,u) = \sum_{\lambda'} d^{(j)}_{\lambda_1'\lambda_1}\left(-\frac{\theta}{2}\right) d^{(j)}_{\lambda_2'\lambda_2}\left(-\frac{\theta}{2}\right) d^{(j)}_{\lambda_3'\lambda_3}\left(\frac{\theta}{2}\right) d^{(j)}_{\lambda_4'\lambda_4}\left(\frac{\theta}{2}\right) A^{\lambda_3',\lambda_4'}_{\lambda_1',\lambda_2'}(s,t,u), \tag{1.135}$$

where the new scattering amplitude A is defined as

$$A^{\lambda_3,\lambda_4}_{\lambda_1,\lambda_2}(s,t,u) \equiv \left(\langle\vec{0},\lambda_3|X_-^\dagger \otimes \langle\vec{0},\lambda_4|X_-^\dagger e^{-i\pi J_2}\right) T \left(X_+|\vec{0},\lambda_1\rangle \otimes e^{+i\pi J_2} X_+|\vec{0},\lambda_2\rangle\right). \tag{1.136}$$

From this explicit expression we see that at $s = 4m^2$ the amplitude A is completely regular due to (1.134), more precisely

$$A^{\lambda_3,\lambda_4}_{\lambda_1,\lambda_2}(s,t,u) = O\left((s-4m^2)^0\right). \tag{1.137}$$

As a result the non-analytic behavior (1.133) at $s = 4m^2$ enters the amplitude T only

[20] The relation $e^{-i\chi J_2} e^{i\pi J_3} = e^{i\pi J_3} e^{+i\chi J_2}$ is used for the states 2 and 4.

[21] The same property holds obviously true for the T operators because of (1.45). The invariance we use here is $e^{i\frac{\theta}{2}J_2} T e^{-i\frac{\theta}{2}J_2} = T$.

through the Wigner d-matrices in (1.135). Now in order to extract the precise behaviour of the poles in the COM amplitude in practice we simply need to expand (1.135) around $s = 4m^2$ to the leading order using the explicit expression of the Wigner d matrices (1.9), taking into account (1.133) and the fact that the functions A are regular at $s = 4m^2$.

The expression (1.135) together with (1.136) can also be used to address kinematic constraints. Expanding (1.135) to the next to leading order one finds that some linear combinations should vanish as $O\Big((s-4m^2)^1\Big)$ instead of $O\Big((s-4m^2)^0\Big)$ or $O\Big((s-4m^2)^{-1}\Big)$. For simple examples as in section 2.1 such linear combinations can be found manually. For more complicated cases one can invoke group theoretic arguments similar to ones in [51].

Special points: $t = 0$ and $u = 0$

Kinematic branch points $\sqrt{t}$ and $\sqrt{u}$ enter the center of mass scattering amplitudes via $\sin\theta$ given (1.130). Their presence can be deduced by looking at the partial wave decomposition (1.105) and noticing that the Wigner d matrix there can be written in the form

$$d^{(\ell)}_{\lambda'\lambda}(\theta) = \left(\cos\frac{\theta}{2}\right)^{|\lambda+\lambda'|}\left(\sin\frac{\theta}{2}\right)^{|\lambda-\lambda'|} P^{\ell}_{\lambda'\lambda}(\cos\theta), \tag{1.138}$$

where $P^{\ell}_{\lambda'\lambda}$ is a polynomial whose precise definition is irrelevant here but can be deduced from (4.1.19) and (4.1.23) in [54]. The important point is that the polynomial $P^{\ell}_{\lambda'\lambda}$ depends only on $\cos\theta$ and therefore does not have any branch points as can be seen from (1.130). Using the above, (1.133) and (1.105) we conclude that

$$T^{\lambda_3,\lambda_4}_{\lambda_1,\lambda_2}(s,t,u) \sim d^{(\ell)}_{\lambda_{12}\lambda_{34}}(\theta) \sim \left(\sqrt{-u}\right)^{|\lambda_{12}+\lambda_{34}|}\left(\sqrt{-t}\right)^{|\lambda_{12}-\lambda_{34}|}. \tag{1.139}$$

The $SO(2)$ enhancement of symmetry at $t = 0$ ($\theta = 0$) and $u = 0$ ($\theta = \pi$), see (1.127), leads to kinematic constraints at these two points. This is the simplest case among all the special points and can be easily addressed in full generality. In order to deduce the implications of this $SO(2)$ invariance we inject the identity in the form $1 = e^{-i\gamma J_3}e^{+i\gamma J_3}$ to the left and to the right of the T operator in (1.61), where γ is some angle. Using the invariance of the T operator (1.44) and the fact that the 1PS states along the z-direction are the eigenstates of J_3, we arrive at

$$T^{\lambda_3,\lambda_4}_{\lambda_1,\lambda_2}(s,t=0) = e^{i\gamma(\lambda_1-\lambda_2-\lambda_3+\lambda_4)}T^{\lambda_3,\lambda_4}_{\lambda_1,\lambda_2}(s,t=0), \tag{1.140}$$

$$T^{\lambda_3,\lambda_4}_{\lambda_1,\lambda_2}(s,u=0) = e^{i\gamma(\lambda_1-\lambda_2+\lambda_3-\lambda_4)}T^{\lambda_3,\lambda_4}_{\lambda_1,\lambda_2}(s,u=0). \tag{1.141}$$

These constraints should be satisfied for any value of the angle γ. Thus, the amplitudes must vanish unless $\lambda_1 - \lambda_2 - \lambda_3 + \lambda_4 = 0$ in the first case and $\lambda_1 - \lambda_2 + \lambda_3 - \lambda_4 = 0$ in

the second case. This is just conservation of angular momentum along the z–axis.

Special point: $s = 0$

Finally let us address the most complicated $s = 0$ case. In the vicinity of $s = 0$, the rapidity parameter η can be written as

$$\eta = \frac{i\pi}{2} - \frac{i\sqrt{s}}{2m} + O(s^{3/2}). \tag{1.142}$$

Let us now define the new rapidity ξ as

$$\xi \equiv \eta - \frac{i\pi}{2} = -\frac{i\sqrt{s}}{2m} + O(s^{3/2}). \tag{1.143}$$

By using (A.45) - (A.47) and the following property of the small Wigner d-matrix

$$d^{(j)}_{\lambda'\lambda}(-\pi) = (-1)^{j+\lambda}\delta_{\lambda',-\lambda}, \tag{1.144}$$

we can rewrite the states (1.129) in the following way

$$\begin{aligned}
|m, +\vec{p}_z; j, \lambda_1\rangle &= e^{+\frac{\pi}{2}K_3}\left(e^{-i\xi K_3}|m, \vec{0}; j, \lambda_1\rangle\right), \\
|m, -\vec{p}_z; j, \lambda_2\rangle &= (-1)^{j+\lambda_2}e^{-\frac{\pi}{2}K_3}\left(e^{+i\xi K_3}|m, \vec{0}; j, -\lambda_2\rangle\right), \\
|m, +\vec{p}_\theta; j, \lambda_3\rangle &= e^{-i\theta J_2}e^{+\frac{\pi}{2}K_3}\left(e^{-i\xi K_3}|m, \vec{0}; j, \lambda_3\rangle\right), \\
|m, -\vec{p}_\theta; j, \lambda_4\rangle &= (-1)^{j+\lambda_4}e^{-i\theta J_2}e^{-\frac{\pi}{2}K_3}\left(e^{+i\xi K_3}|m, \vec{0}; j, -\lambda_4\rangle\right).
\end{aligned} \tag{1.145}$$

These can be further rewritten as[22]

$$\begin{aligned}
|m,+\vec{p}_z;j,\lambda_1\rangle &= e^{+\frac{\pi}{2}K_1}e^{+\frac{\pi}{2}K_3}e^{-i\xi K_1}\left(e^{-i\frac{\pi}{2}J_2}|m,\vec{0};j,\lambda_1\rangle\right),\\
|m,-\vec{p}_z;j,\lambda_2\rangle &= e^{+\frac{\pi}{2}K_1}e^{-\frac{\pi}{2}K_3}e^{-i\xi K_1}\left((-1)^{j+\lambda_2}e^{+i\frac{\pi}{2}J_2}|m,\vec{0};j,-\lambda_2\rangle\right),\\
|m,+\vec{p}_\theta;j,\lambda_3\rangle &= e^{+\frac{\pi}{2}K_1}e^{-(\theta-\frac{\pi}{2})K_3}e^{-i\xi K_1}\left(e^{-i\frac{\pi}{2}J_2}|m,\vec{0};j,\lambda_3\rangle\right),\\
|m,-\vec{p}_\theta;j,\lambda_4\rangle &= e^{+\frac{\pi}{2}K_1}e^{-(\theta+\frac{\pi}{2})K_3}e^{-i\xi K_1}\left((-1)^{j+\lambda_4}e^{+i\frac{\pi}{2}J_2}|m,\vec{0};j,-\lambda_4\rangle\right).
\end{aligned} \tag{1.146}$$

We use now invariance of the scattering operator under boosts and the action of rotations on the center of mass states (1.7), which for the second and fourth particles become

$$\begin{aligned}
(-1)^{j+\lambda}e^{+i\frac{\pi}{2}J_2}|m,\vec{0};j,-\lambda\rangle &= (-1)^{j+\lambda}\sum_{\lambda'}d^j_{\lambda',-\lambda}(-\frac{\pi}{2})|m,\vec{0};j,\lambda'\rangle\\
&= (-1)^{2j}\sum_{\lambda'}d^j_{\lambda',\lambda}(+\frac{\pi}{2})|m,\vec{0};j,\lambda'\rangle,
\end{aligned} \tag{1.147}$$

to obtain the final expression

$$T^{\lambda_3,\lambda_4}_{\lambda_1,\lambda_2}(s,t,u)=\sum_{\lambda'}d^{(j)}_{\lambda_1'\lambda_1}\left(\frac{\pi}{2}\right)d^{(j)}_{\lambda_2'\lambda_2}\left(\frac{\pi}{2}\right)d^{(j)}_{\lambda_3'\lambda_3}\left(\frac{\pi}{2}\right)d^{(j)}_{\lambda_4'\lambda_4}\left(\frac{\pi}{2}\right)B^{\lambda_3',\lambda_4'}_{\lambda_1',\lambda_2'}(s,t,u), \tag{1.148}$$

where the amplitude B is defines as

$$\begin{aligned}
B^{\lambda_3,\lambda_4}_{\lambda_1,\lambda_2}(s,t,u) \equiv &\left(\langle m,\vec{0};j,\lambda_3|e^{+i\xi K_1}e^{+\frac{\pi}{2}K_3}\otimes\langle m,\vec{0};j,\lambda_4|e^{+i\xi K_1}e^{-\frac{\pi}{2}K_3}\right)e^{-\theta K_3}T\\
&\left(e^{+\frac{\pi}{2}K_3}e^{-i\xi K_1}|m,\vec{0};j,\lambda_1\rangle\otimes e^{-\frac{\pi}{2}K_3}e^{-i\xi K_1}|m,\vec{0};j,\lambda_2\rangle\right).
\end{aligned} \tag{1.149}$$

Let us inspect the structure of this amplitude. We expand it around $\xi=0$ or equivalently around $s=0$ according to (1.143). Schematically speaking, each term in this expansion will contain $(\xi K_1)^n$ with some non-negative integer n. We then notice that $(\xi K_1)^n$ are

[22]The steps involved here are as follows. First, we inject the identity operators $\mathbb{I}=e^{\pm i\frac{\pi}{2}J_2}e^{\mp i\frac{\pi}{2}J_2}$ to the left and right of the $e^{\pm i\xi K_3}$ operator and use the following relations

$$e^{-iJ_2\frac{\pi}{2}}e^{\pm i\xi K_3}e^{+iJ_2\frac{\pi}{2}}=e^{\pm i\xi K_1},\qquad e^{+iJ_2\frac{\pi}{2}}e^{\pm i\xi K_3}e^{-iJ_2\frac{\pi}{2}}=e^{\mp i\xi K_1}.$$

Second, we use the following relations

$$e^{\pm\frac{\pi}{2}K_3}e^{+iJ_2\frac{\pi}{2}}=e^{+iJ_2\frac{\pi}{2}}e^{\pm\frac{\pi}{2}K_1},\qquad e^{\pm\frac{\pi}{2}K_3}e^{-iJ_2\frac{\pi}{2}}=e^{-iJ_2\frac{\pi}{2}}e^{\mp\frac{\pi}{2}K_1}$$

to bring all the exponents containing J_2 to the left. Finally, we use

$$e^{-i\theta J_2}e^{\frac{\pi}{2}K_1}=e^{\frac{\pi}{2}K_1}e^{-\theta K_3}.$$

the only operators which change helicities of particles.[23] Now, the only non-zero terms will be the ones with equal total helicity of the states to the left and to the right of the scattering operator T. Given a set of helicities λ_i, the leading term in the $\xi = 0$ expansion will contain $(\xi K_1)^n$ with $n = |\lambda_1 + \lambda_2 - \lambda_3 - \lambda_4|$. Using (1.143) we conclude that

$$B^{\lambda_3,\lambda_4}_{\lambda_1,\lambda_2}(s,t,u) = \left(\sqrt{s}\right)^{|\lambda_1+\lambda_2-\lambda_3-\lambda_4|} \times O(s^0). \tag{1.150}$$

From (1.148) and (1.150) it follows that the COM amplitudes T get a $\sqrt{s}$ branch point only for odd values of $|\lambda_1 + \lambda_2 - \lambda_3 - \lambda_4|$. The relations (1.148) and (1.150) can be also used to address kinematic singularities. Expanding (1.148) around $s = 0$ at the leading order one can find linear combinations of the amplitudes which behave as $O(s^1)$ instead of $O(s^0)$.

[23] One can define the following operators

$$K_\pm \equiv K_1 \pm iK_2 \quad \Rightarrow \quad K_1 = \frac{1}{2}(K_+ + K_-).$$

According to (A.40) these operators rise and lower helicities of the center of mass states as

$$J_3 K_\pm |m, \vec{0}; j, \lambda\rangle = (\lambda \pm 1) K_\pm |m, \vec{0}; j, \lambda\rangle.$$

2 Application: identical Majorana fermions

We will now use the machinery set up in the previous chapter to study the two to two scattering of identical neutral[1] spin $\frac{1}{2}$ fermions also known as Majorana fermions. We will require invariance under parity. As a result we need to specify the intrinsic parity η defined in (1.16). In the two to two scattering of identical particles we are sensitive only to the value of η^2. According to (1.18) there are two possibilities

$$\eta^2 = -1 \quad \text{or} \quad \eta^2 = +1. \tag{2.1}$$

For concreteness we assume the former in this section. In the latter situation everything in this section still remains valid except that the meaning of parity even and odd states in section 2.2 is flipped and the role of scalar and pseudoscalar particles is exchanged in section 2.3. Helicity of a spin $\frac{1}{2}$ particle takes only two values: $+\frac{1}{2}$ and $-\frac{1}{2}$. Thus a priori, we have $2^4 = 16$ helicity amplitudes. However due to the fact that the particles are all identical these amplitudes are related according to (1.86) - (1.90). As a result we can write the following 9 relations

$$\begin{aligned} &T^{--}_{--} = T^{++}_{++}, \qquad T^{+-}_{--} = T^{-+}_{--}, \qquad T^{--}_{-+} = T^{+-}_{++}, \qquad T^{-+}_{-+} = T^{+-}_{+-}, \qquad T^{+-}_{-+} = T^{-+}_{+-}, \\ &T^{++}_{-+} = T^{-+}_{--}, \qquad T^{--}_{+-} = T^{+-}_{++}, \qquad T^{++}_{+-} = T^{-+}_{--}, \qquad T^{-+}_{++} = T^{+-}_{++}, \end{aligned} \tag{2.2}$$

where $+$ and $-$ stand for $+\frac{1}{2}$ and $-\frac{1}{2}$ helicities respectively. Hence out of the 16 amplitudes we are left with 7 independent ones. Requiring parity invariance and noticing that due to (2.1) the product of intrinsic parities $\eta_1\eta_2\eta_3^*\eta_4^* = +1$, due to (1.64) we get in addition the following 2 constraints

$$T^{-+}_{--} = -T^{+-}_{++}, \qquad T^{++}_{--} = +T^{--}_{++}. \tag{2.3}$$

[1] By neutral we mean particles not carrying any $U(1)$ charge and in general not transforming in any non-trivial representation of the global group. In common words it means that the particle is its own antiparticle.

As a result out of the 16 helicity amplitudes we are left with only 5 independent ones, in agreement with (1.97), which we denote as

$$\begin{aligned}
\Phi_1(s,t,u) &\equiv T^{++}_{++}(s,t,u),\\
\Phi_2(s,t,u) &\equiv T^{--}_{++}(s,t,u),\\
\Phi_3(s,t,u) &\equiv T^{+-}_{+-}(s,t,u),\\
\Phi_4(s,t,u) &\equiv T^{-+}_{+-}(s,t,u),\\
\Phi_5(s,t,u) &\equiv T^{+-}_{++}(s,t,u).
\end{aligned} \tag{2.4}$$

It is interesting to note that the scattering of identical neutral fermions preserving parity is automatically time-reversal invariant, this can be intuitively understood from the CPT symmetry since charge conjugation is trivial for neutral particles, see appendix A.2.3.

As discussed in section 1.3.3, in the case of scattering of uncharged identical particles, the crossing equations (1.74) and (1.76) form highly non-trivial constraints on the scattering amplitudes. For instance, in the case of identical Majorana particles these crossing equations give rise to two sets of 16 linear equations. Taking into account the relations (2.2) and (2.3) we simply obtain two sets of 5 linear equations on the independent amplitudes (2.4). They read as

$$\Phi_I(s,t,u) = \sum_{J=1}^{5} C^{IJ}_{st}(s,t,u)\Phi_J(t,s,u), \tag{2.5}$$

$$\Phi_I(s,t,u) = \sum_{J=1}^{5} C^{IJ}_{su}(s,t,u)\Phi_J(u,t,s), \tag{2.6}$$

where the $s-t$ crossing matrix C_{st} is given by

$$C_{st} = -\frac{\epsilon'_{23}}{2}\begin{pmatrix}
-\sin^2\alpha & \sin^2\alpha & -\sin^2\alpha & 1+\cos^2\alpha & 4\cos\alpha\sin\alpha\\
\sin^2\alpha & 1+\cos^2\alpha & \sin^2\alpha & \sin^2\alpha & -4\cos\alpha\sin\alpha\\
-\sin^2\alpha & \sin^2\alpha & 1+\cos^2\alpha & -\sin^2\alpha & 4\cos\alpha\sin\alpha\\
1+\cos^2\alpha & \sin^2\alpha & -\sin^2\alpha & -\sin^2\alpha & 4\cos\alpha\sin\alpha\\
\cos\alpha\sin\alpha & -\cos\alpha\sin\alpha & \cos\alpha\sin\alpha & \cos\alpha\sin\alpha & 2(\sin^2\alpha-\cos^2\alpha)
\end{pmatrix}, \tag{2.7}$$

and the $s-u$ crossing matrix C_{su} is given by

$$C_{su} = -\frac{\epsilon'_{24}}{2}\begin{pmatrix}
-\sin^2\beta & \sin^2\beta & 1+\cos^2\beta & -\sin^2\beta & 4\cos\beta\sin\beta\\
\sin^2\beta & 1+\cos^2\beta & \sin^2\beta & \sin^2\beta & -4\cos\beta\sin\beta\\
1+\cos^2\beta & \sin^2\beta & -\sin^2\beta & -\sin^2\beta & 4\cos\beta\sin\beta\\
-\sin^2\beta & \sin^2\beta & -\sin^2\beta & 1+\cos^2\beta & 4\cos\beta\sin\beta\\
\cos\beta\sin\beta & -\cos\beta\sin\beta & \cos\beta\sin\beta & \cos\beta\sin\beta & 2(\sin^2\beta-\cos^2\beta)
\end{pmatrix}. \tag{2.8}$$

The angles α and β are defined as follows. Looking at the expressions (1.75) and (1.77)

we can make the following choice of Wigner angles

$$\alpha_1 = \alpha, \quad \alpha_2 = \pi + \alpha, \quad \alpha_3 = \pi - \alpha, \quad \alpha_4 = -\alpha. \tag{2.9}$$

$$\beta_1 = \beta, \quad \beta_2 = \pi + \beta, \quad \beta_3 = -\beta, \quad \beta_4 = \pi - \beta, \tag{2.10}$$

where the angles α and β obey

$$\cos\alpha = \frac{st}{\sqrt{s(s-4m^2)}\sqrt{t(t-4m^2)}}, \quad \sin\alpha = -\frac{2m\sqrt{stu}}{\sqrt{s(s-4m^2)}\sqrt{t(t-4m^2)}}, \tag{2.11}$$

$$\cos\beta = \frac{su}{\sqrt{s(s-4m^2)}\sqrt{u(u-4m^2)}}, \quad \sin = +\frac{2m\sqrt{stu}}{\sqrt{s(s-4m^2)}\sqrt{u(u-4m^2)}}. \tag{2.12}$$

The correct choice of the phases at (2.7) and (2.8) will be explained at the end of section 2.1. Here we simply state the correct result, which is

$$\epsilon'_{23} = \epsilon'_{24} = -1. \tag{2.13}$$

There are two non-trivial consistency checks our matrices (2.7) and (2.8) pass. First, these matrices are involutory, namely they satisfy the following conditions[2]

$$\Big(C_{st}(s,t,u)\Big)^2 = 1, \qquad \Big(C_{su}(s,t,u)\Big)^2 = 1. \tag{2.14}$$

Second, we can obtain the crossing matrix appearing in the $t-u$ crossing equations as

$$C_{tu}(s,t,u) = C_{st}(s,t,u)C_{su}(t,s,u)C_{st}(u,s,t). \tag{2.15}$$

In our case it reads as

$$C_{tu}(s,t,u) = \begin{pmatrix} 1 & 0 & 0 & 0 & 0 \\ 0 & 1 & 0 & 0 & 0 \\ 0 & 0 & 0 & 1 & 0 \\ 0 & 0 & 1 & 0 & 0 \\ 0 & 0 & 0 & 0 & -1 \end{pmatrix}. \tag{2.16}$$

This is in perfect agreement with the result (1.85).

[2]More accurately one should write

$$C_{st}(s,t,u)C_{st}(t,s,u) = 1, \qquad C_{su}(s,t,u)C_{su}(u,t,s) = 1.$$

However, these conditions reduce to (2.14) by noticing that the matrices $C_{st}(s,t,u)$ and $C_{st}(u,t,s)$ are symmetric in the exchange of $s \leftrightarrow t$ and $s \leftrightarrow u$ respectively. This follows from the fact that the expressions for the angles α and β given by (2.11) and (2.12) obey the symmetry $s \leftrightarrow t$ and $s \leftrightarrow u$ respectively.

2.1 Improved amplitudes

It is important to study the analytic structure (presence of poles and branch cuts) of helicty amplitudes when all the Mandelstam variables s, t and u are promoted to the full complex plane. As explained in section 1.7 in the case of scattering of spinning particles such amplitudes develop non-analytic behaviour purely due to kinematic reasons. In this section we show how to isolate such kinematic features in the case of Majorana fermions and define improved amplitudes which do not have them.

Due to (1.135) all the amplitudes have a pole at $s = 4m^2$. Expanding (1.135) around this point we get

$$\begin{aligned}
\Phi_1 &= \frac{a_1}{s-4m^2} + b_1 + O(s-4m^2),\\
\Phi_2 &= \frac{a_2}{s-4m^2} + b_2 + O(s-4m^2),\\
\Phi_3 &= \frac{a_3}{s-4m^2} + b_3 + O(s-4m^2),\\
\Phi_4 &= \frac{a_4}{s-4m^2} + b_4 + O(s-4m^2),\\
\Phi_5 &= \frac{a_5}{s-4m^2} + b_5 + O(s-4m^2),
\end{aligned} \tag{2.17}$$

where a_i and b_i are some factors which are regular at $s = 4m^2$. We do not write them explicitly, their form can be obtained straightforwardly using computer algebra.[3] We only note that

$$a_1 = -a_2 = a_3 = a_4 = -ia_5. \tag{2.18}$$

Using (2.17) we can verify the following kinematic relation at the singular point[4]

$$\Phi_1 - \Phi_2 + \Phi_3 + \Phi_4 + 4i\Phi_5 = 0 + O(s-4m^2). \tag{2.19}$$

Now due to (1.148) the amplitude Φ_5 also develops a branch point at $s = 0$ as

$$\Phi_5 \sim \sqrt{s}, \tag{2.20}$$

whereas all the other amplitudes are regular at $s = 0$. Expanding (1.148) to the leading

[3] Notice that identical particles and parity imply constraints on the amplitudes T according to (2.2) and (2.3). In order to proceed with the expansion one needs to deduce the analogues of these expressions on the regular $A(s,t,u)$ amplitudes entering (1.135) by solving an appropriate system of linear equations.

[4] We expand around $s = 4m^2$ keeping t independent. Then in the right-hand side of (2.19) the leading and the next to leading order terms appear to be proportional to the following expression

$$t - u - 2i\sqrt{tu} = 2t + (s-4m^2) - 2i\sqrt{t(4m^2-s-t)} = 0 + O(s-4m^2).$$

In the last equality we have used the domain where $t < 0$ and s has a small positive imaginary part.

order we can verify the following kinematical constraint

$$\Phi_1 + \Phi_2 - \Phi_3 - \Phi_4 = 0 + O(s). \tag{2.21}$$

Finally we consider the behavior of the amplitudes at $t = 0$ and $u = 0$ points. Due to (1.139) the amplitudes Φ_1, Φ_2, Φ_3 and Φ_4 are all analytic at these points. In contrast the amplitude Φ_5 develops a branch point both at $t = 0$ and $u = 0$ as

$$\Phi_5 \sim \sqrt{tu}. \tag{2.22}$$

In addition due to (1.140) and (1.141) we have the following constraints

$$\begin{aligned} \Phi_4 &= 0 + O(t), \quad \Phi_5 = 0 + O(t), \\ \Phi_3 &= 0 + O(u), \quad \Phi_5 = 0 + O(u). \end{aligned} \tag{2.23}$$

Now that we know precisely the non-analytic behaviour of the amplitudes, we can define new improved amplitudes which are free of the kinematic pole at $s = 4m^2$ and kinematic branch points $\sqrt{s}$, $\sqrt{t}$ and $\sqrt{u}$. We denote such improved amplitudes by $H_I(s,t,u)$. The old amplitudes and the new improved amplitudes can be related as

$$\Phi_I(s,t,u) = \sum_{J=1}^{5} M_{IJ}^{-1}(s,t,u) H_J(s,t,u), \tag{2.24}$$

where $M(s,t,u)$ is some matrix to be determined. It is constructed by requiring that

$$\Phi_I \sim \frac{1}{s-4m^2}, \quad \Phi_5 \sim \sqrt{stu} \tag{2.25}$$

and that the relations (2.17) along with (2.18), (2.19), (2.21) and (2.23) are fulfilled. These requirements do not fix the matrix $M_{IJ}(s,t,u)$ completely. One possible choice is

$$M_{IJ}(s,t,u) = \begin{pmatrix} \frac{4}{s-4m^2} & \frac{-4}{s-4m^2} & \frac{2\,(1-t/u)}{s-4m^2} & \frac{2(1-u/t)}{s-4m^2} & \frac{s+4m^2}{s-4m^2} \times \frac{2(t-u)}{m\sqrt{stu}} \\ 0 & 0 & \frac{2}{u} & -\frac{2}{t} & -\frac{8m}{\sqrt{stu}} \\ 0 & 0 & \frac{2}{u} & -\frac{2}{t} & -\frac{2s}{m\sqrt{stu}} \\ 0 & 0 & \frac{2}{u} & \frac{2}{t} & 0 \\ -\frac{4}{s} & -\frac{4}{s} & \frac{2}{u} + \frac{4}{s} & \frac{2}{t} + \frac{4}{s} & \frac{2(t-u)}{m\sqrt{stu}} \end{pmatrix}. \tag{2.26}$$

We motivate this choice in section 2.4.1.

Having established the relation (2.24) we can write the crossing equations (2.5) and (2.6)

directly in terms of the improved amplitudes as

$$H_I(s,t,u) = \sum_{J=1}^{5} \widetilde{C}^{IJ}_{st}(s,t,u) H_J(t,s,u), \tag{2.27}$$

$$H_I(s,t,u) = \sum_{J=1}^{5} \widetilde{C}^{IJ}_{su}(s,t,u) H_J(u,t,s), \tag{2.28}$$

where the crossing matrices $\widetilde{C}_{st}$ and $\widetilde{C}_{su}$ read as

$$\widetilde{C}_{st} \equiv M(s,t,u) C_{st}(s,t,u) M^{-1}(t,s,u), \tag{2.29}$$

$$\widetilde{C}_{su} \equiv M(s,t,u) C_{su}(s,t,u) M^{-1}(u,t,s). \tag{2.30}$$

Plugging here the explicit expressions (2.7), (2.8) and (2.26) we get

$$\widetilde{C}_{st} = \begin{pmatrix} -\frac{1}{4} & -1 & \frac{3}{2} & 1 & -\frac{1}{4} \\ -\frac{1}{4} & \frac{1}{2} & 0 & \frac{1}{2} & \frac{1}{4} \\ \frac{1}{4} & 0 & \frac{1}{2} & 0 & \frac{1}{4} \\ \frac{1}{4} & \frac{1}{2} & 0 & \frac{1}{2} & -\frac{1}{4} \\ -\frac{1}{4} & 1 & \frac{3}{2} & -1 & -\frac{1}{4} \end{pmatrix}, \qquad \widetilde{C}_{su} = \begin{pmatrix} -\frac{1}{4} & 1 & -\frac{3}{2} & 1 & -\frac{1}{4} \\ \frac{1}{4} & \frac{1}{2} & 0 & -\frac{1}{2} & -\frac{1}{4} \\ -\frac{1}{4} & 0 & \frac{1}{2} & 0 & -\frac{1}{4} \\ \frac{1}{4} & -\frac{1}{2} & 0 & \frac{1}{2} & -\frac{1}{4} \\ -\frac{1}{4} & -1 & -\frac{3}{2} & -1 & -\frac{1}{4} \end{pmatrix}. \tag{2.31}$$

It is remarkable that both matrices turn out to be purely numerical! Just like the original matrices C_{st} and C_{su}, the matrices $\widetilde{C}_{st}$ and $\widetilde{C}_{su}$ are also involutory, *i.e* $\widetilde{C}^2_{st} = 1$ and $\widetilde{C}^2_{su} = 1$. This follows from the definitions (2.29), (2.30) and the condition (2.14). Note that similar to (2.15) we can compute the tu crossing matrix $\widetilde{C}_{tu} = \widetilde{C}_{st}\widetilde{C}_{su}\widetilde{C}_{st}$, it reads as

$$\widetilde{C}_{tu} = \begin{pmatrix} 1 & 0 & 0 & 0 & 0 \\ 0 & -1 & 0 & 0 & 0 \\ 0 & 0 & -1 & 0 & 0 \\ 0 & 0 & 0 & 1 & 0 \\ 0 & 0 & 0 & 0 & 1 \end{pmatrix}. \tag{2.32}$$

It says that the improved amplitudes defined via (2.24) are all eigenfunctions of tu crossing.

The overall sign of the crossing matrices (2.31) depends on the choice of phases in (2.13). The choice made in (2.13) is the only correct one. In order to see that we can take the Fermi lagrangian and compute the scattering of Majorana fermions to the leading order. We do it in appendix A.6.1, the final result for the improved amplitudes is given in (A.346). It automatically satisfies the crossing equations (2.27) and (2.28). Any other choice of phases (2.13) leads to crossing equations which are inconsistent with the perturbative computation of appendix A.6.1. This phase choice is independent of any particular model and holds non-perturbatively.

2.2 Unitarity

The general strategy for imposing unitarity constraints on scattering amplitudes was provided in section 1.6. Here we apply that strategy to the case of Majorana fermions. According to section 1.6 one needs to consider all possible states transforming in the irreducible representations which appear in the decomposition of the two particle state formed from two (identical) Majorana particles. These are

$$|c,\vec{p},\ell,\lambda;\lambda_1,\lambda_2\rangle_{id}, \tag{2.33}$$

where $\lambda_i = \pm\frac{1}{2}$. Since the particles are identical we can further restrict our attention to the states with $\lambda_1 \geq \lambda_2$. As a result we are left with only three states of the form

$$|c,\vec{p},\ell,\lambda;+,+\rangle_{id}, \qquad |c,\vec{p},\ell,\lambda;-,-\rangle_{id}, \qquad |c,\vec{p},\ell,\lambda;+,-\rangle_{id}. \tag{2.34}$$

We further notice that due to (1.38), the first two states in (2.34) exist only for even spins ℓ, whereas the last state in (2.34) exists for both even and odd spins ℓ. Using (A.145) we can form the following three parity eigenstates out of the states (2.34)

$$|1\rangle \equiv \frac{1}{\sqrt{2}}\left(|c,\vec{p},\ell,\lambda;+,+\rangle_{id} + |c,\vec{p},\ell,\lambda;-,-\rangle_{id}\right), \quad \ell \geq 0 \quad (\ell \text{ even}), \tag{2.35}$$

$$|2\rangle \equiv \frac{1}{\sqrt{2}}\left(|c,\vec{p},\ell,\lambda;+,+\rangle_{id} - |c,\vec{p},\ell,\lambda;-,-\rangle_{id}\right), \quad \ell \geq 0 \quad (\ell \text{ even}), \tag{2.36}$$

$$|3\rangle \equiv \sqrt{2}\,|c,\vec{p},\ell,\lambda;+,-\rangle_{id}, \quad \ell \geq 1. \tag{2.37}$$

The state $|1\rangle$ is parity odd while the states $|2\rangle$ and $|3\rangle$ are parity even. The states (2.35) - (2.37) can either be *in* or *out* asymptotic states. We now form all possible inner products between such states taking into account that parity eigenstates do not mix since we assumed parity invariance. The states (2.35) lead to

$$\ell \geq 0 \ \text{ (even)}: \qquad \mathcal{H}_\ell^-(s) \times \delta_{\ell\ell'}\delta_{\lambda\lambda'}(2\pi)^4\delta^{(4)}(p-p') \equiv \begin{pmatrix} {}_{in}\langle 1'|1\rangle_{in} & {}_{in}\langle 1'|1\rangle_{out} \\ {}_{out}\langle 1'|1\rangle_{in} & {}_{out}\langle 1'|1\rangle_{out} \end{pmatrix}, \tag{2.38}$$

where the primed states have the labels c', $\vec{p}\,'$, ℓ' and λ'. Analogously the states (2.36) for $\ell = 0$ and the states (2.37) for odd $\ell \geq 1$ lead to

$$\ell = 0: \qquad \mathcal{H}_\ell^+(s) \times \delta_{\ell\ell'}\delta_{\lambda\lambda'}(2\pi)^4\delta^{(4)}(p-p') \equiv \begin{pmatrix} {}_{in}\langle 2'|2\rangle_{in} & {}_{in}\langle 2'|2\rangle_{out} \\ {}_{out}\langle 2'|2\rangle_{in} & {}_{out}\langle 2'|2\rangle_{out} \end{pmatrix}, \tag{2.39}$$

$$\ell \geq 1 \ \text{ (odd)}: \qquad \mathcal{H}_\ell^+(s) \times \delta_{\ell\ell'}\delta_{\lambda\lambda'}(2\pi)^4\delta^{(4)}(p-p') \equiv \begin{pmatrix} {}_{in}\langle 3'|3\rangle_{in} & {}_{in}\langle 3'|3\rangle_{out} \\ {}_{out}\langle 3'|3\rangle_{in} & {}_{out}\langle 3'|3\rangle_{out} \end{pmatrix}. \tag{2.40}$$

Finally for even $\ell \geq 2$, the states (2.36) and (2.37) can mix. They lead to

$$H^{+}_{\ell\geq 2}(s) \times \delta_{\ell\ell'}\delta_{\lambda\lambda'}(2\pi)^4\delta^{(4)}(p-p') \equiv \begin{pmatrix} {}_{in}\langle 2'|2\rangle_{in} & {}_{in}\langle 2'|3\rangle_{in} & {}_{in}\langle 2'|2\rangle_{out} & {}_{in}\langle 2'|3\rangle_{out} \\ {}_{in}\langle 3'|2\rangle_{in} & {}_{in}\langle 3'|3\rangle_{in} & {}_{in}\langle 3'|2\rangle_{out} & {}_{in}\langle 3'|3\rangle_{out} \\ {}_{out}\langle 2'|2\rangle_{in} & {}_{out}\langle 2'|3\rangle_{in} & {}_{out}\langle 2'|2\rangle_{out} & {}_{out}\langle 2'|3\rangle_{out} \\ {}_{out}\langle 3'|2\rangle_{in} & {}_{out}\langle 3'|3\rangle_{in} & {}_{out}\langle 3'|2\rangle_{out} & {}_{out}\langle 3'|3\rangle_{out} \end{pmatrix}. \tag{2.41}$$

Let us explicitly write the components of these matrices. The inner product of only *in* or *out* states are fixed by our normalization conventions, which read

$${}_{in}\langle a'|b\rangle_{in} = {}_{out}\langle a'|b\rangle_{out} = \delta_{ab} \times \delta_{\ell\ell'}\delta_{\lambda\lambda'}(2\pi)^4\delta^{(4)}(p-p'). \tag{2.42}$$

The inner products between *in* and *out* states lead to partial amplitudes, we have

$$\begin{aligned} {}_{out}\langle 1'|1\rangle_{in} &= \delta_{\ell\ell'}\delta_{\lambda\lambda'}(2\pi)^4\delta^{(4)}(p-p') \times \left(1 + i\,\left(T^{++}_{\ell++}(s) + T^{--}_{\ell++}(s)\right)\right), \\ {}_{out}\langle 2'|2\rangle_{in} &= \delta_{\ell\ell'}\delta_{\lambda\lambda'}(2\pi)^4\delta^{(4)}(p-p') \times \left(1 + i\,\left(T^{++}_{\ell++}(s) - T^{--}_{\ell++}(s)\right)\right), \\ {}_{out}\langle 3'|3\rangle_{in} &= \delta_{\ell\ell'}\delta_{\lambda\lambda'}(2\pi)^4\delta^{(4)}(p-p') \times \left(1 + 2i\,T^{+-}_{\ell+-}(s)\right), \\ {}_{out}\langle 3'|2\rangle_{in} &= \delta_{\ell\ell'}\delta_{\lambda\lambda'}(2\pi)^4\delta^{(4)}(p-p') \times \left(2i\,T^{+-}_{\ell++}(s)\right). \end{aligned} \tag{2.43}$$

The partial amplitudes entering these expressions are related to scattering amplitudes via (1.112). We recall the relation here for the reader's convenience

$$T^{\lambda_3,\lambda_4}_{\ell\,\lambda_1,\lambda_2}(s) = \frac{\sqrt{s-4m^2}}{32\pi\sqrt{s}} \times \int_0^\pi d\theta \sin\theta d^{(\ell)}_{\lambda_{12}\lambda_{34}}(\theta) T^{\lambda_3,\lambda_4}_{\lambda_1,\lambda_2}(s,t,u), \quad \lambda_{ij} \equiv \lambda_i - \lambda_j. \tag{2.44}$$

As discussed in section 1.6 unitarity requires that the matrices $\mathcal{H}^-_\ell(s)$ and $\mathcal{H}^+_\ell(s)$ should all be positive semi-definite for all $s \geq 4m^2$ and ℓ. In what follows we will write these conditions in the final form.

In (2.4) we denoted the five independent amplitudes by $\Phi_I(s,t,u)$. In accordance we define the five partial amplitudes as

$$\begin{aligned} \Phi^\ell_1(s) &\equiv T^{++}_{\ell++}(s), \\ \Phi^\ell_2(s) &\equiv T^{--}_{\ell++}(s), \\ \Phi^\ell_3(s) &\equiv T^{+-}_{\ell+-}(s), \\ \Phi^\ell_4(s) &\equiv T^{-+}_{\ell+-}(s), \\ \Phi^\ell_5(s) &\equiv T^{+-}_{\ell++}(s). \end{aligned} \tag{2.45}$$

Plugging (2.42) and (2.43) into (2.38) - (2.41) we can write the semi-definite positivity

conditions on the matrices $\mathcal{H}_\ell^-(s)$ and $\mathcal{H}_\ell^+(s)$ as

$$\ell \geq 0 \ \text{(even)}: \qquad \begin{pmatrix} 1 & 1 \\ 1 & 1 \end{pmatrix} + i \begin{pmatrix} 0 & -\Phi_1^{\ell *}(s) - \Phi_2^{\ell *}(s) \\ \Phi_1^\ell(s) + \Phi_2^\ell(s) & 0 \end{pmatrix} \succeq 0, \tag{2.46}$$

$$\ell = 0: \qquad \begin{pmatrix} 1 & 1 \\ 1 & 1 \end{pmatrix} + i \begin{pmatrix} 0 & -\Phi_1^{\ell *}(s) + \Phi_2^{\ell *}(s) \\ \Phi_1^\ell(s) - \Phi_2^\ell(s) & 0 \end{pmatrix} \succeq 0, \tag{2.47}$$

$$\ell \geq 1 \ \text{(odd)}: \qquad \begin{pmatrix} 1 & 1 \\ 1 & 1 \end{pmatrix} + 2i \begin{pmatrix} 0 & -\Phi_3^{\ell *}(s) \\ \Phi_3^\ell(s) & 0 \end{pmatrix} \succeq 0. \tag{2.48}$$

Finally, the matrix (2.41) leads to the following condition

$$\ell \geq 2 \ \text{(even)}: \qquad \begin{pmatrix} \mathbb{I}_{2\times 2} & \mathbb{S}_{2\times 2}^{\ell \dagger}(s) \\ \mathbb{S}_{2\times 2}^\ell(s) & \mathbb{I}_{2\times 2} \end{pmatrix} \succeq 0, \tag{2.49}$$

where we have defined

$$\mathbb{I}_{2\times 2} \equiv \begin{pmatrix} 1 & 0 \\ 0 & 1 \end{pmatrix}, \qquad \mathbb{S}_{2\times 2}^\ell(s) \equiv \begin{pmatrix} 1 & 0 \\ 0 & 1 \end{pmatrix} + i \begin{pmatrix} \Phi_1^\ell(s) - \Phi_2^\ell(s) & 2\Phi_5^{\ell *}(s) \\ 2\Phi_5^\ell(s) & 2\Phi_3^\ell(s) \end{pmatrix}. \tag{2.50}$$

It is interesting to note that the equations above do not contain the partial amplitude $\Phi_4^\ell(s)$ at all. This is because due to the $t-u$ crossing equations, see (2.16), one has

$$\Phi_4(s,t,u) = \Phi_3(s,u,t) \tag{2.51}$$

Using this inside (2.44) we get the following relation among the partial amplitudes[5]

$$\Phi_4^\ell(s) = (-1)^{\ell+1}\Phi_3^\ell(s). \tag{2.52}$$

2.3 Non-perturbative couplings

We can use the Majorana fermion scattering amplitude to define several non-perturbative coupling constants. These are useful parameters to describe the allowed space of QFTs.

Quartic coupling

We begin by considering the value of the amplitude at the crossing symmetric point

$$s = t = u = \frac{4m^2}{3}. \tag{2.53}$$

[5] In order to show this, we use (1.59) and change the integration variable in (2.44) as $\theta \to \pi - \theta$. Using the properties of the small Wigner d matrix we get then $T_{\ell\,+,-}^{-,+}(s) = (-1)^{\ell+1} T_{\ell\,+,-}^{+,-}(s)$.

At this point, the improved amplitudes H_I must be invariant under both the s-t (2.27) and the s-u (2.28) crossing equations

$$\begin{aligned} H_I\left(\frac{4m^2}{3},\frac{4m^2}{3},\frac{4m^2}{3}\right) &= \sum_{J=1}^{5}\tilde{C}_{st}^{IJ}H_J\left(\frac{4m^2}{3},\frac{4m^2}{3},\frac{4m^2}{3}\right), \\ H_I\left(\frac{4m^2}{3},\frac{4m^2}{3},\frac{4m^2}{3}\right) &= \sum_{J=1}^{5}\tilde{C}_{su}^{IJ}H_J\left(\frac{4m^2}{3},\frac{4m^2}{3},\frac{4m^2}{3}\right). \end{aligned} \tag{2.54}$$

The most general solution reads

$$\vec{H}(4m^2/3,4m^2/3,4m^2/3) = \frac{\lambda}{m^2}\times\begin{pmatrix}1\\0\\0\\1\\-1\end{pmatrix}, \tag{2.55}$$

where $\vec{H}$ represents the five amplitudes collectively and λ is some parameter. We refer to λ as the non-perturbative quartic coupling. By comparing (2.55) with the perturbative result (A.346) we see that λ can be identified with the coupling in front of the $(\overline{\Psi}\Psi)(\overline{\Psi}\Psi)$ interaction term in the Fermi theory.

Cubic (Yukawa) couplings

Suppose now that our theory is described not only by the Majorana asymptotic state but also by a scalar (spin zero) asymptotic state with mass M. We restrict our attention to the values of M in the range $(m,2m)$, where m is the mass of the Majorana asymptotic state. This ensures that the Majorana fermion is the lightest particle in the theory and that the scalar boson is stable.

From general principles we expect such a scalar asymptotic state to manifest itself as a simple pole in the improved scattering amplitudes of Majorana fermions. In full generality one can then write

$$\vec{H}_{bound}(s,t,u) = \begin{pmatrix}\frac{g_1^2}{s-M^2}\\ \frac{g_2^2}{s-M^2}\\ \frac{g_3^2}{s-M^2}\\ \frac{g_4^2}{s-M^2}\\ \frac{g_5^2}{s-M^2}\end{pmatrix} + \begin{pmatrix}\frac{g_1'^2}{t-M^2}\\ \frac{g_2'^2}{t-M^2}\\ \frac{g_3'^2}{t-M^2}\\ \frac{g_4'^2}{t-M^2}\\ \frac{g_5'^2}{t-M^2}\end{pmatrix} + \begin{pmatrix}\frac{g_1''^2}{u-M^2}\\ \frac{g_2''^2}{u-M^2}\\ \frac{g_3''^2}{u-M^2}\\ \frac{g_4''^2}{u-M^2}\\ \frac{g_5''^2}{u-M^2}\end{pmatrix} + \text{regular}, \tag{2.56}$$

where g_I, g_I' and g_I'' are 15 arbitrary parameters. In (2.56) we have written only the poles and omitted all the regular terms at $s,t,u=M^2$. Due to the crossing equations (2.27) and (2.28), the values of g_I' and g_I'' get fixed in terms of g_I. As a result we are left with 5

undetermined parameters g_I. We further require that the $s = M^2$ poles contribute only to the zero spin partial amplitudes. This enforces the fact that the particle generating the poles is a scalar. This leads to the following three additional constraints

$$g_2 = g_3 = g_4 = 0. \tag{2.57}$$

Thus we are left with only two parameters g_1 and g_5.

According to the discussion of section 2.2, more precisely due to the formulas (2.46) and (2.47) one can take combinations of components of partial amplitudes to form parity odd (-) and parity even (+) partial amplitudes which read as

$$\Phi^\ell_-(s) \equiv \Phi^\ell_1 + \Phi^\ell_2, \qquad \Phi^\ell_+(s) \equiv \Phi^\ell_1 - \Phi^\ell_2. \tag{2.58}$$

The $s = M^2$ poles with the parameter g_1 contribute only to the parity even partial amplitude $\Phi^{\ell=0}_+$. We thus interpret g_1 as the non-perturbative coupling describing the interaction between two Majorana particles and a scalar parity even particle. The corresponding pole structure of the amplitude reads as

$$\vec{H}_{scalar}(s,t,u) = \frac{1}{2}\, g^2 \times \vec{P}_{scalar}(s,t,u) + \text{regular}, \tag{2.59}$$

where $g \equiv g_1$ and we have defined

$$\vec{P}_{scalar}(s,t,u) \equiv \begin{pmatrix} -\frac{4}{s-M^2} + \frac{1}{t-M^2} + \frac{1}{u-M^2} \\ \frac{1}{t-M^2} - \frac{1}{u-M^2} \\ -\frac{1}{t-M^2} + \frac{1}{u-M^2} \\ -\frac{1}{t-M^2} - \frac{1}{u-M^2} \\ \frac{1}{t-M^2} + \frac{1}{u-M^2} \end{pmatrix} \tag{2.60}$$

The $s = M^2$ poles with the parameter g_5 instead contribute only to the parity odd partial amplitude $\Phi^{\ell=0}_-$. Thus, the second parameter g_5 describes non-perturbatively the interaction between two Majorana particles and a scalar parity odd (pseudoscalar) particle. The corresponding pole structure of the amplitude reads as

$$\vec{H}_{pseudoscalar}(s,t,u) = \frac{1}{2}\, \tilde{g}^2 \times \vec{P}_{pseudoscalar}(s,t,u) + \text{regular}, \tag{2.61}$$

where $\tilde{g} \equiv g_5$ and we have defined

$$\vec{P}_{pseudoscalar}(s,t,u) \equiv \begin{pmatrix} \frac{1}{t-M^2} + \frac{1}{u-M^2} \\ -\frac{1}{t-M^2} + \frac{1}{u-M^2} \\ -\frac{1}{t-M^2} + \frac{1}{u-M^2} \\ \frac{1}{t-M^2} + \frac{1}{u-M^2} \\ -\frac{4}{s-M^2} + \frac{1}{t-M^2} + \frac{1}{u-M^2} \end{pmatrix}. \tag{2.62}$$

The cubic couplings $g \equiv g_1$ and $\tilde{g} \equiv g_5$ can also be called the non-perturbative Yukawa coupling constants. We also remark that the masses M in (2.60) and (2.62) do not have to be the same.

In the discussion above we fixed the overall sign in (2.59) and (2.61) so that the residue at $s = M^2$ has the appropriate sign in the unitarity equations (2.46) and (2.47). Alternatively one can compare (2.59) and (2.61) to the perturbative results (A.350) and (A.354). This comparison not only fixes the correct signs but also shows that g and $\tilde{g}$ here can be identified with the couplings appearing in front of the $\varphi\overline{\Psi}\Psi$ and $\tilde{\varphi}\overline{\Psi}\gamma^5\Psi$ Yukawa interactions respectively in (A.347) and (A.351).

2.4 An alternative approach to crossing equations

We have so far carefully discussed the construction of crossing equations in the COM frame and explicitly showed it in the case of Majorana particle scattering. There is an alternative way of approaching this topic, namely using fully covariant language based on constructing tensor structures. This relies on the most general representation of a scattering amplitude given in (1.56).

In what follows we will construct tensor structures in the particular example of Majorana particle scattering and re-derive the crossing equations. We will describe a general procedure of constructing tensor structures for particles with spin in appendix A.8.

2.4.1 Tensor structures

As we know from the COM analysis, there are 5 independent amplitudes in the case of identical Majorana particles. As a result there will be 5 linearly independent tensor structures. A particular choice of these tensor structures was made in [55]. It reads

$$\mathbb{T}_{I\,\lambda_1,\lambda_2}^{\lambda_3,\lambda_4}(p_1,p_2,p_3,p_4) = -\frac{1}{2}\,[\bar{u}_{\lambda_4}(p_4)\mathcal{O}_I v_{\lambda_3}(p_3)]\cdot[\bar{v}_{\lambda_2}(p_2)\mathcal{O}_I u_{\lambda_1}(p_1)], \tag{2.63}$$

where the five 4×4 matrices $\mathcal{O}_I$ are given by

$$\mathcal{O}_1 \equiv 1_{4\times 4}, \quad \mathcal{O}_2 \equiv \gamma^\mu, \quad \mathcal{O}_3 \equiv \sqrt{2}\,\sigma^{\mu\nu}, \quad \mathcal{O}_4 \equiv i\,\gamma^5\gamma^\mu, \quad \mathcal{O}_5 \equiv \gamma^5. \tag{2.64}$$

The symbol "$\cdot$" in (2.63) means contraction of all the Lorentz indices among $\mathcal{O}_I$ matrices. Notice also that there is no summation over the repeated index I in (2.63). For the

readers convenience we also write (2.63) explicitly

$$\begin{aligned}
\mathbb{T}_1{}^{\lambda_3,\lambda_4}_{\lambda_1,\lambda_2}(p_1,p_2,p_3,p_4) &= -\frac{1}{2}[\bar{u}_{\lambda_4}(p_4)v_{\lambda_3}(p_3)][\bar{v}_{\lambda_2}(p_2)u_{\lambda_1}(p_1)],\\
\mathbb{T}_2{}^{\lambda_3,\lambda_4}_{\lambda_1,\lambda_2}(p_1,p_2,p_3,p_4) &= -\frac{1}{2}[\bar{u}_{\lambda_4}(p_4)\gamma_\mu v_{\lambda_3}(p_3)][\bar{v}_{\lambda_2}(p_2)\gamma^\mu u_{\lambda_1}(p_1)],\\
\mathbb{T}_3{}^{\lambda_3,\lambda_4}_{\lambda_1,\lambda_2}(p_1,p_2,p_3,p_4) &= -[\bar{u}_{\lambda_4}(p_4)\sigma_{\mu\nu} v_{\lambda_3}(p_3)][\bar{v}_{\lambda_2}(p_2)\sigma^{\mu\nu}u_{\lambda_1}(p_1)],\\
\mathbb{T}_4{}^{\lambda_3,\lambda_4}_{\lambda_1,\lambda_2}(p_1,p_2,p_3,p_4) &= +\frac{1}{2}[\bar{u}_{\lambda_4}(p_4)\gamma_5\gamma_\mu v_{\lambda_3}(p_3)][\bar{v}_{\lambda_2}(p_2)\gamma_5\gamma^\mu u_{\lambda_1}(p_1)],\\
\mathbb{T}_5{}^{\lambda_3,\lambda_4}_{\lambda_1,\lambda_2}(p_1,p_2,p_3,p_4) &= -\frac{1}{2}[\bar{u}_{\lambda_4}(p_4)\gamma_5 v_{\lambda_3}(p_3)][\bar{v}_{\lambda_2}(p_2)\gamma_5 u_{\lambda_1}(p_1)].
\end{aligned} \tag{2.65}$$

The objects $u_\lambda(p)$ and $v_\lambda(p)$ are the usual 4-spinor solutions to the Dirac equation and

$$\bar{u}_\lambda(p) \equiv u^\dagger_\lambda(p)\gamma^0, \quad \bar{v}_\lambda(p) \equiv v^\dagger_\lambda(p)\gamma^0. \tag{2.66}$$

We use the Weyl (also known as chiral) basis for the Dirac γ^μ matrices given in (A.102) and the helicity basis of states. With these conventions the spinor solutions to the Dirac equation read

$$\begin{aligned}
u_{\frac{1}{2}}(p) &= \frac{1}{\sqrt{2}}\begin{pmatrix} \sqrt{p^0-\boldsymbol{p}}\cos\frac{\theta}{2} & \\ \sqrt{p^0-\boldsymbol{p}}\sin\frac{\theta}{2} & e^{+i\phi} \\ \sqrt{p^0+\boldsymbol{p}}\cos\frac{\theta}{2} & \\ \sqrt{p^0+\boldsymbol{p}}\sin\frac{\theta}{2} & e^{+i\phi}\end{pmatrix},\ u_{-\frac{1}{2}}(p) = \frac{1}{\sqrt{2}}\begin{pmatrix} -\sqrt{p^0+\boldsymbol{p}}\sin\frac{\theta}{2} & e^{-i\phi} \\ \sqrt{p^0+\boldsymbol{p}}\cos\frac{\theta}{2} & \\ -\sqrt{p^0-\boldsymbol{p}}\sin\frac{\theta}{2} & e^{-i\phi} \\ \sqrt{p^0-\boldsymbol{p}}\cos\frac{\theta}{2} & \end{pmatrix},\\
v_{\frac{1}{2}}(p) &= \frac{1}{\sqrt{2}}\begin{pmatrix} -\sqrt{p^0+\boldsymbol{p}}\sin\frac{\theta}{2} & e^{-i\phi} \\ \sqrt{p^0+\boldsymbol{p}}\cos\frac{\theta}{2} & \\ \sqrt{p^0-\boldsymbol{p}}\sin\frac{\theta}{2} & e^{-i\phi} \\ -\sqrt{p^0-\boldsymbol{p}}\cos\frac{\theta}{2} & \end{pmatrix},\ v_{-\frac{1}{2}}(p) = \frac{1}{\sqrt{2}}\begin{pmatrix} -\sqrt{p^0-\boldsymbol{p}}\cos\frac{\theta}{2} & \\ -\sqrt{p^0-\boldsymbol{p}}\sin\frac{\theta}{2} & e^{+i\phi} \\ \sqrt{p^0+\boldsymbol{p}}\cos\frac{\theta}{2} & \\ \sqrt{p^0+\boldsymbol{p}}\sin\frac{\theta}{2} & e^{+i\phi}\end{pmatrix}.
\end{aligned} \tag{2.67}$$

We notice that the objects $u_\lambda(p)$ and $\bar{v}_\lambda(p)$ transform in the spin-1/2 representation, namely they get rotated by $D^{(1/2)}_{\lambda'\lambda}$, whereas the objects $v_\lambda(p)$ and $\bar{u}_\lambda(p)$ transform in the conjugate spin-1/2 representation, namely they get rotated by $D^{*(1/2)}_{\lambda'\lambda}$. The tensor structures (2.65) are constructed in such a way that all the Lorentz indices are contracted. They depend only on the helicity labels and thus transform only in the Little group induced representation.

The choice of tensor structures (2.65) is very convenient because of the following reason. Plugging (2.65) into (1.56) and evaluating the amplitudes in the COM frame we get

$$T^{\lambda_3,\lambda_4}_{\lambda_1,\lambda_2}(s,t,u) = \sum_{I=1}^{5} H_I(s,t,u)\mathbb{T}_I{}^{\lambda_3,\lambda_4}_{\lambda_1,\lambda_2}(p_1^{com},p_2^{com},p_3^{com},p_4^{com}). \tag{2.68}$$

In the left-hand side of (2.68) we get the 16 COM amplitudes. They are related by (2.2) and (2.3). The 5 independent amplitudes were chosen in (2.4) and given special names

$\Phi_I(s,t,u)$. For the five independent amplitudes $\Phi_I(s,t,u)$ the right-hand side of (2.68) simply becomes (2.24). In other words the functions $H_I(s,t,u)$ appearing in (2.68) are precisely the kinematic singularity free amplitudes found in section 2.1. This means that all the kinematic singularities and constraints are taken care of by the tensor structures! Having established this we can write (1.56) explicitly in the case of identical Majorana fermions. It reads

$$T^{\lambda_3,\lambda_4}_{\lambda_1,\lambda_2}(p_1,p_2,p_3,p_4) = \sum_{I=1}^{5} H_I(s,t,u)\ \mathbb{T}_I{}^{\lambda_3,\lambda_4}_{\lambda_1,\lambda_2}(p_1,p_2,p_3,p_4), \tag{2.69}$$

where the basis of tensor structures is given by (2.65) and the functions $H_I(s,t,u)$ in this basis are precisely the improved amplitudes defined in section 2.1.

2.4.2 Verification of crossing matrices

In this section we will re-derive the crossing equations (2.27) and (2.28).

The amplitude (2.69) is defined for $p_i^0 \geq 0$ $(i = 1,2,3,4)$ as usual. It can however be analytically continued to $p_i^0 < 0$ domain. There are several options for such an analytic continuation. Throughout this paper we use option (A.256). Let us now analytically continue both sides of (2.69) in p_2 and p_3 to their negative values, we obtain

$$T^{\lambda_3,\lambda_4}_{\lambda_1,\lambda_2}(p_1,-p_2,-p_3,p_4) = \sum_{I=1}^{5} H_I(s,t,u)\ \mathbb{T}_I{}^{\lambda_3,\lambda_4}_{\lambda_1,\lambda_2}(p_1,-p_2,-p_3,p_4), \tag{2.70}$$

Exchanging the role of labels 2 and 3 we get then

$$T^{\lambda_2,\lambda_1}_{\lambda_1,\lambda_3}(p_1,-p_3,-p_2,p_4) = \sum_{I=1}^{5} H_I(t,s,u)\ \mathbb{T}_I{}^{\lambda_2,\lambda_4}_{\lambda_1,\lambda_3}(p_1,-p_3,-p_2,p_4). \tag{2.71}$$

Plugging (2.69) and (2.71) into the crossing equation (1.71) taken with the positive sign for fermions, see (A.295) for details, one gets

$$\sum_{I=1}^{5} H_I(s,t,u)\ \mathbb{T}_I{}^{\lambda_3,\lambda_4}_{\lambda_1,\lambda_2}(p_1,p_2,p_3,p_4) = \sum_{I=1}^{5} H_I(t,s,u)\ \mathbb{T}_I{}^{-\lambda_2,+\lambda_4}_{+\lambda_1,-\lambda_3}(p_1,-p_3,-p_2,p_4). \tag{2.72}$$

The analytic continuations of u and v objects are given in (A.293). Using these and the explicit form of tensor structures (2.63) one gets

$$\begin{aligned}
\mathbb{T}_I{}^{-\lambda_2,+\lambda_4}_{+\lambda_1,-\lambda_3}(p_1,-p_3,-p_2,p_4) &= [\bar{u}_{\lambda_4}(p_4)\mathcal{O}_I v_{-\lambda_2}(-p_2)]\cdot[\bar{v}_{-\lambda_3}(-p_3)\mathcal{O}_I u_{\lambda_1}(p_1)] \\
&= -\,[\bar{u}_{\lambda_4}(p_4)\mathcal{O}_I u_{\lambda_2}(p_2)]\cdot[\bar{u}_{\lambda_3}(p_3)\mathcal{O}_I u_{\lambda_1}(p_1)] \\
&= \sum_{I=1}^{5} \widetilde{C}^{st}_{IJ}\mathbb{T}_I{}^{\lambda_3,\lambda_4}_{\lambda_1,\lambda_2}(p_1,p_2,p_3,p_4),
\end{aligned} \tag{2.73}$$

where the matrix $\widetilde{C}^{st}_{IJ}$ is precisely the crossing matrix (2.31). In the third line of (2.73) we have used the Fierz identities, see for example [56]. Plugging (2.73) into (2.72) and using the fact that the structures (2.63) form a basis, we obtain the final crossing equations

$$H_I(s,t,u) = \sum_{J=1}^{5} \widetilde{C}^{st}_{IJ} H_J(t,s,u), \tag{2.74}$$

which coincide with (2.27). Using identical arguments one can obtain the $s-u$ crossing equations (2.28).

At first glance, it might seem that the way of deriving crossing equations using tensor structures is much simpler than the COM frame approach. This is not necessarily the case especially if one works with higher spin particles. The main issue here is the construction of a linearly independent basis of tensor structures. In practice there are many different looking tensor structures one can write. They are however related via a complicated set of Fierz-like identities. Luckily in the case of identical Majorana particles the problem was already thoroughly studied and the set of linearly independent tensor structures (2.65) was well known.

Once the linearly independent basis of structures is chosen the troubles are unfortunately not over. In the process of deriving the crossing equations all allowed tensor structures reappear and they need to be expressed back in terms of the chosen basis of structures via the Fierz-like identities. In the case of identical Majorana fermions this is precisely the step done in the last line of (2.73) which can be quite tedious for the general spin case.

2.5 Numerics

In this section we numerically estimate non-perturbative bounds on quantum field theories where the scattering of Majorana particles can be defined.

In sections 2.1 and 2.2 we carefully derived the crossing equations and the unitarity constraints which any scattering amplitude of Majorana particles must satisfy. Our precise goal here is to derive various bounds on the non-perturbative coupling constants that we defined in section 2.3. In section 2.5.1 we explain the numerical setup which allows for this. We present the numerical results in sections 2.5.2 and 2.5.3.

2.5.1 Setup

We use the numerical approach of [4]. The first step of this approach is to write the most general ansatz for the scattering amplitude. Before addressing Majorana fermions let us quickly recap the scalar case. The non-trivial part of the scattering of identical scalars with mass m is described by a function of three Mandelstam variables $T(s,t,u)$. To proceed it is crucial to assume maximal analyticity, namely that the amplitude is an analytic function of s, t and u complex variables independently modulo the standard branch cuts at

$$s \in [4m^2, +\infty], \qquad t \in [4m^2, +\infty], \qquad u \in [4m^2, +\infty], \tag{2.75}$$

where m is the mass of the scalar particle. Given a z complex plane, to mimic the above situation, one can define a function which is analytic in the whole complex plane modulo $z \in [4m^2, +\infty]$ branch cut. We choose[6]

$$\mathfrak{r}(z; z_0) \equiv \frac{\sqrt{4m^2 - z_0} - \sqrt{4m^2 - z}}{\sqrt{4m^2 - z_0} + \sqrt{4m^2 - z}}. \tag{2.76}$$

Here $z_0 < 4m^2$ is a free parameter which can be chosen at our will. We can then represent the interacting part of the scalar amplitude as a simple power series in terms of the functions (2.76) in the following way

$$T(s,t,u) = \sum_{a=0}^{\infty} \sum_{b=0}^{\infty} \sum_{c=0}^{\infty} \alpha_{abc}\, \mathfrak{r}(s, s_0)^a \mathfrak{r}(t, t_0)^b \mathfrak{r}(u, u_0)^c, \tag{2.77}$$

where α_{abc} are some real parameters. The ansatz (2.77) has a lot of redundancies due to the condition $s + t + u = 4m^2$. One can attempt to remove them in various ways. In this

[6] The physical domain is defined via $s + i\epsilon$ with $\epsilon > 0$. We can thus rotate the cuts using the identity

$$\sqrt{4m^2 - s} = -i\sqrt{s - 4m^2}.$$

paper we do it in a slightly drastic manner by imposing

$$\alpha_{abc} = 0 \qquad \text{if} \qquad abc \neq 0\,. \tag{2.78}$$

This choice is motivated by the Mandelstam representation [57], see appendix C in [4] for further details. It is convenient to choose the values of s_0, t_0 and u_0 to all be the crossing symmetric point

$$s_0 = t_0 = u_0 = \frac{4}{3}\,m^2. \tag{2.79}$$

The $s-t$ and $s-u$ crossing equations for the scalar amplitude are very simple. They read

$$T(s,t,u) = T(t,s,u) = T(u,t,s). \tag{2.80}$$

Plugging here the ansatz (2.77) we see that the coefficients α_{abc} must be fully symmetric under the permutation of indices a, b and c. The scalar amplitude $T(s,t,u)$ can also have poles when other particles exist in the theory or if the asymptotic state is allowed to have self-interactions. In this case one should extend the ansatz (2.77) to include such poles. We will see how it works in the case of Majorana fermions and skip further discussion of the scalar case.

In the case of Majorana fermions we defined five amplitudes $\vec{\Phi}$, where the vector denotes the five components Φ_1, Φ_2, Φ_3, Φ_4 and Φ_5 collectively. These amplitudes contain kinematic non-analyticities. In order to remove them in section 2.1 we introduced a new set of improved amplitudes denoted by $\vec{H}$. Again the vector here denotes the five components H_1, H_2, H_3, H_4 and H_5 collectively. We assume now that these five improved amplitudes are maximally analytic. Analogously to the scalar case, this allows us to write the following most general ansatz

$$\begin{aligned}\vec{H}(s,t,u) = \frac{1}{2}\,g^2 \times \vec{P}_{scalar}(s,t,u) + \frac{1}{2}\,\tilde{g}^2 \times \vec{P}_{pseudoscalar}(s,t,u)\\ + \sum_{a=0}^{\infty}\sum_{b=0}^{\infty}\sum_{c=0}^{\infty} \vec{\alpha}_{abc}\;\mathfrak{r}(s,s_0)^a \mathfrak{r}(t,t_0)^b \mathfrak{r}(u,u_0)^c,\end{aligned} \tag{2.81}$$

where $\vec{P}_{scalar}$ and $\vec{P}_{pseudoscalar}$ are the terms containing poles defined in (2.60) and (2.62) and $\vec{\alpha}_{abc}$ are some real parameters. In order to remove the redundancies in the ansatz (2.81) as in the scalar case we require

$$\vec{\alpha}_{abc} = 0 \qquad \text{if} \qquad abc \neq 0\,. \tag{2.82}$$

The ansatz (2.81) has an infinite number of terms. In order to work with it one has to introduce the following truncation

$$\sum_{a=0}^{\infty}\sum_{b=0}^{\infty}\sum_{c=0}^{\infty} \longrightarrow \sum_{a=0}^{a+}\sum_{b=0}^{b+c\,\leq N_{max}}\sum_{c=0}, \tag{2.83}$$

where N_{max} is some cut-off parameter. In practice its value is taken to be around 20.

We now require the ansatz (2.81) to satisfy the crossing equations (2.27) and (2.28). The pole terms have been already constructed to obey the crossing equations. However, for the parameters $\vec{\alpha}_{abc}$ we get a non-trivial system of linear algebraic equations with constant coefficients (independent of s, t and u variables). For a chosen N_{max} we solve this system with computer algebra and plug the solution into (2.81). As a result we get a fully crossing invariant expression. From now on when we refer to (2.81) we assume that the above procedure has been done and that (2.81) is fully crossing symmetric.

The second step is to compute the partial amplitudes. In order to do that we need to obtain the amplitudes $\vec{\Phi}(s,t,u)$ (containing all the kinematic non-analyticities) by plugging the ansatz (2.81) into (2.24). We then compute the partial amplitudes $\vec{\Phi}^{\ell}(s)$ using (2.44), see also (2.4) and (2.45). In doing this one needs to perform a set of integrals which have the following form

$$\int_0^{\pi} d\theta \sin\theta \, d_{ij}^{(\ell)}(\theta) \; \mathfrak{r}\Big(t(s,\theta),t_0\Big)^a \mathfrak{r}\Big(u(s,\theta),u_0\Big)^b \tag{2.84}$$

for the following set of indices in the d-matrix

$$(i,j) = \{(0,0),\,(1,1),\,(1,-1),\,(0,1)\}. \tag{2.85}$$

The integral (2.84) is hard to compute analytically. Hence, we perform the integration numerically for some tabulated values a, b, ℓ and s. We do it with Mathematica requiring between 20 and 30 digits of precision. The computed partial amplitudes can then be plugged into the unitarity constraints (2.46) - (2.49). These become a set of numerical semi-definite positivity conditions for different values of spin ℓ and s.

It is important to explain how we choose the values of ℓ and s. Let us start with the former. In principle one needs to consider unitarity conditions for all the spins up to $\ell = \infty$. However, realistically this is not possible and one needs to introduce another truncation, namely we impose unitarity only for a finite set of spins

$$\ell = 0, 1, 2, \ldots, L_{max}. \tag{2.86}$$

In the majority of computations we take the values of L_{max} to be as follows

$$L_{max} = N_{max} + 20. \tag{2.87}$$

In the next section we justify our choice by varying L_{max} and N_{max} separately. Let us address the choice of s values now. The unitarity constraints (2.46) - (2.49) are imposed in the region

$$s \in [4m^2, +\infty] \tag{2.88}$$

slightly above the branch cut. We take 300 different values of s in the region (2.88). One can spread these points differently, in practice we use the Chebyshev distribution.[7]

To summarize, we wrote the unitarity constraints in terms of the unknown real coefficients $\{g^2, \tilde{g}^2, \vec{\alpha}_{abc}\}$ originally appearing in the (crossing symmetric) ansatz (2.81). These conditions were written in a positive semi-definite form. We can now look for these coefficients numerically using semi-definite programming. For this we employ SDPB [43, 58].[8] In the following sections we define two different optimization problems and provide the numerical results. All the optimization problems we consider below use the following normalization

$$m = 1. \tag{2.90}$$

This simply means that all the dimensionful quantities are measured in terms of the mass of the Majorana asymptotic state.

A word about choosing various parameters of the setup such as the number of s values or the precision of the numerical approximation for the integrals (2.84). When performing the numerical analysis we made sure that our results do not depend on these parameters. This is simply done by performing the same computation with two different sets of parameters and confirming that the outcome is stable under such a change. The choice we made in this work guarantees at least two digits of precision in the final answer.

In order to obtain the numerical results presented below we consumed 0.4 million CPU Hours on the EPFL SCITAS cluster.

2.5.2 Quartic coupling

We now apply the strategy described in the previous section to bound the quartic coupling defined in (2.55) in the absence of poles

$$g = \tilde{g} = 0. \tag{2.91}$$

At the crossing symmetric point (2.79) the $\mathfrak{r}$ function vanishes and thus the ansatz (2.81) depends only on the five coefficients $\vec{\alpha}_{000}$. Crossing implies that only one of those coefficients is really independent. By comparing the ansatz at the crossing symmetric

[7] More precisely, we define a variable $\phi(s)$ by $\mathfrak{r}(s, s_0) = e^{i\phi(s)}$. Notice that $s \in [4m^2, +\infty]$ corresponds to $\phi \in [0, \pi]$. Then, we pick a grid $\phi_k = \frac{\pi}{2}\left[1 - \cos\frac{\pi(k-1/2)}{n}\right]$ with $n = 300$ and $k = 1, \ldots, n$.

[8] SDPB works only with real matrices. The unitarity conditions (2.46) - (2.49) are formulated in terms of the hermitian matrices. In order to recast those conditions into the form used by SDPB one needs to use the equivalence

$$H \succeq 0 \quad \Leftrightarrow \quad \begin{pmatrix} Re(H) & -Im(H) \\ Im(H) & Re(H) \end{pmatrix} \succeq 0, \tag{2.89}$$

where H is some hermitian matrix.

point with (2.55) we conclude that

$$\alpha^2_{000} = \alpha^3_{000} = 0, \qquad \alpha^1_{000} = \alpha^4_{000} = -\alpha^5_{000} = \lambda, \tag{2.92}$$

where λ is the non-perturbative quartic coupling.

Optimization problem: we search for the coefficients $\vec{\alpha}_{abc}$ such that the non-perturbative quartic coupling λ has the smallest/largest value and the unitarity constraints (2.46) - (2.49) are satisfied. By solving this problem numerically we conclude that the quartic coupling must be in the following interval

$$\frac{\lambda}{32\pi} \in [-3.25,\ +1.74]. \tag{2.93}$$

This is reasonably compatible with the expectation $\lambda \lesssim (4\pi)^2$ from *naive dimensional analysis* [59, 60].

Let us now discuss the details of this result. Among other parameters our numerical setup depends on N_{max}. In figures 2.1 and 2.2 we present the upper and lower bound on λ as a function of N_{max}^{-1}. The highest value we probe is $N_{max} = 24$. One can see that the bounds get weaker as we increase N_{max}. Intuitively this is easy to understand: upon increasing N_{max} the ansatz becomes more general and thus a larger/smaller coupling is attainable. We then perform an extrapolation of our results to $N_{max} = \infty$. The bound (2.93) already includes this extrapolation.

In making figures 2.1 and 2.2 we have used the spin cut-off value $L_{max} = N_{max} + 20$ as indicated in (2.87). Let us now relax that condition and see the dependence of the bounds also on L_{max}. In figures 2.3 and 2.4 we present the upper and lower bound on the quartic coupling λ as a function of L_{max}^{-1} for various values of N_{max}. We also perform a linear extrapolation to $L_{max} = \infty$.

When constructing figures 2.1 and 2.2 one could have used the points extrapolated to $L_{max} = \infty$ and only then perform the extrapolation to $N_{max} = \infty$. We have done this exercise and found the bound $[-3.34, +1.73]$ which is not too different from (2.93). The reader may use the difference between these results as an indicator of the precision with which we have estimated the optimal bounds for the quartic coupling λ.

2.5.3 Cubic Yukawa couplings

Let us now present the upper bound on the cubic (Yukawa) couplings. All the plots below are made using (2.87) spin cut-off value. One should in principle perform the extrapolation to $L_{max} = \infty$. However, as seen in the previous section, the difference is very small between the two procedures.

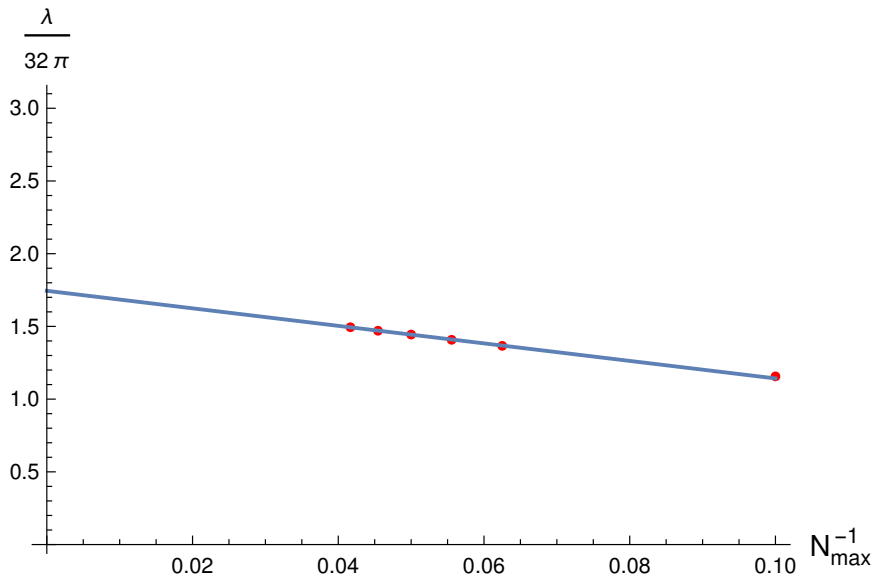

Figure 2.1: Upper bound on the quartic coupling λ as a function of N_{max}^{-1}. The numerical results are indicated by the red dots. They correspond to $N_{max} = 10$, 16, 18, 20, 22 and 24. The blue line represents the linear fit of the three points $N_{max} = 20$, 22 and 24. It is described by $\lambda/(32\pi) = 1.74 - 6.02\, N_{max}^{-1}$ equation. The spin cut-off parameter used here is $L_{max} = N_{max} + 20$.

We start with the situation where we have a scalar particle with mass M and no pseudoscalar particles. In other words $\tilde{g} = 0$. The bound on g as a function of M for various values of N_{max} is given in figure 2.5. As in the previous section the bound gets weaker when the value of N_{max} increases. For each M we perform a linear extrapolation to $N_{max} \to \infty$ analogously to the previous section. The final extrapolated bound is also shown in figure 2.5.

Now consider the case where there is a pseudoscalar particle in the theory and no scalar particle, namely $g = 0$. We can construct an upper bound on the $\tilde{g}$ coupling as a function of the pseudoscalar mass M. The result for different N_{max} is given in figure 2.6. In the figure we also present the extrapolated bound to $N_{max} \to \infty$. It is interesting to note that the bound gets stronger when we approach $M^2 = 4$ point. At $M^2 = 4$ we are forced to have $\tilde{g} = 0$. This situation is very different from figure 2.5. As a consistency check we compute in appendix A.7 an analytic expression for the upper bound in the vicinity of the threshold $M^2 = 4$. It is given by (A.376). In figure 2.6 it is indicated by the black solid line. We see that our numerical result is in agreement with the analytic one.

Similarly to the case of the quartic coupling λ, the order of magnitude of our bounds on Yukawa and pseudo-Yukawa couplings is compatible with the expectation $g \sim \tilde{g} \lesssim 4\pi$ from *naive dimensional analysis* [59, 60].

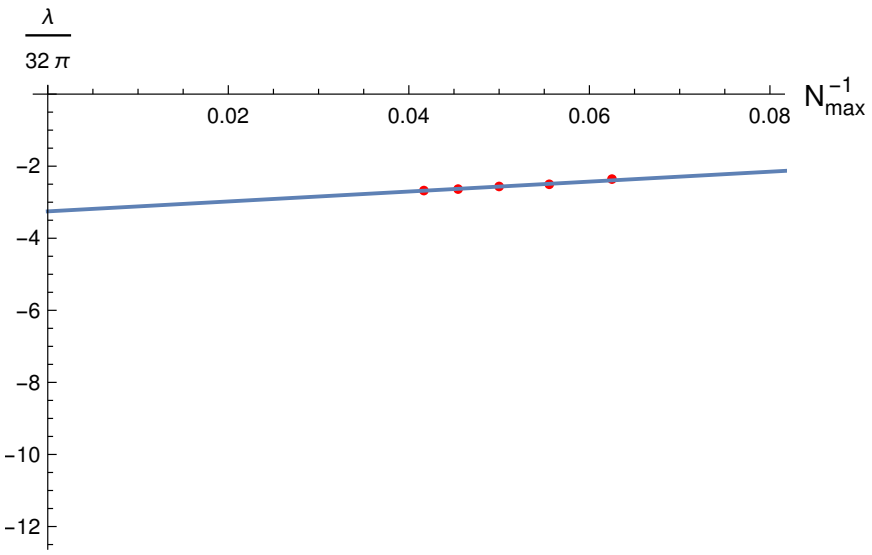

Figure 2.2: Lower bound on the quartic coupling λ as a function of N_{max}^{-1}. The numerical results are indicated by the red dots. They correspond to $N_{max} = 10$, 16, 18, 20, 22 and 24. The blue line represents the linear fit of the three points $N_{max} = 20$, 22 and 24. It is described by $\lambda/(32\pi) = -3.25 + 13.76\, N_{max}^{-1}$ equation. The spin cut-off parameter used here is $L_{max} = N_{max} + 20$.

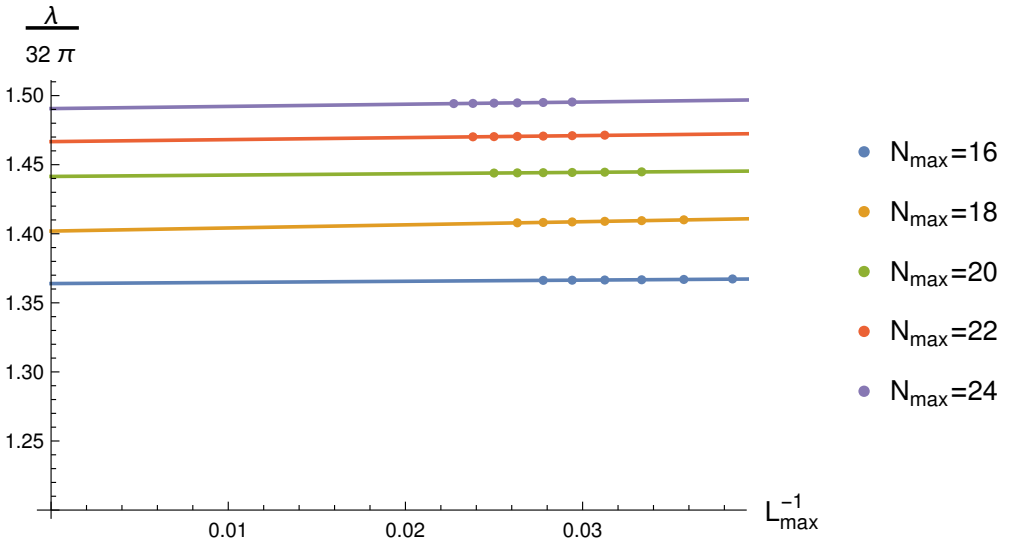

Figure 2.3: Upper bound on the quartic coupling λ as a function of L_{max}^{-1}. The dots represent the numerical results. The solid lines represent the linear extrapolation in L_{max}^{-1} based on the last four points for each N_{max}. Different colours correspond to different values of N_{max} indicated in the right-hand side of the plot.

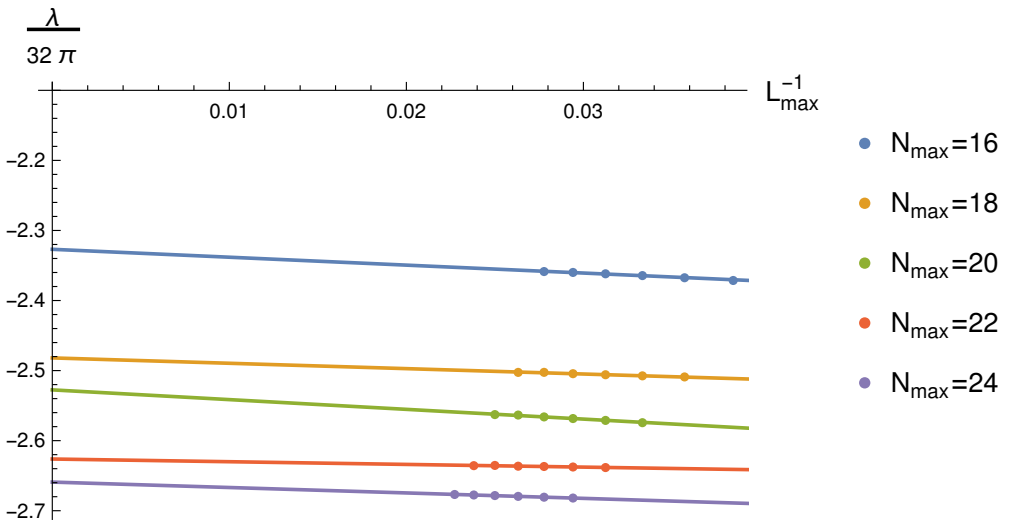

Figure 2.4: Lower bound on the quartic coupling λ as a function of L_{max}^{-1}. The dots represent the numerical results. The solid lines represent the linear extrapolation in L_{max}^{-1} based on the last four points for each N_{max}. Different colours correspond to different values of N_{max} indicated in the right-hand side of the plot.

2.6 Conclusion

We setup the formalism for the numerical S-matrix bootstrap approach to scattering amplitudes of spinning particles in 4d QFTs. We explained the general case and performed the numerical analysis for the particular case of 2 to 2 scattering of identical massive neutral spin $\frac{1}{2}$ fermions, *i.e.* Majorana fermions. In principle, our nonperturbative bound (2.93) on the quartic coupling applies to neutrinos but this is purely academic because neutrinos are very weakly coupled with $\lambda \sim G_F m_\nu^2 \lesssim 10^{-24}$. Goldstinos are massless Majorana fermions in QFTs with spontaneously broken supersymmetry and naturally light if there is also a small explicit breaking. Our bounds also apply to such pseudo Goldstinos.

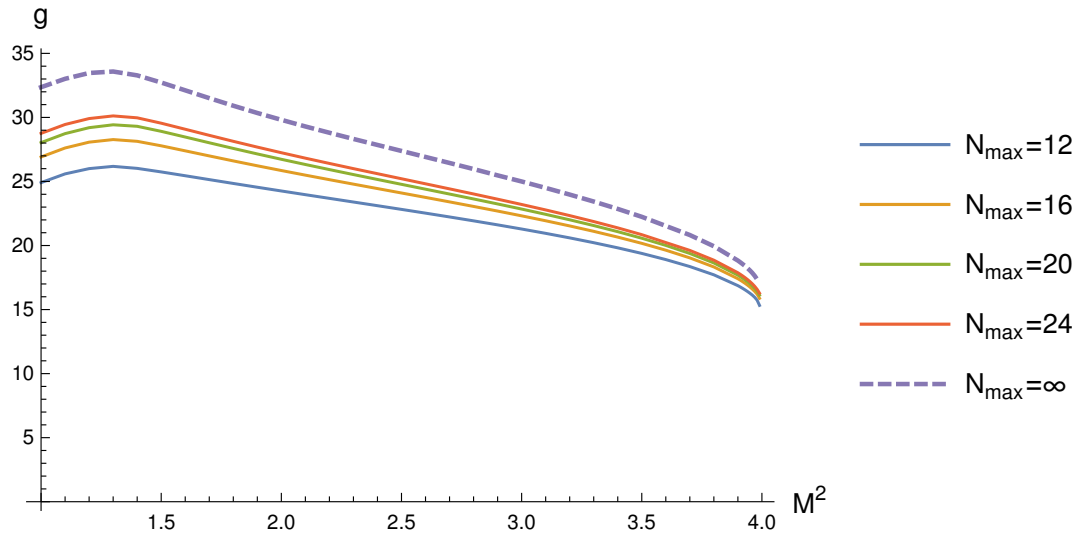

Figure 2.5: Upper bound on the cubic Yukawa coupling g as a function of the scalar particle mass M. The bound is constructed for $N_{max} = 12, 16, 20, 24$ and $L_{max} = N_{max} + 20$. Using $N_{max} = 20$ and $N_{max} = 24$ we also perform a linear extrapolation of the bound to $N_{max} = \infty$. The latter is indicated by the dashed line.

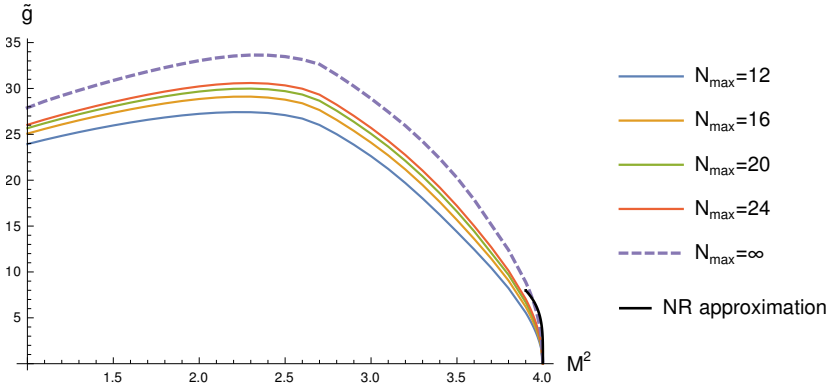

Figure 2.6: Upper bound on the cubic pseudo-Yukawa coupling $\tilde{g}$ as a function of the scalar particle mass M. The bound is constructed for $N_{max} = 12, 16, 20, 24$ and $L_{max} = N_{max} + 20$. Using $N_{max} = 20$ and $N_{max} = 24$ we also perform a linear extrapolation of the bound to $N_{max} = \infty$. The latter is indicated by the dashed line. The black line indicates an analytic prediction for the upper bound in the vicinity of $M^2 = 4$ computed in (A.376).

3 Application: Photons

In this chapter, we will consider photon-photon scattering. The photon is a massless spin 1 particle. The Little group for massless particles is $ISO(2)$.[1] The inhomogeneous part of this group is represented trivially in order to remove continuous degrees of freedom. As a result the Little group effectively becomes $SO(2) \simeq U(1)$ together with the requirement of the gauge invariance (to be defined shortly). Spin 1 massless particles are defined as the collection of $+1$ and -1 $U(1)$ representations (referred to as helicities of the particle). The formalism we developed in chapter 1 was for massive particles, however as we will see most of the formulae can adopted with only minor modifications.

We note that photons are derivatively coupled and therefore their scattering amplitudes do not have IR divergences. Another way to state this is that since they are derivatively coupled, they are free in the IR. In other words they are free at large separation which allows the definition of asymptotic states and the scattering amplitude. This is in contrast to other theories with massless particles where there is long-range interaction ($\sim \frac{1}{R}$).

Kinematics

We begin with one photon states, which we denote by

$$|\vec{p};\lambda\rangle \equiv |m=0,\vec{p};j=1,\lambda\rangle. \tag{3.1}$$

The right-hand side of (3.1) is the standard notation for one-particle states, where m is the mass of the particle, j is its spin, $\vec{p}$ is the spatial momentum and λ is the helicity. As explained above for massless spin $j=1$ particles helicity can only take two values

[1] The Little group is defined as the group of transformations leaving invariant the standard center of mass frame of a massless particle in momentum space which is $\bar{p}^\mu \equiv \{E,0,0,E\}$, where $E \geq 0$ is the energy. The symmetry leaving $\bar{p}^\mu$ invariant is $ISO(2)$. See for example section 2.5 in [17].

$\lambda = \pm 1$. The one photon states are normalized according to

$$\langle \vec{p}_1; \lambda_1 | \vec{p}_2; \lambda_2 \rangle = 2\boldsymbol{p}_1 \delta^{\lambda_2}_{\lambda_1} \times (2\pi)^3 \delta^{(3)}(\vec{p}_1 - \vec{p}_2). \tag{3.2}$$

It is now straightforward to define two photon states:

$$|\kappa_1, \kappa_2\rangle_{id} \equiv \frac{1}{\sqrt{2}} \Big(|\vec{p}_1; \lambda_1\rangle \otimes |\vec{p}_2; \lambda_2\rangle + |\vec{p}_2; \lambda_2\rangle \otimes |\vec{p}_1; \lambda_1\rangle \Big), \tag{3.3}$$

where the symbol $\otimes$ stands for the ordered tensor product. By construction it obeys the condition $|\kappa_1, \kappa_2\rangle_{id} = |\kappa_2, \kappa_1\rangle_{id}$. The $\sqrt{2}$ factor in the definition is part of our conventions.

The normalization of two-particle states follows from (3.3) and (3.2). It reads

$${}_{id}\langle \kappa_3, \kappa_4 | \kappa_1, \kappa_2 \rangle_{id} = 4\boldsymbol{p}_1 \boldsymbol{p}_2 (2\pi)^6 \left(\delta^{(3)}(\vec{p}_1 - \vec{p}_3) \delta^{(3)}(\vec{p}_2 - \vec{p}_4) \delta^{\lambda_3}_{\lambda_1} \delta^{\lambda_4}_{\lambda_2} + (3 \leftrightarrow 4) \right). \tag{3.4}$$

The scattering amplitude for the two to two scattering of photons is then given by

$$(2\pi)^4 \delta^{(4)}(p_1^\mu + p_2^\mu - p_3^\mu - p_4^\mu) \times \mathcal{S}^{\lambda_3, \lambda_4}_{\lambda_1, \lambda_2}(p_1, p_2, p_3, p_4) \equiv {}_{id}\langle \kappa_3, \kappa_4 | S | \kappa_1, \kappa_2 \rangle_{id}, \tag{3.5}$$

where S is the scattering operator.

As usual, we separate out the free propagation $\mathbb{I}$ and the interacting part $\mathbb{T}$ of the scattering operator

$$S = \mathbb{I} + i\mathbb{T}. \tag{3.6}$$

This leads to the definition of the interacting scattering amplitude

$$(2\pi)^4 \delta^{(4)}(p_1^\mu + p_2^\mu - p_3^\mu - p_4^\mu) \times \mathcal{T}^{\lambda_3, \lambda_4}_{\lambda_1, \lambda_2}(p_1, p_2, p_3, p_4) \equiv {}_{id}\langle \kappa_3, \kappa_4 | T | \kappa_1, \kappa_2 \rangle_{id}, \tag{3.7}$$

Using (3.6) we can write the explicit relation between the scattering amplitude and its interacting part. It reads

$$\mathcal{S}^{\lambda_3, \lambda_4}_{\lambda_1, \lambda_2}(p_1, p_2, p_3, p_4) = \frac{{}_{id}\langle \kappa_3, \kappa_4 | \kappa_1, \kappa_2 \rangle_{id}}{(2\pi)^4 \delta^{(4)}(p_1^\mu + p_2^\mu - p_3^\mu - p_4^\mu)} + i\mathcal{T}^{\lambda_3, \lambda_4}_{\lambda_1, \lambda_2}(p_1, p_2, p_3, p_4). \tag{3.8}$$

The first term in the right-hand side of (3.8) is a formal expression. It can be however straightforwardly evaluated in the center of mass frame in spherical coordinates.

3.1 Non-perturbative S-matrix setup

The goal of this section is to derive crossing equations and unitarity constraints for the scattering amplitude of identical spin one massless particles. In order to proceed it is important to define the center of mass scattering amplitudes. This is crucial for

addressing unitarity constraints. The crossing equations can be studied both in a general frame and in the center of mass frame. We will discuss both options for completeness.

The center of mass frame is defined by the following configuration of four-momenta

$$\begin{aligned} p_1^{\text{com}} &\equiv \frac{\sqrt{s}}{2} \times (1,0,0,+1), \\ p_2^{\text{com}} &\equiv \frac{\sqrt{s}}{2} \times (1,0,0,-1), \\ p_3^{\text{com}} &\equiv \frac{\sqrt{s}}{2} \times (1,+\sin\theta,0,+\cos\theta), \\ p_4^{\text{com}} &\equiv \frac{\sqrt{s}}{2} \times (1,-\sin\theta,0,-\cos\theta), \end{aligned} \tag{3.9}$$

where $\theta \in [0,\pi]$ is the scattering angle. It is related to the Mandelstam variables as

$$\sin\theta = \frac{2\sqrt{tu}}{s}, \quad \cos\theta = \frac{t-u}{s} \quad \Leftrightarrow \quad t = -\frac{s}{2}(1-\cos\theta), \quad u = -\frac{s}{2}(1+\cos\theta). \tag{3.10}$$

The center of mass amplitude is defined as

$$\mathcal{T}^{\lambda_3,\lambda_4}_{\lambda_1,\lambda_2}(s,t,u) \equiv \mathcal{T}^{\lambda_3,\lambda_4}_{\lambda_1,\lambda_2}(p_1^{\text{com}}, p_2^{\text{com}}, p_3^{\text{com}}, p_4^{\text{com}}). \tag{3.11}$$

Keep in mind the difference between the three distinct objects

$$\mathcal{T}^{\lambda_3,\lambda_4}_{\lambda_1,\lambda_2}(p_1,p_2,p_3,p_4), \qquad \mathcal{A}_I(s,t,u), \qquad \mathcal{T}^{\lambda_3,\lambda_4}_{\lambda_1,\lambda_2}(s,t,u). \tag{3.12}$$

Due to the presence of identical particles and parity, there are only 5 independent center of mass amplitudes, our choice here is

$$\begin{aligned} \Phi_1(s,t,u) &\equiv \mathcal{T}^{++}_{++}(s,t,u), \\ \Phi_2(s,t,u) &\equiv \mathcal{T}^{--}_{++}(s,t,u), \\ \Phi_3(s,t,u) &\equiv \mathcal{T}^{+-}_{+-}(s,t,u), \\ \Phi_4(s,t,u) &\equiv \mathcal{T}^{-+}_{+-}(s,t,u), \\ \Phi_5(s,t,u) &\equiv \mathcal{T}^{+-}_{++}(s,t,u). \end{aligned} \tag{3.13}$$

The rest of the center of mass amplitudes are related to the above 5 ones via 11 relations. Due to the presence of identical particles we get the following 9 constraints

$$\begin{aligned} &\mathcal{T}^{--}_{--} = \Phi_1, \quad \mathcal{T}^{+-}_{--} = \mathcal{T}^{-+}_{--}, \quad \mathcal{T}^{--}_{-+} = \Phi_5, \quad \mathcal{T}^{-+}_{-+} = \Phi_3, \quad \mathcal{T}^{+-}_{-+} = \Phi_4, \\ &\mathcal{T}^{++}_{-+} = \mathcal{T}^{-+}_{--}, \quad \mathcal{T}^{--}_{+-} = \Phi_5, \quad \mathcal{T}^{++}_{+-} = \mathcal{T}^{-+}_{--}, \quad \mathcal{T}^{-+}_{++} = \Phi_5. \end{aligned} \tag{3.14}$$

Due to the requirement of parity invariance we get in addition another two relations

which read

$$\mathcal{T}^{--++} = \Phi_5, \qquad \mathcal{T}^{++--} = \Phi_2. \tag{3.15}$$

Both (3.14) and (3.15) follow straightforwardly from equations (1.64), (1.84), (1.89) and (1.90).

Tensor structures

An alternative approach to using the centre of mass frame is to decompose the interacting scattering amplitude (1.47) via tensor structures as follows

$$\mathcal{T}^{\lambda_3,\lambda_4}_{\lambda_1,\lambda_2}(p_1,p_2,p_3,p_4) = \sum_{I=1}^{n} \mathcal{A}_I(s,t,u)\mathbf{T}_I{}^{\lambda_3,\lambda_4}_{\lambda_1,\lambda_2}(p_1,p_2,p_3,p_4). \tag{3.16}$$

Here the objects $\mathbf{T}_I$ take care of the correct Lorentz transformation properties. They are called tensor structures. Their form is completely fixed by the kinematics. There are n linearly independent tensor structures. The objects $\mathcal{A}_I(s,t,u)$ are referred to as the components of the interacting scattering amplitude. They are invariant under Lorentz transformations. As a result they depend only on the Mandelstam variables defined as

$$s \equiv -(p_1+p_2)^2, \quad t \equiv -(p_1-p_3)^2, \quad u \equiv -(p_1-p_4)^2, \quad s+t+u=0. \tag{3.17}$$

The physical range of the Mandelstam variables is

$$s \geq 0, \quad t \in [-s, 0], \quad u \in [-s, 0]. \tag{3.18}$$

Contrary to tensor structures the components of interacting amplitudes $\mathcal{A}_I(s,t,u)$ carry the dynamical information of the theory. Before we construct these tensor structures let us first define polarization vectors which transform under both Lorentz and little group transformations:

$$\epsilon^{\alpha}_{\lambda}(p) = \frac{e^{i\lambda\phi}}{\sqrt{2}} \begin{pmatrix} 0 \\ \cos\theta\cos\phi - i\lambda\sin\phi \\ \cos\theta\sin\phi + i\lambda\cos\phi \\ -\sin\theta \end{pmatrix} \tag{3.19}$$

Here $\alpha = 0,1,2,3$ is the Lorentz index and $\lambda = \pm 1$ is the $U(1)$ little group charge, also called helicity. The polarizations enjoy gauge symmetry which is the symmetry under the following transformations

$$\epsilon^{\alpha}_{\lambda}(p) \to \epsilon^{\alpha}_{\lambda}(p) + c\, p^{\alpha}, \tag{3.20}$$

called the gauge transformations. Here c is some real constant.[2] The tensor structures in (3.16) are Lorentz invariant but Little group covariant. They are thus built out of

[2]Gauge invariance is the reminiscence of the full $ISO(2)$ Little group. See section 5.9 of [17] for details.

4-momenta, polarizations and the Levi-Civita symbol, namely

$$p_i^\alpha, \quad \epsilon^\alpha_{\lambda_i}(p_i), \quad \varepsilon^{\alpha\beta\gamma\rho}. \tag{3.21}$$

The structures which contain the Levi-Civita symbol are parity odd and the structures which do not contain it are manifestly parity even. Due to the presence of gauge invariance all the tensor structure must be invariant under the gauge transformations (3.20). As a result the polarizations must only enter through the following basic gauge invariant building blocks

$$\begin{aligned} H^{\alpha\beta}_{\lambda_i} &\equiv p_i^\alpha\, \epsilon^\beta_{\lambda_i}(p_i) - p_i^\beta\, \epsilon^\alpha_{\lambda_i}(p_i), \\ H^{\lambda_i,\alpha\beta} &\equiv \left(H^{\alpha\beta}_{\lambda_i}\right)^*. \end{aligned} \tag{3.22}$$

Notice also that due to (3.19) the following property holds

$$H^{\lambda_i,\alpha\beta} = H^{\alpha\beta}_{-\lambda_i}. \tag{3.23}$$

The number of linearly independent tensor structure of generic massless particles is obviously $2^4 = 16$. When the particles are identical or when we impose parity the number of linearly independent structures decreases. In section 1.4, we showed that there are only 5 parity even amplitudes for the scattering of identical massless particles of spin $j = 1$. As a result there must be only

$$n = 5 \tag{3.24}$$

linearly independent tensor structures. In this paper we choose the following basis of 5 such tensor structures

$$\begin{aligned} \mathbf{T}_1{}^{\lambda_3,\lambda_4}_{\lambda_1,\lambda_2} &= \mathrm{tr}(H_{\lambda_1}H_{\lambda_2})\,\mathrm{tr}(H^{\lambda_3}H^{\lambda_4}), \\ \mathbf{T}_2{}^{\lambda_3,\lambda_4}_{\lambda_1,\lambda_2} &= \mathrm{tr}(H_{\lambda_1}H^{\lambda_3})\,\mathrm{tr}(H_{\lambda_2}H^{\lambda_4}), \\ \mathbf{T}_3{}^{\lambda_3,\lambda_4}_{\lambda_1,\lambda_2} &= \mathrm{tr}(H_{\lambda_1}H^{\lambda_4})\,\mathrm{tr}(H_{\lambda_2}H^{\lambda_3}), \\ \mathbf{T}_4{}^{\lambda_3,\lambda_4}_{\lambda_1,\lambda_2} &= \mathrm{tr}(H_{\lambda_1}H^{\lambda_3}H_{\lambda_2}H^{\lambda_4}), \\ \mathbf{T}_5{}^{\lambda_3,\lambda_4}_{\lambda_1,\lambda_2} &= -\left(p_2H_{\lambda_1}p_3\right)\ \mathrm{tr}\left(H_{\lambda_2}H^{\lambda_3}H^{\lambda_4}\right) + \left(p_1H_{\lambda_2}p_4\right)\ \mathrm{tr}\left(H_{\lambda_1}H^{\lambda_3}H^{\lambda_4}\right) \\ &\quad - \left(p_2H^{\lambda_4}p_3\right)\mathrm{tr}\left(H_{\lambda_1}H_{\lambda_2}H^{\lambda_3}\right) + \left(p_1H^{\lambda_3}p_4\right)\mathrm{tr}\left(H_{\lambda_1}H_{\lambda_2}H^{\lambda_4}\right). \end{aligned} \tag{3.25}$$

Here we used a short-hand notation for contraction of Lorentz indices. For instance

$$\begin{aligned} \mathrm{tr}(H_{\lambda_1}H_{\lambda_2}) &= H_{\lambda_1,\alpha\beta}H^{\beta\alpha}_{\lambda_2}, \\ \mathrm{tr}(H_{\lambda_1}H_{\lambda_2}H_{\lambda_3}H_{\lambda_4}) &= H_{\lambda_1,\alpha\beta}H^{\beta\gamma}_{\lambda_2}H_{\lambda_3,\gamma\rho}H^{\rho\alpha}_{\lambda_4}, \\ (p_2H_{\lambda_1}p_3) &= p_{2,\alpha}H^{\alpha\beta}_{\lambda_1}p_{3,\beta}. \end{aligned} \tag{3.26}$$

Identical definitions hold for any other configuration of helicities.

Evaluating (3.16) in the center of mass frame (3.9) and using the basis of tensor structures (3.25) one establishes the relation between two sets of amplitudes defined in (3.16) and (3.13). This relation reads

$$\Phi_I(s,t,u) = \sum_{J=1}^{5} M_{IJ}(s,t,u)\mathcal{A}_J(s,t,u), \tag{3.27}$$

where the matrix M reads as

$$M(s,t,u) = \begin{pmatrix} s^2 & 0 & 0 & \frac{s^2}{4} & 0 \\ s^2 & t^2 & u^2 & -\frac{tu}{2} & stu \\ 0 & 0 & u^2 & \frac{u^2}{4} & 0 \\ 0 & t^2 & 0 & \frac{t^2}{4} & 0 \\ 0 & 0 & 0 & 0 & \frac{stu}{4} \end{pmatrix}. \tag{3.28}$$

3.2 Crossing equations

The s-t and s-u crossing equations for the center of mass amplitudes in the case of massless $j = 1$ particles can be obtained up to an overall phase using the arguments of Trueman and Wick [47]. Their derivation was reviewed in chapter 1, see equations (1.81) and (1.82), and is presented in detail in A.5. Here we simply state the result which reads

$$\begin{aligned} \mathcal{T}^{\lambda_3,\lambda_4}_{\lambda_1,\lambda_2}(s,t,u) &= \chi_{st}\, \mathcal{T}^{+\lambda_2,-\lambda_4}_{-\lambda_1,+\lambda_3}(t,s,u), \\ \mathcal{T}^{\lambda_3,\lambda_4}_{\lambda_1,\lambda_2}(s,t,u) &= \chi_{su}\, \mathcal{T}^{-\lambda_3,+\lambda_2}_{-\lambda_1,+\lambda_4}(u,t,s), \end{aligned} \tag{3.29}$$

where the overall phases χ_{st} and χ_{su} remain undetermined. Using (3.13), (3.14) and (3.15) we can rewrite the crossing equations (3.29) in terms of the 5 independent amplitudes only. They read

$$\Phi_I(s,t,u) = \chi_{st} \sum_{J=1}^{5} C^{st}_{IJ}\Phi_J(t,s,u), \qquad \Phi_I(s,t,u) = \chi_{su} \sum_{J=1}^{5} C^{su}_{IJ}\Phi_J(u,t,s), \tag{3.30}$$

where the crossing matrices read

$$C^{st} \equiv \begin{pmatrix} 0 & 0 & 0 & 1 & 0 \\ 0 & 1 & 0 & 0 & 0 \\ 0 & 0 & 1 & 0 & 0 \\ 1 & 0 & 0 & 0 & 0 \\ 0 & 0 & 0 & 0 & 1 \end{pmatrix}, \qquad C^{su} \equiv \begin{pmatrix} 0 & 0 & 1 & 0 & 0 \\ 0 & 1 & 0 & 0 & 0 \\ 1 & 0 & 0 & 0 & 0 \\ 0 & 0 & 0 & 1 & 0 \\ 0 & 0 & 0 & 0 & 1 \end{pmatrix}. \tag{3.31}$$

Both matrices have the following eigenvalues $\{-1,1,1,1,1\}$. They cannot however be simultaneously diagonalized.

The easiest way to fix the unknown phases χ_{st} and χ_{su} in (3.30) is to plug the explicit expressions for the scattering amplitudes (3.81) computed for the photon scattering into the crossing equations (3.30). One then immediately concludes that

$$\chi_{st} = \chi_{su} = +1. \tag{3.32}$$

Even though this result is found in perturbation theory for a particular model, the conclusion (3.32) remains valid in the most general situation.

For completeness let us re-derive the crossing equations (3.30) together with (3.32) in a different way using tensor structures. We start by stating the crossing equations in a general frame which read

$$\begin{aligned}\mathcal{T}^{\lambda_3,\lambda_4}_{\lambda_1,\lambda_2}(p_1,p_2,p_3,p_4) &= \mathcal{T}^{-\lambda_2,+\lambda_4}_{+\lambda_1,-\lambda_3}(p_1,-p_3,-p_2,p_4),\\ \mathcal{T}^{\lambda_3,\lambda_4}_{\lambda_1,\lambda_2}(p_1,p_2,p_3,p_4) &= \mathcal{T}^{+\lambda_3,-\lambda_2}_{+\lambda_1,-\lambda_4}(p_1,-p_4,p_3,-p_2).\end{aligned} \tag{3.33}$$

They can be straightforwardly derived using the LSZ procedure, see appendix A.5.3. It is important to recall that the scattering amplitudes are defined for non-negative energies only, namely $p_i^0 \geq 0$ for every particle $i = 1,2,3,4$. The amplitudes in the right-hand side of (3.33) however explicitly contain negative energies and must be properly defined via the analytic continuation

$$p^\mu \to \text{complex values} \to -p^\mu \tag{3.34}$$

in the appropriate four-momenta. This procedure is ambiguous. We make a particular choice of the analytic continuation, which in spherical coordinates reads as[3]

$$p^0 \to -p^0, \quad \boldsymbol{p} \to -\boldsymbol{p}, \quad \theta \to \theta, \quad \phi \to \phi. \tag{3.36}$$

From the definitions (3.19) and (3.22) it also follows that

$$\epsilon^\alpha_\lambda(-p) = \epsilon^\alpha_\lambda(p), \qquad H^{\alpha\beta}_{\lambda_i}(-p) = -H^{\alpha\beta}_{\lambda_i}(p). \tag{3.37}$$

Let us now inspect the basis of tensor structures (3.25). Using the properties (3.23) and

[3]The other choice of the analytic continuations is

$$p^0 \to -p^0, \quad \boldsymbol{p} \to +\boldsymbol{p}, \quad \theta \to \pi - \theta, \quad \phi \to \pi + \phi. \tag{3.35}$$

Clearly both (3.35) and (3.36) lead to (3.34). For more details see appendix A.5.1.

(3.37) we can straightforwardly write the following relations

$$\begin{aligned}\mathbf{T}_{I\,+\lambda_1,-\lambda_3}^{\;-\lambda_2,+\lambda_4}(p_1,-p_3,-p_2,p_4) &= \sum_{J=1}^{5}\widetilde{C}_{IJ}^{st}(s,t,u)\,\mathbf{T}_{J\,\lambda_1,\lambda_2}^{\;\lambda_3,\lambda_4}(p_1,p_2,p_3,p_4),\\ \mathbf{T}_{I\,+\lambda_1,-\lambda_4}^{\;+\lambda_3,-\lambda_2}(p_1,-p_4,p_3,-p_2) &= \sum_{J=1}^{5}\widetilde{C}_{IJ}^{su}(s,t,u)\,\mathbf{T}_{J\,\lambda_1,\lambda_2}^{\;\lambda_3,\lambda_4}(p_1,p_2,p_3,p_4),\end{aligned} \tag{3.38}$$

where the matrices $\widetilde{C}^{st}$ and $\widetilde{C}^{su}$ read as

$$\widetilde{C}_{IJ}^{st}(s,t,u)=\begin{pmatrix}0&1&0&0&0\\1&0&0&0&0\\0&0&1&0&0\\\frac{s^2-t^2}{4s^2}&\frac{s^2-t^2}{4s^2}&\frac{s^2-t^2}{4s^2}&\frac{t^2}{s^2}&0\\0&0&0&0&1\end{pmatrix},\quad \widetilde{C}_{IJ}^{su}(s,t,u)=\begin{pmatrix}0&0&1&0&0\\0&1&0&0&0\\1&0&0&0&0\\\frac{s^2-u^2}{4s^2}&\frac{s^2-u^2}{4s^2}&\frac{s^2-u^2}{4s^2}&\frac{u^2}{s^2}&0\\0&0&0&0&1\end{pmatrix}. \tag{3.39}$$

Plugging the decomposition (3.16) into the crossing equations (3.33) and using the relations (3.38) we obtain

$$\mathcal{A}_I(s,t,u)=\sum_{J=1}^{5}\mathcal{A}_J(t,s,u)\,\widetilde{C}_{JI}^{st}(s,t,u),\qquad \mathcal{A}_I(s,t,u)=\sum_{J=1}^{5}\mathcal{A}_J(u,t,s)\,\widetilde{C}_{JI}^{su}(s,t,u). \tag{3.40}$$

Using (3.27) we can rewrite these equations in the form (3.30). The following consistency relations must hold then

$$\begin{aligned}\chi_{st}C^{st} &= M(s,t,u)(\widetilde{C}^{st}(s,t,u))^T(M(t,s,u))^{-1},\\ \chi_{su}C^{su} &= M(s,t,u)(\widetilde{C}^{su}(s,t,u))^T(M(u,t,s))^{-1}.\end{aligned} \tag{3.41}$$

Plugging here the explicit form of the matrices (3.28), (3.31), (3.39) and taking into account (3.32) we can explicitly verify the validity of (3.41).

The crossing equations (3.40) can be explicitly solved by introducing the three functions

$$f_1(s|t,u),\quad f_2(s|t,u),\quad f_3(s,t,u). \tag{3.42}$$

The first two functions are symmetric under the exchange of their last two arguments. Instead the last function is symmetric under any exchange of its arguments. One can

then show that the 5 amplitude components written as

$$\begin{aligned}
\mathcal{A}_1(s,t,u) &= f_1(s|t,u) + \frac{f_2(u|s,t)+f_2(t|s,u)}{4} - \frac{u^2 f_2(u|s,t)+t^2 f_2(t|s,u)}{4s^2},\\
\mathcal{A}_2(s,t,u) &= f_1(t|s,u) + \frac{f_2(u|s,t)+f_2(t|s,u)}{4} - \frac{u^2 f_2(u|s,t)+t^2 f_2(t|s,u)}{4s^2},\\
\mathcal{A}_3(s,t,u) &= f_1(u|s,t) + \frac{f_2(u|s,t)+f_2(t|s,u)}{4} - \frac{u^2 f_2(u|s,t)+t^2 f_2(t|s,u)}{4s^2},\\
\mathcal{A}_4(s,t,u) &= f_2(s|t,u) + \frac{u^2 f_2(u|s,t)+t^2 f_2(t|s,u)}{s^2},\\
\mathcal{A}_5(s,t,u) &= f_3(s,t,u)
\end{aligned} \tag{3.43}$$

automatically obey the crossing equations (3.40).

3.3 Unitarity

We now discuss the constraints on the amplitudes due to unitarity. This subsection is an application of the general construction presented in section 1.6, which the reader is referred to for more details. We begin by defining a short hand notation for two photon direct product states in the COM frame:

$$|(\boldsymbol{p},\theta,\phi);\lambda_1,\lambda_2\rangle_{id} \equiv \frac{1}{\sqrt{2}}(|\vec{p};\lambda_1\rangle\otimes|-\vec{p};\lambda_2\rangle + |-\vec{p};\lambda_2\rangle\otimes|\vec{p};\lambda_1\rangle) \tag{3.44}$$

where (θ,ϕ) are the angular coordinates of $\vec{p}$ and $\boldsymbol{p}=|\vec{p}|$. We now construct two photon Wigner irreps in the COM frame:

$$|c,\vec{0},\ell,\lambda;\lambda_1,\lambda_2\rangle_{id} = \frac{2\ell+1}{4\pi\sqrt{2}C_\ell}\int_0^{2\pi}d\phi\int_0^{\pi}d\theta\sin\theta e^{-i\phi(\lambda_1+\lambda_2-\lambda)}d^{\ell}_{\lambda,\lambda_{12}}(\theta)|(\boldsymbol{p},\theta,\phi);\lambda_1,\lambda_2\rangle_{id} \tag{3.45}$$

where $\lambda_{12}\equiv\lambda_1-\lambda_2$, $c=2\boldsymbol{p}$ is the COM frame energy and

$$C_\ell = \sqrt{8\pi(2\ell+1)} \tag{3.46}$$

Two photon Wigner irreps in a general frame are then defined by boosting them from the COM frame. The benefit of using these states is that physically these are two particle states with definite spin and therefore by conservation of angular momentum, scattering amplitudes are diagonal in this basis:

$${}_{id}\langle c',\vec{p}\,',\ell',\lambda';\lambda_3,\lambda_4|T|c,\vec{p},\ell,\lambda;\lambda_1,\lambda_2\rangle_{id} = (2\pi)^4\delta^4(p^\mu-p'^\mu)\delta_{\ell\ell'}\delta_{\lambda\lambda'}T_\ell{}^{\lambda_3,\lambda_4}_{\lambda_1,\lambda_2}(s) \tag{3.47}$$

The functions $T_\ell{}^{\lambda_3,\lambda_4}_{\lambda_1,\lambda_2}(s)$ are called partial wave amplitudes and are related to scattering amplitudes as follows

$$T_\ell{}^{\lambda_3,\lambda_4}_{\lambda_1,\lambda_2}(s) = \frac{1}{32\pi}\int_0^\pi d\theta \sin\theta\, d^\ell_{\lambda_{12},\lambda_{34}}(\theta) T^{\lambda_3,\lambda_4}_{\lambda_1,\lambda_2}\Big(s, t(s,\theta), u(s,\theta)\Big) \tag{3.48}$$

with $t(s,\theta)$ and $u(s,\theta)$ given as in (3.10).

For the case of two photons, there are three possible Wigner irreps. We list them using the notation $+$ for helicity $+1$ and $-$ for helicity -1 [4]

$$|c,\vec{p},\ell,\lambda;+,+\rangle_{id}, \quad |c,\vec{p},\ell,\lambda;-,-\rangle_{id}, \quad |c,\vec{p},\ell,\lambda;+,-\rangle_{id} \tag{3.49}$$

Bose symmetry of the photons also implies the selection rule that the first two states in the list above only exist for even ℓ. The third state exists for all spin $\ell \geq 2$ [5]. Under a Parity transformation, the three states transform as follows

$$\begin{aligned}
\mathcal{P}|c,\vec{0},\ell,\lambda;+,+\rangle_{id} &= (-1)^\ell |c,\vec{0},\ell,\lambda;-,-\rangle_{id} \\
\mathcal{P}|c,\vec{0},\ell,\lambda;-,-\rangle_{id} &= (-1)^\ell |c,\vec{0},\ell,\lambda;+,+\rangle_{id} \\
\mathcal{P}|c,\vec{0},\ell,\lambda;+,-\rangle_{id} &= |c,\vec{0},\ell,\lambda;+,-\rangle_{id}
\end{aligned} \tag{3.50}$$

Since we consider Parity invariant theories, it is convenient to define new linear combinations which are Parity eigenstates:

Parity even

$$\begin{aligned}
|1\rangle &= \frac{1}{\sqrt{2}}\Big(|c,\vec{p},\ell,\lambda;+,+\rangle_{id} + |c,\vec{p},\ell,\lambda;-,-\rangle_{id}\Big) \quad \ell \geq 0 \quad \text{and} \quad \ell \quad \text{even} \\
|2\rangle &= \sqrt{2}\,|c,\vec{p},\ell,\lambda;+,-\rangle_{id} \quad \forall \quad \ell \geq 2
\end{aligned} \tag{3.51}$$

Parity odd

$$|3\rangle = \frac{1}{\sqrt{2}}\Big(|c,\vec{p},\ell,\lambda;+,+\rangle_{id} - |c,\vec{p},\ell,\lambda;-,-\rangle_{id}\Big) \quad \ell \geq 0 \quad \text{and} \quad \ell \quad \text{even} \tag{3.52}$$

In a unitary quantum theory, the norm of any state in the theory must be non-negative.

[4] Note that $|c,\vec{p},\ell,\lambda;-,+\rangle_{id} = (-1)^\ell |c,\vec{p},\ell,\lambda;+,-\rangle_{id}$ by Bose symmetry.

[5] The total spin ℓ must always be greater than the difference in helicity $\lambda_1 - \lambda_2$ of the two particles

Consider the following set of six states:

$$\begin{aligned} &|1\rangle_{in} && |1\rangle_{out} \\ &|2\rangle_{in} && |2\rangle_{out} \\ &|3\rangle_{in} && |3\rangle_{out} \end{aligned} \tag{3.53}$$

Any linear combination of these states must have non-negative norm. This statement is equivalent to the statement that the 6×6 Hermitian matrix formed by the inner products between the six states is positive semi-definite. Factoring out the overall delta functions we write

$$\begin{pmatrix} {}_{in}\langle a'|b\rangle_{in} & {}_{in}\langle a'|b\rangle_{out} \\ {}_{out}\langle a'|b\rangle_{in} & {}_{out}\langle a'|b\rangle_{out} \end{pmatrix} = \mathcal{H}_\ell(s) \times (2\pi)^4 \delta^4(p^\mu - p'^\mu)\delta_{\ell\ell'}\delta_{\lambda\lambda'} \tag{3.54}$$

Unitarity as stated above then implies that

$$\mathcal{H}_\ell(s) \succeq 0 \quad \forall \quad \ell \quad \text{and} \quad s \geq 0. \tag{3.55}$$

The inner products between two incoming states or two outgoing states are fixed by the normalization of these states [6]

$${}_{in}\langle a'|b\rangle_{in} = {}_{out}\langle a'|b\rangle_{out} = \delta_{a'b} \times \delta_{\ell\ell'}\delta_{\lambda\lambda'}(2\pi)^4\delta^4(p^\mu - p'^\mu) \tag{3.56}$$

The inner products between incoming and outgoing states are, by definition, the matrix elements of the scattering operator $\mathcal{S} = 1 + i\mathcal{T}$ and therefore we have

$$\begin{aligned} {}_{out}\langle 1'|1\rangle_{in} &= \delta_{\ell\ell'}\delta_{\lambda\lambda'}(2\pi)^4\delta^4(p^\mu - p'^\mu)\left(1 + i\left(T_\ell{}^{+,+}_{+,+}(s) + T_\ell{}^{-,-}_{+,+}(s)\right)\right) \\ {}_{out}\langle 2'|2\rangle_{in} &= \delta_{\ell\ell'}\delta_{\lambda\lambda'}(2\pi)^4\delta^4(p^\mu - p'^\mu)\left(1 + 2i\, T_\ell{}^{+,-}_{+,-}(s)\right) \\ {}_{out}\langle 2'|1\rangle_{in} &= \delta_{\ell\ell'}\delta_{\lambda\lambda'}(2\pi)^4\delta^4(p^\mu - p'^\mu)\left(2i\, T_\ell{}^{+,-}_{+,+}(s)\right) \\ {}_{out}\langle 1'|2\rangle_{in} &= \delta_{\ell\ell'}\delta_{\lambda\lambda'}(2\pi)^4\delta^4(p^\mu - p'^\mu)\left(2i\, T_\ell{}^{+,-}_{+,+}(s)\right) \\ {}_{out}\langle 3'|3\rangle_{in} &= \delta_{\ell\ell'}\delta_{\lambda\lambda'}(2\pi)^4\delta^4(p^\mu - p'^\mu)\left(1 + i\left(T_\ell{}^{+,+}_{+,+}(s) - T_\ell{}^{-,-}_{+,+}(s)\right)\right) \end{aligned} \tag{3.57}$$

Due to invariance under Parity, there is no scattering between states with different parity eigenvalues. Hence the inner products ${}_{out}\langle 3'|1\rangle_{in}$ and ${}_{out}\langle 3'|2\rangle_{in}$ are 0. Therefore the positive semi-definite condition in (3.55) simplifies into smaller matrices. Taking into account the selection rules for the two photon Wigner irreps due to Bose symmetry, we have

[6] The pre-factors in (3.51) and (3.52) ensure that all three states have the same normalization

Parity even sector

We begin by considering parity even eigenstates (3.51). For even spin $\ell \geq 2$, we have

$$\mathcal{H}_\ell^+(s) \times \delta_{\ell\ell'}\delta_{\lambda\lambda'}(2\pi)^4\delta^{(4)}(p-p') \equiv \begin{pmatrix} {}_{in}\langle 1'|1\rangle_{in} & {}_{in}\langle 1'|2\rangle_{in} & {}_{in}\langle 1'|1\rangle_{out} & {}_{in}\langle 1'|2\rangle_{out} \\ {}_{in}\langle 2'|1\rangle_{in} & {}_{in}\langle 2'|2\rangle_{in} & {}_{in}\langle 2'|1\rangle_{out} & {}_{in}\langle 2'|2\rangle_{out} \\ {}_{out}\langle 1'|1\rangle_{in} & {}_{out}\langle 1'|2\rangle_{in} & {}_{out}\langle 1'|1\rangle_{out} & {}_{out}\langle 1'|2\rangle_{out} \\ {}_{out}\langle 2'|1\rangle_{in} & {}_{out}\langle 2'|2\rangle_{in} & {}_{out}\langle 2'|1\rangle_{out} & {}_{out}\langle 2'|2\rangle_{out} \end{pmatrix} \tag{3.58}$$

The case of spin $\ell = 0$ is special because the state $|2\rangle$ does not exist and therefore we get a smaller matrix:

$$\mathcal{H}_0^+(s) \times \delta_{\lambda\lambda'}(2\pi)^4\delta^{(4)}(p-p') \equiv \begin{pmatrix} {}_{in}\langle 1'|1\rangle_{in} & {}_{in}\langle 1'|1\rangle_{out} \\ {}_{out}\langle 1'|1\rangle_{in} & {}_{out}\langle 1'|1\rangle_{out} \end{pmatrix}, \tag{3.59}$$

We now consider odd $\ell \geq 3$, in which case the only state that exists is state $|2\rangle$ and therefore we have

$$\mathcal{H}_\ell^+(s) \times \delta_{\ell\ell'}\delta_{\lambda\lambda'}(2\pi)^4\delta^{(4)}(p-p') \equiv \begin{pmatrix} {}_{in}\langle 2'|2\rangle_{in} & {}_{in}\langle 2'|2\rangle_{out} \\ {}_{out}\langle 2'|2\rangle_{in} & {}_{out}\langle 2'|2\rangle_{out} \end{pmatrix} \tag{3.60}$$

Parity odd sector

We now turn to the parity odd eigenstate (3.52) which exists for even spin $\ell \geq 0$. We have

$$\mathcal{H}_\ell^-(s) \times \delta_{\ell\ell'}\delta_{\lambda\lambda'}(2\pi)^4\delta^{(4)}(p-p') \equiv \begin{pmatrix} {}_{in}\langle 3'|3\rangle_{in} & {}_{in}\langle 3'|3\rangle_{out} \\ {}_{out}\langle 3'|3\rangle_{in} & {}_{out}\langle 3'|3\rangle_{out} \end{pmatrix}. \tag{3.61}$$

We can now plug in (3.56) and (3.57) for the inner products between states along with (3.55) to arrive at the unitarity constrains on our scattering amplitudes. Before presenting them, it is convenient to use the following notation for the partial amplitudes of the independent amplitudes introduced in (3.13):

$$\begin{aligned} \Phi_1^\ell(s) &\equiv T_{\ell\,++}^{++}(s), \\ \Phi_2^\ell(s) &\equiv T_{\ell\,++}^{--}(s), \\ \Phi_3^\ell(s) &\equiv T_{\ell\,+-}^{+-}(s), \\ \Phi_4^\ell(s) &\equiv T_{\ell\,+-}^{-+}(s), \\ \Phi_5^\ell(s) &\equiv T_{\ell\,++}^{+-}(s). \end{aligned} \tag{3.62}$$

The final unitarity equations read

Even $\ell \geq 0$

$$\begin{pmatrix} 1 & 1 \\ 1 & 1 \end{pmatrix} + i \begin{pmatrix} 0 & -\Phi_1^{\ell *}(s) + \Phi_2^{\ell *}(s) \\ \Phi_1^{\ell}(s) - \Phi_2^{\ell}(s) & 0 \end{pmatrix} \succeq 0, \tag{3.63}$$

Even $\ell \geq 2$

$$\begin{pmatrix} \mathbb{I}_{2\times 2} & \mathbb{S}_{2\times 2}^{\ell \dagger}(s) \\ \mathbb{S}_{2\times 2}^{\ell}(s) & \mathbb{I}_{2\times 2} \end{pmatrix} \succeq 0, \tag{3.64}$$

where we defined

$$\mathbb{I}_{2\times 2} \equiv \begin{pmatrix} 1 & 0 \\ 0 & 1 \end{pmatrix}, \qquad \mathbb{S}_{2\times 2}^{\ell}(s) \equiv \begin{pmatrix} 1 & 0 \\ 0 & 1 \end{pmatrix} + i \begin{pmatrix} \Phi_1^{\ell}(s) + \Phi_2^{\ell}(s) & 2\Phi_5^{\ell}(s) \\ 2\Phi_5^{\ell}(s) & 2\Phi_3^{\ell}(s) \end{pmatrix}. \tag{3.65}$$

Odd $\ell \geq 3$

$$\begin{pmatrix} 1 & 1 \\ 1 & 1 \end{pmatrix} + 2i \begin{pmatrix} 0 & -\Phi_3^{\ell *}(s) \\ \Phi_3^{\ell}(s) & 0 \end{pmatrix} \succeq 0. \tag{3.66}$$

And $\ell = 0$

$$\begin{pmatrix} 1 & 1 \\ 1 & 1 \end{pmatrix} + i \begin{pmatrix} 0 & -\Phi_1^{0 *}(s) - \Phi_2^{0 *}(s) \\ \Phi_1^{0}(s) + \Phi_2^{0}(s) & 0 \end{pmatrix} \succeq 0, \tag{3.67}$$

The equations above hold for arbitrarily high spin ℓ and high energy s. However a numerical implementation of the above constraints implies discretizing the range energy s and imposing the constraints upto some maximum spin L_{max}. During our preliminary numerical explorations, we found that imposing constraints from analyzing unitarity equations at large spin (see appendix B.3.1) and large energy (see appendix B.3.2) were important for convergence of the numerics.

3.4 Effective field theory of photon scattering

In the previous section, we worked out the crossing and unitarity constraints on the photon-photon amplitude. However functions $\mathcal{T}_I$ in eq. (1.101) parametrize the most general Lorentz invariant amplitude of identical spin 1 massless particles. To specific that the particles are actually photons, we need to choose a specific low energy behavior. A convenient and physically transparent way to do this is through the low energy effective field theory (EFT). The choice of an EFT is essentially the choice of an action

for the low energy degrees of freedom. We would like to describe a world where photons are the only massless particles. Furthermore, we assume parity to be an exact symmetry. The most general Lorentz and gauge invariant Lagrangian is then a function of (derivatives) of the field strength $F_{\mu\nu} = \partial_\mu A_\nu - \partial_\nu A_\mu$. In other words, photons are derivatively coupled, hence free at low energies.

Let us consider the quantum electrodynamics (QED). It is defined by the standard Lagrangian density which reads

$$\mathcal{L}_{QED} = \bar{\psi}(i\not{D} - m)\psi - \frac{1}{4}F_{\mu\nu}F^{\mu\nu} - \frac{1}{2\xi}(\partial_\mu A^\mu)^2. \tag{3.68}$$

Here $\psi(x)$ is the Dirac fermion field and the covariant derivative is

$$D_\mu \equiv \partial_\mu + ieA_\mu, \tag{3.69}$$

where e is the electric charge of ψ. The excitations of $\psi(x)$ describe electrons with mass m. The electromagnetic field strength tensor $F_{\mu\nu}(x)$ is given by

$$F_{\mu\nu}(x) \equiv \partial_\mu A_\nu(x) - \partial_\nu A_\mu(x), \tag{3.70}$$

where $A_\mu(x)$ is the electromagnetic potential. The excitations of $A_\mu(x)$ describe photons.

For the range of energies E much smaller than the electron mass m, namely when $E << m$ we can write the effective field theory (EFT) of the photons scattering. It reads as

$$\mathcal{L}_{EFT} = -\frac{1}{4}F_{\mu\nu}F^{\mu\nu} + \mathcal{L}_8 + \dots, \tag{3.71}$$

where $\mathcal{L}_8$ describes the first non-trivial interaction part between four photons. The subscript 8 indicates its mass dimension. The ellipsis indicate terms with higher mass dimensions. The form of $\mathcal{L}_8$ can be straightforwardly obtained from (3.68) and reads as

$$\mathcal{L}_8 = c_1(F_{\mu\nu}F^{\nu\mu})(F_{\alpha\beta}F^{\beta\alpha}) + c_2 F_{\mu\nu}F^{\nu\rho}F_{\rho\sigma}F^{\sigma\mu}, \tag{3.72}$$

where the coefficients c_1 and c_2 are given in terms of the electromagnetic structure constant $\alpha \equiv e^2/4\pi$ by [61]

$$c_1 = -\frac{1}{36}\frac{\alpha^2}{m^4} \qquad c_2 = \frac{7}{90}\frac{\alpha^2}{m^4}. \tag{3.73}$$

Using (3.72) we can compute the leading non-trivial part of the photon scattering. It

reads

$$\begin{aligned}
&\mathcal{T}^{Tree\,\lambda_3,\lambda_4}_{EFT\;\lambda_1,\lambda_2}(p_1,p_2,p_3,p_4) = \\
&\quad 8c_1\Big(\operatorname{tr}(H_{\lambda_1}H_{\lambda_2})\operatorname{tr}(H^{\lambda_3}H^{\lambda_4}) + \operatorname{tr}(H_{\lambda_1}H^{\lambda_3})\operatorname{tr}(H_{\lambda_2}H^{\lambda_4}) + \operatorname{tr}(H_{\lambda_1}H^{\lambda_4})\operatorname{tr}(H_{\lambda_2}H^{\lambda_3})\Big) \\
&+8c_2\Big(\operatorname{tr}(H_{\lambda_1}H_{\lambda_2}H^{\lambda_3}H^{\lambda_4}) + \operatorname{tr}(H_{\lambda_1}H^{\lambda_3}H_{\lambda_2}H^{\lambda_4}) + \operatorname{tr}(H_{\lambda_1}H_{\lambda_2}H^{\lambda_4}H^{\lambda_3})\Big).
\end{aligned} \tag{3.74}$$

We can decompose this result into the basis of tensor structures (3.25) using (3.16). We get then

$$\begin{aligned}
\mathcal{A}_1^{EFT}(s,t,u) &= 8c_1 + 2c_2 \times \frac{s^2-2st-2t^2}{s^2} + O(s^2), \\
\mathcal{A}_2^{EFT}(s,t,u) &= 8c_1 + 2c_2 \times \frac{s^2-2st-2t^2}{s^2} + O(s^2), \\
\mathcal{A}_3^{EFT}(s,t,u) &= 8c_1 + 2c_2 \times \frac{s^2-2st-2t^2}{s^2} + O(s^2), \\
\mathcal{A}_4^{EFT}(s,t,u) &= 16c_2 \times \frac{s^2+st+t^2}{s^2} + O(s^2), \\
\mathcal{A}_5^{EFT}(s,t,u) &= 0 + O(s^2).
\end{aligned} \tag{3.75}$$

We can do the same for the dimension 10 operator as well:

$$\mathcal{L}_{10} = c_3 F_{ab}\partial^b F_{\mu\nu}\partial^a F^{\nu\rho}F_\rho{}^\mu + +c_4(\partial_a F_{\mu\nu}\partial^a F^{\nu\mu})(F_{\rho\sigma}F^{\sigma\rho}) + c_5\partial_a F_{\mu\nu}F^{\nu\rho}\partial^a F_{\rho\sigma}F^{\sigma\mu}, \tag{3.76}$$

Computing the tree-level amplitude of this $\mathcal{L}_{10}$, we obtained:

$$\begin{aligned}
\mathcal{T}_{10}(s,t,u) = 6c_3\Big\{ &-(p_2H_{\lambda_1}p_3)\ \operatorname{tr}\left(H_{\lambda_2}H^{\lambda_3}H^{\lambda_4}\right) + (p_1H_{\lambda_2}p_4)\ \operatorname{tr}\left(H_{\lambda_1}H^{\lambda_3}H^{\lambda_4}\right) \\
&- \left(p_2H^{\lambda_4}p_3\right)\operatorname{tr}\left(H_{\lambda_1}H_{\lambda_2}H^{\lambda_3}\right) + \left(p_1H^{\lambda_3}p_4\right)\operatorname{tr}\left(H_{\lambda_1}H_{\lambda_2}H^{\lambda_4}\right)\Big\} \\
&+ 4c_4\Big(s\ \operatorname{tr}(H_{\lambda_1}H_{\lambda_2})\operatorname{tr}(H^{\lambda_3}H^{\lambda_4}) + t\ \operatorname{tr}(H_{\lambda_1}H^{\lambda_3})\operatorname{tr}(H_{\lambda_2}H^{\lambda_4}) + u\ \operatorname{tr}(H_{\lambda_1}H^{\lambda_4})\operatorname{tr}(H_{\lambda_2}H^{\lambda_3})\Big) \\
&+ 4c_5\Big(s\ \operatorname{tr}(H_{\lambda_1}H^{\lambda_3}H_{\lambda_2}H^{\lambda_4}) + t\ \operatorname{tr}(H_{\lambda_1}H_{\lambda_2}H^{\lambda_3}H^{\lambda_4}) + u\ \operatorname{tr}(H_{\lambda_1}H_{\lambda_2}H^{\lambda_4}H^{\lambda_3})\Big)
\end{aligned} \tag{3.77}$$

Therefore, in terms of the functions $f's$, the tree-level amplitude is parametrized by

$$f_1(s|t,u) = 8c_1 + 4c_4 s \tag{3.78}$$

$$f_2(s|t,u) = 8c_2 + 4c_5 s \tag{3.79}$$

$$f_3(s,t,u) = 6c_3 \tag{3.80}$$

In terms of the COM frame amplitudes, we have

$$\begin{aligned}
\Phi_1^{EFT}(s,t,u) &= 2(4c_1+3c_2)s^2+4c_4s^3+O(s^4),\\
\Phi_2^{EFT}(s,t,u) &= 2(4c_1+c_2)(s^2+t^2+u^2)\\
&\quad +(12c_4-6c_5+6c_3)stu+O(s^4),\\
\Phi_3^{EFT}(s,t,u) &= 2(4c_1+3c_2)u^2+4c_4u^3+O(s^4),\\
\Phi_4^{EFT}(s,t,u) &= 2(4c_1+3c_2)t^2+4c_4t^3+O(s^4),\\
\Phi_5^{EFT}(s,t,u) &= \frac{3}{2}c_3stu+O(s^5).
\end{aligned} \tag{3.81}$$

This is the soft behaviour that we will impose on our amplitudes and in fact take to be the distinguishing feature of photon scattering.

Allowed space in c_1 and c_2

Consider the dimension 8 Wilson coefficients c_1 and c_2. From the work of [62] it is known that the following two quantities must be positive

$$2c_1+c_2\geq 0 \quad \text{and} \quad c_2\geq 0 \tag{3.82}$$

These inequalities are saturated by free theories. We now plot the values of dimensionless ratio $\frac{c_2}{2(c_1+c_2)}\in[0,1]$ for two perturbative examples - scalar QED *i.e* photon coupled to a massive charged scalar and spinor QED *i.e* photon coupled to a massive Dirac fermion.

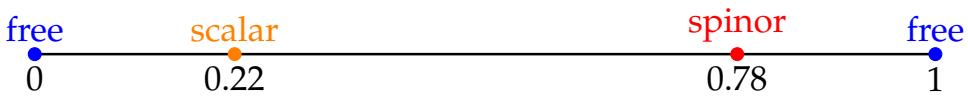

Figure 3.1: Allowed space of $\frac{c_2}{2c_1+2c_2}$ with some known examples.

Future plans

In the future we would like to bound the allowed space at the next order *i.e* in the space of the dimension 10 Wilson coefficients c_3, c_4 and c_5.

Flux-Tubes and Glueballs Part II

Overview of Part II

The first part of the thesis was concerned with scattering of particles in four spacetime dimensions. In this second part of the thesis, we will instead be considering quantum field theories which have long string-like excitations in D spacetime dimensions [7]. Examples of such QFTs are Yang-Mills, QCD, the Abelian Higgs model, Ising model in 3d etc. While the string itself lives in D dimensional spacetime (called the target space), scattering that takes place on it is naturally described by a 2 spacetime dimensional theory. The scattering amplitude $S(s,t,u)$ of the massless branons is now a function of only 1 variable due to the kinematical fact that in 2d we have to have either forward scattering

$$t = -s \quad \text{and} \quad u = 0 \tag{3.83}$$

or backward scattering

$$u = -s \quad \text{and} \quad u = 0 \tag{3.84}$$

As a function of s, the amplitude $S(s)$ is defined for

$$s \geq 0 \tag{3.85}$$

As usual, we can analytically continue this function to the complex plane which allows us to use the machinery of complex analysis to gain insights about the space of S matrices.

In chapter 4, we consider the two to two scattering of excitations (a.k.a branons) on these long strings which we will refer to henceforth as flux-tubes. As mentioned in the introduction to the thesis, our goal in this chapter is to bound the low energy EFT of these branons. In section 4.1, we introduce the problem in more detail and then set up the bootstrap problem in section 4.2. Using the Schwarz-Pick theorem we are able to get bounds for $D = 3$ and $D = 4$ flux-tubes. The bounds from Schwarz-Pick are optimal for $D = 3$ but not $D = 4$ flux tubes as they only use part of the unitarity constraints. We therefore use numerics to augment these bounds. In 4.3, we translate these bounds to constraints on the non-universal corrections to the energy spectrum of flux tubes. These two sections constitute the major results of this part of the thesis. Finally in 4.4 we look at the resonance spectrum of the S-matrices that lie on the boundary of our allowed

[7] We will mainly focus on the cases of $D = 3$ or $D = 4$

space of S-matrices.

In chapter 5, which describes work in progress, we add a glueball to the branon system considered above. At present we only consider the case of $D = 3$ target space. We set up the bootstrap problem and we will shortly run numerics to bound for example the coupling of the glueball to the fluxtube. Another possibility is to add input from the lattice about the mass of the glueball and then see how this effects the space of S-matrices found in chapter 4.

4 Fluxtube S-matrix Bootstrap

4.1 Introduction

Unraveling the dual string description of Yang-Mills theory is an old-standing problem. A first step towards achieving this goal is solving for the spectrum of long strings or confining flux tubes of pure glue. At low energies, the massless flux tube excitations (or branons) decouple from the massive short strings (or glueballs)[1] and can be described by a two dimensional worldsheet theory which can be formulated in terms of an effective Lagrangian or in terms of the branon S-matrix. Both approaches have their advantages and limitations.

The flux tube's effective Lagrangian density is built out of derivatives of the fields X^μ describing the embedding of the worldsheet in spacetime. At low energies, it is dominated by the square root of the induced metric determinant $h = \det h_{\alpha\beta} = \det \partial_\alpha X^\mu \partial_\beta X^\nu \eta_{\mu\nu}$, i.e. the Nambu-Goto lagrangian. Any interaction consistent with the bulk D-dimensional Poincaré symmetry is also permitted. Thus, the action is written in terms of curvature invariants [63, 64],

$$A = \int d^2\sigma \sqrt{-h} \left[\ell_s^{-2} + \mathcal{R} + K^2 + \ell_s^2 K^4 + \dots \right] , \tag{4.1}$$

where $\mathcal{R}(h_{\alpha\beta})$ is the Ricci scalar and $K^\mu_{\alpha\beta} = \nabla_\alpha \partial_\beta X^\mu$ is the extrinsic curvature tensor and implicit are Wilson coefficients multiplying any of these structures in the effective Lagrangian. The parameter ℓ_s is called the string length. In static gauge $X^\mu(\sigma) = (\sigma^\alpha, X^i)$, where $i = 1, \dots, D-2$ are the transverse excitations of the flux tube.

Nicely, Ricci is a total derivative and K^2 vanishes on-shell so the first two terms in the effective field theory expansion can be dropped. Therefore, the low energy dynamics of (4.1) is tightly constrained by the non-linearly realized target Poincaré symmetry. This

[1] If the number of colours N_c tends to infinity, then the flux tubes decouple from the glueballs at any energy (independent of N_c).

is known as low energy universality [63–65]. The leading deviations from the Nambu-Goto predictions for physical observables arise from K^4 operators in (4.1), namely effects of $O(\partial^8 X^4)$. More precisely, there are two K^4 operators, differing by the contractions of the indices and correspondingly two coefficients α_3 and β_3 which do depend on the specific underlying confining theory.

We will constrain them in this paper and thus bound interesting physical quantities which depend on them. To constrain these parameters we turn to the on-shell approach to the flux tube world-sheet theory pioneered by [63] which is based on the branon *S-matrix*. The $2 \to 2$ scattering amplitudes can be decomposed into channels, i.e. irreducible representations of the symmetry group $O(D-2)$. The low energy expansion of the phase shifts in each channel can be written as (see 4.2.1 for details)

$$\begin{aligned} 2\delta_{sym} &= \frac{s}{4} + \alpha_2 s^2 + \alpha_3 s^3 + O(s^4) \\ 2\delta_{anti} &= \frac{s}{4} - \alpha_2 s^2 + (\alpha_3 + 2\beta_3) s^3 + O(s^4) \\ 2\delta_{sing} &= \frac{s}{4} - (D-3)\alpha_2 s^2 + (\alpha_3 - (D-2)\beta_3) s^3 + O(s^4) \end{aligned} \tag{4.2}$$

where $\alpha_2 = \frac{D-26}{384\pi}$ and s is the square of the center of mass energy. Here and below we set $\ell_s = 1$. The low energy universality mentioned above is manifest here up to $O(s^2)$ included [63]. The non-universal K^4 terms in (4.1) contribute at $O(s^3)$ and are encoded in the parameters α_3 and β_3 in (4.2). The high degree of universality of the branon S-matrix is to be contrasted with a theory of compact goldstones like the Pion, whose S-matrix shows departures from universality already at $O(s^2)$. To this order, the phase shifts are real because inelastic processes like $2 \to 4$ give rise to imaginary contributions of $O(s^6)$.

We will see below that by requiring a consistent UV completion of the branon S-matrix, we can put bounds on its low energy expansion and thus bound the effective field theory parameters. This immediately leads to many interesting bounds on various low energy physical observables. One such interesting observable is the finite volume energy spectrum which we can compute in perturbation theory from the action (4.1) above. For example, for the ground state, we will find

$$E_0(R) = \sqrt{R^2 - \tfrac{\pi}{3}(D-2)} + \frac{\delta(D)}{R^7} + O(1/R^9)\,, \tag{4.3}$$

where R is the length of the flux tube loop and

$$\delta(D) = \frac{32\pi^6 (2-D)((D-2)\alpha_3 + (D-4)\beta_3)}{225}\,. \tag{4.4}$$

Note that the leading confining potential $E_0(R) \sim R$ all the way upto the sub-sub-sub-leading corrections of $O(1/R^5)$ are universal and captured by the square root term in (4.3).

Similar formulae governing the first few universal terms of the large R expansion can be written for excited states as well [63, 64]. A particular feature of those results is that they exhibit quite a lot of degeneracy: for very large radius the energy levels typically depend only on the total left and right moving momentum but not on the individual momenta of the branons. Level splitting of these energy levels starts at $O(1/R^7)$ and directly probes the non-universal parameters α_3 and β_3 introduced above (see equation (4.27) below for a concrete example).

In summary, at very low energy, i.e. very long flux tubes, universality powerfully constrains everything. Eventually non-universal terms kick in. We then have a triangle of three important players: the effective field theory Lagrangian (4.1), the branon S-matrix (4.2) and the finite volume spectrum (4.3). The main result of this paper is a bound on the low energy expansion of the S-matrix following from the existence of its consistent UV completion. This immediately translates into rigorous bounds for the other two players in the triangle.

More speculatively, we will also study the boundary of the allowed S-matrix space and find a remarkable numerical coincidence: on that boundary lies an S-matrix exhibiting a resonance with the quantum numbers, mass and width exactly as predicted in [66, 67] and dubbed as the QCD worldsheet axion there. Amusingly, at that same point, the S-matrix we obtain also contains three further heavier excitations which we call the dilaton, the symmetron and the axion*. Given the remarkable numerical coincidence w.r.t. the QCD axion, it is tempting to speculate that they should be present in the QCD flux tube.

Lattice Monte Carlo simulations of pure Yang-Mills provide precious information on the dynamics of confining flux tubes. The measurements of the low energy spectrum support the outlined picture of universality at large radius – see [68] for a review – and should hopefully be sensitive to the non-universal corrections soon, e.g. [69] for D=3. They also favor the existence of the conjectured axion excitation [66, 67, 70, 71]; it would be very interesting to look for other more massive excitations.

4.2 2D massless S-matrix Bootstrap

Massless excitations in 2D can be left (L) or right (R) movers. In this section, we study the L-R scattering amplitude of branons.[2]

[2] A general 2D massless S-matrix has non-trivial L-L, L-R and R-R components [72]. Lorentz invariance implies that the L-L components is a function of the ratio p_1^L / p_2^L of the momenta of the incoming left-moving particles. This means that the L-L and the R-R amplitudes are independent of the energy scale. Therefore, the branons must have trivial L-L and R-R scattering because their interactions turn off at low energies [73].

4.2.1 Setup

A long flux tube in D dimensions breaks the target Poincaré symmetry to $ISO(1,1) \times O(D-2)$.[3] This leads to $D-2$ Goldstone bosons or branons. Consider now the $2 \to 2$ scattering amplitude of these branons,

$$S_{ab}^{cd}(s) = \sigma_1(s)\delta_{ab}\delta^{cd} + \sigma_2(s)\delta_a^c\delta_b^d + \sigma_3(s)\delta_a^d\delta_b^c\,, \tag{4.5}$$

where the indices run over the $D-2$ transverse directions and s is the square of the center-of-mass energy. Crossing symmetry leads to

$$\sigma_2(-s) = \sigma_2(s)\,, \qquad \sigma_3(-s) = \sigma_1(s)\,. \tag{4.6}$$

The amplitude (4.5) can also be decomposed in partial waves of $O(D-2)$ namely, the singlet, the anti-symmetric tensor and the symmetric traceless tensor (see [6, 7] for details),

$$\begin{aligned} S_{sing} &= e^{2i\delta_{sing}} = (D-2)\sigma_1 + \sigma_2 + \sigma_3 \\ S_{anti} &= e^{2i\delta_{anti}} = \sigma_2 - \sigma_3 \\ S_{sym} &= e^{2i\delta_{sym}} = \sigma_2 + \sigma_3 \end{aligned} \tag{4.7}$$

where δ_{rep} may have an imaginary part due to particle production. In this basis, unitarity is simply

$$|S_{rep}(s)|^2 \leq 1\,, \quad \forall s > 0\,. \tag{4.8}$$

The amplitudes $\sigma_i(s)$ are analytic functions of s in the upper and the lower half plane related by [4]

$$\sigma_i(s^*) = [\sigma_i(s)]^*\,. \tag{4.9}$$

Therefore, it is enough to know the amplitudes in the upper half plane, where equations (4.6) and (4.9) lead to

$$\sigma_2(-s^*) = [\sigma_2(s)]^*\,, \qquad \sigma_3(-s^*) = [\sigma_1(s)]^*\,. \tag{4.10}$$

The Nambu-Goto lagrangian leads to the low energy expansion of the phase shifts as $2\delta_{rep} = \frac{s}{4} + O(s^2)$. In principle, higher order terms may also include non-analytic terms of the form $s^p(\log s)^k$ with $p > k > 0$. Furthermore, we know that $\operatorname{Im}\delta_{rep} = O(s^6)$ because particle production starts with $|\mathcal{M}_{2\to 4}|^2 \sim l_s^{12}$ [74]. Using just these facts and (4.10) we can derive the low energy expansion (4.2) with α_2, α_3 and β_3 as real parameters. In the context of the flux tube theory $\alpha_2 = \frac{D-26}{384\pi}$ is universal and α_3 and β_3 are non-

[3] We assume that the D-dimensional theory and the flux tube preserve parity. It would be interesting to generalize our study of branon scattering in the absence of parity, e.g. due to a θ-term.

[4] This is just real analyticity for massive particles. For massless particles, the s-channel and the t-channel cuts touch at $s = 0$ and cover the entire real axis of s.

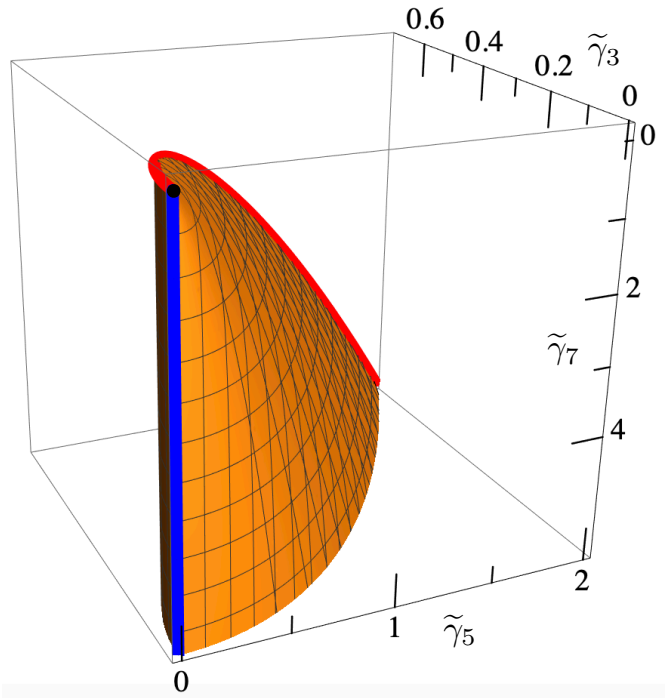

Figure 4.1: Allowed region in the $\{\tilde{\gamma}_3, \tilde{\gamma}_5, \tilde{\gamma}_7\}$ space for a generic D=3 flux tube S-matrix, with $\tilde{\gamma}_n = \gamma_n + (-1)^{(n+1)/2} \frac{1}{n 2^{3n-1}}$. The S-matrix at the cusp (black point) is associated to the goldstone (goldstino) S-matrix describing the flow from tricritical Ising to free fermions: it saturates the Schwarz-Pick inequality. The edge in red corresponds to double CDD solutions, saturating the 2-point Schwarz-Pick bound and the full orange surface is determined by the 3-point Schwarz-Pick inequality and it is saturated by a triple CDD family.

universal coefficients related to the two independent K^4 terms in (4.1). In appendix C.1, we push this expansion up to $O(s^6)$ and find perfect agreement with the $O(s^4)$ results of [75].

4.2.2 $D = 3$ Flux Tubes

To start with, we focus on the $D = 3$ target space. In this case, only $\delta_{sing} \equiv \delta$ is meaningful and the amplitude $S = e^{2i\delta}$ obeys $S(-s^*) = [S(s)]^*$ for s in the upper half plane. Furthermore, it was shown in [76] that $\mathrm{Im}\,\delta = O(s^8)$. This implies

$$2\delta(s) = \frac{s}{4} + \gamma_3 s^3 + \gamma_5 s^5 + \gamma_7 s^7 + i\gamma_8 s^8 + O(s^9)\,, \tag{4.11}$$

where $\gamma_3, \gamma_5, \gamma_7$ are non-universal parameters. On the other hand, γ_8 is determined by the probability of particle production at leading order $P_{2\to n\geq 4} = 2\gamma_8 s^8 + O(s^9)$. As explained in [76], $\gamma_8 \propto \gamma_3^2$ is not an independent parameter. We shall now show that the coefficients $\gamma_3, \gamma_5, \gamma_7$ can only take values in the region depicted in figure 4.1.

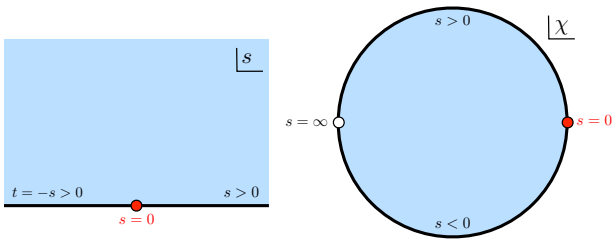

Figure 4.2: Left: domain of analyticity of a generic massless two-dimensional S-matrix. The cut, in black, is all over the real axis; the threshold at $s = 0$ it is in general a branch point singularity. Right: we map the upper half plane to the unit disc through $s \to \chi = (4 + is)/(4 - is)$. The real axis is mapped to the boundary of the unit circle, the threshold to $\chi = 1$ and $s = \infty$ to $\chi = -1$.

The S-matrix $S(z)$ is a holomorphic function from the upper half plane $\mathbb{H}$ to the the unit disc $\mathbb{D}$ because unitarity on the real axis along with the maximum modulus principle implies that $|S(z)| \leq 1$ in the full upper half plane. Next, we construct a new function

$$S^{(1)}(z|w) \equiv \frac{S(z) - S(w)}{1 - S(z)\overline{S(w)}} \Big/ \frac{z - w}{z - \overline{w}}, \tag{4.12}$$

where w is any point in the upper half plane. It is easy to see that (as a holomorphic function of z) this function (a) has no singularities in the upper half plane and (b) is again bounded by 1 for z on the real line.[5] By the maximum modulus principle, it is bounded everywhere on the upper half plane: $|S^{(1)}(z|w)|_{\mathrm{Im}(z)\geq 0} \leq 1$. This is the content of the so-called Schwarz-Pick theorem.

Inserting (4.11) in the Schwarz-Pick combination (4.12) and expanding for small and imaginary z and w, we find

$$S^{(1)}(ix|iy) = -1 + \left(\frac{1}{96} + 8\gamma_3\right) x\, y + \cdots \geq -1\,. \tag{4.13}$$

This leads to our first bound

$$\gamma_3 \geq -\frac{1}{768}\,. \tag{4.14}$$

In Appendix C.2, we show that the bound cannot be improved by approaching the origin $z{=}w{=}0$ in any other direction in the upper half plane. The authors of [67, 76] estimated $\gamma_3 \approx 3 \times 10^{-4}$ from lattice data for $SU(6)$ YM [77].

Similarly, one can define $S^{(2)}(z|q, w)$ by replacing $S(z)$ by $S^{(1)}(z|q)$ in (4.12). Such

[5] For z on the real line, $|z - w|/|z - \overline{w}| = 1$ and notice that $S(z)$, $S(w) \in \mathbb{D}$ and $\frac{S(z)-S(w)}{1-S(z)\overline{S(w)}}$ is a Mobius transformation that maps the unit disc $\mathbb{D}$ to itself.

Schwarz-Pick multi-point generalizations [78] can be used to derive (see appendix C.2)

$$\begin{aligned} \tilde{\gamma}_3 &\geq 0 \\ \tilde{\gamma}_5 &\geq 4\tilde{\gamma}_3^2 - \frac{1}{64}\tilde{\gamma}_3 \\ \tilde{\gamma}_7 &\geq \frac{\tilde{\gamma}_5^2}{\tilde{\gamma}_3} + \frac{1}{4096}\tilde{\gamma}_3 + \frac{1}{64}\tilde{\gamma}_5 - \frac{1}{16}\tilde{\gamma}_3^2 \end{aligned} \tag{4.15}$$

where $\tilde{\gamma}_n{=}\gamma_n + (-1)^{(n+1)/2}\frac{1}{n2^{3n-1}}$. The allowed region is shown in figure 4.1.

It is interesting that Schwarz-Pick inequalities exploit both unitarity and analyticity by exploring the region of purely imaginary Mandelstam s – orthogonal to real physical s – to efficiently bound the space of $2 \to 2$ S-matrices.

4.2.3 $D = 4$ Flux Tubes

In $D = 4$ dimensions, the branon S-matrix possesses an $O(2)$ symmetry. In addition, the crossing and unitary equations are invariant under $S_{\text{sing}} \leftrightarrow S_{\text{anti}}$ interchange corresponding to $\beta_3 \leftrightarrow -\beta_3$ in (4.2). Universality fixes the low energy expansion of the phase shifts up to order s^2 included. The leading non-universal behavior depends on the two coefficients α_3 and β_3 introduced in (4.2).

Crossing mixes the various irreps but the symmetric channel S-matrix is still bounded by 1 along all the real s-axis[6] so we can still apply the first Schwarz-Pick inequality in this channel as in the previous section. Moreover, it can be applied to the two crossing symmetric combinations in $D = 4$: $S_\pm = 1/2(S_{sing} \pm S_{sym})$. This analysis leads to

$$\alpha_3 \geq -\frac{1}{768} + \frac{121}{9216\pi^2}\,, \tag{4.16}$$

$$\alpha_3 \geq -\frac{1}{768} + |\beta_3|\,. \tag{4.17}$$

This is however not the full allowed $\{\alpha_3, \beta_3\}$ space as we have yet to explore all channels and their interrelations. To find the optimal bounds we proceed numerically in the spirit of [3,4,8]. We map the upper half plane to the unit disk with the real axis mapped to the unit circle, see figure 4.2. By assumption the S-matrix is analytic in the interior of the disk and we can represent it as a Taylor expansion. Our numerical ansatz is then given by the truncated Taylor series

$$S_{\text{ansatz}} = \sum_{n=0}^{N_{max}} a_n \chi^n\,, \qquad |\chi| \leq 1\,. \tag{4.18}$$

[6] By crossing $|S_{\text{sym}}^{\text{crossed}}| = \frac{1}{2}|S_{\text{sing}} + S_{\text{anti}}| \leq 1$. This actually holds for any $O(N = D-2)$ theory as pointed out in [7].

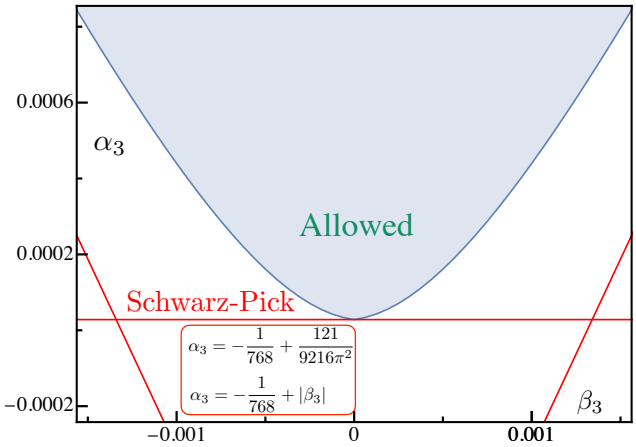

Figure 4.3: Allowed region in the $\{\beta_3, \alpha_3\}$ parameter space of flux tube S-matrice in $D = 4$ as obtained by numerics. The horizontal red line represents the absolute minimum of α_3 as predicted analytically by the Schwarz-Pick theorem applied to the symmetric channel. The additional red lines can be obtained applying Schwarz-Pick to the additional crossing symmetric combinations $S_\pm(s)$.

Then we minimize the linear functional α_3 in the vector space of the Taylor coefficients $\{a_n\}$ as a function of β_3, given the quadratic constraints $|S_{\text{ansatz}}(\chi)| \leq 1$ for each χ on the upper boundary of the disk and for each S_{rep}. Further details are given in appendix C.4 along with more general numerical results obtained as byproduct of our explorations but that are not relevant in the context of flux tube theories.

The numerical result of the optimization problem is shown in figure 4.3. The analytic bound in (4.17) would allow all the points above the Schwarz-Pick line (in red), while we see numerically that the effect of bounding the other channels produces the region depicted in blue. When $\beta_3 = 0$ the numerical bound and the analytic one coincide. At this point, the S-matrix satisfies Yang-Baxter and it is a pure phase in all channels. Its expression can be predicted analytically and is given in appendix C.3.

4.3 Energy spectrum in finite volume

We just saw how many constraints on the long Flux Tube follow from the general principles of the S-matrix theory. Here we translate them into constraints on large volume observables. We start with the flux tube ground state energy $E_0(R)$.

At very large R we read off the string tension from $E_0(R) \simeq R/\ell_s^2$. Recall that the corrections up to $1/R^5$ to this confining result are universal and given by the square root in (4.3). The sub-sub-sub-subleading term is *not* uniquely fixed by symmetry and is the subject of this section.

Computing the non-universal correction in (4.3) is straightforward in perturbation

theory (sum of connected vacuum Feynman diagrams), albeit increasingly complex as we move to higher orders in $1/R$. The leading correction $\delta(D)$ comes from the two K^4 possible interactions which we parametrize as

$$\begin{aligned}\mathcal{L}_{\text{non-univ}} = \partial_a\partial_b X^i \partial_a\partial_b X^j \partial_c\partial_d X^k \partial_c\partial_d X^l \times \\ \times \left[4\delta_{ik}\delta_{jl}(\alpha_3+\beta_3) - 2\delta_{ij}\delta_{kl}(\alpha_3+3\beta_3)\right] .\end{aligned} \tag{4.19}$$

Here we parametrize the coefficient of the two invariant structures so to match the eye pleasing expressions (4.2), as can be verified by a straightforward tree level computation. Thus, the leading order non-universal contribution to the vacuum energy density is


$$= f(D)\left[\partial_\mu\partial_\nu\partial_\rho\partial_\sigma\Delta_R(0)\right]^2 , \tag{4.20}$$

where $f(D) = 4(2-D)((D-2)\alpha_3+(D-4)\beta_3)$. The derivative of the finite volume propagator is given by $\partial_\mu\Delta_R(x)=\sum_n \partial_\mu\Delta(x+n)$, where $\partial_\mu\Delta(x) = -x_\mu/(2\pi\, x^2)$ and $n_\mu = (0, nR)$ is a displacement vector in the winding direction. The zero mode $n_\mu = (0,0)$ gives a short-distance divergence in the limit $x \to 0$ leading to (4.20). This is regulated by a local counter-term, which at this order simply amounts to neglecting the zero mode. Thus, after a bit of algebra and excluding the zero mode, we are led to $\left[\partial_\mu\partial_\nu\partial_\rho\partial_\sigma\Delta_R(0)\right]^2_{\text{ren.}} = 288/\pi^2\sum_{n,m=1}^{\infty} 1/(R^8 n^4 m^4) = 8\pi^6/225R^8$, which gives the desired relation (4.4) between the first non-universal correction to the energy and the first non-universal low energy S-matrix parameters or Wilson coefficients. See appendix C.6 for further details. (In $D = 3$, physical quantities only depend on the combination $\alpha_3 - \beta_3 = \gamma_3$.)

Since we bounded the later low energy parameters, see figures 4.1 and 4.3, we automatically obtain bounds on the Wilson coefficients and on the ground state energy. In three and four dimensions, for instance, we find the following bound on the deviation from the square root formula

$$\delta(3) = -\frac{32\pi^6\gamma_3}{225} \leq \frac{\pi^6}{5400} , \tag{4.21}$$

and

$$\delta(4) = -\frac{128\pi^6\alpha_3}{225} \leq \frac{\pi^6}{1350} - \frac{121\pi^4}{16200} . \tag{4.22}$$

Note that the right hand side of (4.22) is negative so the square root formula *must* be corrected; the right hand side of (4.21) is positive, in nice agreement with the fact that integrable $D = 3$ Strings have precisely $E_0^{\text{int}} = \sqrt{R^2 - \frac{\pi}{3}}$. Note also that the four dimensional bound (4.22) is saturated when $\beta_3 = 0$ (see figure 4.3) which corresponds to the particular point where integrability is preserved.

In fact, if we exploit the low energy integrability of the theory we can bypass the Lagrangian approach altogether and, by means of the so called Thermodynamic Bethe Ansatz (TBA), compute (4.3) in terms of the S-matrix.

This is particularly clean in $D = 3$ since there is only a single branon and a single corresponding pseudo-energy in this case. The ground state energy then reads

$$E_0(R) = R + \frac{1}{\pi R}\int_0^\infty dx\, \log(1 - e^{-\varepsilon(x)})\,, \tag{4.23}$$

where the pseudo-energy ε is the solution to the integral equation

$$\varepsilon(x) = x + \frac{1}{2\pi}\int_0^\infty \frac{dx'}{x'}\mathcal{K}\log(1 - e^{-\varepsilon(x')})\,, \tag{4.24}$$

with the kernel $\mathcal{K} = x'\frac{\partial}{\partial x'}\,\delta(\frac{4xx'}{R^2})$ and the phase shift is given by the low energy expansion (4.11). (The TBA aficionado might notice that this equation is a bit unusual; in terms of $x = e^\theta$ we see that a *sum* of rapidities shows up as opposed to the more conventional *difference*. This is because of the pure L/R scattering of our problem.) Expanding the pseudo-energy as

$$\varepsilon(x) = x + \frac{a(x)}{R^2} + \frac{b(x)}{R^4} + \frac{c(x)}{R^6} + \mathcal{O}\left(\frac{1}{R^8}\right)\,, \tag{4.25}$$

and collecting powers of R we can straightforwardly find all the functions $a, b, c, \ldots$ and hence the ground state energy,

$$E_0 = R - \frac{\pi}{6R} - \frac{\pi^2}{72R^3} - \frac{\pi^3}{432R^5} - \frac{5\pi^4}{10368R^7} - \frac{32\pi^6\gamma_3}{225R^7} + \ldots \tag{4.26}$$

We recognize that the first five terms are precisely the expansion of the square root in (4.3) while the last term is nothing but (4.4) with $D = 3$ and $\alpha_3 - \beta_3 \equiv \gamma_3$.

For $D = 4$ we can proceed in the same fashion as long as we restrict ourselves to the integrable subspace $\beta_3 = 0$. In this case, we get a set of TBA equations [67] which can also be simplified into a single equation and solved in a large R expansion, see appendix C.5.1 for details.

Next we have excited states which we can analyze in a similar way, either through perturbation theory or through the *excited state* TBA. Of particular relevance is the level splitting between the first few energy levels since this degeneracy lifting is a sharp signature of the non-universal terms. For instance, in $D = 3$ the first level splitting between the second and third excited states (in the zero momentum sector) reads

$$\begin{aligned} &E_{2\,\text{branons}}(2,-2) - E_{4\,\text{branons}}(1,1,-1,-1) \\ &\quad = -\frac{2455552\pi^6\gamma_3}{5R^7} + O\left(1/R^9\right)\,, \end{aligned} \tag{4.27}$$

where the arguments refer to the individual mode numbers. The basic logic that goes into computing (4.27) is analogous to the derivation of (4.26), therefore the details are

given in appendix C.5.2. There we also establish the bound on (4.27), that immediately follows from (4.15), and comment on potential comparisons with LMC data in the future.

Note that in our current logic, we can not completely ignore the Lagrangian since we are exploiting the thermodynamic Bethe ansatz, which only allows us to relate the S-matrix and the energy levels when the system is integrable. It should be possible – and very interesting – to relate more generally the various energy levels with the two-to-two S-matrix, together with all higher point amplitudes of non-integrable theories. The Lüscher corrections [79] provide the leading term and generalized Lüscher corrections have been recently explored e.g. in [80]. Perhaps the recent rederivation of the TBA in more diagrammatic terms, see e.g. [81], can provide some insights for such putative description. Or, developing the approach of [82] for the flux tube may turn out useful. It would be great to adapt these ideas to our setup and re-derive (4.22) without expanding around the integrable theory.

4.4 Resonances

Given the bounds in figures 4.1 and 4.3 it is natural to ask which S-matrices lie on those boundaries. This is particularly relevant in 4D since Lattice MC shows a rich phenomenology, with the presence of a parity odd resonance [70, 71], dubbed QCD worldsheet axion in the S-matrix approach to the long flux tube [66, 67].

In $D = 3$ we can find the S-matrices at the boundary of figure 4.1 analytically. Given that in this case there is no strong evidence for resonances from the lattice data, we present this analysis in appendix C.2.4. Furthermore, ref. [83] suggests that indeed the $D = 3$ QCD Flux-Tube has no resonances, in appendix C.7 we discuss how our bounds can be improved if we incorporate this further assumption into the analytic properties of the S-matrix. Finally, let us mention that at the cusp of figure 4.1 $S_{\text{cusp}} = (8i - s)/(8i + s)$. Nicely, this is an important S-matrix, albeit in a different context: it describes the RG flow from the tricritical Ising fixed point to the free fermion theory [84]. [7]

Next we turn to $D = 4$, where the boundary must be studied numerically. Here we find some remarkable surprises. A first nice surprise is that the S-matrices which saturate the bound have zeros, which physically correspond to resonances. Figure 4.4 describes the position of these resonances in the anti-symmetric channel as we move along the boundary of figure 4.3. Depending on whether we are to the right or left of the integrable $\beta_3 = 0$ point, there is one ($\beta_3 < 0$) or two zeros there ($\beta_3 > 0$). As we move along the boundary in the region $\beta_3 > 0$, the sharpest of these resonances passes spot on by the values of the worldsheet axion. The two dots correspond to estimates based on $SU(3)$ [66, 67] and $SU(5)$ [83] lattice MC simulations [70]. Because of these encouraging

[7] Precisely, $S_{\text{Goldstino}} = -S_{\text{cusp}}$, where the overall minus sign could be easily incorporated in the formulas of the main text.

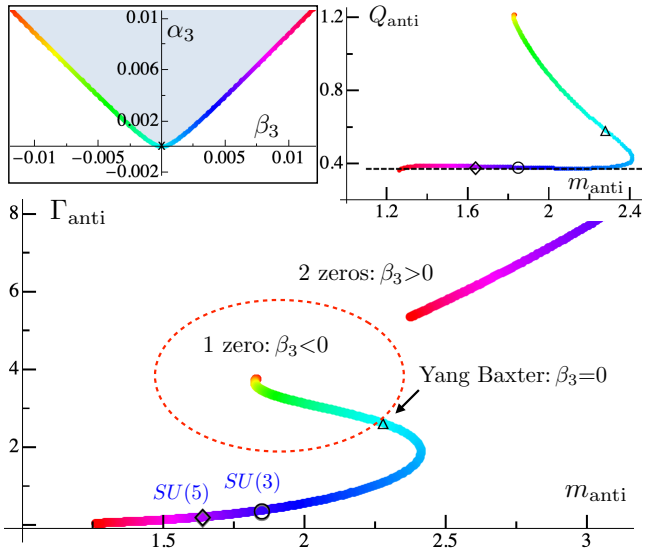

Figure 4.4: At the S-matrix space boundary we encounter S-matrices with zeros, that is resonances. In the antisymmetric channel, to the left of the integrable point there is one single resonance while to the right of the integrable point there are two resonances, a broad one and a sharp one. Curiously, as we move along the boundary we encounter S-matrices whose resonance mass and with are in precise agreement with those predicted in [67, 83] as extracted from $SU(3)$ (right point) and $SU(5)$ (left point) lattice data.

numerical coincidences we will denote these two points along the boundary as the $SU(3)$ point and $SU(5)$ point.

Remarkably, at these points, we find other zeros in the S-matrices. One broader resonance shows up in the same anti-symmetric channel along with a resonance in each of the other two channels. The spectrum, measured as $s_0 = (m + i\Gamma/2)^2$ at the position $S_{rep}(s_0) = 0$, for the $SU(3)$ and $SU(5)$ points is given by

spectrum $[m, \Gamma]$	$SU(3)$	$SU(5)$
axion	[1.85, 0.39]	[1.64, 0.22]
axion*	[3.25, 8.84]	[2.83, 7.02]
symmetron	[2.36, 4.99]	[2.34, 4.54]
dilaton	[1.88, 3.37]	[1.84, 3.52]

Even though these values should obviously be taken as benchmark values only, could these resonances be further excitations present in the Yang-Mills long flux tubes? Of course, these explorations must be taken with a grain of salt since there is a priori no strong reason for the real flux tube to be close to the boundary (recall that these S-matrices cannot represent the elastic scattering of branons all the way up to the UV since particle production kicks in eventually [74]).

Furthermore, we find that the axion coupling to the world-sheet branons $Q \approx \sqrt{8\Gamma}/m^{5/2}$ (valid for $\Gamma \ll m$) shows a plateau for almost all the values of $\beta_3 > 0$, apart from an initial transient. The value of this plateau surprisingly coincides within a good numerical accuracy with $Q_{\text{integrable}} = \sqrt{7/(16\pi)}$ [83]. The integrable value of Q is fixed by demanding that the presence of the axion results in a vanishing $2 \to 4$ scattering amplitude as the axion mass goes to zero. It is plausible, given our current numerical explorations, that this plateau holds all the way up to $\beta_3 \to \infty$, where the axion becomes massless. Since the family of S-matrices we find, coincidentally, contain the $SU(3)$ and $SU(5)$ axions, it would be tempting to believe that all $SU(N)$ axions lie somewhere along the trajectory in figure 4.4 and a natural candidate for the large-N axion would be the massless resonance in the limit $\beta_3 \to \infty$. However, this is excluded by current lattice simulations [71] and it is an open question how to relate a "blind to color" S-matrix approach to the large-N limit. In appendix C.4.4 we give further details on the resonances.

Finally let us mention a small curiosity. The world-sheet axion is the sharpest excitation by far. One could imagine a dilation like excitation, governing the flux tube thickness, to be the lightest scalar mode in some flux tube theories. Could it be that perhaps the broad dilaton identified here becomes sharper in some other circumstances? As it turns out, there is a region where the dilaton and axion swap their roles; it is nothing but the reflection symmetry of figure 4.3 discussed in section 4.2.3. So it is natural to expect flux tube theories – albeit with very different physics – living on the left shore. The left and right shores of figure 4.3 can therefore also be called the dilaton and axion shores respectively. In recent QCD explorations [8] a boundary of the physical S-matrix of pions was analyzed and there also the two shores had somehow mirror physical properties (as far as which channels are attractive/repulsive, which ones contain the ρ particle etc); the two dimensional setup here highlights in a very sharp way some of the features which are quite challenging to probe numerically there.

5 Glueball-Branon Bootstrap

We consider the scattering between branons on a long flux tube in $3d$ [1] and a scalar glueball in the bulk. The presence of the long flux tube breaks the 3 dimensional Poincare group to the 2 dimensional one: ISO(1,1). We further assume that the full theory is Parity invariant which means that there is an additional Z_2 symmetry which is essentially a reflection about the flux tube.

We begin by describing the kinematics.

5.1 Kinematics

5.1.1 Branon states

One particle branon states $|p\rangle$ are normalized according to

$$\langle p'|p\rangle = (2\pi)2|p|\delta(p-p') \tag{5.1}$$

where p refers to the spatial momentum of the branon states, $p > 0$ for right-movers and $p < 0$ for left-movers. Since the branons are massless $E = |p|$.

It is then straightforward to describe two branon states:

$$\langle p_3, p_4|p_1, p_2\rangle = (2\pi)^2(2|p_1|)(2|p_2|)\left(\delta(p_1-p_3)\delta(p_1-p_4) + 3 \leftrightarrow 4\right) \tag{5.2}$$

Branon states have eigenvalue $(-1)^N$ under the Z_2 symmetry, where N is the number of branons. In particular, the two branon state is Z_2 invariant.

[1] We stick to $3d$ for simplicity.

5.1.2 Glueball states

One particle glueball states are labelled by their mass m, p which is their spatial momentum in the direction of the flux tube and q is their transverse momentum:

$$|m, p, q, +\rangle \tag{5.3}$$

The energy of the glueball is given by $E = (p^2 + q^2 + m^2)^{1/2}$. The '+' sign in the states above indicates that these states are the Z_2 even combination of glueball states: $|m, p, q, +\rangle = \frac{1}{\sqrt{2}} (|m, p, q\rangle + |m, p, -q\rangle)$ [2]. These single glueball states are normalized as follows:

$$\langle m, p', q', +|m, p, q, +\rangle = (2\pi)^2(2E)\delta(p - p')\delta(q - q'). \tag{5.4}$$

Due to the above fact, we restrict $q \geq 0$.

5.2 Scattering amplitudes

We define the interacting part of the S matrix via the equation

$$S = \mathbf{1} + iT \tag{5.5}$$

Scattering amplitudes are now defined as matrix elements of the T matrix:

Branon-Branon amplitude

$$\langle p_3, p_4|T|p_1, p_2\rangle = (2\pi)^2\delta^{(2)}(p_1^a + p_2^a - p_3^a - p_4^a)M(s) \tag{5.6}$$

Here $s = -(p_1 + p_2)^2$.

Glueball-Glueball amplitude

$$\langle m, p_2, q_2, +|T|m, p_1, q_1, +\rangle = (2\pi)^2\delta^{(2)}(p_1^a - p_2^a)G(s) \tag{5.7}$$

For a glueball state, $p_i^a = (E_i, p_i)$ and q_i is fixed by the mass shell condition. Note that $s = E_i^2 - p_i^2 = q_i^2 + m^2$.

Glueball-Branon amplitude

$$\langle m, p_3, q_3, +|T|p_1, p_2\rangle = (2\pi)^2\delta^{(2)}(p_1^a + p_2^a - p_3^a)F(s) \tag{5.8}$$

[2] Z_2 invariance implies that there is no scattering of two branon states to the Z_2 odd glueball states.

CPT invariance implies that the amplitude for incoming glueball going to two outgoing branons is the same as the above amplitude:

$$\langle p_1, p_2|T|m, p_3, q_3, +\rangle = (2\pi)^2\delta^{(2)}(p_1^a + p_2^a - p_3^a)F(s) \tag{5.9}$$

5.3 Properties of the amplitudes

5.3.1 Crossing symmetry

Crossing relates the s channel branon-branon amplitude to the t channel:

$$M(-s) = M(s) \tag{5.10}$$

5.3.2 Unitarity

The unitarity of the S matrix $S^\dagger S = \mathbf{1}$ implies that the T matrix satisfies $-i(T - T^\dagger) = T^\dagger T$. We can now take appropriate matrix elements of this equation and plugging in a complete set of states on the right hand side we get the following unitarity relations [3]:

$$2\,\mathrm{Im}\,M(s) = \frac{1}{2s}|M(s)|^2 + \frac{1}{2\sqrt{s-m^2}}|F(s)|^2\Theta(s-m^2) + ... \tag{5.11}$$

$$2\,\mathrm{Im}\,G(s) = \frac{1}{2\sqrt{s-m^2}}|G(s)|^2\Theta(s-m^2) + \frac{1}{2s}|F(s)|^2 + ... \tag{5.12}$$

$$2\,\mathrm{Im}\,F(s) = \frac{1}{2\sqrt{s-m^2}}G^*(s)F(s)\Theta(s-m^2) + \frac{1}{2s}F^*(s)M(s) + ... \tag{5.13}$$

These equations hold for $s > 0$ and the ... correspond to contributions from four or higher particle branon states and multi-particle glueball states.

We can write the above equations in matrix form as follows:

$$2\,\mathrm{Im}\,\mathbb{M} \succeq \mathbb{M}^\dagger\rho\mathbb{M} \tag{5.14}$$

where the matrix $\mathbb{M}$ is given by:

$$\mathbb{M} = \begin{pmatrix} M & F \\ F & G \end{pmatrix} \tag{5.15}$$

[3] For the derivation, see appendix D.1

and the matrix ρ is given by:

$$\rho = \begin{pmatrix} \frac{1}{2s}\Theta(s) & 0 \\ 0 & \frac{1}{2\sqrt{s-m^2}}\Theta(s-m^2) \end{pmatrix} \tag{5.16}$$

The unitarity condition in equation 5.14 is equivalent to the following semi-definite condition:

$$\begin{pmatrix} \mathbf{1} & \sqrt{\rho}\mathbb{M} \\ (\sqrt{\rho}\mathbb{M})^\dagger & 2\,\mathrm{Im}\,\mathbb{M} \end{pmatrix} \succeq 0 \tag{5.17}$$

5.3.3 Analyticity

We assume that the only non-analyticities are the ones mandated by unitarity and crossing, which means that we expect that the branon-branon scattering amplitude $M(s)$ has a branch cut all across the real line $s \in R$. The glueball-glueball amplitude $G(s)$ and glueball-branon amplitude $F(s)$ just have a cut on the positive real axis $s \geq 0$.

Moreover, the amplitudes are real analytic:

$$M(s^*) = [M(s)]^* \tag{5.18}$$
$$G(s^*) = [G(s)]^* \tag{5.19}$$
$$F(s^*) = [F(s)]^* \tag{5.20}$$

5.4 Numerics

In this section we will set the glueball mass $m = 1$.

5.4.1 Mapping the functions to unit disk

For the branon-branon amplitude, we use the same map as before:

$$s \to \chi = \frac{4+is}{4-is} \tag{5.21}$$

For the glueball-branon and glueball-glueball amplitude, we use the ρ map:

$$s \to \rho = \frac{\sqrt{-s_0}-\sqrt{-s}}{\sqrt{-s_0}+\sqrt{-s}} \tag{5.22}$$

where $s_0 < 0$ can be chosen arbitrarily. (For example we could chose it to be -1 in units of m^2.)

5.4.2 Taylor expansion in terms of χ and ρ variables

From analyticity and crossing, we have the following properties:

$$\begin{aligned} M(-s^*) &= [M(s)]^* \\ G(s^*) &= [G(s)]^* \\ F(s^*) &= [F(s)]^* \end{aligned} \tag{5.23}$$

in terms of the χ and ρ variables this translates to [4]:

$$\begin{aligned} M(\chi^*) &= [M(\chi)]^* \\ G(\rho^*) &= [G(\rho)]^* \\ F(\rho^*) &= [F(\rho)]^* \end{aligned} \tag{5.24}$$

Therefore we make the following Taylor expansions:

$$\begin{aligned} M(\chi) &= \sum_{j=1}^{N} c_j (\chi - 1)^j \\ G(\rho) &= \sum_{j=0}^{N} g_j \, (\rho - 1)^j \\ F(\rho) &= \sum_{j=0}^{N} f_j \, (\rho - 1)^j \end{aligned} \tag{5.25}$$

here all the coefficients are real as a result of equation 5.24.

To simplify the relation between the coefficients c_j, g_j and f_j and the coefficients in an expansion in powers of s, we expand around $\chi = 1$ and $\rho = 1$.

5.4.3 Relation to low energy $s \to 0$ expansion

In $2d$, there is a simple relation between the full 2 to 2 amplitude $S(s)$ and interacting amplitude $M(s)$:

$$S(s) = 1 + \frac{i}{2s} M(s) \tag{5.26}$$

[4] Here we have used the fact that $\chi(-s^*) = \chi(s)^*$ and $\rho(s^*) = \rho(s)^*$

Since we fixed the glueball mass $m = 1$, the string length l_s is a parameter in the low energy expansion:

$$2\delta(s) = \frac{s}{4\,l_s^2} + \mathcal{O}(s^2) \tag{5.27}$$

where $S(s) = e^{2i\delta(s)}$, this implies that the two branon amplitude in the χ plane has the following leading behaviour at $\chi = 1$:

$$M(\chi) = -\frac{2}{l_s^2}(\chi - 1)^2 + \mathcal{O}((\chi - 1)^3) \tag{5.28}$$

Comparing with (5.25), we see that this means that $c_0 = c_1 = 0$ and $c_2 = -\frac{2}{l_s^2}$. For the glueball-glueball amplitude $G(s)$ and branon-glueball amplitude $F(s)$, we assume the following behavour at low energy, taking inspiration from low energy EFT:

$$G(s) = \tilde{g}s + \frac{\lambda^2}{16\pi m} s \log s \tag{5.29}$$

and

$$F(s) = \frac{\lambda}{2\sqrt{m}} s \tag{5.30}$$

This behaviour comes from the simplest interaction we can write between the glueball field ϕ and the branon field π: $\lambda\phi\,(\partial\pi)^2$. Since $s \sim (\rho - 1)^2$, the f_2 coefficient is a measure of the strength of coupling of the glueball to the flux tube so an interesting question we can ask is - what is the allowed space in f_2 vs l_s?

5.4.4 Slow glueball $s \to m^2$

We can also consider the point $s \to m^2$. We can re-write the unitarity equations 5.11 and 5.12 in the following form where the left hand sides are the probabilities of two branon to two branon scattering and glueball transmission respectively:

$$\begin{aligned} \left|1 + \frac{iM(s)}{2s}\right|^2 &= 1 - \frac{|F(s)|^2}{4s\sqrt{s - m^2}}\Theta(s - m^2) - \dots, \qquad s \geq 0 \\ \left|1 + \frac{iG(s)}{2\sqrt{s - m^2}}\right|^2 &= 1 - \frac{|F(s)|^2}{4s\sqrt{s - m^2}} - \dots, \qquad s \geq m^2 \end{aligned} \tag{5.31}$$

Thus the behaviour of $G(s)$ near $s = m^2$ is directly related to the probability of transmission of a very slow moving glueball.

The simplest behaviour consistent with the above unitarity equations is to have

$$\begin{aligned} M(s) &\sim (s - m^2)^0 \\ G(s) &\sim (s - m^2)^{1/2} \\ F(s) &\sim (s - m^2)^{1/4} \end{aligned} \tag{5.32}$$

The point $s = m^2$ is far from the regime of validity of the low energy EFT but we can use non-relativistic QM to see what the amplitudes behave like. This is a good approximaton because the glueball has low momenta near this point.

NR approximation for glueball transmission near $s = m^2$

Due to translational symmetry along the flux tube we can ignore one of the dimensions and therefore we have a $1d$ NRQM problem with a delta function potential:

$$V(x) = \alpha\delta(x) \tag{5.33}$$

This is of course a standard problem in QM, only thing we have to remember is that our scattering states are the parity invariant combination of plane wave states:

$$\psi_+(x) = e^{-iq|x|} + S_g(q)e^{iq|x|} \tag{5.34}$$

where q is the transverse momentum and $S_g(q)$ is the scattering amplitude for the glueball.

$$S_g(q) = \frac{2iq + \alpha}{2iq - \alpha} = -1 - \frac{4iq}{\alpha} + \dots \tag{5.35}$$

We can expand for small q and use the fact that $S_g(q) = 1 + \frac{iG(s)}{2\sqrt{s-m^2}}$

$$G(s) = 4i\sqrt{s - m^2} - \frac{8q\sqrt{s - m^2}}{\alpha} + \dots \tag{5.36}$$

where the transverse momentum $q = \sqrt{s - k^2 - m^2}$. So it appears that the leading behaviour of the glueball transmission amplitude is fixed and independent of the coupling to the flux tube.

5.4.5 Future plans

We intend use our numerical ansatz (5.25) to estimate the allowed space in glueball coupling λ as a function of string length l_s. In addition we plan to follow [85] and formulate the corresponding dual problem which would allow us to approach the optimum bound from both the allowed (primal) and the disallowed (dual) side.

Conclusion

In this thesis we extended the modern S-matrix Bootstrap program in two ways. In part I, we generalized the numerical approach of [4] to particles with any spin and mass in four space-time dimensions. Prior to our work, the S-matrix bootstrap had only been used to study scattering of scalar particles in various contexts in four spacetime dimensions. This thesis therefore unlocks a much broader class of scattering problems to be studied using the S-matrix bootstrap. We then used our formalism to find novel bounds on the quartic and Yukawa couplings of identical Majorana fermions. Our work paves the way for investigations of more physically relevant systems such as pion-nucleon scattering. This would give access to observables such as the mass of the deuteron.

We could also consider pure Yang-Mills which have stable glueballs (both with and without spin). We could bootstrap the scattering amplitude of these particles and see if the $SU(3)$ theory has a special place near the boundary of the allowed space of these scattering amplitudes.

Another direction of future study would be massless Majorana fermions. This could be used to derive bounds on the low energy effective field theories for massless Goldstinos [86, 87].

In part I, we also analysed the scattering of photons and we will shortly bound the space of low energy effective field theories of photons.

One could try to repeat the same for gravitons. However in four dimensions, we run into IR divergences which actually implies that the usual S-matrix does not exist. One way to bypass this would be to work in higher dimensions, say five spacetime dimensions.

Of course the general idea to bound low energy effective field theory using the consistency and UV completeness of the S-matrix is not new [20–33]. The numerical techniques we use in this thesis are in some sense a systematic method to optimize such bounds.

In this context, we would like to comment that our numerical problem is formulated as a primal problem, in the language of convex optimization. In other words at each step we construct consistent S-matrices and approach the boundary of the space of S-matrices

from the inside. In the dual approach, at each step physically inconsistent S-matrices are ruled out. The dual formulation of the S-matrix bootstrap was recently set up for 2d systems in [85] and for scalars in 4d in [88]. Generalizing this to Majorana particles in 4d and then comparing with our primal bounds in (2.93) and figures 2.5 and 2.6 would be very interesting.

In part II of the thesis, we found a new application of S-matrix bootstrap techniques, using them to constrain the non-universal corrections to dynamics of flux tubes. These bounds also apply to any string-like object that exhibits the same symmetry breaking pattern.

A possible direction of future study would be to specialize further and use input from lattice studies of Yang-Mills flux tubes to narrow down the space of flux-tube S-matrices. By studying the space it should be possible to in turn make predictions for the lattice [5].

Another possibility which we also pursue in part II is to input (and extract) information about Yang-Mills theory by including scattering to glueballs in the bulk with the flux tube.

Having listed some concrete problems that can be treated using the methods used in this thesis, we now discuss some more open directions of future research.

Open directions

The modern S-matrix bootstrap while still in the nascent stage, has already proven to be remarkably successful in 2d where many integrable theories have been found to lie on the boundary of allowed space of S-matrices [3,7,11]. Note that the S-matrices of these integrable theories in 2d were already known. However in 4d spacetime, we do not yet have even a single example of a non-perturbatively defined scattering amplitude. Finding such an S-matrix would be a fantastic outcome for the S-matrix bootstrap. More pragmatically, one can hope to find perturbative scattering amplitudes lying on or close to the boundary of allowed space of theories.

We must also remark on the additional features of S-matrices in four dimensions that we do not yet describe with the modern S-matrix bootstrap. As pointed out in [14] the properties of elastic unitarity and particle production are important aspects of scattering amplitudes. In particular, they would be crucial in the endeavour of finding examples of non-perturbative physical S-matrices.

In addition we know from theories such as QCD that there exist bounds states of spin $J \geq 2$. At present there is no easy way to include such bound states in the numerical ansatz we use for the S-matrix bootstrap. This problem is related to that of including

[5] See appendix C.4.3 for a sample of such a study

Regge trajectories in the S-matrix bootstrap since it is known that a spin $J \geq 2$ bound state or resonance must lie on a Regge trajectory of higher spin bound states/resonances [89].

We could also ask about theories with massless particles which are not free in the IR, such as QED. In these cases the usual S-matrix is not defined and instead one needs to consider the "dressed" S-matrix [90]. However hardly anything is known about the analytic structure of these dressed S-matrices. On a related note, celestial CFT correlators were proposed as more natural objects for the study of scattering involving photons and gravitons in [91].

It is curious to note that while there have been a large number of studies of the S-matrix bootstrap in two and four spacetime dimensions, the case of 2+1d scattering has been mostly neglected until now. Recall that in 2+1d, particles no longer have to be either bosons or fermions and can in fact be anyons [92]. As shown by computations in Chern-Simons-matter theories [93], crossing equations have to be modified to account for non-trivial phases of anyon statistics. It would interesting to develop a relativistic S-matrix theory for these anyons. A related problem with applications to quantum computation is the system of $3+1d$ photons coupled to $2+1d$ anyons on the boundary [94].

On the technical side, the results on the analyticity of scattering amplitudes that we quoted in part I are from the 70s. Perhaps it is time to revisit them more seriously and try to improve them either using newer developments in multi-variable complex analysis or by using our improved understanding of QFTs from the past 50 years. In this regard it may be fruitful to consider scattering amplitudes as the flat space limit of AdS boundary correlators. A concrete position-space prescription to extract scattering amplitudes from boundary correlators was given recently in [95]. It might be possible to leverage the proven boundedness and analyticity properties of these correlators to deduce analyticity of flat space amplitudes.

Appendices Part

A Appendices to spinning S-matrix bootstrap

A.1 Details of working with spin

In this appendix we provide many technical details which support the discussion in the main text of part I of the thesis. We start in appendix A.1.1 by reviewing 3d Euclidean rotations and then move to the discussion of the Poincaré group in appendix A.1.2. These cover most of the basics required in section 1.1. We define the vector and spinor representations in appendix A.1.3. Finally we derive the Wigner angles in a particular situation (crucial for appendix A.5.4) in appendix A.1.4.

A.1.1 Euclidean rotations in 3d

Rotations in $3d$ are generated by three generators J_1, J_2 and J_3 which satisfy the algebra

$$[J_i, J_j] = i\epsilon_{ijk}J_k\,. \tag{A.1}$$

Physically, these three generators correspond to infinitesimal rotations about the 3 axes. The Casimir operator which commutes with all the generators is

$$J^2 \equiv J_1^2 + J_2^2 + J_3^2, \qquad [J^2, J_i] = 0. \tag{A.2}$$

Any generic rotation can be written as

$$R(\theta_i) = \exp\left(-\sum_{k=1}^{3} i\theta_k J_k\right). \tag{A.3}$$

For our purposes a more useful way to write a rotation is to use the Euler angles (α, β, γ) instead of angles θ_i. A generic rotation in the Euler form reads as

$$R(\alpha, \beta, \gamma) \equiv \exp(-i\alpha J_3)\exp(-i\beta J_2)\exp(-i\gamma J_3). \tag{A.4}$$

The Euler angles α, β and γ can be related to the θ_i angles in (A.3). We do not write this relation explicitly since it is complicated and not very illuminating.

In quantum mechanical theories, the classical group of symmetries gets extended and therefore in the case at hand, we need to consider the central extension of $SO(3)$ which is the $SU(2)$ group. Henceforth when we talk about rotations we will mean the $SU(2)$ group. The unitary representations of the $SU(2)$ are finite-dimensional and are classified by the eigenvalue of the Casimir operator J^2. The usual basis for these representations is formed by choosing eigenvectors of the J_3 operator and thus these vectors are labelled by two parameters ℓ and λ:

$$\begin{aligned} J^2|\ell,\lambda\rangle &= \ell(\ell+1)|\ell,\lambda\rangle, \\ J_3|\ell,\lambda\rangle &= \lambda|\ell,\lambda\rangle, \end{aligned} \tag{A.5}$$

where ℓ is a non-negative integer or half-integer and $\lambda = -\ell, -\ell+1, \ldots, \ell-1, \ell$.

Given such a spin ℓ representation, a generic rotation parametrized using Euler angles as in (A.4) acts on it in the following way

$$R(\alpha,\beta,\gamma)|\ell,\lambda\rangle = \sum_{\lambda} |\ell,\lambda'\rangle\langle\ell,\lambda'|R|\ell,\lambda\rangle = \sum_{\lambda'} \mathscr{D}^{\ell}_{\lambda'\lambda}(\alpha,\beta,\gamma)|\ell,\lambda'\rangle, \tag{A.6}$$

where in the first equality we inject an identity operator as a sum over all the states and in the second equality we have defined the Wigner $\mathscr{D}$-matrix

$$\mathscr{D}^{\ell}_{\lambda'\lambda}(\alpha,\beta,\gamma) \equiv \langle\ell,\lambda'|R(\alpha,\beta,\gamma)|\ell,\lambda\rangle = \exp\left(-i(\alpha\lambda'+\gamma\lambda)\right) \times d^{\ell}_{\lambda'\lambda}(\beta), \tag{A.7}$$

and the (small) Wigner d-matrix

$$d^{\ell}_{\lambda'\lambda}(\beta) \equiv \langle\ell,\lambda'|\exp(-i\beta J_2)|\ell,\lambda\rangle. \tag{A.8}$$

Since the rotation operator is unitary, the inverse of a rotation can be written in terms of the complex conjugate of a $\mathscr{D}$-matrix as

$$\langle\ell,\lambda'|R^{-1}(\alpha,\beta,\gamma)|\ell,\lambda\rangle = \langle\ell,\lambda|R(\alpha,\beta,\gamma)|\ell,\lambda'\rangle^* = \mathscr{D}^{\ell\,*}_{\lambda\lambda'}(\alpha,\beta,\gamma). \tag{A.9}$$

The general form of (A.8) has the following simple expression

$$\begin{aligned} d^{\ell}_{\lambda'\lambda}(\beta) = &\sqrt{(j+\lambda')!(j-\lambda')!(j+\lambda)!(j-\lambda)!} \\ &\times \sum_{\nu} (-1)^{\nu} \frac{(\cos(\beta/2))^{2j+\lambda-\lambda'-2\nu}\,(-\sin(\beta/2))^{\lambda'-\lambda+2\nu}}{\nu!(j-\lambda'-\nu)!(j+\lambda-\nu)!(\nu+\lambda'-\lambda)!}. \end{aligned} \tag{A.10}$$

Note that setting the λ' and λ indices to 0 gives the familiar Legendre polynomials

$$d^{\ell}_{00}(\beta) = P_{\ell}(\cos\beta). \tag{A.11}$$

The small Wigner d-matrix is real. From its explicit expression one can conclude

$$d^{\ell}_{\lambda'\lambda}(\beta) = (-1)^{\lambda'-\lambda} d^{\ell}_{-\lambda',-\lambda}(\beta) = (-1)^{\lambda'-\lambda} d^{\ell}_{\lambda\lambda'}(\beta). \tag{A.12}$$

As a consequence we also have

$$\mathscr{D}^{\ell *}_{\lambda'\lambda}(\alpha,\beta,\gamma) = (-1)^{\lambda'-\lambda} \mathscr{D}^{\ell}_{-\lambda',-\lambda}(\alpha,\beta,\gamma). \tag{A.13}$$

The Wigner D-matrix satisfies the following important orthogonality relations

$$\sum_{\lambda'} \mathscr{D}^{\ell *}_{\lambda'\lambda_2}(\alpha,\beta,\gamma) \mathscr{D}^{\ell}_{\lambda'\lambda_1}(\alpha,\beta,\gamma) = \delta_{\lambda_1\lambda_2}, \tag{A.14}$$

$$\int_0^{2\pi} d\alpha \int_{-1}^{+1} d\cos\beta \int_0^{2\pi} d\gamma \; \mathscr{D}^{\ell_1 *}_{\lambda_1'\lambda_1}(\alpha,\beta,\gamma) \mathscr{D}^{\ell_2}_{\lambda_2'\lambda_2}(\alpha,\beta,\gamma) = \frac{8\pi^2}{2\ell_1+1} \delta_{\ell_1\ell_2}\delta_{\lambda_1'\lambda_2'}\delta_{\lambda_1\lambda_2}. \tag{A.15}$$

The small Wigner d matrix satisfies the following orthogonality condition instead

$$\int_0^{\pi} d\beta \sin\beta \, d^{\ell_1}_{\lambda'\lambda}(\beta) d^{\ell_2}_{\lambda'\lambda}(\beta) = \frac{2}{2\ell_1+1} \delta_{\ell_1\ell_2} \tag{A.16}$$

Since the spin ℓ representations described above are unitary, the dual representation is the same as the complex conjugate representation and moreover, as the spin ℓ representations are irreducible, the complex conjugate representations are also irreducible. We denote the basis of states in the dual spin ℓ representation by

$$|\ell,\lambda'\rangle^{\text{dual}}.$$

Under rotations they transform as

$$R(\alpha,\beta,\gamma)|\ell,\lambda\rangle^{\text{dual}} = \sum_{\lambda'} \mathscr{D}^{\ell *}_{\lambda'\lambda}(\alpha,\beta,\gamma)|\ell,\lambda'\rangle^{\text{dual}}. \tag{A.17}$$

The dual representations are actually equivalent to the standard spin ℓ representations. In order to show that let us rewrite (A.13) in the following form

$$\mathscr{D}^{\ell *}_{\lambda'\lambda}(\alpha,\beta,\gamma) = \sum_{\lambda_1,\lambda_2} \left(U^{-1}\right)_{\lambda'\lambda_1} \mathscr{D}^{\ell}_{\lambda_1\lambda_2}(\alpha,\beta,\gamma) U_{\lambda_2\lambda}, \tag{A.18}$$

where we have defined

$$\begin{aligned} U_{\lambda'\lambda} &\equiv d^{\ell}_{\lambda'\lambda}(+\pi) = (-1)^{\ell-\lambda}\delta_{\lambda',-\lambda}, \\ \left(U^{-1}\right)_{\lambda'\lambda} &= (-1)^{\ell+\lambda}\delta_{\lambda',-\lambda}. \end{aligned} \tag{A.19}$$

In order to confirm that $U^{-1}U = UU^{-1} = 1$ and to show the results below, notice the

following identity

$$1 = (-1)^{2(\ell \pm \lambda)}, \tag{A.20}$$

which holds true since $\ell \pm \lambda$ is always an integer. Using (A.19) we can then relate the basis states in two representation as follows

$$|\ell, \lambda\rangle^{\text{dual}} = \sum_{\lambda'} U_{\lambda'\lambda} |\ell, \lambda'\rangle = (-1)^{\ell-\lambda} |\ell, -\lambda\rangle. \tag{A.21}$$

In order to show this, we simply rotate both sides of (A.21). It then follows that

$$\begin{aligned} R(\alpha,\beta,\gamma)|\ell,\lambda\rangle^{\text{dual}} &= \sum_{\lambda',\lambda''} \mathscr{D}^{\ell}_{\lambda''\lambda'}(\alpha,\beta,\gamma) U_{\lambda'\lambda} |\ell,\lambda''\rangle \\ &= \sum_{\mu,\lambda',\lambda'',\lambda'''} U_{\lambda''\mu} \left(U^{-1}\right)_{\mu\lambda'''} \mathscr{D}^{\ell}_{\lambda'''\lambda'}(\alpha,\beta,\gamma) U_{\lambda'\lambda} |\ell,\lambda''\rangle \\ &= \sum_{\mu,\lambda''} U_{\lambda''\mu} \mathscr{D}^{\ell *}_{\mu\lambda}(\alpha,\beta,\gamma) |\ell,\lambda''\rangle \\ &= \sum_{\mu} \mathscr{D}^{\ell *}_{\mu\lambda}(\alpha,\beta,\gamma) |\ell,\mu\rangle^{\text{dual}}. \end{aligned} \tag{A.22}$$

Where in the first line we used (A.6), in the second line we inserted the identity, we used (A.18) in the third line and finally we used (A.21) in the fourth line. Thus we see that the identification (A.21) leads consistently to (A.17).

A.1.2 Poincaré group

We now consider the group of symmetries of Minkowski space *i.e.* the Poincaré group. We begin by recalling its defining representation, mainly to set the notation, and then we recall its algebra and unitary representations.

Defining representation

Given a 4-vector

$$x^{\mu} \equiv \{t, \vec{x}\}, \quad \mu = 0, 1, 2, 3, \tag{A.23}$$

one can define the following transformation

$$x^{\mu} \longrightarrow x'^{\mu} = a^{\mu} + \Lambda(\omega)^{\mu}{}_{\nu} x^{\nu}, \tag{A.24}$$

where a^{μ} and $\omega_{\rho\sigma}$ are Lie parameters of the transformation. The transformation matrix Λ obeys the constraint

$$\eta^{\mu\nu} = \Lambda^{\mu}{}_{\rho} \Lambda^{\nu}{}_{\sigma} \eta^{\rho\sigma}, \quad \eta_{\mu\nu} = \{-+++\}, \tag{A.25}$$

where $\eta_{\mu\nu}$ is the metric. This implies that $\omega_{\rho\sigma} = -\omega_{\sigma\rho}$.

The transformations (A.24) form the Poincaré group, which is also known as the inhomogeneous Lorentz group. It is denoted by

$$ISO(1,3) \equiv R^{1,3} \rtimes O(1,3), \qquad O(1,3) = SO^{+}(1,3) \rtimes P \rtimes T, \tag{A.26}$$

where $R^{1,3}$ is the group of 4d Minkowski translations, $SO^{+}(1,3)$ is the proper orthochronous Lorentz group and P and T are discrete transformations called parity and time reversal which act on the coordinates as follows

$$x^{\mu} \longrightarrow (t, -\vec{x}), \quad x^{\mu} \longrightarrow (-t, \vec{x}). \tag{A.27}$$

We restrict the $O(1,3)$ group to its $SO^{+}(1,3)$ subgroup by requiring that the generic Lorentz transformation $\Lambda(a,\omega)$ obeys

$$\det \Lambda = +1, \quad \Lambda^{0}{}_{0} \geq +1. \tag{A.28}$$

We require our quantum system to be invariant only under the restricted Poincaré group denoted by

$$ISO^{+}(1,3) \equiv R^{1,3} \rtimes SO^{+}(1,3). \tag{A.29}$$

Parity or time reversal symmetry may or may not be present. The discussion above was about the classical group of symmetries. Once again, in quantum mechanical theories the Lorentz group $SO(1,3)$ is centrally extended to its double-cover, the $SL(2,\mathbb{C})$ group.

Poincaré Algebra

A generic Poincaré transformation can be written in terms of infinitesimal generators

$$U(a,\omega) = \exp(-ia_{\mu}P^{\mu})\Lambda(\omega), \quad \Lambda(\omega) \equiv \exp\left(-\frac{i}{2}\,\omega_{\rho\sigma}M^{\rho\sigma}\right). \tag{A.30}$$

Here P^{μ} and $M^{\rho\sigma}$ are the generators of translations and $4d$ Lorentz tranformations respectively. The generators satisfy the following algebra

$$[P_{\mu}, P_{\nu}] = 0, \tag{A.31}$$
$$[M_{\mu\nu}, P_{\lambda}] = i\,(\eta_{\mu\lambda}P_{\nu} - \eta_{\nu\lambda}P_{\mu}), \tag{A.32}$$
$$[M_{\mu\nu}, M_{\lambda\sigma}] = i\,(\eta_{\mu\lambda}M_{\nu\sigma} - \eta_{\nu\lambda}M_{\mu\sigma} + \eta_{\mu\sigma}M_{\lambda\nu} - \eta_{\nu\sigma}M_{\lambda\mu}). \tag{A.33}$$

There are two Casimir operators which commute with all the generators, they are

$$C_1 \equiv -P^2, \quad C_2 \equiv W^2, \quad W^{\mu} \equiv \epsilon^{\mu\nu\rho\sigma}M_{\nu\rho}P_{\sigma}. \tag{A.34}$$

where W^μ is called the Pauli-Lubanski pseudovector. Using the definitions (A.34) and the commutation relations (A.31) and (A.32) we can write[1]

$$W^2 = -2\, M_{\mu\nu} M^{\nu\mu}\, C_1 - 4\, P_\mu M^{\mu\nu} M_{\nu\sigma} P^\sigma. \tag{A.36}$$

Let us consider the purely Lorentz part $\Lambda(\omega)$ of the generic Poincaré transformation (A.30). It is convenient to split it into two parts. First, we define boosts

$$B(\vec{\eta}) \equiv \exp\left(-i\eta_i K^i\right), \quad K^i \equiv M^{0i}, \quad \eta_i \equiv \omega_{0i}, \tag{A.37}$$

where K^i are the three boost generators. Second, we define rotations

$$R(\vec{\theta}) \equiv \exp\left(-i\theta_i J^i\right), \quad J^i \equiv \frac{1}{2}\epsilon^{ijk} M^{jk}, \quad \theta_i \equiv \epsilon_{ijk}\omega_{jk}, \tag{A.38}$$

where J^i are the generators of rotations around ith axis and θ_i are the angles of rotations around the ith axis. For completeness we also write explicitly

$$\vec{J} = \{M^{23},\, M^{31},\, M^{12}\}, \quad \vec{\theta} = \{\omega^{23},\, \omega^{31},\, \omega^{12}\}. \tag{A.39}$$

Pure rotations form an $SO(3)$ subgroup of the Lorentz group which one can verify by computing the algebra of the operators $\vec{J} = \{M^{23},\, M^{31},\, M^{12}\}$ and seeing that it matches (A.1). In terms of boost and rotation generator the Lorentz algebra (A.33) can be rewritten as

$$[J_i, J_j] = +i\epsilon_{ijk} J_k, \quad [J_i, K_j] = +i\epsilon_{ijk} K_k, \quad [K_i, K_j] = -i\epsilon_{ijk} J_k. \tag{A.40}$$

We can use the above commutation relations along with the Baker-Campbell-Hausdorff formula

$$e^{\xi A} B e^{-\xi A} = B + \xi[A, B] + \frac{\xi^2}{2}[A, [A, B]] + \ldots \tag{A.41}$$

to get commutation relations between finite boosts and rotations. We list here three such relations that will turn out to be useful later

$$e^{-iJ_2\theta} e^{-iK_3\eta} e^{iJ_2\theta} = e^{-i(K_3\cos\theta + K_1\sin\theta)\eta}, \tag{A.42}$$

$$e^{-iJ_2\theta} e^{-iJ_3\phi} e^{iJ_2\theta} = e^{-i(J_3\cos\theta + J_1\sin\theta)\phi}, \tag{A.43}$$

$$e^{-iJ_3\phi} e^{-iJ_2\theta} e^{iJ_3\phi} = e^{-i(J_2\cos\phi - J_1\sin\phi)\theta}. \tag{A.44}$$

[1]The Lorentzian 4d epsilon symbol $\epsilon^{\mu\nu\lambda\sigma}$ is fully antisymmetric. It is defined by $\epsilon^{0123} = -\epsilon_{0123} = +1$. Instead the Euclidean 4d epsilon symbol obeys instead $\epsilon^{1234} = \epsilon_{1234} = +1$. It has the following property

$$\sum_{a=1}^{4} \epsilon^{abcd}\epsilon_{ab'c'd'} = \delta^b_{b'}\delta^c_{c'}\delta^d_{d'} - \delta^b_{b'}\delta^c_{d'}\delta^d_{c'} - \delta^b_{c'}\delta^c_{b'}\delta^d_{d'} + \delta^b_{c'}\delta^c_{d'}\delta^d_{b'} - \delta^b_{d'}\delta^c_{c'}\delta^d_{b'} + \delta^b_{d'}\delta^c_{b'}\delta^d_{c'}. \tag{A.35}$$

In particular, we will use the following special cases of the above equations repeatedly

$$e^{\pm i\pi J_2} e^{-iK_3\eta} = e^{iK_3\eta} e^{\pm i\pi J_2}, \tag{A.45}$$

$$e^{\pm i\pi J_2} e^{-iJ_3\phi} = e^{iJ_3\phi} e^{\pm i\pi J_2}, \tag{A.46}$$

$$e^{\pm i\pi J_3} e^{-iJ_2\theta} = e^{iJ_2\theta} e^{\pm i\pi J_3}. \tag{A.47}$$

Unitary representation

We now review the unitary representation of the restricted Poincaré group $ISO^+(1,3)$. We refer to vectors in this representation as states. The unitary representation is characterized by the eigenvalues of two Casimirs $-P^2$ and W^2 as defined in (A.34).

Let us denote the eigenvalue of the first Casimir $-P^2$ by

$$c^2 = -P^2 = -p^2. \tag{A.48}$$

We focus on the case when $c^2 > 0$ only. We can chose the basis of states to be eigenvalues of $\vec{P}$. We denote such a basis by

$$|c, \vec{p}; \ldots\rangle, \tag{A.49}$$

where the dots stand for other labels yet to be discussed. Notice that the energy p^0 is related to c as

$$c^2 = -p^2 \quad \Rightarrow \quad p^0 = +\sqrt{c^2 + \vec{p}^2}. \tag{A.50}$$

Thus, we can also use p^0 instead of c to label the representation. There are two disconnected but equivalent regions for p^0 which can be related by time-reversal. We consider only positive energy states i.e those with $p^0 > 0$.

We now focus on the center of mass states, namely the states with $\vec{p} = 0$. We notice that 3d spatial rotations leave the $\vec{p} = 0$ condition invariant. This means that the set of states (A.49) with $\vec{p} = 0$ must furnish a representation of the $SU(2)$ group.[2] We often refer to this group as the Little group. $SU(2)$ representations were already discussed in section A.1.1. They are labeled by the (half)integer ℓ. The basis of states is labeled by the eigenvalues of the J_3 generator. We can thus fill the dots in (A.49) when $\vec{p} = 0$

$$|c, \vec{0}; \ell, \lambda\rangle. \tag{A.51}$$

Under 3d rotation the state (A.51) transforms according to (A.4),

$$R(\alpha,\beta,\gamma)|c, \vec{0}; \ell, \lambda\rangle = \sum_{\lambda'} \mathscr{D}^{\ell}_{\lambda'\lambda}(\alpha,\beta,\gamma)|c, \vec{0}; \ell, \lambda'\rangle. \tag{A.52}$$

[2]This follows for example from the equality $W^2|c, \vec{0}; \ldots\rangle = -4\, P^2 J^2\, |c, \vec{0}; \ldots\rangle$, which can be deduced using the results of appendix A.1.2. We see that the second Casimir W^2 for the center of mass states simply reduces to the J^2 Casimir of the $SU(2)$ group defined in (A.2).

We now need to define a basis of states with generic values of $\vec{p}$ from (A.51) by applying an appropriate Lorentz transformation which we denote by $U_h(\vec{p})$. In other words

$$|c,\vec{p};\ell,\lambda\rangle = U_{\rm h}(\vec{p})|c,\vec{0};\ell,\lambda\rangle. \tag{A.53}$$

The most convenient choice of the transformation $U_h(\vec{p})$ is as follows

$$U_{\rm h}(\vec{p}) = R(\phi,\theta,-\phi)\exp(-i\eta K_3), \tag{A.54}$$

where $(\phi,\theta,-\phi)$ are the three Wigner angles and η is the rapidity related to the four-momentum by (1.6). Here the boost generates a non-zero 3-momentum along the z-axis. The rotation then brings this 3-momentum to the required direction $\vec{p}$, where (ϕ,θ) are the spherical angles of $\vec{p}$.[3]

The choice (A.54) is known as the helicity boost and the basis (A.53) is known as the helicity basis. This name comes from the fact that the states are the eigenstates of the helicity operator defined as

$$\mathbb{H} \equiv (\vec{J}\cdot\vec{P}). \tag{A.55}$$

In other words one has

$$\mathbb{H}|c,\vec{p};\ell,\lambda\rangle = \lambda\,\boldsymbol{p}\,|c,\vec{p};\ell,\lambda\rangle, \tag{A.56}$$

where $\boldsymbol{p}$ is the length of $\vec{p}$. Moreover the helicity label λ remains invariant under any 3d rotation as can be seen from

$$\begin{aligned}
R(\alpha,\beta,\gamma)|c,\vec{p};\ell,\lambda;\gamma\rangle &= R(\alpha,\beta,\gamma)R(\phi,\theta,-\phi)B_3(\eta)|c,\vec{0};\ell,\lambda;\gamma\rangle\\
&= R(\alpha',\beta',\gamma')B_3(\eta)|c,\vec{0};\ell,\lambda;\gamma\rangle\\
&= R(\alpha',\beta',-\alpha')\exp(-i(\alpha'+\gamma')J_3)B_3(\eta)|c,\vec{0};\ell,\lambda;\gamma\rangle\\
&= \exp(-i\lambda(\alpha'+\gamma'))R(\alpha',\beta',-\alpha')B_3(\eta)|c,\vec{0};\ell,\lambda;\gamma\rangle\\
&= \exp(-i\lambda(\alpha'+\gamma'))U_h(\vec{p}\,')|c,\vec{0};\ell,\lambda;\gamma\rangle,\\
&= \exp(-i\lambda(\alpha'+\gamma'))|c,\vec{p}\,';\ell,\lambda;\gamma\rangle.
\end{aligned} \tag{A.57}$$

Here in the second line we use the fact two rotations give another rotation, and the parameters (α',β',γ') can be expressed in terms of $(\alpha,\beta,\gamma,\phi,\theta)$. In the fourth line we use the fact that J_3 commutes with K_3. Finally we obtain the three-momentum $\vec{p}\,'$ which has (α',β') spherical angles and $|\vec{p}\,'| = |\vec{p}\,|$. Thus, contrary to the rotations of the center of mass states (A.52), the rotation of a state in a generic frame with non-zero momentum $\vec{p}$ only changes the direction of its three-momentum but not its helicity. This can be understood intuitively since the helicities in the helicity eigenstates are always aligned with the three-momentum.

[3] Notice that a rotation $R(\phi,\theta,\gamma)$ with any value of γ would do the job. Such a rotation is 4π periodic in ϕ. With the particular choice $\gamma = -\phi$, the rotation becomes instead 2π periodic in ϕ, namely $R(\phi+2\pi,\theta,-(\phi+2\pi)) = R(\phi,\theta,-\phi)$.

Finally let us discuss transformation properties of the states (A.53) under a generic Poincaré transformation $U(a,\omega)$, where a and ω are its Lie parameters as discussed in appendix (A.1.2). One has

$$\begin{aligned} U(a,\omega)|c,\vec{p};\ell,\lambda;\gamma\rangle &= \exp(-ia_\mu P^\mu)\Lambda(\omega)|c,\vec{p};\ell,\lambda;\gamma\rangle \\ &= \exp(-ia_\mu P^\mu)U_{\rm h}(\vec{p}\,')U_{\rm h}(\vec{p}\,')^{-1}\Lambda(\omega)U_{\rm h}(\vec{p})|c,\vec{0};\ell,\lambda;\gamma\rangle \\ &= \exp(-ia_\mu P^\mu)U_{\rm h}(\vec{p}\,')R(\alpha,\beta,\gamma)|c,\vec{0};\ell,\lambda;\gamma\rangle \\ &= \exp(-ia_\mu p'^\mu)\sum_{\lambda'}\mathscr{D}^\ell_{\lambda'\lambda}(\alpha,\beta,\gamma)|c,\vec{p}\,';\ell,\lambda';\gamma\rangle. \end{aligned} \tag{A.58}$$

Here in the second line we inserted the identity operator in the form

$$\mathbb{I} = U_{\rm h}(\vec{p}\,')U_{\rm h}(\vec{p}\,')^{-1}. \tag{A.59}$$

The key point lies in the third line where we notice that the following product of Lorentz group elements is a pure rotation

$$R(\alpha(p,\omega),\beta(p,\omega),\gamma(p,\omega)) = U_{\rm h}(\vec{p}\,')^{-1}\Lambda(\omega)U_{\rm h}(\vec{p}), \quad p'^\mu \equiv \Lambda^\mu{}_\nu(w)p^\nu. \tag{A.60}$$

This can be seen as follows. The transformation (A.60) takes rest frame states to rest frames states in the following way: $\vec{0}\to\vec{p}\to\vec{p}\,'\to\vec{0}$. The rotation (A.60) is known as a Wigner rotation. In the third line of (A.58) we use (A.52). Finally the action of $U_h(\vec{p}\,')$ just sends the COM frame state to the helicity state with final momentum $\vec{p}\,'$.

The Wigner angles (α,β,γ) in the left-hand side of (A.60) are determined in terms of (p,ω). They can be computed for example by choosing a particular finite dimensional representation and comparing the final matrices in the left- and right-hand side of (A.60). However these expressions are too cumbersome to be presented in the most general case. In practice we only need to consider a few special cases. The most important one for our paper is discussed in appendix A.1.4.

Clebsch-Gordan coefficients

In this appendix we compute in detail the Clebsch-Gordan coefficient C^ℓ_λ defined in (1.23). For convenience let us recall its definition here

$$(2\pi)^4\delta^{(4)}(p^\mu - p_1^\mu - p_2^\mu)\delta_{\alpha\gamma}\times C^\ell_\lambda(\vec{p}_1,\vec{p}_2,\alpha) \equiv \langle c,\vec{p};\ell,\lambda;\gamma|\kappa_1,\kappa_2\rangle, \tag{A.61}$$

where κ_1 and κ_2 are the one-particle states (with masses m_1, m_2, spins j_1, j_2, helicities λ_1, λ_2 and three-momenta $\vec{p}_1$, $\vec{p}_2$) and α is the multiplicity label of the two-particle states which reads as

$$\alpha = (m_1,m_2,j_1,j_2,\lambda_1,\lambda_2). \tag{A.62}$$

Using it the decomposition of generic two particle states can be written as

$$|\kappa_1, \kappa_2\rangle = \sum_{\ell,\lambda} C^{\ell}_{\lambda}(\vec{p}_1, \vec{p}_2, \alpha)|c, \vec{p}; \ell, \lambda; \alpha\rangle. \tag{A.63}$$

We start by bringing the states in the right-hand side of (A.61) to the center of mass frame. This is done by injecting an identity operator

$$\mathbb{I} = U_{\mathrm{h}}(\vec{p})U_{\mathrm{h}}^{-1}(\vec{p}) \tag{A.64}$$

composed out of the helicity boosts (A.54) into the definition of the Clebsch-Gordan coefficient (A.61), we then have

$$C^{\ell}_{\lambda}(\vec{p}_1, \vec{p}_2) = C^{\ell}_{\lambda}(\vec{p}_1{}', -\vec{p}_1{}', \alpha) \times \mathscr{D}^{j_1}_{\lambda_1'\lambda_1}(\vec{\omega}_1)\mathscr{D}^{j_2}_{\lambda_2'\lambda_2}(\vec{\omega}_2). \tag{A.65}$$

The value of $\vec{p}$ in (A.64) is chosen in such a way that the inverse helicity boost $U_{\mathrm{h}}^{-1}(\vec{p})$ brings the pair of vectors $(\vec{p}_1, \vec{p}_2)$ to $(\vec{p}_1{}', -\vec{p}_1{}')$ which are in the center of mass frame. The Wigner angles $\vec{\omega}_1$ and $\vec{\omega}_2$ correspond to the Wigner rotations W_1 and W_2 defined as

$$W_i \equiv U_h^{-1}(\Lambda\vec{p}_i)\Lambda U_h(\vec{p}_i), \quad \Lambda = U_h^{-1}(\vec{p}). \tag{A.66}$$

In practice we never need the general expression (A.65). We will therefore not attempt to derive the Wigner angles $\vec{\omega}_1$ and $\vec{\omega}_2$. What we will need instead is the Clebsch-Gordan coefficient in the center of mass frame

$$C^{\ell}_{\lambda}(\vec{p}, -\vec{p}, \alpha), \tag{A.67}$$

which enters in the right-hand side of (A.65). Notice that we dropped the primes and the subscripts compared to (A.65). Recalling the definition of the two-particle center of mass states (1.26)

$$|(\boldsymbol{p}, \theta, \phi); \lambda_1, \lambda_2\rangle \equiv |m_1, \vec{p}; j_1, \lambda_1\rangle \otimes |m_2, -\vec{p}; j_2, \lambda_2\rangle, \tag{A.68}$$

where $(\boldsymbol{p}, \theta, \phi)$ are the spherical coordinates of $\vec{p}$, and using the definition (A.61) we can write the Clebsch-Gordan coefficient (A.67) as

$$(2\pi)^4\delta^{(4)}(0) \times C^{\ell}_{\lambda}(\vec{p}, -\vec{p}, \alpha) \equiv \langle c, \vec{0}; \ell, \lambda; \lambda_1, \lambda_2|(\boldsymbol{p}, \theta, \phi); \lambda_1, \lambda_2\rangle. \tag{A.69}$$

We also notice that the state (A.68) obeys the following relation

$$R(\phi, \theta, -\phi)|(\boldsymbol{p}, 0, 0); \lambda_1, \lambda_2\rangle = e^{-2i\phi\lambda_2}|(\boldsymbol{p}, \theta, \phi); \lambda_1, \lambda_2\rangle. \tag{A.70}$$

We prove it later in this section.

In order to compute the Clebsch-Gordan coefficient (A.69) we inject the identity operator

$$\mathbb{I} = R(\phi, \theta, -\phi) R^{-1}(\phi, \theta, -\phi) \tag{A.71}$$

in the right-hand side of (A.69). Due to (A.52) and (A.70) the matrix element in the right-hand side of (A.69) becomes

$$\begin{aligned} \langle c, 0, \ell, \lambda | (\boldsymbol{p}, \theta, \phi); \lambda_1, \lambda_2 \rangle &= e^{+2i\phi\lambda_2} \sum_{\lambda'} \mathscr{D}^{\ell}_{\lambda\lambda'}(\phi, \theta, -\phi) \ \langle c, 0, \ell, \lambda' | (\boldsymbol{p}, 0, 0); \lambda_1, \lambda_2 \rangle \\ &= e^{+2i\phi\lambda_2} \mathscr{D}^{\ell}_{\lambda\, \lambda_{12}}(\phi, \theta, -\phi) \ \langle c, 0, \ell, \lambda_{12} | (\boldsymbol{p}, 0, 0); \lambda_1, \lambda_2 \rangle. \end{aligned} \tag{A.72}$$

In the second line we have used the fact that the states here are eigenvectors of the J_3 generator and we have defined

$$\lambda_{12} \equiv \lambda_1 - \lambda_2. \tag{A.73}$$

Finally, we denote the matrix element in the right-hand side of the second line in (A.72) by

$$(2\pi)^4 \delta^{(4)}(0) \times C_\ell(\boldsymbol{p}) \equiv \langle c_1, 0, \ell, \lambda_{12} | (\boldsymbol{p}, 0, 0); \lambda_1, \lambda_2 \rangle. \tag{A.74}$$

As indicated, the coefficient $C_\ell(\boldsymbol{p})$ can only depend on the spin label ℓ and the length $\boldsymbol{p}$. Its value is fixed by the choice of normalization. We will derive it shortly. Plugging (A.72) and (A.74) into (A.69) we derive the final expression of the Clebsch-Gordan coefficient

$$C^{\ell}_{\lambda}(\vec{p}, -\vec{p}, \alpha) = C_\ell(\boldsymbol{p}) e^{+2i\phi\lambda_2} \mathscr{D}^{\ell}_{\lambda\, \lambda_{12}}(\phi, \theta, -\phi). \tag{A.75}$$

Using (A.75), see also (A.68), we can write the decomposition (A.63) in the center of mass frame. It reads

$$\begin{aligned} |(\boldsymbol{p}, \theta, \phi); \lambda_1, \lambda_2 \rangle &= e^{+2i\phi\lambda_2} \sum_{\ell, \lambda} C_\ell(\boldsymbol{p}) \ \mathscr{D}^{\ell}_{\lambda\lambda_{12}}(\phi, \theta, -\phi) | c, \vec{0}; \ell, \lambda; \alpha \rangle \\ &= \sum_{\ell, \lambda} C_\ell(\boldsymbol{p}) \ e^{i(\lambda_1 + \lambda_2 - \lambda)\phi} d^{\ell}_{\lambda\lambda_{12}}(\theta) | c, \vec{0}; \ell, \lambda; \alpha \rangle. \end{aligned} \tag{A.76}$$

We can invert the above equation using (A.15) and the orthogonality of the exponential function

$$|c, \vec{0}; \ell, \lambda; \alpha\rangle = \frac{2\ell + 1}{4\pi C_\ell(\boldsymbol{p})} \int_0^{2\pi} d\phi \int_{-1}^{+1} d\cos\theta e^{-i(\lambda_1 + \lambda_2 - \lambda)\phi} d^{\ell}_{\lambda\lambda_{12}}(\theta) | (\boldsymbol{p}, \theta, \phi); \lambda_1, \lambda_2 \rangle. \tag{A.77}$$

Derivation of (A.70)

Let us denote the vector $\vec{p}$ aligned with the direction of the z-axis by $\vec{p}_z$. Notice that as defined both $\vec{p}$ and $\vec{p}_z$ have the same length $\boldsymbol{p}$. Using the definition (A.68) we can write

$$R(\phi,\theta,-\phi)|(\boldsymbol{p},0,0);\lambda_1,\lambda_2\rangle = \\ (R(\phi,\theta,-\phi)|m_1,\vec{p}_z;j_1,\lambda_1\rangle)\otimes(R(\phi,\theta,-\phi)|m_2,-\vec{p}_z;j_2,\lambda_2\rangle)\,. \quad \text{(A.78)}$$

From (A.57) it is clear that the rotation operators bring the two one-particle states from $\vec{p}_z$ and $-\vec{p}_z$ configuration to the $\vec{p}$ and $-\vec{p}$ configuration with some additional phases ξ_1 and ξ_2. In other words

$$R(\phi,\theta,-\phi)|(\boldsymbol{p},0,0);\lambda_1,\lambda_2\rangle = e^{i(\xi_1+\xi_2)}|(\boldsymbol{p},\theta,\phi);\lambda_1,\lambda_2\rangle \quad \text{(A.79)}$$

The goal of this section is to compute the phases ξ_1 and ξ_2.

Let us start from the state with $\vec{p}_z$. Its spherical angles are $(0,0)$. Using the definition of the helicity basis (A.53) we can simply write

$$\begin{aligned} R(\phi,\theta,-\phi)|m_1,\vec{p}_z;j_1,\lambda_1\rangle &= R(\phi,\theta,-\phi)R(0,0,0)e^{-i\eta K_3}|m_1,\vec{0};j_1,\lambda_1\rangle \\ &= |m_1,\vec{p};j_1,\lambda_1\rangle. \end{aligned} \quad \text{(A.80)}$$

Thus, we conclude that

$$\xi_1 = 0. \quad \text{(A.81)}$$

Let us now address the state with $-\vec{p}_z$. According to (1.27) its spherical angles are (π,π) instead. Using again the definition of the helicity basis (A.53) we can write

$$\begin{aligned} R(\phi,\theta,-\phi)|m_2,\vec{p}_z;j_2,\lambda_2\rangle &= R(\phi,\theta,-\phi)R(\pi,\pi,-\pi)e^{-i\eta K_3}|m_2,\vec{0};j_2,\lambda_2\rangle \\ &= R(\pi+\phi,\pi-\theta,-\pi-\phi)e^{-2i\phi J_3}e^{-i\eta K_3}|m_2,\vec{0};j_2,\lambda_2\rangle \\ &= e^{-2i\phi\lambda_2}|m_2,-\vec{p};j_2,\lambda_2\rangle. \end{aligned} \quad \text{(A.82)}$$

In the second line of (A.82) we have repeatedly used the identities (A.46) and (A.47). In the last line we have used the fact that J_3 and K_3 commute and that the center of mass state is the eigenstate of the J_3 generator. Thus, we conclude that

$$\xi_2 = -2\lambda_2\phi. \quad \text{(A.83)}$$

Combining (A.79) with (A.81) and (A.83) we arrive at the desired property (A.70).

Computation of (A.74)

The coefficient $C_\ell(\boldsymbol{p})$ in (A.74) is fixed by the normalization condition (1.14). In what follows we carefully compute it. Using (1.20) and performing the change of variables, see appendix A of [13] for details, we get

$$\langle \kappa_1', \kappa_2' | \kappa_1, \kappa_2 \rangle = (2\pi)^6 4 p_1^0 p_2^0 \, \delta^{(3)}(\vec{p}_1' - \vec{p}_1) \delta^{(3)}(\vec{p}_2' - \vec{p}_2) \delta_{\alpha'\alpha} \tag{A.84}$$

$$= (2\pi)^6 4 \sqrt{\frac{-p^2}{\boldsymbol{p}^2}} \, \delta^{(4)}(p'^\mu - p^\mu) \delta(\cos\theta' - \cos\theta) \delta(\phi' - \phi) \delta_{\alpha'\alpha}, \tag{A.85}$$

where α is given by (A.62) and

$$\delta_{\alpha'\alpha} \equiv \delta_{m_1' m_1} \delta_{m_2' m_2} \delta_{j_1' j_1} \delta_{j_2' j_2} \delta_{\lambda_1' \lambda_1} \delta_{\lambda_2' \lambda_2}. \tag{A.86}$$

Now let us take the norm of both sides of (A.77) and use (1.22) and (A.85) to get

$$\begin{aligned} \delta_{\ell'\ell} \, \delta_{\lambda'\lambda} \, \delta_{\gamma'\gamma} = \left(\frac{2\ell+1}{4\pi |C_\ell(\boldsymbol{p})|} \right)^2 (2\pi)^2 4 \sqrt{\frac{-p^2}{\boldsymbol{p}^2}} \\ \times \int_0^{2\pi} d\phi \int_{-1}^{+1} d\cos\theta e^{-i(\lambda_1+\lambda_2-\lambda)\phi} d^\ell_{\lambda\lambda_{12}}(\theta) \\ \times \int_0^{2\pi} d\phi' \int_{-1}^{+1} d\cos\theta' e^{i(\lambda_1'+\lambda_2'-\lambda')\phi'} d^\ell_{\lambda'\lambda_{12}'}(\theta') \\ \times \delta(\cos\theta' - \cos\theta) \delta(\phi' - \phi) \delta_{\alpha'\alpha}. \end{aligned} \tag{A.87}$$

The delta functions over the angular coordinates removes two of the integrals and sets $\phi' = \phi$ and $\cos\theta' = \cos\theta$. We can then use the orthogonality of the small Wigner d matrix (A.16) along with the orthogonality of the exponential function to obtain

$$1 = \left(\frac{2\ell+1}{4\pi |C_\ell(\boldsymbol{p})|} \right)^2 (2\pi)^2 4 \sqrt{\frac{-p^2}{\boldsymbol{p}^2}} \, \frac{4\pi}{2\ell+1}. \tag{A.88}$$

Noticing that in the center of mass frame $-p^2 = c^2$, we immediately get

$$|C_\ell(\boldsymbol{p})|^2 = 4\pi(2\ell+1) \times \frac{c}{\boldsymbol{p}}. \tag{A.89}$$

The phase of the $C_\ell(\boldsymbol{p})$ coefficient is unobservable. In all the final formulas it will enter in the form (A.89). Thus we can simply set this phase to zero and obtain the final expression

$$C_\ell(\boldsymbol{p}) = \sqrt{4\pi(2\ell+1) \times \frac{c}{\boldsymbol{p}}}. \tag{A.90}$$

A.1.3 Finite dimensional Lorentz representations

Let us discuss two particular finite-dimensional representations on the Lorentz group, namely the vector and spinor representations.

Vector representation

The generators of the Lorentz transformation (A.30) obey the algebra (A.33). In the vector representation of the Lorentz group, the generators satisfying (A.33) can be written as

$$\left[M^{\mu\nu}\right]_{\rho\sigma} = -i\left(\delta^{\mu}{}_{\rho}\delta^{\nu}{}_{\sigma} - \delta^{\mu}{}_{\sigma}\delta^{\nu}{}_{\rho}\right) \quad \Rightarrow \quad \left[M^{\mu\nu}\right]^{\rho}{}_{\sigma} = -i\left(\eta^{\mu\rho}\delta^{\nu}_{\sigma} - \delta^{\mu}_{\sigma}\eta^{\nu\rho}\right). \tag{A.91}$$

According to (A.37) and (A.38) they split into generators of boosts and rotations as

$$\begin{aligned}
\left[K^1\right]^{\rho}{}_{\sigma} &= i\begin{pmatrix} 0 & +1 & 0 & 0 \\ +1 & 0 & 0 & 0 \\ 0 & 0 & 0 & 0 \\ 0 & 0 & 0 & 0 \end{pmatrix}, & \left[J^1\right]^{\rho}{}_{\sigma} &= -i\begin{pmatrix} 0 & 0 & 0 & 0 \\ 0 & 0 & 0 & 0 \\ 0 & 0 & 0 & +1 \\ 0 & 0 & -1 & 0 \end{pmatrix}, \\
\left[K^2\right]^{\rho}{}_{\sigma} &= i\begin{pmatrix} 0 & 0 & +1 & 0 \\ 0 & 0 & 0 & 0 \\ +1 & 0 & 0 & 0 \\ 0 & 0 & 0 & 0 \end{pmatrix}, & \left[J^2\right]^{\rho}{}_{\sigma} &= -i\begin{pmatrix} 0 & 0 & 0 & 0 \\ 0 & 0 & 0 & -1 \\ 0 & 0 & 0 & 0 \\ 0 & +1 & 0 & 0 \end{pmatrix}, \\
\left[K^3\right]^{\rho}{}_{\sigma} &= i\begin{pmatrix} 0 & 0 & 0 & +1 \\ 0 & 0 & 0 & 0 \\ 0 & 0 & 0 & 0 \\ +1 & 0 & 0 & 0 \end{pmatrix}, & \left[J^3\right]^{\rho}{}_{\sigma} &= -i\begin{pmatrix} 0 & 0 & 0 & 0 \\ 0 & 0 & +1 & 0 \\ 0 & -1 & 0 & 0 \\ 0 & 0 & 0 & 0 \end{pmatrix}.
\end{aligned} \tag{A.92}$$

Using (A.37) the matrices of finite transformations follow straightforwardly, for instance for the boost along the z-axis we get

$$B_3(\eta)^{\mu}{}_{\nu} = \begin{pmatrix} \cosh\eta & 0 & 0 & \sinh\eta \\ 0 & 1 & 0 & 0 \\ 0 & 0 & 1 & 0 \\ \sinh\eta & 0 & 0 & \cosh\eta \end{pmatrix}. \tag{A.93}$$

Similarly using (A.38) for the rotation around the y-axis and z-axis we get respectively

$$R_2(\beta)^{\mu}{}_{\nu} = \begin{pmatrix} 1 & 0 & 0 & 0 \\ 0 & \cos\beta & 0 & \sin\beta \\ 0 & 0 & 1 & 0 \\ 0 & -\sin\beta & 0 & \cos\beta \end{pmatrix}, \quad R_3(\gamma)^{\mu}{}_{\nu} = \begin{pmatrix} 1 & 0 & 0 & 0 \\ 0 & \cos\gamma & -\sin\gamma & 0 \\ 0 & \sin\gamma & \cos\gamma & 0 \\ 0 & 0 & 0 & 1 \end{pmatrix}. \tag{A.94}$$

In defining a 1PS we apply a boost along the positive direction of the z-axis to the particle at rest. The boost parameter can be found from

$$\begin{pmatrix} p^0 \\ 0 \\ 0 \\ \boldsymbol{p} \end{pmatrix} = B_3(\eta) \begin{pmatrix} m \\ 0 \\ 0 \\ 0 \end{pmatrix}, \qquad \eta \geq 0. \tag{A.95}$$

Using (A.93) we get

$$\cosh\eta = \frac{p^0}{m}, \quad \sinh\eta = \frac{\boldsymbol{p}}{m}. \tag{A.96}$$

Consider now a state with the three-momentum $\vec{p}$ constrained to the xz-plane

$$p^\mu = \{p^0, p_x, 0, p_z\}. \tag{A.97}$$

In terms of rapidity and spherical coordinates it is described by the following parameters

$$p^\mu : \quad (\eta, \theta). \tag{A.98}$$

The components of the vector (A.97) can be expressed in terms of the components (A.98) as

$$p^0 = m\cosh\eta, \quad \boldsymbol{p} = m\sinh\eta, \quad p_x = \boldsymbol{p}\sin\theta, \qquad p_z = \boldsymbol{p}\cos\theta. \tag{A.99}$$

By definition (1.5) the helicity state is constructed by applying (A.54) to the center of mass states. We have

$$\begin{pmatrix} p^0 \\ p_x \\ 0 \\ p_z \end{pmatrix} = U_{\mathrm{h}}(p) \begin{pmatrix} m \\ 0 \\ 0 \\ 0 \end{pmatrix}, \tag{A.100}$$

where in the vector representation the matrix $U_{\mathrm{h}}(p)$ reads as

$$U_{\mathrm{h}}(p) = R_2(\theta)B_3(\eta) = \begin{pmatrix} \cosh\eta & 0 & 0 & \sinh\eta \\ \sinh\eta\sin\theta & \cos\theta & 0 & \cosh\eta\sin\theta \\ 0 & 0 & 1 & 0 \\ \sinh\eta\cos\theta & -\sin\theta & 0 & \cosh\eta\cos\theta \end{pmatrix}. \tag{A.101}$$

Spinor representation

In order to define the spinor representation of the Lorentz group, we first define the 4×4 gamma matrices in our conventions[4]

$$\gamma^\mu \equiv \begin{pmatrix} 0 & \sigma^\mu \\ \bar{\sigma}^\mu & 0 \end{pmatrix}, \tag{A.102}$$

where

$$\sigma^\mu = (I, \vec{\sigma}) \quad \text{and} \quad \bar{\sigma}^\mu = (I, -\vec{\sigma}) \tag{A.103}$$

and $\vec{\sigma}$ are the usual 2×2 Pauli matrices:

$$\sigma_1 = \begin{pmatrix} 0 & 1 \\ 1 & 0 \end{pmatrix}, \quad \sigma_2 = \begin{pmatrix} 0 & -i \\ i & 0 \end{pmatrix}, \quad \sigma_3 = \begin{pmatrix} 1 & 0 \\ 0 & -1 \end{pmatrix}. \tag{A.104}$$

From the explicit form of the gamma matrices it is easy to verify that they satisfy

$$\{\gamma^\mu, \gamma^\nu\} = -2\eta^{\mu\nu}, \tag{A.105}$$

where $\{A, B\} \equiv AB + BA$ is the anti-commutator. We can now define the generators of the spinorial representation of the Lorentz group:

$$S^{\mu\nu} \equiv \frac{i}{4}[\gamma^\mu, \gamma^\nu]. \tag{A.106}$$

These generators satisfy the Lorentz algebra (A.33) and we can split them into boost generators $K^i = S^{0i}$ and rotation generators $J^i = \frac{1}{2}\epsilon^{ijk}S^{jk}$. For the reader's convenience, we write out these matrices explicitly

$$K^1 = \begin{pmatrix} 0 & -\frac{i}{2} & 0 & 0 \\ -\frac{i}{2} & 0 & 0 & 0 \\ 0 & 0 & 0 & \frac{i}{2} \\ 0 & 0 & \frac{i}{2} & 0 \end{pmatrix}, \quad K^2 = \begin{pmatrix} 0 & -\frac{1}{2} & 0 & 0 \\ \frac{1}{2} & 0 & 0 & 0 \\ 0 & 0 & 0 & \frac{1}{2} \\ 0 & 0 & -\frac{1}{2} & 0 \end{pmatrix}, \quad K^3 = \begin{pmatrix} -\frac{i}{2} & 0 & 0 & 0 \\ 0 & \frac{i}{2} & 0 & 0 \\ 0 & 0 & \frac{i}{2} & 0 \\ 0 & 0 & 0 & -\frac{i}{2} \end{pmatrix},$$

$$J^1 = \begin{pmatrix} 0 & \frac{1}{2} & 0 & 0 \\ \frac{1}{2} & 0 & 0 & 0 \\ 0 & 0 & 0 & \frac{1}{2} \\ 0 & 0 & \frac{1}{2} & 0 \end{pmatrix}, \quad J^2 = \begin{pmatrix} 0 & -\frac{i}{2} & 0 & 0 \\ \frac{i}{2} & 0 & 0 & 0 \\ 0 & 0 & 0 & -\frac{i}{2} \\ 0 & 0 & \frac{i}{2} & 0 \end{pmatrix}, \quad J^3 = \begin{pmatrix} \frac{1}{2} & 0 & 0 & 0 \\ 0 & -\frac{1}{2} & 0 & 0 \\ 0 & 0 & \frac{1}{2} & 0 \\ 0 & 0 & 0 & -\frac{1}{2} \end{pmatrix}.$$

[4]Note that we work in the Weyl (also known as chiral) basis for the gamma matrices.

Using (A.37) and (A.38) the matrices of finite transformations follow straightforwardly, for instance for a boost along the z-axis by rapidity η we get

$$B_3(\eta) = \begin{pmatrix} e^{-\frac{\eta}{2}} & 0 & 0 & 0 \\ 0 & e^{\eta/2} & 0 & 0 \\ 0 & 0 & e^{\eta/2} & 0 \\ 0 & 0 & 0 & e^{-\frac{\eta}{2}} \end{pmatrix}, \tag{A.107}$$

while for rotations about the y-axis by an angle θ we get

$$R_2(\theta) = \begin{pmatrix} \cos\left(\frac{\theta}{2}\right) & -\sin\left(\frac{\theta}{2}\right) & 0 & 0 \\ \sin\left(\frac{\theta}{2}\right) & \cos\left(\frac{\theta}{2}\right) & 0 & 0 \\ 0 & 0 & \cos\left(\frac{\theta}{2}\right) & -\sin\left(\frac{\theta}{2}\right) \\ 0 & 0 & \sin\left(\frac{\theta}{2}\right) & \cos\left(\frac{\theta}{2}\right) \end{pmatrix}. \tag{A.108}$$

In case of a rotation about the z-axis by an angle ϕ we have

$$R_3(\phi) = \begin{pmatrix} e^{-\frac{i\phi}{2}} & 0 & 0 & 0 \\ 0 & e^{\frac{i\phi}{2}} & 0 & 0 \\ 0 & 0 & e^{-\frac{i\phi}{2}} & 0 \\ 0 & 0 & 0 & e^{\frac{i\phi}{2}} \end{pmatrix}. \tag{A.109}$$

A.1.4 An example of the Wigner rotation

Consider now the vector (A.98) and the following Lorentz transformation applied to it

$$\Lambda = R_2(\psi_2)B_3(\chi)R_2(\psi_1), \quad \psi_i \in [0, \pi], \tag{A.110}$$

which implements a rotation around the y-axis by an angle ψ_1 followed by a boost along the positive z-axis with the rapidity parameter χ and another rotation around the y-axis by an angle ψ_2. As a result we get the following 4-momentum

$$p'^{\mu} = \Lambda^{\mu}{}_{\nu} p^{\nu} \tag{A.111}$$

which is described by the parameters

$$p'^{\mu}: \quad (\eta', \theta'). \tag{A.112}$$

and also lies in the xz-plane. The four-vector p'^{μ} can be generated using the helicity boost $U_{\mathrm{h}}(p') = U_{\mathrm{h}}(\eta', \theta')$ analogously to (A.100). The components of p'^{μ} can be found from (A.111). The values of (η', θ') in the helicity boost matrix then follow straightforwardly.

The Wigner rotation associated to generic Lorentz transformations are defined in (A.60). In case of the Lorentz transformation (A.110), upon plugging the above results in the

definition (A.60), we get the following explicit result

$$R_{\text{wigner}} = U_{\text{h}}^{-1}(p')\,\Lambda\,U_{\text{h}}(p) = \begin{pmatrix} 1 & 0 & 0 & 0 \\ 0 & \cos\omega & 0 & \sin\omega \\ 0 & 0 & 1 & 0 \\ 0 & -\sin\omega & 0 & \cos\omega \end{pmatrix}, \tag{A.113}$$

where the Wigner angle written in compact form read as

$$\cos\omega = \frac{p^0 p'^0 - m^2\cosh\chi}{\boldsymbol{p}\,\boldsymbol{p}'}, \quad \sin\omega = \frac{m\sinh\chi}{\boldsymbol{p}'}\,\sin(\theta+\psi_1). \tag{A.114}$$

The Wigner angle ω depends on five parameters $(\eta,\theta,\chi,\psi_1,\psi_2)$. The full form of the angle ω reads as

$$\cos\omega = \frac{A}{\sqrt{B^2-1}}, \quad \sin\omega = \frac{\sin(\theta+\psi_1)\sinh\chi}{\sqrt{B^2-1}}, \tag{A.115}$$

where we have defined

$$A \equiv \sinh\eta\cosh\chi + \cosh\eta\sinh\chi\cos(\theta+\psi_1), \tag{A.116}$$

$$B \equiv \cosh\eta\cosh\chi + \sinh\eta\sinh\chi\cos(\theta+\psi_1). \tag{A.117}$$

A.2 Parity and time-reversal

In this section we will discuss the discrete symmetries of the full Poincaré group, namely parity $\mathcal{P}$ and time-reversal $\mathcal{T}$.

A.2.1 Parity

Parity in the defining vector representation of the Lorentz group is given by the following matrix

$$\mathcal{P} = \begin{pmatrix} 1 & 0 & 0 & 0 \\ 0 & -1 & 0 & 0 \\ 0 & 0 & -1 & 0 \\ 0 & 0 & 0 & -1 \end{pmatrix}. \tag{A.118}$$

We denote the parity operator in the (infinite-dimensional) unitary representation by the same symbol $\mathcal{P}$. It obeys the following commutation relations with the generators of the Poincaré group

$$\mathcal{P}P^\mu\mathcal{P}^\dagger = (P^0,-\vec{P}), \quad \mathcal{P}K^i\mathcal{P}^\dagger = -K^i, \quad \mathcal{P}J^i\mathcal{P}^\dagger = J^i. \tag{A.119}$$

In what follows we will use (A.119) to derive the action of parity on one- and two-particle states. We will then derive constraints on the scattering amplitudes due to parity. Let us begin with the following preliminary computation of the parity transformation property of the helicity boost operator (A.54),

$$\begin{aligned}\mathcal{P}U_{\rm h}(\vec{p})\mathcal{P}^\dagger =&\mathcal{P}R(\phi,\theta,-\phi)\mathcal{P}^\dagger\mathcal{P}B_3(\eta)\mathcal{P}^\dagger\\ =&R(\phi,\theta,-\phi)B_3(-\eta)\\ =&R(\phi,\theta,-\phi)R(0,\pi,0)B_3(\eta)R^\dagger(0,\pi,0).\end{aligned}\tag{A.120}$$

Here in the first line we injected the identity $\mathbb{I}=\mathcal{P}^\dagger\mathcal{P}$, we then used the commutation properties (A.119) in the second line. Finally, in the third line we used (A.45).

One-particle states

Consider the action of parity on a one-particle state (1.13) in the rest frame. Since parity commutes with all of the rotation generators J_i, it must leave the helicity of the particle invariant.[5] Therefore the most general possible action is a simple multiplication by a phase which we denote by η. In other words

$$\mathcal{P}|m,\vec{0};j,\lambda\rangle=\eta|m,\vec{0};j,\lambda\rangle.\tag{A.121}$$

This phase η is called the intrinsic parity of the particle. Due to the discussion of section 3.3 in [17], one can always define parity operator $\mathcal{P}$ in such a way that either $\mathcal{P}^2=+1$ or $\mathcal{P}^2=-1$. As a result, applying (A.121) consecutively we conclude that

$$\eta^2=+1\quad\text{or}\quad\eta^2=-1.\tag{A.122}$$

We can now deduce the action of parity on a generic one-particle state (1.13), see also (A.53). One has

$$\begin{aligned}\mathcal{P}|m,\vec{p};j,\lambda\rangle&=\mathcal{P}U_h(\vec{p})|m,\vec{0};j,\lambda\rangle\\ &=\mathcal{P}U_h(\vec{p})\mathcal{P}^\dagger\mathcal{P}|m,\vec{0};j,\lambda\rangle\\ &=\eta R(\phi,\theta,-\phi)R(0,\pi,0)B_3(\eta)R^\dagger(0,\pi,0)|m,\vec{0};j,\lambda\rangle\\ &=\eta(-1)^{j+\lambda}R(\phi,\theta,-\phi)R(0,\pi,0)B_3(\eta)|m,\vec{0};j,-\lambda\rangle.\end{aligned}\tag{A.123}$$

Here in the third line we used (A.120) and (A.121), instead in the fourth line we used (A.52), (A.6) and the following property of the small Wigner d-matrix

$$d^j_{\lambda'\lambda}(-\pi)=(-1)^{j+\lambda'}\delta_{-\lambda,\lambda'}.\tag{A.124}$$

[5] This can be seen by applying parity to the eigenvector conditions (A.5).

Next, by repeatedly using (A.46) and (A.47) one can show that

$$R(\phi,\theta,-\phi)R(0,\pi,0) = R(\phi+\pi,\pi-\theta,-(\phi+\pi))e^{-i(2\pi+2\phi)J_3}. \tag{A.125}$$

Inserting this relation into (A.123) and using the fact that J_3 commutes with K_3 and that the $\vec{p}=0$ state is the eigenstate of J_3 we conclude that

$$\begin{aligned}\mathcal{P}|m,\vec{p};j,\lambda\rangle &= \eta(-1)^{j+\lambda}e^{+i(2\pi+2\phi)\lambda}R(\phi+\pi,\pi-\theta,-(\phi+\pi))B_3(\eta)|m,\vec{0};j,-\lambda\rangle \\ &= \eta(-1)^{j+3\lambda}e^{2i\lambda\phi}U_h(-\vec{p})|m,\vec{0};j,-\lambda\rangle \\ &= \eta(-1)^{j-\lambda}e^{2i\lambda\phi}|m,-\vec{p};j,-\lambda\rangle.\end{aligned} \tag{A.126}$$

Here in the second line we used (1.27) and (A.54). In the third line we used (A.53) and the fact that

$$e^{4i\pi\lambda} = e^{4i\pi j} = +1 \tag{A.127}$$

for any λ and j which are integer or half-integer. Summarizing, the final expression for the action of the parity operator on a one-particle states reads as

$$\mathcal{P}|m,\vec{p};j,\lambda\rangle = \eta(-1)^{j-\lambda}e^{2i\lambda\phi}|m,-\vec{p};j,-\lambda\rangle. \tag{A.128}$$

Two-particle COM states

From the action of parity on one-particle states (A.128), one can conclude the action of parity on two-particle center of mass states defined in (1.26). One has

$$\begin{aligned}\mathcal{P}|(\boldsymbol{p},\theta,\phi),\lambda_1,\lambda_2\rangle &= \mathcal{P}\left(|m_1,\vec{p};j_1,\lambda_1\rangle\otimes|m_2,-\vec{p};j_2,\lambda_2\rangle\right) \\ &= \eta_1\eta_2(-1)^{j_1-\lambda_1}(-1)^{j_2-\lambda_2}e^{2i\phi\lambda_1}e^{2i(\phi+\pi)\lambda_2}|m_1,-\vec{p};j_1,-\lambda_1\rangle\otimes|m_2,\vec{p};j_2,-\lambda_2\rangle \\ &= \eta_1\eta_2(-1)^{j_1-j_2-\lambda_1-\lambda_2}e^{2i\phi(\lambda_1+\lambda_2)}|(\boldsymbol{p},\pi-\theta,\phi+\pi),-\lambda_1,-\lambda_2\rangle,\end{aligned}$$

where η_1 and η_2 are the intrinsic parities of the first and the second particle respectively. Notice also that in the third line we used for the second particle the identity

$$1 = e^{2\pi i(\lambda\pm j)}, \tag{A.129}$$

which holds true since $\lambda\pm j$ is always an integer. To summarize, we have

$$\mathcal{P}|(\boldsymbol{p},\theta,\phi),\lambda_1,\lambda_2\rangle = \eta_1\eta_2(-1)^{j_1-j_2-\lambda_1-\lambda_2}e^{2i\phi(\lambda_1+\lambda_2)}|(\boldsymbol{p},\pi-\theta,\phi+\pi),-\lambda_1,-\lambda_2\rangle. \tag{A.130}$$

In principle (A.130) is our final answer. However, for applications to scattering amplitudes we need to bring (A.130) to a different form. We focus on the case where $\phi=0$,

when (A.130) simplifies to

$$\mathcal{P}|(\boldsymbol{p},\theta,0),\lambda_1,\lambda_2\rangle = \eta_1\eta_2(-1)^{j_1-j_2-\lambda_1-\lambda_2}|(\boldsymbol{p},\pi-\theta,\pi),-\lambda_1,-\lambda_2\rangle. \tag{A.131}$$

Here the two-particle state in the right-hand side by definition reads as

$$|(\boldsymbol{p},\pi-\theta,\pi),-\lambda_1,-\lambda_2\rangle = |m_1,-\vec{p},j_1,-\lambda_1\rangle\otimes|m_2,\vec{p},j_2,-\lambda_2\rangle, \tag{A.132}$$

where the three-vector $\vec{p}$ has $(\theta,0)$ spherical angles and the three-vector $-\vec{p}$ has $(\pi-\theta,\pi)$ spherical angles. Using (A.46) and (A.47) one can derive the following relations

$$R(\pi,\pi-\theta,-\pi) = e^{-i\pi J_2}R(0,\theta,-2\pi), \tag{A.133}$$

$$R(0,\theta,0) = e^{-i\pi J_2}R(\pi,\pi-\theta,-\pi). \tag{A.134}$$

Using the definition of helicity states (A.53) and the relation (A.133) we conclude that the first one-particle state in (A.132) can be written as

$$\begin{aligned}|m_1,-\vec{p};j_1,-\lambda_1\rangle &= R(\pi,\pi-\theta,-\pi)B(\eta)|m_1,\vec{0};j_1,-\lambda_1\rangle\\ &= e^{-i\pi J_2}R(0,\theta,0)e^{2\pi i J_3}B_3(\eta)|m_1,\vec{0};j_1,-\lambda_1\rangle\\ &= e^{-2\pi i\lambda_1}e^{-i\pi J_2}R(0,\theta,0)B_3(\eta)|m_1,\vec{0};j_1,-\lambda_1\rangle\\ &= (-1)^{-2j_1}e^{-i\pi J_2}|m_1,\vec{p};j_1,-\lambda_1\rangle.\end{aligned} \tag{A.135}$$

In the third line we used the fact that J_3 commutes with K_3 and that the state with $\vec{p}=0$ is the eigenstate of J_3. In the last equality we used (A.129). Analogously using (A.134) for the second one-particle state in (A.132) we conclude that

$$|m_2,\vec{p};j_2,-\lambda_2\rangle = e^{-i\pi J_2}|m_2,-\vec{p};j_2,-\lambda_2\rangle. \tag{A.136}$$

Plugging (A.135) and (A.136) into (A.132) we obtain the following relation

$$|(\boldsymbol{p},\pi-\theta,\pi),-\lambda_1,-\lambda_2\rangle = (-1)^{-2j_1}e^{-i\pi J_2}|(\boldsymbol{p},\theta,0),-\lambda_1,-\lambda_2\rangle. \tag{A.137}$$

Finally, plugging (A.137) into (A.131) and using an obvious identity $(-1)^{-j-\lambda}=(-1)^{j+\lambda}$ which holds true since $j+\lambda$ is always an integer, we obtain the desired expression

$$\mathcal{P}|(\boldsymbol{p},\theta,0);\lambda_1,\lambda_2\rangle = \eta_1\eta_2(-1)^{j_1+j_2+\lambda_1+\lambda_2}e^{-i\pi J_2}|(\boldsymbol{p},\theta,0);-\lambda_1,-\lambda_2\rangle. \tag{A.138}$$

The benefit of this equation is that the states in the left- and right-hand side are in the same configuration contrary to (A.131).

Two-particle irreps

The two-particle states can be decomposed into states in the irreducible representation of the Poincaré group. We refer to them as the two-particle irreps. In the center of mass

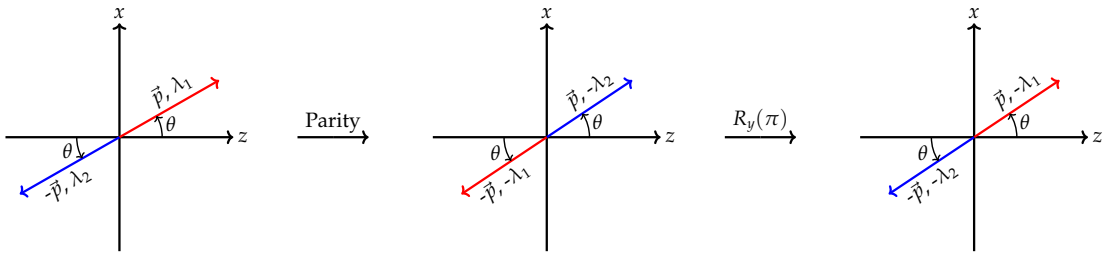

Figure A.1: The geometric picture behind (A.131) and (A.137). Particle 1 is red and particle 2 is blue.

frame such a decomposition and its inverse are given by (A.76) and (A.77) respectively. Applying parity to (A.77) and using (A.130) we get

$$\mathcal{P}|c,0;\ell,\lambda;\lambda_1,\lambda_2\rangle = \mathcal{N}\int_0^{2\pi} d\phi \int_0^{\pi} d\theta \sin\theta\, e^{-i\phi(\lambda_1+\lambda_2-\lambda)} d^{(\ell)}_{\lambda\lambda_{12}}(\theta)\mathcal{P}|(\boldsymbol{p},\theta,\phi);\lambda_1,\lambda_2\rangle \tag{A.139}$$

$$= \eta_{12}^{\text{com}}\mathcal{N}\int_0^{2\pi} d\phi \int_0^{\pi} d\theta \sin\theta\, e^{i(\lambda_1+\lambda_2+\lambda)\phi} d^{(\ell)}_{\lambda\lambda_{12}}(\theta)|(\boldsymbol{p},\pi-\theta,\phi+\pi),-\lambda_1,-\lambda_2\rangle,$$

where we have defined

$$\mathcal{N} \equiv \frac{2\ell+1}{4\pi C_\ell(\boldsymbol{p})}, \qquad \eta_{12}^{\text{com}} \equiv \eta_1\eta_2(-1)^{j_1-j_2-\lambda_1-\lambda_2}. \tag{A.140}$$

Changing the integration variables from θ and ϕ to $\theta' \equiv \pi-\theta$ and $\phi' \equiv \phi+\pi$, using the following property of the small Wigner d-matrix

$$d^{(\ell)}_{\lambda'\lambda}(\pi-\theta) = (-1)^{\ell+\lambda'} d^{(\ell)}_{\lambda',-\lambda}(\theta), \tag{A.141}$$

the second line of (A.139) can be written as

$$\mathcal{P}|c,0;\ell,\lambda;\lambda_1,\lambda_2\rangle = (-1)^{-\lambda_1-\lambda_2-\lambda}(-1)^{\ell+\lambda}\eta_{12}^{com}\mathcal{N}$$
$$\times \int_\pi^{3\pi} d\phi' \int_0^{\pi} d\theta' \sin\theta' e^{i(\lambda_1+\lambda_2+\lambda)\phi'} d^{(\ell)}_{\lambda,-\lambda_{12}}(\theta')|(p,\theta',\phi'),-\lambda_1,-\lambda_2\rangle. \tag{A.142}$$

Consider now a function $f(\phi)$ which is 2π periodic in ϕ. The following property then holds

$$\int_0^{2\pi} d\phi f(\phi) = \int_{\phi_0}^{\phi_0+2\pi} d\phi f(\phi) \tag{A.143}$$

for any real ϕ_0. We notice that both $e^{i(\lambda_1+\lambda_2+\lambda)\phi'}$ and $|(p,\theta',\phi'),-\lambda_1,-\lambda_2\rangle$ are 2π periodic in ϕ'. The former follows from the fact that $\lambda_1+\lambda_2+\lambda$ is always an integer. The latter follows from our definition of the helicity basis (A.54), see in particular footnote 3.

We can then use the definition (A.77) one more time to conclude that

$$\mathcal{P}|c,0;\ell,\lambda;\lambda_1,\lambda_2\rangle = (-1)^{-\lambda_1-\lambda_2-\lambda}(-1)^{\ell+\lambda}\eta_{12}^{\text{com}}|c,0;\ell,\lambda;-\lambda_1,-\lambda_2\rangle. \tag{A.144}$$

Plugging in (A.140) and using (A.129) the above can be brought to the following final form

$$\mathcal{P}|c,0;\ell,\lambda;\lambda_1,\lambda_2\rangle = \eta_1\eta_2(-1)^{\ell-j_1+j_2}|c,0;\ell,\lambda;-\lambda_1,-\lambda_2\rangle. \tag{A.145}$$

Constraints on scattering amplitudes

In parity invariant theories the scattering operators S and T obey

$$S = \mathcal{P}S\mathcal{P}^\dagger = \mathcal{P}^\dagger S\mathcal{P}, \qquad T = \mathcal{P}T\mathcal{P}^\dagger = \mathcal{P}^\dagger T\mathcal{P}. \tag{A.146}$$

Using (A.146) in the definition of the center of mass amplitude (1.61) we obtain the following constraint on the COM scattering amplitudes

$$\langle(\boldsymbol{p}',\theta,0);\lambda_3,\lambda_4|T|(\boldsymbol{p},0,0);\lambda_1,\lambda_2\rangle = \langle(\boldsymbol{p}',\theta,0);\lambda_3,\lambda_4|\mathcal{P}^\dagger T\mathcal{P}|(\boldsymbol{p},0,0);\lambda_1,\lambda_2\rangle. \tag{A.147}$$

Using (A.138) the right-hand side of this equation can be written as

$$\begin{aligned}\langle(\boldsymbol{p}',\theta,0);\lambda_3,\lambda_4|\mathcal{P}^\dagger T\mathcal{P}|(\boldsymbol{p},0,0);\lambda_1,\lambda_2\rangle = \eta_1\eta_2\eta_3^*\eta_4^*(-1)^{j_1+j_2+\lambda_1+\lambda_2}(-1)^{j_3+j_4+\lambda_3+\lambda_4}\\ \langle(\boldsymbol{p}',\theta,0);-\lambda_3,-\lambda_4|e^{i\pi J_2}Te^{-i\pi J_2}|(\boldsymbol{p},0,0);-\lambda_1,-\lambda_2\rangle.\end{aligned} \tag{A.148}$$

Plugging this into (A.147), using the fact the scattering operator T is invariant under rotations and invoking the definition of the COM amplitudes we obtain the final constraint

$$T_{12\to34}{}^{\lambda_3,\lambda_4}_{\lambda_1,\lambda_2}(s,t,u) = \eta_1\eta_2\eta_3^*\eta_4^*(-1)^{j_1+j_2+j_3+j_4}(-1)^{\lambda_1+\lambda_2+\lambda_3+\lambda_4}T_{12\to34}{}^{-\lambda_3,-\lambda_4}_{-\lambda_1,-\lambda_2}(s,t,u). \tag{A.149}$$

A.2.2 Time-reversal

In the defining vector representation time-reversal is given by the following matrix

$$\mathcal{T} = \begin{pmatrix} -1 & 0 & 0 & 0 \\ 0 & 1 & 0 & 0 \\ 0 & 0 & 1 & 0 \\ 0 & 0 & 0 & 1 \end{pmatrix}. \tag{A.150}$$

We use the same symbol $\mathcal{T}$ to denote the time-reversal operator in the (infinite-dimensional) unitary representation. Using (A.150) one can deduce the following commutation properties of the time-reversal operator with finite rotations and boosts in the unitary

representation

$$\mathcal{T}e^{-i\theta_i J_i}\mathcal{T}^\dagger = e^{-i\theta_i J_i} \quad \text{and} \quad \mathcal{T}e^{-i\eta_i K_i}\mathcal{T}^\dagger = e^{i\eta_i K_i}. \tag{A.151}$$

Similarly, the action of time-reversal on the translation operators is given by

$$\mathcal{T}e^{-iP^0 t}\mathcal{T}^\dagger = e^{+iP^0 t} \quad \text{and} \quad \mathcal{T}e^{+i\vec{P}\cdot\vec{x}}\mathcal{T}^\dagger = e^{+i\vec{P}\cdot\vec{x}}. \tag{A.152}$$

We recall now that $\mathcal{T}$ is anti-unitary, namely it obeys the following condition

$$\mathcal{T}i\mathcal{T}^\dagger = -i. \tag{A.153}$$

Using these facts we deduce the following commutation relations of $\mathcal{T}$ with the generators of the Poincaré group

$$\mathcal{T}P^\mu\mathcal{T}^\dagger = (P^0, -\vec{P}), \qquad \mathcal{T}K^i\mathcal{T}^\dagger = K^i, \qquad \mathcal{T}J^i\mathcal{T}^\dagger = -J^i. \tag{A.154}$$

In what follows we will use (A.154) to derive the action of time-reversal on one- and two-particle states. Then (as in the previous section) we will derive constraints on the scattering amplitudes. As before, we begin by computing the the transformation property of the helicity eigenstate boost (A.54) under time-reversal,

$$\begin{aligned}\mathcal{T}U_{\rm h}(\vec{p})\mathcal{T}^\dagger =& \mathcal{T}R(\phi,\theta,-\phi)\mathcal{T}^\dagger\mathcal{T}B_3(\eta)\mathcal{T}^\dagger \\ =& R(\phi,\theta,-\phi)B_3(-\eta) \\ =& R(\phi,\theta,-\phi)R(0,\pi,0)B_3(\eta)R^\dagger(0,\pi,0).\end{aligned} \tag{A.155}$$

Here in the first line we injected the identity $\mathbb{I} = \mathcal{T}^\dagger\mathcal{T}$, we then used the commutation properties (A.154) together with (A.153) in the second line. Finally, in the third line we used (A.45). Interestingly enough, (A.155) is the same as (A.120). Thus, we expect that in what follows we will be able to utilize many intermediate results from the previous section.

One-particle states

Let us first deduce the action of time-reversal on a one-particle state in the rest frame. Consider the following relation

$$\begin{aligned}\mathcal{T}R(\alpha,\beta,\gamma)|m,\vec{0};j,\lambda\rangle &= \mathcal{T}R(\alpha,\beta,\gamma)\mathcal{T}^\dagger\mathcal{T}|m,\vec{0};j,\lambda\rangle \\ &= R(\alpha,\beta,\gamma)\mathcal{T}|m,\vec{0};j,\lambda\rangle,\end{aligned} \tag{A.156}$$

which holds true due to (A.153) and (A.154). On the other hand we also have

$$\begin{aligned}\mathcal{T}R(\alpha,\beta,\gamma)|m,\vec{0};j,\lambda\rangle &= \mathcal{T}\mathscr{D}^\ell_{\lambda'\lambda}(\alpha,\beta,\gamma)|m,\vec{0};j,\lambda\rangle \\ &= \mathscr{D}^{\ell *}_{\lambda'\lambda}(\alpha,\beta,\gamma)\mathcal{T}|m,\vec{0};j,\lambda'\rangle.\end{aligned} \tag{A.157}$$

Here in the first line we simply used (A.52). Instead the second line follows from (A.153) and the explicit form of the large Wigner D-matrix, see (A.7) and (A.10). Comparing the above two expressions we conclude that

$$R(\alpha,\beta,\gamma)\mathcal{T}|m,\vec{0};j,\lambda\rangle = \mathscr{D}^{\ell *}_{\lambda'\lambda}(\alpha,\beta,\gamma)\mathcal{T}|m,\vec{0};j,\lambda'\rangle. \tag{A.158}$$

By comparing (A.158) with (A.17), we see that the time reversal transformed one-particle states (in the center of mass) are in the dual spin ℓ representation. Using (A.21) we conclude that[6]

$$\mathcal{T}|m,\vec{0};j,\lambda\rangle = \varepsilon\,(-1)^{j-\lambda}|m,\vec{0};j,-\lambda\rangle, \tag{A.159}$$

where ε is the proportionality coefficient obeying $|\varepsilon|^2 = 1$. One can always define $\mathcal{T}$ in such a way that $\mathcal{T}^2 = +1$ or $\mathcal{T}^2 = -1$. Thus, we have

$$\varepsilon^2 = +1 \quad \text{or} \quad \varepsilon^2 = -1. \tag{A.160}$$

In order to obtain the action of time-reversal on a one-particle state, we use the definition of the helicity basis (A.53) and (A.155). We have

$$\begin{aligned}
\mathcal{T}|m,\vec{p};j,\lambda\rangle &= \mathcal{T}U_h(\vec{p})|m,\vec{0},j,\lambda\rangle \\
&= \mathcal{T}U_h(\vec{p})\mathcal{T}^\dagger\mathcal{T}|m,\vec{0},j,\lambda\rangle \\
&= R(\phi,\theta,-\phi)R(0,\pi,0)B(+\vec{\eta})R^\dagger(0,\pi,0)\mathcal{T}|m,\vec{0},j,\lambda\rangle \\
&= \varepsilon(-1)^{j-\lambda}R(\phi,\theta,-\phi)R(0,\pi,0)B(+\eta)R^\dagger(0,\pi,0)|m,\vec{0},j,-\lambda\rangle \\
&= \varepsilon R(\phi,\theta,-\phi)R(0,\pi,0)B(+\vec{\eta})|m,\vec{0},j,\lambda\rangle.
\end{aligned} \tag{A.161}$$

In going from the fourth to the fifth line we used (A.124) and (A.129). Utilizing (A.125) and (A.129) the above result can be brought to the following final form

$$\mathcal{T}|m,\vec{p};j,\lambda\rangle = \varepsilon(-1)^{2j}e^{-2i\lambda\phi}|m,-\vec{p},j;\lambda\rangle. \tag{A.162}$$

Two-particle COM states

From the action of time-reversal on one-particle states (A.128), one deduces the action of time-reversal on two-particle center of mass states defined in (1.26). One has

$$\begin{aligned}
\mathcal{T}|(\boldsymbol{p},\theta,\phi);\lambda_1,\lambda_2\rangle &= \mathcal{T}\left(|m_1,\vec{p},j_1,\lambda_1\rangle\otimes|m_2,-\vec{p},j_2,\lambda_2\rangle\right) \\
&= \varepsilon_1\varepsilon_2(-1)^{2j_1}(-1)^{2j_2}e^{-2i\phi\lambda_1}e^{-2i(\phi+\pi)\lambda_2}|m_1,-\vec{p},j_1,\lambda_1\rangle\otimes|m_2,\vec{p},j_2,\lambda_2\rangle.
\end{aligned} \tag{A.163}$$

Using (A.129) we can bring the above to the final form

$$\mathcal{T}|(\boldsymbol{p},\theta,\phi);\lambda_1,\lambda_2\rangle = \varepsilon_1\varepsilon_2(-1)^{2j_1}e^{-2i(\lambda_1+\lambda_2)\phi}|(\boldsymbol{p},\pi-\theta,\phi+\pi);\lambda_1,\lambda_2\rangle. \tag{A.164}$$

[6] From $J_3\mathcal{T} = -\mathcal{T}J_3$ and (A.5) we could have only concluded that helicity flips under-time reversal.

Two-particle irreps

Let us repeat that the two-particle states can be decomposed into states in the irreducible representation of the Poincaré group. We refer to them as the two-particle irreps. In the center of mass frame such a decomposition and its inverse were given by (A.76) and (A.77) respectively. Applying time-reversal to (A.77) and using (A.164) we get

$$\begin{aligned}\mathcal{T}|c,0;\ell,\lambda;\lambda_1,\lambda_2\rangle &= \mathcal{N}\int_0^{2\pi}d\phi\int_0^{\pi}d\theta\sin\theta\,\mathcal{T}e^{-i(\lambda_1+\lambda_2-\lambda)\phi}d^{(\ell)}_{\lambda\lambda_{12}}(\theta)|(\boldsymbol{p},\theta,\phi);\lambda_1,\lambda_2\rangle\\ &= \mathcal{N}\int_0^{2\pi}d\phi\int_0^{\pi}d\theta\sin\theta\,e^{+i(\lambda_1+\lambda_2-\lambda)\phi}d^{(\ell)}_{\lambda\lambda_{12}}(\theta)\mathcal{T}|(\boldsymbol{p},\theta,\phi);\lambda_1,\lambda_2\rangle\\ &= \varepsilon_{12}^{\text{com}}\mathcal{N}\int_0^{2\pi}d\phi\int_0^{\pi}d\theta\sin\theta\,e^{-i(\lambda_1+\lambda_2+\lambda)\phi}d^{(\ell)}_{\lambda\lambda_{12}}(\theta)|(\boldsymbol{p},\pi-\theta,\phi+\pi),\lambda_1,\lambda_2\rangle.\end{aligned} \tag{A.165}$$

Notice that in going from the first to the second line we used (A.153). The constant $\mathcal{N}$ was defined in (A.140) and we have introduced for brevity

$$\varepsilon_{12}^{\text{com}}\equiv\varepsilon_1\varepsilon_2(-1)^{2j_1}. \tag{A.166}$$

Changing the integration variables from θ and ϕ to $\theta'\equiv\pi-\theta$ and $\phi'\equiv\phi+\pi$, using the following property of the small Wigner d-matrix

$$d^{(\ell)}_{\lambda'\lambda}(\pi-\theta)=(-1)^{\lambda-\ell}d^{(\ell)}_{-\lambda'\lambda}(\theta), \tag{A.167}$$

we can bring (A.165) to the following form

$$\begin{aligned}\mathcal{T}|c,0;\ell,\lambda;\lambda_1,\lambda_2\rangle &= \varepsilon_{12}^{\text{com}}\mathcal{N}e^{i(\lambda_1+\lambda_2+\lambda)\pi}(-1)^{\lambda_1-\lambda_2-\ell}\\ &\times\int_{\pi}^{3\pi}d\phi'\int_0^{\pi}d\theta'\sin\theta'\,e^{-i(\lambda_1+\lambda_2+\lambda)\phi}d^{(\ell)}_{-\lambda\lambda_{12}}(\theta')|(\boldsymbol{p},\theta',\pi'),\lambda_1,\lambda_2\rangle.\end{aligned} \tag{A.168}$$

Using (A.77) and (A.143) we conclude that

$$\mathcal{T}|c,0;\ell,\lambda;\lambda_1,\lambda_2\rangle=\varepsilon_{12}^{\text{com}}e^{i(\lambda_1+\lambda_2+\lambda)\pi}(-1)^{\lambda_1-\lambda_2-\ell}|c,0;\ell,-\lambda;\lambda_1,\lambda_2\rangle. \tag{A.169}$$

Using (A.166) and the obvious identity $(-1)^{\ell-\lambda}=(-1)^{\lambda-\ell}$ which holds true since $\ell-\lambda$ is always an integer, we obtain our final expression

$$\mathcal{T}|c,0,\ell,\lambda;\lambda_1,\lambda_2\rangle=\varepsilon_1\varepsilon_2(-1)^{\ell-\lambda}|c,0,\ell,-\lambda;\lambda_1,\lambda_2\rangle. \tag{A.170}$$

Constraints on scattering amplitudes

In time-reversal invariant theories the scattering operators S and T obey

$$\mathcal{T}S\mathcal{T}^\dagger = S^\dagger, \qquad \mathcal{T}T\mathcal{T}^\dagger = T^\dagger. \tag{A.171}$$

Consider the states

$$|\psi\rangle = |(\boldsymbol{p}', \theta, 0); \lambda_3, \lambda_4\rangle, \qquad |\phi\rangle = T|(\boldsymbol{p}, 0, 0); \lambda_1, \lambda_2\rangle. \tag{A.172}$$

By definition the anti-unitary time-reversal operator $\mathcal{T}$ satisfies

$$\langle \mathcal{T}\psi|\mathcal{T}\phi\rangle^* = \langle\psi|\phi\rangle, \tag{A.173}$$

where

$$|\mathcal{T}\phi\rangle \equiv \mathcal{T}|\phi\rangle \quad \text{and} \quad |\mathcal{T}\psi\rangle \equiv \mathcal{T}|\psi\rangle. \tag{A.174}$$

Using (A.164) and time-reversal invariance of the T operator (A.171), we have

$$\begin{aligned} |\mathcal{T}\phi\rangle &= T\mathcal{T}|(\boldsymbol{p}, 0, 0); \lambda_1, \lambda_2\rangle \\ &= \varepsilon_1\varepsilon_2(-1)^{2j_1}T^\dagger|(\boldsymbol{p}, \pi, \pi), \lambda_1, \lambda_2\rangle \end{aligned} \tag{A.175}$$

and

$$\langle \mathcal{T}\psi| = \varepsilon_3^*\varepsilon_4^*(-1)^{2j_3}\langle(\boldsymbol{p}, \pi-\theta, \pi), \lambda_3, \lambda_4|. \tag{A.176}$$

Plugging (A.175) and (A.176) along with the definitions (A.172) into (A.173), we arrive at

$$\begin{aligned} \langle(\boldsymbol{p}', \theta, 0); \lambda_3, \lambda_4|T|(\boldsymbol{p}, 0, 0); \lambda_1, \lambda_2\rangle = \\ \varepsilon_1^*\varepsilon_2^*\varepsilon_3\varepsilon_4(-1)^{2j_1}(-1)^{2j_3}\langle(\boldsymbol{p}', \pi-\theta, \pi); \lambda_3, \lambda_4|T^\dagger|(\boldsymbol{p}, \pi, \pi); \lambda_1, \lambda_2\rangle^* \\ \varepsilon_1^*\varepsilon_2^*\varepsilon_3\varepsilon_4(-1)^{2j_1}(-1)^{2j_3}\langle(\boldsymbol{p}, \pi, \pi); \lambda_1, \lambda_2|T|(\boldsymbol{p}', \pi-\theta, \pi); \lambda_3, \lambda_4\rangle. \end{aligned} \tag{A.177}$$

We are now left with bringing the matrix element in the last line of (A.177) to the standard COM frame. For that we will use the following identity

$$R(\pi, \pi+\theta'-\theta, -\pi) = R(\pi, \pi-\theta, 0)R(0, \theta', 0)e^{i\pi J_3}, \tag{A.178}$$

which is a simple reorganization of exponents in the definition of the Euler rotation (A.4).

Let us start by the following rewriting of the 34 two-particle state

$$\begin{aligned} |(\boldsymbol{p}', \pi-\theta, \pi); \lambda_3, \lambda_4\rangle &= e^{2i\pi\lambda_4}R(\pi, \pi-\theta, -\pi)|(\boldsymbol{p}', 0, 0); \lambda_3, \lambda_4\rangle \\ &= e^{2i\pi\lambda_4}R(\pi, \pi-\theta, 0)R(0, 0, 0)e^{i\pi J_3}|(\boldsymbol{p}', 0, 0); \lambda_3, \lambda_4\rangle \\ &= e^{i\pi(\lambda_3+\lambda_4)}R(\pi, \pi-\theta, 0)|(\boldsymbol{p}', 0, 0); \lambda_3, \lambda_4\rangle. \end{aligned} \tag{A.179}$$

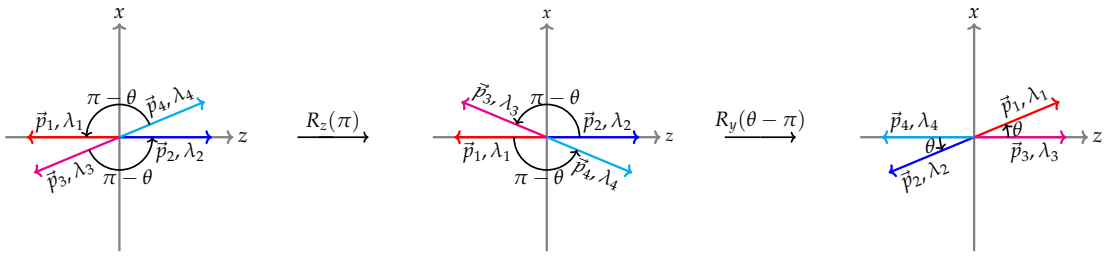

Figure A.2: The geometric picture involved in going from (A.177) to (A.181). Particle 1 is red, particle 2 is blue, particle 3 is magenta and particle 4 is cyan.

Here in the first line we used (A.70). We used (A.178) with $\theta' = 0$ in the second line. Finally we used the fact that the states with the momentum along the z-axis are eigenstates of J_3 generators. Analogously we can write the 12 two-particle state as

$$\begin{aligned}|(\boldsymbol{p},\pi,\pi);\lambda_1,\lambda_2\rangle &= e^{2i\pi\lambda_2}R(\pi,\pi,-\pi)|(\boldsymbol{p},0,0);\lambda_1,\lambda_2\rangle \\ &= e^{2i\pi\lambda_2}R(\pi,\pi-\theta,0)R(0,\theta,0)e^{i\pi J_3}|(\boldsymbol{p},0,0);\lambda_1,\lambda_2\rangle \\ &= e^{i\pi(\lambda_1+\lambda_2)}R(\pi,\pi-\theta,0)|(\boldsymbol{p},\theta,0);\lambda_1,\lambda_2\rangle,\end{aligned} \tag{A.180}$$

where in the second line we used (A.178) with $\theta' = \theta$. Plugging both (A.179) and (A.180) into the last line of (A.177) we conclude that

$$\begin{aligned}\langle(\boldsymbol{p}',\theta,0);\lambda_3,\lambda_4|T|(\boldsymbol{p},0,0);\lambda_1,\lambda_2\rangle &= \varepsilon_1^*\varepsilon_2^*\varepsilon_3\varepsilon_4(-1)^{2j_1}(-1)^{2j_3}e^{i\pi(-\lambda_1-\lambda_2+\lambda_3+\lambda_4)} \\ \langle(\boldsymbol{p},\theta,0);\lambda_1,\lambda_2|\left(R(\pi,\pi-\theta,0)\right)^\dagger TR(\pi,\pi-\theta,0)|(\boldsymbol{p}',0,0);\lambda_3,\lambda_4\rangle.\end{aligned} \tag{A.181}$$

Using the fact that the scattering operator is invariant under rotations and that according to (A.230) - (A.232) the Mandelstam variables remain invariant under the exchange $\boldsymbol{p} \leftrightarrow \boldsymbol{p}'$, we can use the definition of the center of mass amplitudes (1.61) and write (A.181) in its final form

$$T_{12\to34}{}^{\lambda_3,\lambda_4}_{\lambda_1,\lambda_2}(s,t,u) = \varepsilon_1^*\varepsilon_2^*\varepsilon_3\varepsilon_4(-1)^{\lambda_1-\lambda_2-\lambda_3+\lambda_4}T_{34\to12}{}^{\lambda_1,\lambda_2}_{\lambda_3,\lambda_4}(s,t,u). \tag{A.182}$$

Here we also simplified the phases according to (A.129). Notice that whereas parity (1.64) imposes a constraint on the same amplitude, time reversal relates the process $12 \to 34$ to the process $34 \to 12$, which are in general different.

A.2.3 $\mathcal{PT}$

Let us conclude this appendix by discussing the situation when our physical system is symmetric under simultaneous application of parity and time-reversal, in other words under the $\mathcal{PT}$ transformation. Due to (A.128) and (A.162), the one-particle states

transform under $\mathcal{PT}$ as follows

$$\mathcal{PT}|m,\vec{p};j,\lambda\rangle = \eta\varepsilon(-1)^{j-\lambda}|m,\vec{p};j,-\lambda\rangle. \tag{A.183}$$

One can then derive constraints posed by $\mathcal{PT}$ on scattering amplitudes. The simplest way to obtain them is to combine (A.149) and (A.182). One then has

$$T_{12\to 34}{}^{\lambda_3,\lambda_4}_{\lambda_1,\lambda_2}(s,t,u) = \zeta_1^*\zeta_2^*\zeta_3\zeta_4(-1)^{j_1-j_2-j_3+j_4}T_{34\to 12}{}^{-\lambda_1,-\lambda_2}_{-\lambda_3,-\lambda_4}(s,t,u), \tag{A.184}$$

where we have defined the phases as

$$\zeta_i \equiv \varepsilon_i\eta_i. \tag{A.185}$$

It is interesting to consider the case of identical neutral particles with spin j and the phase ζ. Then the equation (A.184) becomes

$$T^{\lambda_3,\lambda_4}_{\lambda_1,\lambda_2}(s,t,u) = T^{-\lambda_1,-\lambda_2}_{-\lambda_3,-\lambda_4}(s,t,u), \tag{A.186}$$

where we have removed the subscript $12\to 34$ since all the particles are identical and used the fact that $|\zeta|^2 = 1$.

Any consistent quantum field theory must be CPT invariant [96]. This means that one can always introduce the so called CPT operator which we denote by Σ. In the system of neutral particles one can choose

$$\Sigma = \mathcal{PT}. \tag{A.187}$$

As a result the constraint (A.186) on the scattering amplitudes of identical particles is not an additional assumption but rather a consequence of the CPT theorem.

A.3 Identical particles

In this appendix we consider the special situation where a two-particle state (2PS) describes a system of two identical particles with mass m and spin j. Such a system possesses Bose or Fermi (anti-)symmetry. In other words, the two-particle state must satisfy

$$|\kappa_1,\kappa_2\rangle_{id} = (-1)^{2j}|\kappa_2,\kappa_1\rangle_{id}. \tag{A.188}$$

Here we have added a subscript *id* to explicitly indicate that the state describes a system of two identical particles. In order to satisfy (A.188), we have to take the symmetrized,

in case of bosons, and the anti-symmetrized, in case of fermions, tensor product, *i.e*

$$|\kappa_1,\kappa_2\rangle_{id} \equiv \frac{1}{\sqrt{2}}\left(|m,\vec{p}_1;j,\lambda_1\rangle\otimes|m,\vec{p}_2;j,\lambda_2\rangle + (-1)^{2j}|m,\vec{p}_2;j,\lambda_2\rangle\otimes|m,\vec{p}_1;j,\lambda_1\rangle\right). \tag{A.189}$$

We remind the reader that $\otimes$ denotes the ordered tensor product that was used in (1.19) to define generic two-particle states. The normalization of the state (A.189) follows from (1.14) and reads

$${}_{id}\langle\kappa_1,\kappa_2|\kappa_3,\kappa_4\rangle_{id} = \delta(\kappa_1-\kappa_3)\delta(\kappa_2-\kappa_4) + (-1)^{2j}\delta(\kappa_1-\kappa_4)\delta(\kappa_2-\kappa_3). \tag{A.190}$$

A.3.1 Two-particle COM states

As before we need to define the identical 2PS in the center of momentum. Adapting (1.26) to the case of identical particles we get

$$|(\boldsymbol{p},\theta,\phi);\lambda_1,\lambda_2\rangle_{id} \equiv \\ \frac{1}{\sqrt{2}}\left(|m,+\vec{p};j,\lambda_1\rangle\otimes|m,-\vec{p};j,\lambda_2\rangle + (-1)^{2j}|m,-\vec{p};j,\lambda_2\rangle\otimes|m,\vec{p};j,\lambda_1\rangle\right). \tag{A.191}$$

In the notation (1.26) this can be equivalently written as

$$|(\boldsymbol{p},\theta,\phi);\lambda_1,\lambda_2\rangle_{id} = \frac{1}{\sqrt{2}}\left(|(\boldsymbol{p},\theta,\phi);\lambda_1,\lambda_2\rangle + (-1)^{2j}|(\boldsymbol{p},\pi-\theta,\pi+\phi);\lambda_2,\lambda_1\rangle\right). \tag{A.192}$$

The normalization of these states is fixed by (1.35). Analogously to (1.28) we can write it in spherical coordinates as

$${}_{id}\langle(\boldsymbol{p},\theta,\phi);\lambda_1,\lambda_2|(\boldsymbol{p}',0,0);\lambda_1',\lambda_2'\rangle_{id} = (2\pi)^4\delta^4(0)\times\frac{16\pi^2\sqrt{s}}{\sqrt{\boldsymbol{p}\boldsymbol{p}'}}\times \\ \left(\frac{\delta(\theta)\delta(\phi)}{\sin\theta}\delta_{\lambda_1\lambda_1'}\delta_{\lambda_2\lambda_2'} + (-1)^{2j}\frac{\delta(\pi-\theta)\delta(\phi+\pi)}{\sin(\pi-\theta)}\delta_{\lambda_2\lambda_1'}\delta_{\lambda_1\lambda_2'}\right). \tag{A.193}$$

The symmetry (A.188) for the two-particle states in the center of mass reads as

$$|(\boldsymbol{p},\theta,\phi);\lambda_1,\lambda_2\rangle_{id} = (-1)^{2j}|(\boldsymbol{p},\pi-\theta,\phi+\pi);\lambda_2,\lambda_1\rangle_{id}. \tag{A.194}$$

Let us now restrict our attention on the special case $\phi = 0$ and derive the following two relations

$$|(\boldsymbol{p},\theta,0);\lambda_1,\lambda_2\rangle_{id} = e^{-i\pi J_2}|(\boldsymbol{p},\theta,0);\lambda_2,\lambda_1\rangle_{id}, \tag{A.195}$$

$$|(\boldsymbol{p},\theta,0);\lambda_1,\lambda_2\rangle_{id} = (-1)^{\lambda_1-\lambda_2}e^{-i\pi J_3}|(\boldsymbol{p},\pi-\theta,0);\lambda_2,\lambda_1\rangle_{id}. \tag{A.196}$$

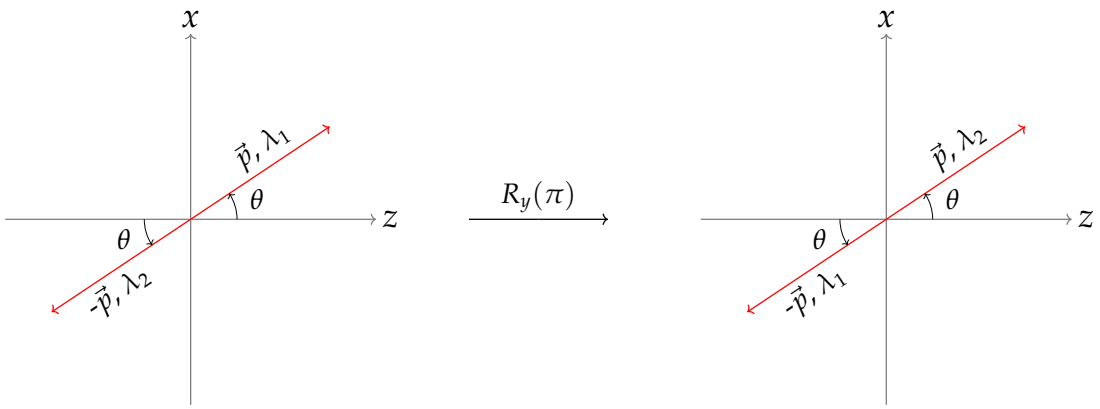

Figure A.3: The geometric picture behind (A.195). The particles are identical and are therefore represented by the same colour.

The first one simply follows from (A.194) with $\phi = 0$ and (A.137). The second one follows from (A.194) with $\phi = 0$ and (A.70). More precisely

$$\begin{aligned}
|(\boldsymbol{p},\theta,\phi);\lambda_1,\lambda_2\rangle_{id} &= (-1)^{2j}e^{2i\pi\lambda_1}R(\pi,\pi-\theta,-\pi)|(\boldsymbol{p},0,0);\lambda_2,\lambda_1\rangle_{id} \\
&= (-1)^{2j}e^{2i\pi\lambda_1}e^{-i\pi J_3}R(0,\pi-\theta,0)e^{+i\pi J_3}|(\boldsymbol{p},0,0);\lambda_2,\lambda_1\rangle_{id} \\
&= (-1)^{2j}e^{i\pi(\lambda_2+\lambda_1)}e^{-i\pi J_3}R(0,\pi-\theta,0)|(\boldsymbol{p},0,0);\lambda_2,\lambda_1\rangle_{id} \\
&= (-1)^{2j}e^{i\pi(\lambda_1+\lambda_2)}e^{-i\pi J_3}|(\boldsymbol{p},\pi-\theta,0);\lambda_2,\lambda_1\rangle_{id}.
\end{aligned} \tag{A.197}$$

In the first and the fourth line we used (A.70). In the second line we simply used the definition of Euler rotations (A.4). Finally in the third line we used the fact that the states with the three-momentum along the z-axis are eigenvector of J_3. Using (A.129) in the last line of (A.197) we obtain (A.196).

A.3.2 Two-particle irreps

We would now like to decompose identical two particle states (A.189) into irreducible representations analogously to the generic two-particle state decomposition (1.29). The two-particle states in the irreducible representation are denoted by

$$|c,0,\ell,\lambda;\lambda_1,\lambda_2\rangle_{id}. \tag{A.198}$$

As before the subscript *id* emphasizes the fact that we do not deal with a generic situation but with the identical particle case. In what follows we need to define the states (A.198) precisely and fix their normalization.

In a generic situation, the two-particle states in the reducible and irreducible representations are related by (A.77). Since the Lorentz transformation property of the states are the same for identical and distinct particles, we can just use the decomposition formula

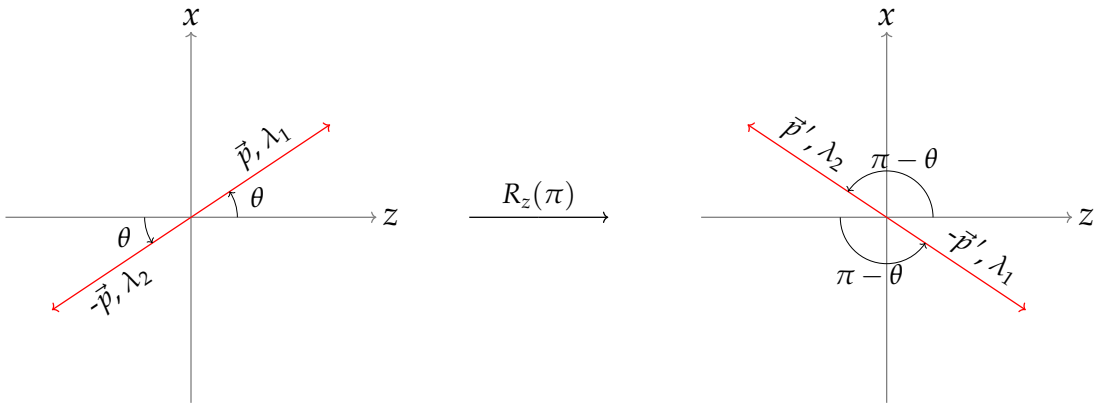

Figure A.4: The geometric picture behind (A.196). The particles are identical and are therefore represented by the same colour.

(A.77) but with an unspecified normalization $\mathcal{N}_{id}$ which we fix later in the section. One has

$$|c, \vec{0}; \ell, \lambda; \lambda_1, \lambda_2\rangle_{id} = \mathcal{N}_{id} \int_0^{2\pi} d\phi \int_{-1}^{+1} d\cos\theta e^{-i(\lambda_1+\lambda_2-\lambda)\phi} d^{\ell}_{\lambda\lambda_{12}}(\theta) |(\boldsymbol{p}, \theta, \phi); \lambda_1, \lambda_2\rangle_{id}. \tag{A.199}$$

We can use this formula to deduce the symmetry property of the state (A.198) under the exchange of two particles. Plugging (A.194) into the right-hand side of (A.199) we get

$$\begin{aligned}
&(-1)^{2j}\mathcal{N}_{id} \int_0^{2\pi} d\phi \int_0^{\pi} d\theta \sin\theta\, e^{-i(\lambda_1+\lambda_2-\lambda)\phi} d^{(\ell)}_{\lambda\lambda_{12}}(\theta) |(\boldsymbol{p}, \pi-\theta, \phi+\pi); \lambda_2, \lambda_1\rangle_{id} = \\
&(-1)^{2j}\mathcal{N}_{id} \int_{\pi}^{3\pi} d\phi' \int_0^{\pi} d\theta' \sin\theta' e^{-i(\lambda_1+\lambda_2-\lambda)(\phi'-\pi)} d^{(\ell)}_{\lambda\lambda_{12}}(\pi-\theta') |(\boldsymbol{p}, \theta', \phi'); \lambda_2, \lambda_1\rangle_{id} = \\
&(-1)^{2j} e^{i\pi(\lambda_1+\lambda_2-\lambda)} (-1)^{\ell+\lambda} \times \\
&\qquad \mathcal{N}_{id} \int_{\pi}^{3\pi} d\phi' \int_0^{\pi} d\theta' \sin\theta' e^{-i(\lambda_1+\lambda_2-\lambda)\phi'} d^{(\ell)}_{\lambda\lambda_{21}}(\theta') |(\boldsymbol{p}, \theta', \phi'); \lambda_2, \lambda_1\rangle_{id}.
\end{aligned} \tag{A.200}$$

In the second line we changed the integration variables from θ and ϕ to $\theta' \equiv \pi - \theta$ and $\phi' \equiv \phi + \pi$. In the third line we used (A.141) to rewrite the small Wigner d-matrix. Also recall the definition

$$\lambda_{12} \equiv \lambda_1 - \lambda_2. \tag{A.201}$$

The last line in (A.200) simply contains the two-particle irrep (A.199). In order to see this, we refer the reader to (A.143) and the discussion below. Combining (A.199) and (A.200), and taking into account (A.129) we finally get[7]

$$|c, \vec{0}; \ell, \lambda; \lambda_1, \lambda_2\rangle_{id} = (-1)^{\ell+\lambda_1-\lambda_2} |c, 0; \ell, \lambda; \lambda_2, \lambda_1\rangle_{id}. \tag{A.202}$$

[7]Notice that due to (A.202) the two-particle irreps with $\lambda_1 = \lambda_2$ exist only for even spins ℓ. When $\lambda_1 \neq \lambda_2$ we can form two linear combinations from two-particle irreps, one of which exists only for even spins ℓ and the other one only for odd ℓ.

We can now define two-particle irreps (A.198) describing identical particles in terms of generic two-particle irreps by requiring that (A.198) automatically satisfies the condition (A.202). Our choice here is as follows

$$|c,0,\ell,\lambda;\lambda_1,\lambda_2\rangle_{id} \equiv \frac{1}{2}\left(|c,0,\ell,\lambda;\lambda_1,\lambda_2\rangle + (-1)^{\ell+\lambda_1-\lambda_2}|c,0,\ell,\lambda;\lambda_2,\lambda_1\rangle\right). \tag{A.203}$$

The normalization of the states (A.203) follows from the normalization of each of the two terms fixed by (1.22) together with (1.25). As a result the normalization of the states (A.203) is given by (1.22) along with

$$\delta_{\gamma'\gamma} = \frac{1}{2}\left(\delta_{\lambda_1\lambda_1'}\delta_{\lambda_2\lambda_2'} + (-1)^{\ell+\lambda_1-\lambda_2}\delta_{\lambda_1\lambda_2'}\delta_{\lambda_2\lambda_1'}\right). \tag{A.204}$$

Having defined (A.203), we can apply (1.29) to both terms in the right-hand side of (A.192). Using the property of the small Wigner d-matrix (A.141) we get

$$|(\boldsymbol{p},\theta,\phi);\lambda_1,\lambda_2\rangle_{\rm id} = \sqrt{2}\sum_{\ell,\lambda} C_\ell(\boldsymbol{p}) e^{i(\lambda_1+\lambda_2-\lambda)\phi} d^{(\ell)}_{\lambda\lambda_{12}}(\theta)|c,0;\ell,\lambda;\lambda_1,\lambda_2\rangle_{id}, \tag{A.205}$$

where the coefficient $C_\ell(\boldsymbol{p})$ is given by (1.32). As before we can invert the above equation to get precisely (A.199) with

$$\mathcal{N}_{id} = \frac{2\ell+1}{4\pi\sqrt{2}C_\ell(\boldsymbol{p})}. \tag{A.206}$$

A.3.3 Constraints on scattering amplitudes

Consider now the scattering of identical particles.[8] The amplitude describing such a situation is defined as

$$T^{\lambda_3,\lambda_4}_{\lambda_1,\lambda_2}(s,t,u)\times(2\pi)^4\delta^{(4)}(0) \equiv {}_{id}\langle(\boldsymbol{p}',\theta,0);\lambda_3,\lambda_4|T|(\boldsymbol{p},0,0);\lambda_1,\lambda_2\rangle_{id}, \tag{A.207}$$

where the identical two-particle states were defined in (A.192). We now deduce constraints the amplitude (A.207) must obey in order to incorporate the symmetry property (A.194). In practice we will use (A.194) rewritten in the form (A.196).

Let us start with the outgoing particles 3 and 4. Using (A.196) one can rewrite the

[8] More generally one can consider scattering processes with only incoming or outgoing particles being identical. As presented, most of the results in this section still apply to these situations.

right-hand side of (A.207) as

$$\begin{aligned}
&{}_{id}\langle(\boldsymbol{p}',\theta,0);\lambda_3,\lambda_4|T|(\boldsymbol{p},0,0);\lambda_1,\lambda_2\rangle_{id}\\
&\qquad=(-1)^{\lambda_3-\lambda_4}{}_{id}\langle(\boldsymbol{p}',\pi-\theta,0);\lambda_4,\lambda_3|e^{i\pi J_3}T|(\boldsymbol{p},0,0);\lambda_1,\lambda_2\rangle_{id}\\
&\qquad=(-1)^{\lambda_3-\lambda_4}{}_{id}\langle(\boldsymbol{p}',\pi-\theta,0);\lambda_4,\lambda_3|e^{i\pi J_3}Te^{-i\pi J_3}e^{i\pi J_3}|(\boldsymbol{p},0,0);\lambda_1,\lambda_2\rangle_{id}\\
&\qquad=(-1)^{\lambda_3-\lambda_4+\lambda_1-\lambda_2}{}_{id}\langle(\boldsymbol{p}',\pi-\theta,0);\lambda_4,\lambda_3|T|(\boldsymbol{p},0,0);\lambda_1,\lambda_2\rangle_{id}.
\end{aligned}\tag{A.208}$$

In the third line we simply injected the identity operator made out of z-rotations. In the fourth line we used the fact that the states with the momentum along the z-axis are eigenstates of J_3 generators. Looking at the definition of the Mandelstam variables (A.231) and (A.232) we see that the exchange $\theta \leftrightarrow \pi-\theta$ simply corresponds to $t \leftrightarrow u$. Combining (A.208) with (A.207) we obtain

$$T^{\lambda_3,\lambda_4}_{\lambda_1,\lambda_2}(s,t,u)=(-1)^{\lambda_1-\lambda_2-\lambda_3+\lambda_4}T^{\lambda_4,\lambda_3}_{\lambda_1,\lambda_2}(s,u,t),\tag{A.209}$$

which is nothing but the (34) $t-u$ crossing equation.

Let now address the incoming particles 1 and 2. First, we need the following relation which holds true for generic two-particle states (and therefore also for identical two-particle states)

$$|(\boldsymbol{p},\theta,0);\lambda_3,\lambda_4\rangle=(-1)^{\lambda_3-\lambda_4}e^{-i\pi J_3}e^{-i\pi J_2}|(\boldsymbol{p},\pi-\theta,0);\lambda_3,\lambda_4\rangle.\tag{A.210}$$

It simply follows from (A.70) and (A.47), see also (A.4) and (A.54). Due to (A.196) and (A.70) we also have the following relation for identical particles

$$|(\boldsymbol{p},0,0);\lambda_1,\lambda_2\rangle_{id}=(-1)^{\lambda_1-\lambda_2}e^{-i\pi J_3}e^{-i\pi J_2}|(\boldsymbol{p},0,0);\lambda_2,\lambda_1\rangle_{id}.\tag{A.211}$$

Using both (A.210) and (A.210) in the right-hand side of (A.207), and the fact that the scattering operator is invariant under rotations we conclude that

$$T^{\lambda_3,\lambda_4}_{\lambda_1,\lambda_2}(s,t,u)=(-1)^{\lambda_1-\lambda_2+\lambda_3-\lambda_4}T^{\lambda_3,\lambda_4}_{\lambda_2,\lambda_1}(s,u,t),\tag{A.212}$$

which is nothing but the (12) $t-u$ crossing equation.

Combining both crossing equations (A.209) and (A.212) we obtain the following purely kinematic constraint

$$T^{\lambda_3,\lambda_4}_{\lambda_1,\lambda_2}(s,t,u)=T^{\lambda_4,\lambda_3}_{\lambda_2,\lambda_1}(s,t,u).\tag{A.213}$$

Here we used the fact that $\lambda_1-\lambda_2+\lambda_3-\lambda_4$ is always an integer.

A.4 Center of mass frame

In this section we define the center of mass frame describing two-, three- and four-point amplitudes.

A.4.1 Two-point amplitudes

We start with the two-point amplitude defined in (1.52). It reads

$$_{free}\langle c_1, \vec{p}_1; \ell_1, \lambda_1; \gamma_1 | T | c_2, \vec{p}_2; \ell_2, \lambda_2; \gamma_2 \rangle_{free}. \tag{A.214}$$

It is non-zero only for $\vec{p}_1 = \vec{p}_2$ due to translation symmetry. By using the three boost generators one can set

$$\vec{p}_1 = \vec{p}_2 = 0. \tag{A.215}$$

The remaining symmetry is $SO(3)$. The matrix element (A.214) at the point (A.215) must be invariant under this $SO(3)$ symmetry. Applying an $SO(3)$ rotation to (A.214) we get

$$\begin{aligned} &_{free}\langle c_1, \vec{0}; \ell_1, \lambda_1; \gamma_1 | T | c_2, \vec{0}; \ell_2, \lambda_2; \gamma_2 \rangle_{free} = \\ &\sum_{\lambda_1', \lambda_2'} {}_{free}\langle c_1, \vec{0}; \ell_1, \lambda_1'; \gamma_1 | T | c_2, \vec{0}; \ell_2, \lambda_2'; \gamma_2 \rangle_{free} \times \mathscr{D}^{*(\ell_1)}_{\lambda_1' \lambda_1}(\vec{\omega}_1) \mathscr{D}^{(\ell_2)}_{\lambda_2' \lambda_2}(\vec{\omega}_2). \end{aligned} \tag{A.216}$$

In order to make the amplitude invariant one has to demand that

$$_{free}\langle c_1, \vec{0}; \ell_1, \lambda_1; \gamma_1 | T | c_2, \vec{0}; \ell_2, \lambda_2; \gamma_2 \rangle_{free} \propto \delta_{\ell_1 \ell_2} \delta_{\lambda_1 \lambda_2}. \tag{A.217}$$

Then due to the orthogonality (A.14) the Wigner D-matrices disappear completely and one recovers the invariance of the two-point amplitude. The condition (A.217) means that there is only one independent two-point amplitude

$$N_2 = 1. \tag{A.218}$$

A.4.2 Three-point amplitudes

Consider the following matrix element

$$_{out}\langle \kappa_1, \kappa_2 | c, \vec{p}; \ell, \lambda; \gamma \rangle_{in} = {}_{free}\langle \kappa_1, \kappa_2 | S | c, \vec{p}; \ell, \lambda; \gamma \rangle_{free}. \tag{A.219}$$

It appears in the discussion of poles, see for example section 2.5.1 in [13]. It also appears in computations of partial amplitudes, see the end of appendix A.8. It is interesting to ask what happens if the ket state in (A.219) is actually a one particle state, namely when

we deal with the following object

$$ {}_{out}\langle \kappa_1, \kappa_2 | \kappa_3 \rangle_{in} = {}_{free}\langle \kappa_1, \kappa_2 | S | \kappa_3 \rangle_{free}. \tag{A.220} $$

It describes the decay process of the asymptotic state 3 into two asymptotic states 1 and 2. Strictly speaking such a matrix element must be zero, since asymptotic states by definition cannot decay.[9] In some circumstances when a particle is unstable but lives long enough it might be useful however to treat it as an approximate asymptotic state and prescribe physical meaning to (A.220).

Let us discuss the spin structure of (A.220) in the COM frame. By using the three boosts we can set $\vec{p}_3 = 0$. By using two rotations we can move to the following final frame

$$ \begin{aligned} p_1^\mu &= \{E_1,\ 0,\ 0,\ +\boldsymbol{p}\}, \\ p_2^\mu &= \{E_2,\ 0,\ 0,\ -\boldsymbol{p}\}, \\ p_3^\mu &= \{E_3,\ 0,\ 0,\ 0\}, \end{aligned} \tag{A.221} $$

where the energies read as

$$ E_1 = \frac{\left| m_3^2 + m_1^2 - m_2^2 \right|}{2\, m_3}, \quad E_2 = \frac{\left| m_3^2 - m_1^2 + m_2^2 \right|}{2\, m_3}, \quad E_3 = m_3 \tag{A.222} $$

and we have

$$ \boldsymbol{p} = \frac{1}{2m_3} \sqrt{(m_3 + m_1 + m_2)(m_3 - m_1 - m_2)(m_3 - m_1 + m_2)(m_3 + m_1 - m_2)}. \tag{A.223} $$

The value $\boldsymbol{p}$ should be real, this enforces the condition

$$ m_3 \geq m_1 + m_2. \tag{A.224} $$

Having chosen the frame (A.221) one is left with a single generator of rotations around the z-axis. This means that one has a remaining $SO(2)$ symmetry and the matrix element (A.220) in the frame (A.221) must be invariant under it. To find the consequence of this symmetry one can inject the identity operator composed out of z-rotations into (A.220) twice and requiring that the matrix element remains invariant. It leads to the following constraint

$$ \lambda_3 = \lambda_1 - \lambda_2. \tag{A.225} $$

Given the condition (A.225) one can easily count the number of different three-point

[9] If a particle is unstable an observer after waiting long enough will see the decay product which is described by true asymptotic states.

amplitudes N_3. It is given by

$$N_3 = \sum_{\lambda_1=-j_1}^{+j_1} \sum_{\lambda_2=-j_2}^{+j_2} \sum_{\lambda_3=-j_3}^{+j_3} \delta_{\lambda_1+\lambda_2,\lambda_3}. \tag{A.226}$$

This expression was rewritten in a compact form in [51], it reads as

$$N_3 = (2j_1+1)(2j_2+1) - r(r+1), \quad r \equiv \max(j_1+j_2-j_3, 0), \quad j_1 \leq j_2 \leq j_3. \tag{A.227}$$

A.4.3 Four-point amplitudes

The four-point amplitude was defined in (1.41). Using all the generators of the Lorentz group, we can bring this amplitude to the following frame

$$\begin{aligned} p_1^\mu &= \{E_1, 0, 0, +\boldsymbol{p}\}, \\ p_2^\mu &= \{E_2, 0, 0, -\boldsymbol{p}\}, \\ p_3^\mu &= \{E_3, +\boldsymbol{p}' \sin\theta, 0, +\boldsymbol{p}' \cos\theta\}, \\ p_4^\mu &= \{E_4, -\boldsymbol{p}' \sin\theta, 0, -\boldsymbol{p}' \cos\theta\}, \end{aligned} \tag{A.228}$$

where $\boldsymbol{p} \geq 0$, $\boldsymbol{p}' \geq 0$ and $\theta \in [0, \pi]$ and the energies are given by

$$E_1 = \sqrt{m_1^2 + \boldsymbol{p}^2}, \quad E_2 = \sqrt{m_2^2 + \boldsymbol{p}^2}, \quad E_3 = \sqrt{m_3^2 + \boldsymbol{p}'^2}, \quad E_4 = \sqrt{m_4^2 + \boldsymbol{p}'^2}. \tag{A.229}$$

The Mandelstam variables in the COM frame (A.228) then read as

$$s = (E_1 + E_2)^2 = (E_3 + E_4)^2, \tag{A.230}$$

$$t = m_1^2 + m_3^2 - 2E_1E_3 + 2\boldsymbol{p}\boldsymbol{p}' \cos\theta, \tag{A.231}$$

$$u = m_1^2 + m_4^2 - 2E_1E_4 - 2\boldsymbol{p}\boldsymbol{p}' \cos\theta. \tag{A.232}$$

In the case of four-point COM amplitudes there is no additional symmetry left. Thus, the total number of amplitudes is obtained by simply counting all possible helicity configurations

$$N_4 = (2\ell_1+1)(2\ell_2+1)(2\ell_3+1)(2\ell_4+1). \tag{A.233}$$

The relations (A.230) - (A.232) express the Mandelstam variables (s, t, u) in terms of $(\boldsymbol{p}, \boldsymbol{p}', \theta)$. We can also invert these relations as follows. From (A.230) we get

$$\boldsymbol{p} = \frac{\mathcal{L}_{12}(s)}{2\sqrt{s}}, \qquad \boldsymbol{p}' = \frac{\mathcal{L}_{34}(s)}{2\sqrt{s}}, \tag{A.234}$$

where we have defined

$$\mathcal{L}_{ij}(s) \equiv \sqrt{\Big(s-(m_i-m_j)^2\Big)\Big(s-(m_i+m_j)^2\Big)}. \tag{A.235}$$

Plugging (A.234) into (A.229) we get the energies

$$E_1 = \frac{s+m_1^2-m_2^2}{2\sqrt{s}},\;\; E_2 = \frac{s-m_1^2+m_2^2}{2\sqrt{s}},\;\; E_3 = \frac{s+m_3^2-m_4^2}{2\sqrt{s}},\;\; E_4 = \frac{s-m_3^2+m_4^2}{2\sqrt{s}}. \tag{A.236}$$

Subtracting (A.232) from (A.231) and using (A.234) and (A.236) we get

$$\cos\theta = \frac{s(t-u)+(m_1^2-m_2^2)(m_3^2-m_4^2)}{\mathcal{L}_{12}(s)\mathcal{L}_{34}(s)}. \tag{A.237}$$

In the range $\theta \in [0,\pi]$ we can also write unambiguously

$$\sin\theta = \sqrt{1-\cos^2\theta} = \frac{2\sqrt{s}\,\sqrt{\Phi}}{\mathcal{L}_{12}(s)\mathcal{L}_{34}(s)}, \tag{A.238}$$

where we have defined

$$\begin{aligned}\Phi &\equiv stu - s(m_2^2-m_4^2)(m_1^2-m_3^2) - t\,(m_1^2-m_2^2)(m_3^2-m_4^2) + \Delta_t\,(m_1^2m_4^2-m_2^2m_3^2)\\ &= stu - s(m_2^2-m_3^2)(m_1^2-m_4^2) + u(m_1^2-m_2^2)(m_3^2-m_4^2) + \Delta_u(m_1^2m_3^2-m_2^2m_4^2)\end{aligned} \tag{A.239}$$

together with

$$\Delta_t \equiv -m_1^2+m_2^2+m_3^2-m_4^2, \qquad \Delta_u \equiv -m_1^2+m_2^2-m_3^2+m_4^2. \tag{A.240}$$

Let us study the physical ranges of the Mandelstam variables. From (A.229) and (A.230) the following inequalities follow

$$s \geq \max\Big((m_1+m_2)^2,\,(m_3+m_4)^2\Big). \tag{A.241}$$

Notice, that due to (A.241) all the energies E_i in (A.236) are positive and $\mathcal{L}_{12}(s)$, $\mathcal{L}_{34}(s)$ are real as they should be. Since the value of $\cos\theta$ is bounded to be in the $[-1,+1]$ interval, we can derive the following constraints on the values of the variable t from (A.237)

$$\begin{aligned}&t \in [v+\frac{\mathcal{L}_{12}(s)\mathcal{L}_{34}(s)}{2s}, v-\frac{\mathcal{L}_{12}(s)\mathcal{L}_{34}(s)}{2s}],\\ &v \equiv \frac{1}{2}\,(m_1^2+m_2^2+m_3^2+m_4^2-s) - \frac{(m_1^2-m_2^2)(m_3^2-m_4^2)}{2s}.\end{aligned} \tag{A.242}$$

From (A.241) and (A.242) in the equal mass case we recover the familiar result

$$s \in [4m^2, \infty), \quad t \in [-(s-4m^2), 0]. \tag{A.243}$$

There is a very special situation when

$$\mathcal{L}_{12}(s) = 0 \quad \textbf{or} \quad \mathcal{L}_{34}(s) = 0. \tag{A.244}$$

From (A.234) we see that this corresponds to when either incoming or outgoing particles are at rest. In such a situation we cannot define the angle between incoming and outgoing particles which can be see from (A.237) which is singular at (A.244). The values of s which lead to (A.244) are

$$s = (m_1 \pm m_2)^2, \quad s = (m_3 \pm m_4)^2 . \tag{A.245}$$

A.5 Crossing equations

The goal of this appendix is to prove the crossing relations in a general frame (1.70) - (1.73) and then derive the crossing equations in the COM frame (1.74) and (1.76) together with the Wigner angles α_i and β_i.

A.5.1 Analytic continuation of four-momenta

Consider the interacting part of the scattering amplitude

$$T^{\lambda_3,\lambda_4}_{\lambda_1,\lambda_2}(p_1^{\mu_1}, p_2^{\mu_2}, p_3^{\mu_3}, p_4^{\mu_4}). \tag{A.246}$$

This function is defined only for non-negative energies $p_i^0 \geq 0$, provided that the following constraint is satisfied

$$p_i^2 = -m_i^2, \tag{A.247}$$

where $m_i \geq 0$ are the masses of particles. However crossing requires us to evaluate the amplitude (A.246) at $-p_i^\mu$ points which means that one must extend the definition of (A.246) also to negative values of energies p_i^0. This can be done by analytically continuing the amplitude (A.246) in each component of four 4-vectors p_i^μ to the full complex plane while keeping the constraints (A.247) satisfied.[10] To perform this analytic continuation, one needs to choose the path in (complexified) momentum space.

To continue the discussion in more detail let us focus for simplicity on a function of a

[10] In other words by using the analytic continuation, the amplitude (A.246) can be defined as a function of $4 \times 4 = 16$ complex variables which satisfy the four constraints (A.247).

single 4-momentum

$$f(p^\mu) \tag{A.248}$$

defined for $p^0 \geq 0$ and $p^2 = -m^2$ with the non-negative mass m. The case of four 4-momenta (A.246) follows straightforwardly by the repeated use of the steps here for each $i = 1, 2, 3, 4$. Using the spherical coordinates $\boldsymbol{p}$, θ and ϕ one can write

$$p^0 = \sqrt{\boldsymbol{p}^2 + m^2}, \qquad \begin{cases} p^1 = \boldsymbol{p} \sin\theta \cos\phi, \\ p^2 = \boldsymbol{p} \sin\theta \sin\phi, \\ p^3 = \boldsymbol{p} \cos\theta, \end{cases} \tag{A.249}$$

where $\boldsymbol{p} \geq 0$ is the length of the 3-vector $\vec{p}$. The relation $p^2 = -m^2$ can be rewritten as

$$\boldsymbol{p} = i\sqrt{(m - p^0)(p^0 + m)}. \tag{A.250}$$

If we promote p^0 to the full complex plane, the function (A.250) will have an analytic structure as depicted on figure A.5 with two branch points $\pm m$ and two branch cuts ending in these points.

In order to study crossing we need to defined (A.248) at the following point

$$f(-p^\mu). \tag{A.251}$$

This can be achieved by performing the following analytic continuation

$$p^0 + i\epsilon \to \text{complex value} \to -p^0 - i\epsilon, \quad \vec{p} \to \text{complex value} \to -\vec{p}. \tag{A.252}$$

In the p^0 complex plane two different paths for such an analytic continuation are depicted in figure A.5 [11]. Note that the original domain of physical energy $p^0 \geq m$ by convention lies slightly above the right-hand branch cut.

Now let us investigate the behavior of the function (A.250) depending on the chosen path of the analytic continuation. If the path does not cross any branch cuts we simply get

$$\boldsymbol{p} \to \text{complex value} \to +\boldsymbol{p}. \tag{A.253}$$

In case we cross once one of the branch cuts we get an extra phase due to the monodromy around the associated branch point which leads to

$$p^0 \pm m \to (p^0 \pm m)e^{2\pi i}.$$

[11] To be precise, the two different paths for analytic continuation take us to two different points on the Riemann surface. We thank Brando Bellazzini for this comment.

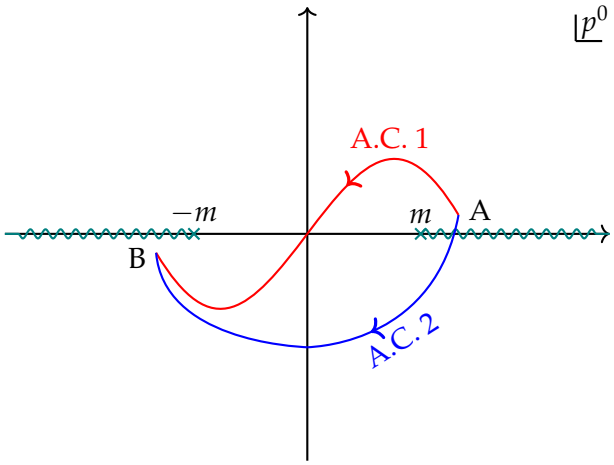

Figure A.5: The complex p^0 plane. We depict the analytic structure of the function $\boldsymbol{p}(p^0)$ defined in (A.250). It has two branch cuts. The original domain of the function $\boldsymbol{p}$ is given by positive values p^0 slightly above the right cut. We define $\boldsymbol{p}$ for negative values of p^0 by an analytic continuation. The two different options are depicted in red and blue. Two paths together encircle the $+m$ branch point and thus differ by a monodromy around that point.

As a result for this path we get the following

$$\boldsymbol{p} \to \text{complex value} \to -\boldsymbol{p}. \tag{A.254}$$

To summarize, the analytic continuation (A.252) can be implemented in two different ways depending on the path chosen on figure A.5. The two distinct options (A.253) and (A.254) due to (A.249) read as

$$p^0 \to -p^0, \quad \boldsymbol{p} \to +\boldsymbol{p}, \quad \theta \to \pi - \theta, \quad \phi \to \pi + \phi, \tag{A.255}$$
$$p^0 \to -p^0, \quad \boldsymbol{p} \to -\boldsymbol{p}, \quad \theta \to \theta, \quad \phi \to \phi. \tag{A.256}$$

The first option (A.255) is commonly used in the literature. The second option (A.256) is more suitable for massless particles since two branch cuts in figure A.5 unite and one cannot choose a path for the analytic continuation without crossing any of the two branch cuts. For treating massless particles one can also use the first option (A.255) and take the limit $m \to 0$ at the very end.

The helicity states are defined via (1.5) and at a practical level depend only on the rapidity and two angles (η, θ, ϕ). Using the definition of rapidity (1.6) we can write

(A.255) and (A.256) as

$$\eta \to i\pi - \eta, \quad \theta \to \pi - \theta, \quad \phi \to \pi + \phi, \tag{A.257}$$
$$\eta \to i\pi + \eta, \quad \theta \to \theta, \quad \phi \to \phi. \tag{A.258}$$

A.5.2 Crossing equations in a general frame

Given an amplitude of the $12 \to 34$ process in a generic frame we would like to relate it in this appendix to the four "crossed" amplitudes associated to the following processes

$$\bar{4}2 \to 3\bar{1}, \qquad 1\bar{3} \to \bar{2}4, \qquad \bar{3}2 \to \bar{1}4, \qquad 1\bar{4} \to 3\bar{2}. \tag{A.259}$$

We refer to these relations as the crossing equations. To be concrete we will focus on writing the crossing equations for $12 \to 34$ and $\bar{4}2 \to 3\bar{1}$ amplitudes, the rest will follow by analogy.

Given an amplitude

$$T_{12\to 34}{}^{\lambda_3,\lambda_4}_{\lambda_1,\lambda_2}(p_1, p_2, p_3, p_4), \tag{A.260}$$

one can obtain the amplitude $\bar{4}2 \to 3\bar{1}$ by crossing particles 1 and 4. The ingoing particle 1 becomes then the outgoing one and the outgoing particle 4 becomes the ingoing one. As a result we need to make the following replacements: $p_1^\mu \to -p_1^\mu$ and $p_4^\mu \to -p_4^\mu$. Moreover if a particle 1 has a charge (or more generally transforms in some representation of a global group) the particle $\bar{i}$ has the opposite charge (transforms in the conjugate representation). As a result (A.260) under crossing 1-4 becomes

$$T_{\bar{4}2\to 3\bar{1}}{}^{\lambda_3,\lambda_1}_{\lambda_4,\lambda_2}(-p_4, p_2, p_3, -p_1). \tag{A.261}$$

In both (A.260) and (A.261) all 4-momenta have positive energies $p_i^0 > 0$ and are on-shell (1.48).

Without using the LSZ reduction formula one can only postulate crossing. It states that one can define a single "mother amplitude" with complex values of 4-momenta such that all the amplitudes in (A.260) and (A.261) are its boundary values. This is known as the Mandelstam hypothesis. One cannot however simply equate (A.260) and (A.261). At the very least these amplitudes should have the same Lorentz transformation properties. We will use this requirement to fix the crossing equations up to an overall phase. This is the original way by which general spin crossing equations were derived in [47].

Consider the transformation property of the amplitude describing the $12 \to 34$ process

under generic Lorentz transformations Λ. According to (1.54) it reads as

$$T_{12\to 34}{}^{\lambda_3,\lambda_4}_{\lambda_1,\lambda_2}(p_1,p_2,p_3,p_4) = \tag{A.262}$$
$$\sum_{\lambda_i'} \mathscr{D}^{(j_1)}_{\lambda_1'\lambda_1}(p_1,\Lambda)\mathscr{D}^{(j_2)}_{\lambda_2'\lambda_2}(p_2,\Lambda)\mathscr{D}^{*(j_3)}_{\lambda_3'\lambda_3}(p_3,\Lambda)\mathscr{D}^{*(j_4)}_{\lambda_4'\lambda_4}(p_4,\Lambda)T_{12\to 34}{}^{\lambda_3',\lambda_4'}_{\lambda_1',\lambda_2'}(p_1',p_2',p_3',p_4').$$

Similarly the crossed amplitude describing the $\bar{4}2\to 3\bar{1}$ process transforms as

$$T_{\bar{4}2\to 3\bar{1}}{}^{\lambda_3,\lambda_1}_{\lambda_4,\lambda_2}(-p_4,p_2,p_3,-p_1) = \tag{A.263}$$
$$\sum_{\lambda_i'} \mathscr{D}^{*(j_1)}_{\lambda_1'\lambda_1}(-p_1,\Lambda)\mathscr{D}^{(j_2)}_{\lambda_2'\lambda_2}(p_2,\Lambda)\mathscr{D}^{*(j_3)}_{\lambda_3'\lambda_3}(p_3,\Lambda)\mathscr{D}^{(j_4)}_{\lambda_4'\lambda_4}(-p_4,\Lambda)T_{\bar{4}2\to 3\bar{1}}{}^{\lambda_3',\lambda_1'}_{\lambda_4',\lambda_2'}(-p_4',p_2',p_3',-p_1').$$

In the equations (A.262) and (A.263) we have schematically denoted the arguments of the Wigner D-matrices by (p_i,Λ). In practice they depend only on three Wigner angles which correspond to the $p_i\to\Lambda p_i$ Lorentz transformation. We denote these angles as

$$\mathscr{D}^{(j_i)}_{\lambda_i'\lambda_i}(\alpha_i,\beta_i,\gamma_i) \equiv \mathscr{D}^{(j_i)}_{\lambda_i'\lambda_i}(+p,\Lambda), \tag{A.264}$$
$$\mathscr{D}^{(j_i)}_{\lambda_i'\lambda_i}(\bar{\alpha}_i,\bar{\beta}_i,\bar{\gamma}_i) \equiv \mathscr{D}^{(j)}_{\lambda'\lambda_i}(-p_i,\Lambda), \tag{A.265}$$

where $i=1,2,3,4$. The Wigner angles $(\alpha_i,\beta_i,\gamma_i)$ generically differ from $(\bar{\alpha}_i,\bar{\beta}_i,\bar{\gamma}_i)$. They are however closely related. The main technical task of this appendix is to understand precisely how.

We would like to equate the amplitudes which transform in the same way under Lorentz transformations. Thus, in practice we need to compare the transformation properties of (A.262) and (A.263). This in turn boils down to comparing the Wigner D-matrices

$$\mathscr{D}^{(j_1)}_{\lambda_1'\lambda_1}(+p_1,\Lambda) \quad \text{vs.} \quad \mathscr{D}^{*(j_1)}_{\lambda_1'\lambda_1}(-p_1,\Lambda) \qquad \textbf{and} \qquad \mathscr{D}^{*(j_4)}_{\lambda_4'\lambda_4}(+p_4,\Lambda) \quad \text{vs.} \quad \mathscr{D}^{(j_4)}_{\lambda_4'\lambda_4}(-p_4,\Lambda).$$

In order to do this recall that according to (A.58) and (A.60) the Wigner rotation matrices are defined as

$$\mathscr{D}^{(j)}_{\lambda'\lambda}(\alpha,\beta,\gamma) = \mathscr{D}^{(j)}_{\lambda'\lambda}(+p,\Lambda): \quad R(\alpha,\beta,\gamma) = U_{\rm h}(+p')^{-1}\Lambda U_{\rm h}(+p), \tag{A.266}$$
$$\mathscr{D}^{(j)}_{\lambda'\lambda}(\bar{\alpha},\bar{\beta},\bar{\gamma}) = \mathscr{D}^{(j)}_{\lambda'\lambda}(-p,\Lambda): \quad R(\bar{\alpha},\bar{\beta},\bar{\gamma}) = U_{\rm h}(-p')^{-1}\Lambda U_{\rm h}(-p), \tag{A.267}$$

where the helicity transformation $U_{\rm h}(+p)$ is defined via (A.54). We repeat this definition here for convenience

$$U_{\rm h}(+p) = R(\phi,\theta,-\phi)\times B_3(\eta). \tag{A.268}$$

The quantity $U_{\rm h}(-p)$ is defined from $U_{\rm h}(+p)$ by analytic continuation. As discussed in the previous section there are two distinct ways to do it, using (A.257) or (A.258). Below we address the two options separately.

Analytic continuation 1

Using (A.268) and (A.257) we get

$$U_{\rm h}(-p) = R(\pi+\phi,\, \pi-\theta,\, -\pi-\phi) \times B_3(i\pi-\eta). \tag{A.269}$$

We can then focus on the vector representation defined in appendix A.1.3 and compute the Wigner angles in (A.266) and (A.267) brute force using computer algebra.[12,13,14] Comparing the results we conclude that

$$\bar\alpha = -\alpha + 2\phi', \quad \bar\beta = -\beta, \quad \bar\gamma = -\gamma - 2\phi. \tag{A.270}$$

From the properties of the Wigner D-matrix it then follows that

$$\begin{aligned} \mathscr{D}^{(j)}_{\lambda',\lambda}(\bar\alpha,\bar\beta,\bar\gamma) &= e^{-2i\phi'\lambda'}\mathscr{D}^{(j)}_{\lambda',\lambda}(-\alpha,-\beta,-\gamma)e^{+2i\phi\lambda} \\ &= e^{i(\pi-2\phi')\lambda'}e^{-i(\pi-2\phi)\lambda}\mathscr{D}^{*(j)}_{\lambda'\lambda}(\alpha,\beta,\gamma), \end{aligned} \tag{A.271}$$

see appendix A.2 of [44] for the summary of properties of D matrices. In other words

$$\mathscr{D}^{(j)}_{\lambda'\lambda}(-p,\Lambda) = e^{i(\pi-2\phi')\lambda'}e^{-i(\pi-2\phi)\lambda}\mathscr{D}^{*(j)}_{\lambda'\lambda}(+p,\Lambda). \tag{A.272}$$

With the help of (A.272) one can rewrite the transformation property (A.263) in the following form[15]

$$T_{\bar 4 2\to 3\bar 1}{}^{\lambda_3,\lambda_1}_{\lambda_4,\lambda_2}(-p_4,p_2,p_3,-p_1) = \sum_{\lambda_i'} e^{-i(\pi-2\phi_1')\lambda_1'}e^{+i(\pi-2\phi_1)\lambda_1}e^{i(\pi-2\phi_4')\lambda_4'}e^{-i(\pi-2\phi_4)\lambda_4} \tag{A.273}$$

$$\mathscr{D}^{(j_1)}_{\lambda_1'\lambda_1}(+p_1,\Lambda)\mathscr{D}^{(j_2)}_{\lambda_2'\lambda_2}(+p_1,\Lambda)\mathscr{D}^{*(j_3)}_{\lambda_3'\lambda_3}(+p_1,\Lambda)\mathscr{D}^{*(j_4)}_{\lambda_4'\lambda_4}(+p_4,\Lambda)T_{\bar 4 2\to 3\bar 1}{}^{\lambda_3',\lambda_1'}_{\lambda_4',\lambda_2'}(-p_4',p_2',p_3',-p_1'),,$$

[12] Given a generic 3×3 rotation matrix it is straightforward to determine $\tan\alpha$, $\cos\beta$ and $\tan\gamma$ without any ambiguity. In order to determine the rest of trigonometric functions it is necessary to choose the region of β angle. One can either have $\beta\in[0,\pi]$ or $\beta\in[0,-\pi]$.

[13] By convention $\beta\in[0,\pi]$, however we are free to choose either $\bar\beta\in[0,\pi]$ or $\bar\beta\in[0,-\pi]$. We make the latter choice, however both options lead to the same conclusion at the very end.

[14] We first perform this computation for a generic infinitesimal Lorentz transformation. We then focus on some simple finite transformations like boosts along the x, y and z axes separately.

[15] In writing this formula we assumed that the relation between $\mathscr{D}^{*(j)}_{\lambda'\lambda}(-p,\Lambda)$ and $\mathscr{D}^{(j)}_{\lambda'\lambda}(+p,\Lambda)$ is obtained from (A.272) by taking complex conjugation. This is not quite correct because we are interested in the analytic continuation along the same path in the p^0 complex plane and not along the complex conjugated path. However, the two continuations are related by a monodromy around square root branch points that can only give rise to an overall helicity-independent phase which is irrelevant for the discussion below.

which can be rewritten as

$$\left(e^{-i(\pi-2\phi_1)\lambda_1}e^{+i(\pi-2\phi_4)\lambda_4}T_{\bar{4}2\to 3\bar{1}}{}^{\lambda_3,\lambda_1}_{\lambda_4,\lambda_2}(-p_4,p_2,p_3,-p_1)\right)=\sum_{\lambda_i'}\mathscr{D}^{(j_1)}_{\lambda_1'\lambda_1}(+p_1,\Lambda)\mathscr{D}^{(j_2)}_{\lambda_2'\lambda_2}(+p_1,\Lambda)$$
$$\mathscr{D}^{*(j_3)}_{\lambda_3'\lambda_3}(+p_1,\Lambda)\mathscr{D}^{*(j_4)}_{\lambda_4'\lambda_4}(+p_4,\Lambda)\left(e^{-i(\pi-2\phi_1')\lambda_1'}e^{i(\pi-2\phi_4')\lambda_4'}T_{\bar{4}2\to 3\bar{1}}{}^{\lambda_3',\lambda_1'}_{\lambda_4',\lambda_2'}(-p_4',p_2',p_3',-p_1')\right). \tag{A.274}$$

Comparing (A.262) and (A.274) we see that the following two objects transform in the same way under generic Lorentz transformations

$$T_{12\to 34}{}^{\lambda_3,\lambda_4}_{\lambda_1,\lambda_2}(p_1,p_2,p_3,p_4)\ \text{ vs. }\ e^{-i(\pi-2\phi_1)\lambda_1}e^{i(\pi-2\phi_4)\lambda_4}T_{\bar{4}2\to 3\bar{1}}{}^{\lambda_3,\lambda_1}_{\lambda_4,\lambda_2}(-p_4,p_2,p_3,-p_1). \tag{A.275}$$

As a result, the only way to write crossing equations which involve objects transforming in the same way under generic Lorentz tranformation is to equate the objects in (A.275). This procedure leaves undetermined an overall helicity independent phase. The other crossing equations follow by simply re-labeling the indices.

Our final answer reads as

$$\begin{aligned}
T_{12\to 34}{}^{\lambda_3,\lambda_4}_{\lambda_1,\lambda_2}(p_1,p_2,p_3,p_4)&=\epsilon_{14}^{(1)}e^{-i(\pi-2\phi_1)\lambda_1}e^{i(\pi-2\phi_4)\lambda_4}T_{\bar{4}2\to 3\bar{1}}{}^{\lambda_3,\lambda_1}_{\lambda_4,\lambda_2}(-p_4,p_2,p_3,-p_1),\\
T_{12\to 34}{}^{\lambda_3,\lambda_4}_{\lambda_1,\lambda_2}(p_1,p_2,p_3,p_4)&=\epsilon_{23}^{(1)}e^{-i(\pi-2\phi_2)\lambda_2}e^{i(\pi-2\phi_3)\lambda_3}T_{1\bar{3}\to\bar{2}4}{}^{\lambda_2,\lambda_4}_{\lambda_1,\lambda_3}(p_1,-p_3,-p_2,p_4),\\
T_{12\to 34}{}^{\lambda_3,\lambda_4}_{\lambda_1,\lambda_2}(p_1,p_2,p_3,p_4)&=\epsilon_{13}^{(1)}e^{-i(\pi-2\phi_1)\lambda_1}e^{i(\pi-2\phi_3)\lambda_3}T_{\bar{3}2\to 1\bar{4}}{}^{\lambda_1,\lambda_4}_{\lambda_3,\lambda_2}(-p_3,p_2,-p_1,p_4),\\
T_{12\to 34}{}^{\lambda_3,\lambda_4}_{\lambda_1,\lambda_2}(p_1,p_2,p_3,p_4)&=\epsilon_{24}^{(1)}e^{-i(\pi-2\phi_2)\lambda_2}e^{i(\pi-2\phi_4)\lambda_4}T_{1\bar{4}\to 3\bar{2}}{}^{\lambda_3,\lambda_2}_{\lambda_1,\lambda_4}(p_1,-p_4,p_3,-p_2),
\end{aligned} \tag{A.276}$$

where $\epsilon_{14}^{(1)}$, $\epsilon_{23}^{(1)}$, $\epsilon_{13}^{(1)}$ and $\epsilon_{24}^{(1)}$ are the helicity independent phases unfixed by this procedure.

Analytic continuation 2

Using (A.268) and (A.258) we get

$$U_{\rm h}(-p)=R(\phi,\,\theta,\,-\phi)\times B_3(i\pi+\eta)=-U_{\rm h}(+p)R(\pi,0,0). \tag{A.277}$$

Plugging it into (A.267) one gets

$$\begin{aligned}
\mathscr{D}^{(j)}_{\lambda'\lambda}(\bar{\alpha},\bar{\beta},\bar{\gamma})=\mathscr{D}^{(j)}_{\lambda'\lambda}(-p,\Lambda):\quad R(\bar{\alpha},\bar{\beta},\bar{\gamma})&=R^{-1}(\pi,0,0)\Big(U_{\rm h}(+p')^{-1}\Lambda U_{\rm h}(+p)\Big)R(\pi,0,0)\\
&=R^{-1}(\pi,0,0)R(\alpha,\beta,\gamma)R(\pi,0,0).
\end{aligned} \tag{A.278}$$

Using the properties of the small Wigner d-matrices we can write then

$$\mathscr{D}^{(j)}_{\lambda'\lambda}(\bar{\alpha},\bar{\beta},\bar{\gamma}) = e^{+i\pi\lambda'}\mathscr{D}^{(j)}_{\lambda'\lambda}(\alpha,\beta,\gamma)e^{-i\pi\lambda} = \mathscr{D}^{*(j)}_{-\lambda',-\lambda}(\alpha,\beta,\gamma). \tag{A.279}$$

In other words we get

$$\mathscr{D}^{(j)}_{\lambda'\lambda}(-p,\Lambda) = \mathscr{D}^{*(j)}_{-\lambda',-\lambda}(+p,\Lambda). \tag{A.280}$$

Using this we can write the transformation property (A.263) as[16]

$$\begin{aligned} &T_{\bar{4}2\to 3\bar{1}}{}^{\lambda_3,\lambda_1}_{\lambda_4,\lambda_2}(-p_4,p_2,p_3,-p_1) = \\ &\sum_{\lambda'_i}\mathscr{D}^{(j_1)}_{-\lambda'_1,-\lambda_1}(+p_1,\Lambda)\mathscr{D}^{(j_2)}_{\lambda'_2\lambda_2}(+p_2,\Lambda)\mathscr{D}^{*(j_3)}_{\lambda'_3\lambda_3}(+p_3,\Lambda)\mathscr{D}^{*(j_4)}_{-\lambda'_4,-\lambda_4}(+p_4,\Lambda)T_{\bar{4}2\to 3\bar{1}}{}^{\lambda'_3,\lambda'_1}_{\lambda'_4,\lambda'_2}(-p'_4,p'_2,p'_3,-p'_1). \end{aligned} \tag{A.281}$$

Let us rename λ_1 and λ_4 and call them $-\lambda_1$ and $-\lambda_4$. We can also do the same for λ'_1 and λ'_4 since they are dummy indices and the summation covers all the options. We get then

$$\begin{aligned} &T_{\bar{4}2\to 3\bar{1}}{}^{+\lambda_3,-\lambda_1}_{-\lambda_4,+\lambda_2}(-p_4,p_2,p_3,-p_1) = \\ &\sum_{\lambda'_i}\mathscr{D}^{(j_1)}_{\lambda'_1,\lambda_1}(+p_1,\Lambda)\mathscr{D}^{(j_2)}_{\lambda'_2\lambda_2}(+p_2,\Lambda)\mathscr{D}^{*(j_3)}_{\lambda'_3\lambda_3}(+p_3,\Lambda)\mathscr{D}^{*(j_4)}_{\lambda'_4,\lambda_4}(+p_4,\Lambda)T_{\bar{4}2\to 3\bar{1}}{}^{+\lambda'_3,-\lambda'_1}_{-\lambda'_4,+\lambda'_2}(-p'_4,p'_2,p'_3,-p'_1). \end{aligned} \tag{A.282}$$

Comparing (A.262) and (A.282) we conclude that the following two objects transform in the same way under the generic Lorentz transformations

$$T_{12\to 34}{}^{\lambda_3,\lambda_4}_{\lambda_1,\lambda_2}(+p_1,p_2,p_3,+p_4) \quad \text{vs.} \quad T_{\bar{4}2\to 3\bar{1}}{}^{+\lambda_3,-\lambda_1}_{-\lambda_4,+\lambda_2}(-p_4,p_2,p_3,-p_1). \tag{A.283}$$

Analogous discussion holds for other crossings we can thus write the following equations

$$\begin{aligned} T_{12\to 34}{}^{\lambda_3,\lambda_4}_{\lambda_1,\lambda_2}(p_1,p_2,p_3,p_4) &= \epsilon^{(2)}_{14}\; T_{\bar{4}2\to 3\bar{1}}{}^{+\lambda_3,-\lambda_1}_{-\lambda_4,+\lambda_2}(-p_4,+p_2,+p_3,-p_1), \\ T_{12\to 34}{}^{\lambda_3,\lambda_4}_{\lambda_1,\lambda_2}(p_1,p_2,p_3,p_4) &= \epsilon^{(2)}_{23}\; T_{1\bar{3}\to\bar{2}4}{}^{-\lambda_2,+\lambda_4}_{+\lambda_1,-\lambda_3}(+p_1,-p_3,-p_2,+p_4), \\ T_{12\to 34}{}^{\lambda_3,\lambda_4}_{\lambda_1,\lambda_2}(p_1,p_2,p_3,p_4) &= \epsilon^{(2)}_{13}\; T_{\bar{3}2\to 1\bar{4}}{}^{-\lambda_1,+\lambda_4}_{-\lambda_3,+\lambda_2}(-p_3,+p_2,-p_1,+p_4), \\ T_{12\to 34}{}^{\lambda_3,\lambda_4}_{\lambda_1,\lambda_2}(p_1,p_2,p_3,p_4) &= \epsilon^{(2)}_{24}\; T_{1\bar{4}\to 3\bar{2}}{}^{+\lambda_3,-\lambda_2}_{+\lambda_1,-\lambda_4}(+p_1,-p_4,+p_3,-p_2), \end{aligned} \tag{A.284}$$

where as before $\epsilon^{(2)}_{14}$, $\epsilon^{(2)}_{23}$, $\epsilon^{(2)}_{13}$ and $\epsilon^{(2)}_{24}$ are the helicity independent phases unfixed by this procedure.

[16] See footnote 15.

A.5.3 Crossing equations in a general frame: LSZ derivation

In this section we derive the crossing equation (1.71) from the LSZ reduction formula in the case of spin 1/2 fermion scattering. The latter is carefully discussed in section 41 of [97]. The LSZ reduction formula in this case reads as

$$\begin{aligned} T_{12\to 34}{}^{\lambda_3,\lambda_4}_{\lambda_1,\lambda_2}(p_1,p_2,p_3,p_4) &= \int d^4x_1\, d^4x_2\, d^4x_3\, d^4x_4 \\ &\times\ e^{-ip_3x_3}\,[\bar{u}_{\lambda_3}(p_3)(-i\not{\partial}_3+m_3)]_{\alpha_3} \\ &\times\ e^{-ip_4x_4}\,[\bar{u}_{\lambda_4}(p_4)(-i\not{\partial}_4+m_4)]_{\alpha_4} \\ &\times\ \langle\Omega|T\{\Psi_{\alpha_4}(x_4)\Psi_{\alpha_3}(x_3)\overline{\Psi}_{\alpha_1}(x_1)\overline{\Psi}_{\alpha_2}(x_2)\}|\Omega\rangle_{connected} \\ &\times\ [(i\overleftarrow{\not{\partial}}_1+m_1)u_{\lambda_1}(p_1)]_{\alpha_1}\,e^{ip_1x_1} \\ &\times\ [(i\overleftarrow{\not{\partial}}_2+m_2)u_{\lambda_2}(p_2)]_{\alpha_2}\,e^{ip_2x_2}, \end{aligned} \tag{A.285}$$

where $|\Omega\rangle$ denotes the vacuum state and $\Psi_i(x)$ are 4-component Majorana or Dirac fields with masses m_i. Analogously one can write

$$\begin{aligned} T_{1\bar{3}\to\bar{2}4}{}^{\lambda_2,\lambda_4}_{\lambda_1,\lambda_3}(p_1,p_3,p_2,p_4) &= \int d^4x_1\, d^4x_2\, d^4x_3\, d^4x_4 \\ &\times\ e^{ip_3x_3}\,[\bar{v}_{\lambda_3}(p_3)(-i\not{\partial}_3+m_3)]_{\alpha_3} \\ &\times\ e^{-ip_4x_4}\,[\bar{u}_{\lambda_4}(p_4)(-i\not{\partial}_4+m_4)]_{\alpha_4} \\ &\times\ \langle\Omega|T\{\Psi_{\alpha_4}(x_4)\overline{\Psi}_{\alpha_2}(x_2)\overline{\Psi}_{\alpha_1}(x_1)\Psi_{\alpha_3}(x_3)\}|\Omega\rangle_{connected} \\ &\times\ [(i\overleftarrow{\not{\partial}}_1+m_1)u_{\lambda_1}(p_1)]_{\alpha_1}\,e^{ip_1x_1} \\ &\times\ [(i\overleftarrow{\not{\partial}}_2+m_2)v_{\lambda_2}(p_2)]_{\alpha_2}\,e^{-ip_2x_2}. \end{aligned} \tag{A.286}$$

In the above equations all the momenta have positive energy, namely $p_i^0 > 0$. In order to relate the two processes (A.285) and (A.286) one can analytically continue the latter process in p_2 and p_3 to allow for negative energies. Assuming such an analytic continuation exists one gets

$$\begin{aligned} T_{1\bar{3}\to\bar{2}4}{}^{\lambda_2,\lambda_4}_{\lambda_1,\lambda_3}(p_1,-p_3,-p_2,p_4) &= \int d^4x_1\, d^4x_2\, d^4x_3\, d^4x_4 \\ &\times\ e^{-ip_3x_3}\,[\bar{v}_{\lambda_3}(-p_3)(-i\not{\partial}_3+m_3)]_{\alpha_3} \\ &\times\ e^{-ip_4x_4}\,[\bar{u}_{\lambda_4}(p_4)(-i\not{\partial}_4+m_4)]_{\alpha_4} \\ &\times\ \langle\Omega|T\{\Psi_{\alpha_4}(x_4)\overline{\Psi}_{\alpha_2}(x_2)\overline{\Psi}_{\alpha_1}(x_1)\Psi_{\alpha_3}(x_3)\}|\Omega\rangle_{connected} \\ &\times\ [(i\overleftarrow{\not{\partial}}_1+m_1)u_{\lambda_1}(p_1)]_{\alpha_1}\,e^{ip_1x_1} \\ &\times\ [(i\overleftarrow{\not{\partial}}_2+m_2)v_{\lambda_2}(-p_2)]_{\alpha_2}\,e^{ip_2x_2}. \end{aligned} \tag{A.287}$$

Notice also that the anticommutation of fermionic operators manifests itself in the following relation

$$\langle\Omega|T\{\Psi_{\alpha_4}(x_4)\overline{\Psi}_{\alpha_2}(x_2)\overline{\Psi}_{\alpha_1}(x_1)\Psi_{\alpha_3}(x_3)\}|\Omega\rangle = \\ -\langle\Omega|T\{\Psi_{\alpha_4}(x_4)\Psi_{\alpha_3}(x_3)\overline{\Psi}_{\alpha_1}(x_1)\overline{\Psi}_{\alpha_2}(x_2)\}|\Omega\rangle. \quad \text{(A.288)}$$

According to appendix A.5.1 there are two ways of choosing the analytic continuation when writing (A.287). Below we discuss both of them in order.

Analytic continuation 1

Using the analytic continuation (A.255) and the definition (2.67) it follows straightforwardly

$$\begin{aligned} u_\lambda(-p) &= e^{i\lambda(\pi+2\phi)}v_\lambda(p), \qquad \bar{u}_\lambda(-p) = e^{i\lambda(\pi-2\phi)}\bar{v}_\lambda(p), \\ v_\lambda(-p) &= e^{i\lambda(\pi-2\phi)}u_\lambda(p), \qquad \bar{v}_\lambda(-p) = e^{i\lambda(\pi+2\phi)}\bar{u}_\lambda(p). \end{aligned} \quad \text{(A.289)}$$

Plugging (A.289) and (A.288) into (A.287) and comparing the result with (A.285) we arrive at the following crossing equation

$$T_{12\to34}{}^{\lambda_3,\lambda_4}_{\lambda_1,\lambda_2}(p_1,p_2,p_3,p_4) = -e^{-i\lambda_2(\pi-2\phi_2)}e^{-i\lambda_3(\pi+2\phi_3)}T_{1\bar{3}\to\bar{2}4}{}^{\lambda_2,\lambda_4}_{\lambda_1,\lambda_3}(p_1,-p_3,-p_2,p_4). \quad \text{(A.290)}$$

Analogously one derives the other three crossing equations. The complete summary of crossing equations reads

$$\begin{aligned} T_{12\to34}{}^{\lambda_3,\lambda_4}_{\lambda_1,\lambda_2}(p_1,p_2,p_3,p_4) &= -e^{-i\lambda_1(\pi-2\phi_1)}e^{-i\lambda_4(\pi+2\phi_4)}T_{\bar{4}2\to3\bar{1}}{}^{\lambda_3,\lambda_1}_{\lambda_4,\lambda_2}(-p_4,p_2,p_3,-p_1), \\ T_{12\to34}{}^{\lambda_3,\lambda_4}_{\lambda_1,\lambda_2}(p_1,p_2,p_3,p_4) &= -e^{-i\lambda_2(\pi-2\phi_2)}e^{-i\lambda_3(\pi+2\phi_3)}T_{1\bar{3}\to\bar{2}4}{}^{\lambda_2,\lambda_4}_{\lambda_1,\lambda_3}(p_1,-p_3,-p_2,p_4), \\ T_{12\to34}{}^{\lambda_3,\lambda_4}_{\lambda_1,\lambda_2}(p_1,p_2,p_3,p_4) &= -e^{-i\lambda_1(\pi-2\phi_1)}e^{-i\lambda_3(\pi+2\phi_3)}T_{\bar{3}2\to\bar{1}4}{}^{\lambda_1,\lambda_4}_{\lambda_3,\lambda_2}(-p_3,p_2,-p_1,p_4), \\ T_{12\to34}{}^{\lambda_3,\lambda_4}_{\lambda_1,\lambda_2}(p_1,p_2,p_3,p_4) &= -e^{-i\lambda_2(\pi-2\phi_2)}e^{-i\lambda_4(\pi+2\phi_4)}T_{1\bar{4}\to3\bar{2}}{}^{\lambda_3,\lambda_2}_{\lambda_1,\lambda_4}(p_1,-p_4,p_3,-p_2). \end{aligned} \quad \text{(A.291)}$$

We can now compare the above to (A.276) and deduce the undetermined phases[17]

$$\epsilon_{14}^{(1)} = \epsilon_{23}^{(1)} = \epsilon_{13}^{(1)} = \epsilon_{24}^{(1)} = +1. \quad \text{(A.292)}$$

Analytic continuation 2

Using the analytic continuation (A.256) and the definition (2.67) it follows straightforwardly

$$\begin{aligned} u_\lambda(-p) &= i\,v_{-\lambda}(p), \qquad \bar{u}_\lambda(-p) = i\,\bar{v}_{-\lambda}(p), \\ v_\lambda(-p) &= i\,u_{-\lambda}(p), \qquad \bar{v}_\lambda(-p) = i\,\bar{u}_{-\lambda}(p). \end{aligned} \quad \text{(A.293)}$$

[17] Here we use the fact that $e^{2i\pi\lambda} = -1$ since λ is half-integer.

Plugging (A.293) and (A.288) into (A.287) and comparing the result with (A.285) we arrive at the following crossing equation

$$T_{12\to34}{}^{\lambda_3,\lambda_4}_{\lambda_1,\lambda_2}(p_1,p_2,p_3,p_4) = T_{1\bar{3}\to\bar{2}4}{}^{-\lambda_2,+\lambda_4}_{+\lambda_1,-\lambda_3}(p_1,-p_3,-p_2,p_4). \tag{A.294}$$

Analogously one derives the other three crossing equations. The complete summary of crossing equations reads

$$\begin{aligned}
T_{12\to34}{}^{\lambda_3,\lambda_4}_{\lambda_1,\lambda_2}(p_1,p_2,p_3,p_4) &= T_{\bar{4}2\to3\bar{1}}{}^{+\lambda_3,-\lambda_1}_{-\lambda_4,+\lambda_2}(-p_4,p_2,p_3,-p_1),\\
T_{12\to34}{}^{\lambda_3,\lambda_4}_{\lambda_1,\lambda_2}(p_1,p_2,p_3,p_4) &= T_{1\bar{3}\to\bar{2}4}{}^{-\lambda_2,+\lambda_4}_{+\lambda_1,-\lambda_3}(p_1,-p_3,-p_2,p_4),\\
T_{12\to34}{}^{\lambda_3,\lambda_4}_{\lambda_1,\lambda_2}(p_1,p_2,p_3,p_4) &= T_{\bar{3}2\to\bar{1}4}{}^{-\lambda_1,+\lambda_4}_{-\lambda_3,+\lambda_2}(-p_3,p_2,-p_1,p_4),\\
tT_{12\to34}{}^{\lambda_3,\lambda_4}_{\lambda_1,\lambda_2}(p_1,p_2,p_3,p_4) &= T_{1\bar{4}\to3\bar{2}}{}^{+\lambda_3,-\lambda_2}_{+\lambda_1,-\lambda_4}(p_1,-p_4,p_3,-p_2).
\end{aligned} \tag{A.295}$$

Comparing the above with (A.284), we see that all the previously undetermined phases are

$$\epsilon_{14}^{(2)} = \epsilon_{23}^{(2)} = \epsilon_{13}^{(2)} = \epsilon_{24}^{(2)} = +1. \tag{A.296}$$

Concluding remarks

We have derived in this appendix the crossing equations for generic spin 1/2 particles in a general frame using the LSZ reduction formula. These depend on the analytic continuation. For the analytic continuation (A.255) our crossing equations are given by (A.291). For the analytic continuation (A.256) our crossing equations are given by (A.295). All these formulas remain (almost) the same even if some of the particles have spin different from 1/2. This follows from the fact that the spin structures of a generic spin particle can be represented by products of u and v objects. The only change in the crossing equations comes in the overall sign since some particles can now commute instead.

A.5.4 Crossing equations in the center of mass frame

The goal of this appendix is to write the crossing equations (A.276) and (A.284) in the center of mass frame. We will see that both analytic continuations lead to the same center of mass equations. The crossing equations 1-4 and 2-3 are called the $s-t$ equations. Since they carry identical information, we focus on only on the 2-3 crossing equation. Instead the crossing equations 1-3 and 2-4 are called the $s-u$ equations. Since they also carry the same information we focus on only the 2-4 crossing equation. The discussion of the $s-u$ center of mass equations is identical to the $s-t$ one, we will therefore only provide the final results without any intermediate steps.

$s-t$ crossing equation

According to appendix A.5.2 the 2-3 crossing equation depending on the analytic continuation can take either of the two forms

$$T_{12\to34}{}^{\lambda_3,\lambda_4}_{\lambda_1,\lambda_2}(p_1,p_2,p_3,p_4) = \epsilon_{23}^{(1)} e^{-i(\pi-2\phi_2)\lambda_2} e^{i(\pi-2\phi_3)\lambda_3} T_{1\bar{3}\to\bar{2}4}{}^{\lambda_2,\lambda_4}_{\lambda_1,\lambda_3}(P_1,P_2,P_3,P_4), \tag{A.297}$$

$$T_{12\to34}{}^{\lambda_3,\lambda_4}_{\lambda_1,\lambda_2}(p_1,p_2,p_3,p_4) = \epsilon_{23}^{(2)}\ T_{1\bar{3}\to\bar{2}4}{}^{-\lambda_2,+\lambda_4}_{+\lambda_1,-\lambda_3}(P_1,P_2,P_3,P_4), \tag{A.298}$$

where we have defined

$$P_1 \equiv p_1, \quad P_2 \equiv -p_3, \quad P_3 \equiv -p_2, \quad P_4 \equiv p_4. \tag{A.299}$$

In the right hand-side of (A.297) and (A.298) P_1 and P_2 describe the incoming particles 1 and $\bar{3}$ respectively, whereas P_3 and P_4 describe the outgoing particles $\bar{2}$ and 4 respectively. The Mandelstam variables associated to the left-hand side are as usual

$$s \equiv -(p_1+p_2)^2, \quad t \equiv -(p_1-p_3)^2, \quad u \equiv -(p_1-p_4)^2. \tag{A.300}$$

Instead the Mandelstam variables associated to the right-hand side are

$$\begin{aligned} S &\equiv -(P_1+P_2)^2 = -(p_1-p_3)^2 = t, \\ T &\equiv -(P_1-P_3)^2 = -(p_1+p_2)^2 = s, \\ U &\equiv -(P_1-P_4)^2 = -(p_1-p_4)^2 = u. \end{aligned} \tag{A.301}$$

The Mandelstam variables remain invariant by definition under any Lorentz transformation.

Let us now evaluate the left-hand side of (A.297) and (A.298) in the center of mass frame of the $12\to34$ process denoted by p_i^{com}. It is defined in (3.9), we write it here again for convenience

$$\begin{aligned} p_1^{\text{com}} &\equiv (E_1, 0, 0, +\boldsymbol{p}), \\ p_3^{\text{com}} &\equiv (E_3, +\boldsymbol{p}'\sin\theta, 0, +\boldsymbol{p}'\cos\theta), \\ p_2^{\text{com}} &\equiv (E_2, 0, 0, -\boldsymbol{p}), \\ p_4^{\text{com}} &\equiv (E_4, -\boldsymbol{p}'\sin\theta, 0, -\boldsymbol{p}'\cos\theta). \end{aligned} \tag{A.302}$$

The main feature of this frame is that it respects the center of mass conditions

$$\begin{aligned} p_1^{\text{com}} + p_2^{\text{com}} &= (E_1+E_2, 0, 0, 0), \\ p_3^{\text{com}} + p_4^{\text{com}} &= (E_3+E_4, 0, 0, 0). \end{aligned} \tag{A.303}$$

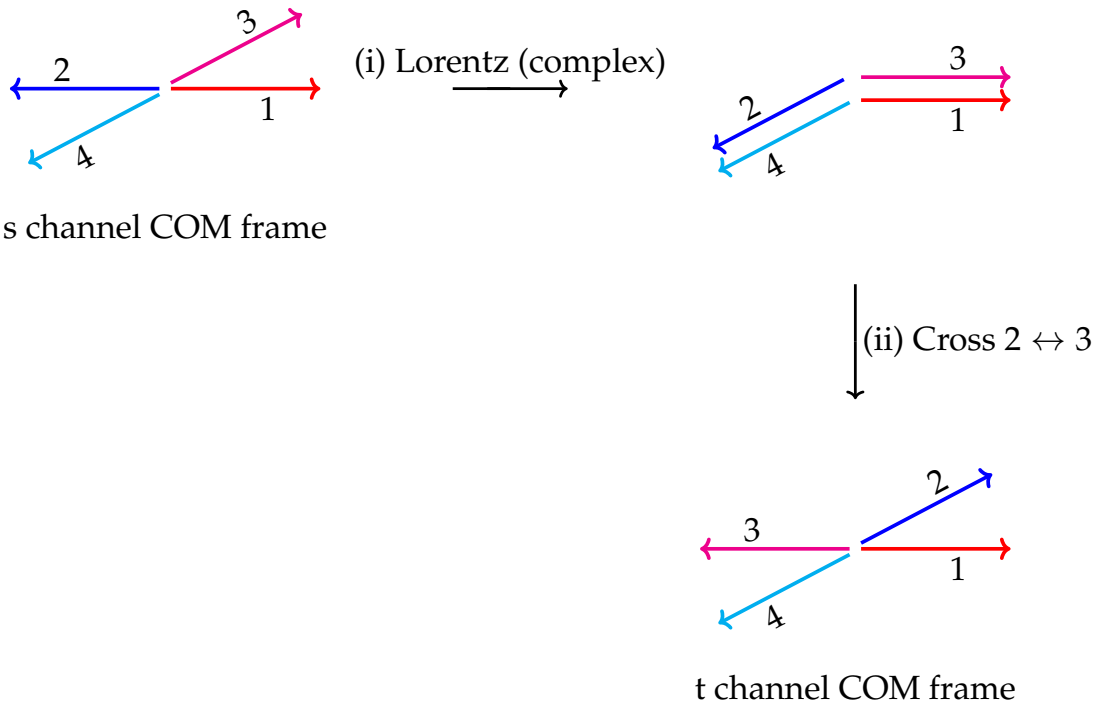

Figure A.6: Schematic picture of (23) crossing for COM frame amplitudes.

Then the right-hand side of (A.297) and (A.298) will depend on

$$\begin{aligned} P_1^{\text{com}} &\equiv (E_1, 0, 0, \boldsymbol{p}), \\ P_2^{\text{com}} &\equiv (-E_3, -\boldsymbol{p}' \sin\theta, 0, -\boldsymbol{p}' \cos\theta), \\ P_3^{\text{com}} &\equiv (-E_2, 0, 0, \boldsymbol{p}), \\ P_4^{\text{com}} &\equiv (E_4, -\boldsymbol{p}' \sin\theta, 0, -\boldsymbol{p}' \cos\theta). \end{aligned} \tag{A.304}$$

The latter obey

$$\begin{aligned} P_1^{\text{com}} - P_3^{\text{com}} &= (E_1 + E_2, 0, 0, 0), \\ P_4^{\text{com}} - P_2^{\text{com}} &= (E_3 + E_4, 0, 0, 0). \end{aligned} \tag{A.305}$$

However, this is not the standard COM frame of the process $1\bar{3} \to \bar{2}4$. We refer to (A.304) as the (23) crossed COM frame.

Once the left-hand sides of (A.297) and (A.298) are evaluated in the $12 \to 34$ COM frame which respects (A.303) we do not get closed expressions since the right-hand side is not in the $1\bar{3} \to \bar{2}4$ COM frame but rather in the (23) crossed COM frame[18]. We therefore need an additional Lorentz transformation. It turns out to be simpler to bring the left-hand side to the (23) crossed COM frame. This way upon (23) crossing we end up in the COM frame for the $1\bar{3} \to \bar{2}4$. This is illustrated in figure A.6.

[18]Recall that we defined the amplitudes as functions of Mandelstam invariants in the COM frame.

We consider the Lorentz transformation Λ such that

$$\begin{aligned} p_1^{\text{com}} &= (E_1, 0, 0, +\boldsymbol{p}) & & \hat{p}_1^{\text{com}} = (\hat{E}_1, 0, 0, +\hat{\boldsymbol{p}}), \\ p_2^{\text{com}} &= (E_2, 0, 0, -\boldsymbol{p}) & & \hat{p}_2^{\text{com}} = (\hat{E}_2, -\hat{\boldsymbol{p}}' \sin\hat{\theta}, 0, -\hat{\boldsymbol{p}}' \cos\hat{\theta}), \\ p_3^{\text{com}} &= (E_3, +\boldsymbol{p}' \sin\theta, 0, +\boldsymbol{p}' \cos\theta) & \Longrightarrow \quad & \hat{p}_3^{\text{com}} = (\hat{E}_3, 0, 0, \hat{\boldsymbol{p}}), \\ p_4^{\text{com}} &= (E_4, -\boldsymbol{p}' \sin\theta, 0, -\boldsymbol{p}' \cos\theta) & & \hat{p}_4^{\text{com}} = (\hat{E}_4, -\hat{\boldsymbol{p}}' \sin\hat{\theta}, 0, -\hat{\boldsymbol{p}}' \cos\hat{\theta}), \end{aligned} \tag{A.306}$$

where $\hat{E}_i$, $\hat{\boldsymbol{p}}$, , $\hat{\boldsymbol{p}}'$ and $\hat{\theta}$ are the components of the 4-momenta in the new frame. The frame described by the right-hand side (A.306) is precisely the (23) crossed frame (A.304) since

$$\begin{aligned} \hat{p}_1^{\text{com}} - \hat{p}_3^{\text{com}} &= (\hat{E}_1 - \hat{E}_3, 0, 0, 0), \\ \hat{p}_4^{\text{com}} - \hat{p}_2^{\text{com}} &= (\hat{E}_4 - \hat{E}_2, 0, 0, 0). \end{aligned} \tag{A.307}$$

Due to the results of appendix A.4.3 we have

$$E_1 = \frac{s + m_1^2 - m_2^2}{2\sqrt{s}}, \quad E_2 = \frac{s - m_1^2 + m_2^2}{2\sqrt{s}}, \quad E_3 = \frac{s + m_3^2 - m_4^2}{2\sqrt{s}}, \quad E_4 = \frac{s - m_3^2 + m_4^2}{2\sqrt{s}}, \tag{A.308}$$

$$\boldsymbol{p} = \frac{\mathcal{L}_{12}(s)}{2\sqrt{s}}, \quad \boldsymbol{p}' = \frac{\mathcal{L}_{34}(s)}{2\sqrt{s}}. \tag{A.309}$$

These are originally defined in the physical range of parameters of the $12 \to 34$ process, where in the case of identical particles we have

$$12 \to 34: \qquad s \geq 4m^2, \quad t \in [4m^2 - s\,, 0]. \tag{A.310}$$

Remember that s is regularized as $s + i\epsilon$, where $\epsilon > 0$. We can unambiguously continue all the formulas valid in the domain (A.310) to the physical domain of the $1\bar{3} \to \bar{2}4$ process which for identical particles read as

$$1\bar{3} \to \bar{2}4: \qquad t \geq 4m^2, \quad s \in [4m^2 - t\,, 0]. \tag{A.311}$$

The Lorentz transformation which allows for (A.306) and (A.307) has the following form

$$\Lambda = R_2(\psi_2) B_3(\chi) R_2(\psi_1), \tag{A.312}$$

where R_2 and B_3 are finite rotations around the y-axis and boost in the z-direction. Their form in the vector representation is given in appendix A.1.3. By requiring (A.307) we can determine the unknown parameters ψ_1, ψ_2 and χ. First, using the rotation $R_2(\psi_1)$ we make the x-components of p_1^{com} and p_3^{com} equal. This is achieved for example with

$$\cos\psi_1 = \frac{\boldsymbol{p} - \boldsymbol{p}' \cos\theta}{\sqrt{\boldsymbol{p}^2 + \boldsymbol{p}'^2 - 2\boldsymbol{p}\boldsymbol{p}' \cos\theta}}, \qquad \sin\psi_1 = \frac{\boldsymbol{p}' \sin\theta}{\sqrt{\boldsymbol{p}^2 + \boldsymbol{p}'^2 - 2\boldsymbol{p}\boldsymbol{p}' \cos\theta}}. \tag{A.313}$$

Second, using the boost $B_3(\chi)$ along the z-axis we make the z-components of the rotated

vectors p_1^{com} and p_3^{com} equal. This is achieved with

$$\cosh\chi = \frac{E_1 - E_3}{\sqrt{(E_1-E_3)^2 - \boldsymbol{p}^2 - \boldsymbol{p}'^2 + 2\boldsymbol{p}\boldsymbol{p}'\cos\theta}} = \frac{m_1^2 - m_2^2 - m_3^2 + m_4^2}{2\sqrt{s}\sqrt{t}}, \tag{A.314}$$

$$\sinh\chi = -\frac{\sqrt{\boldsymbol{p}^2 + \boldsymbol{p}'^2 - 2\boldsymbol{p}\boldsymbol{p}'\cos\theta}}{\sqrt{(E_1-E_3)^2 - \boldsymbol{p}^2 - \boldsymbol{p}'^2 + 2\boldsymbol{p}\boldsymbol{p}'\cos\theta}} = -\frac{\sqrt{s^{-1}(m_1^2 - m_2^2 - m_3^2 + m_4^2)^2 - 4t}}{2\sqrt{t}}.$$

Third, the rotation $R_2(\psi_2)$ brings us to the desired frame. However, we will not need the explicit expression for the angle ψ_2. As a result we get the following expressions

$$\hat{E}_1 = \frac{m_1^2 - m_3^2 + t}{2\sqrt{t}}, \quad \hat{E}_2 = \frac{m_4^2 - m_2^2 - t}{2\sqrt{t}}, \quad \hat{E}_3 = \frac{m_1^2 - m_3^2 - t}{2\sqrt{t}}, \quad \hat{E}_4 = \frac{m_4^2 - m_2^2 + t}{2\sqrt{t}}, \tag{A.315}$$

$$\hat{\boldsymbol{p}}^2 = \frac{(\mathcal{L}_{13}(t))^2}{4t}, \quad \hat{\boldsymbol{p}}'^2 = \frac{(\mathcal{L}_{24}(t))^2}{4t}. \tag{A.316}$$

There were several choices of signs in (A.314). We picked one such that the energy $\hat{E}_1$ in (A.315) is non-negative in the physical domain (A.311) of the process $1\bar{3} \to \bar{2}4$.

Assuming that we have determined the correct values of parameters ψ_1, ψ_2 and χ, we can then straightforwardly compute the Wigner angles using the results of appendix A.1.4, which read

$$\cos\alpha_i = \frac{E_i\,\hat{E}_i - m_i^2\cosh\chi}{\boldsymbol{p}_i\,\hat{\boldsymbol{p}}_i}, \quad \sin\alpha_i = \frac{m_i\sinh\chi}{\hat{\boldsymbol{p}}_i}\,\sin(\theta_i + \psi_1). \tag{A.317}$$

Here the Wigner angles with the subscript $i = 1,2,3,4$ correspond to Lorentz transformations of p_i^{com} in (A.306). The spherical angles of the four-particles in (A.306) before the Lorentz transformation read as

$$\boldsymbol{p}_1 = \boldsymbol{p}_2 = \boldsymbol{p}, \quad \theta_1 = 0, \quad \theta_2 = \pi, \quad \boldsymbol{p}_3 = \boldsymbol{p}_4 = \boldsymbol{p}', \quad \theta_3 = \theta, \quad \theta_4 = \theta + \pi. \tag{A.318}$$

Using the transformation property (1.54) of scattering amplitudes we can then write

$$\begin{aligned} &T_{12\to34}\,{}^{\lambda_3,\lambda_4}_{\lambda_1,\lambda_2}(p_1^{\text{com}}, p_2^{\text{com}}, p_3^{\text{com}}, p_4^{\text{com}}) = \\ &\sum_{\lambda_i'} d^{(j_1)}_{\lambda_1'\lambda_1}(\alpha_1)\, d^{(j_2)}_{\lambda_2'\lambda_2}(\alpha_2)\, d^{(j_3)}_{\lambda_3'\lambda_3}(\alpha_3)\, d^{(j_4)}_{\lambda_4'\lambda_4}(\alpha_4)\, T_{12\to34}\,{}^{\lambda_3',\lambda_4'}_{\lambda_1',\lambda_2'}(\hat{p}_1^{\text{com}}, \hat{p}_3^{\text{com}}, \hat{p}_2^{\text{com}}, \hat{p}_4^{\text{com}}). \end{aligned} \tag{A.319}$$

Analytic continuation 1

Having performed the Lorentz transformations (A.306) we ended up with (A.315). These expressions contain an ambiguity on how to take a square root. This is related to the choice of the analytic continuation discussed in section A.5. For the choice (A.255) in the

domain (A.311) we have

$$\hat{\boldsymbol{p}} = +\frac{\mathcal{L}_{13}(t)}{2\sqrt{t}}, \qquad \hat{\boldsymbol{p}}' = +\frac{\mathcal{L}_{24}(t)}{2\sqrt{t}}. \tag{A.320}$$

The spherical angles of the four-momenta $\hat{p}_i^{\text{com}}$ after the Lorentz transformation read as

$$\hat{\boldsymbol{p}}_1 = \hat{\boldsymbol{p}}_3 = \hat{\boldsymbol{p}}, \quad \hat{\theta}_1 = \hat{\theta}_3 = 0, \quad \hat{\boldsymbol{p}}_2 = \hat{\boldsymbol{p}}_4 = \hat{\boldsymbol{p}}', \quad \hat{\theta}_2 = \hat{\theta}_4 = \hat{\theta} + \pi. \tag{A.321}$$

Using these, the boost (A.314) and (A.317) we obtain in full generality the cosines[19]

$$\begin{aligned}
\cos\alpha_1 &= \frac{+(s+m_1^2-m_2^2)(t+m_1^2-m_3^2)+2m_1^2\,\Delta_t}{\mathcal{L}_{12}(s)\mathcal{L}_{13}(t)},\\
\cos\alpha_2 &= \frac{-(s-m_1^2+m_2^2)(t+m_2^2-m_4^2)+2m_2^2\,\Delta_t}{\mathcal{L}_{12}(s)\mathcal{L}_{24}(t)},\\
\cos\alpha_3 &= \frac{-(s+m_3^2-m_4^2)(t-m_1^2+m_3^2)+2m_3^2\,\Delta_t}{\mathcal{L}_{34}(s)\mathcal{L}_{13}(t)},\\
\cos\alpha_4 &= \frac{+(s+m_4^2-m_3^2)(t+m_4^2-m_2^2)+2m_4^2\,\Delta_t}{\mathcal{L}_{34}(s)\mathcal{L}_{24}(t)},
\end{aligned} \tag{A.322}$$

together with sines

$$\begin{aligned}
\sin\alpha_1 &= -\frac{2m_1\sqrt{\Phi}}{\mathcal{L}_{12}(s)\mathcal{L}_{13}(t)}, \quad \sin\alpha_2 = +\frac{2m_2\sqrt{\Phi}}{\mathcal{L}_{12}(s)\mathcal{L}_{24}(t)},\\
\sin\alpha_3 &= -\frac{2m_3\sqrt{\Phi}}{\mathcal{L}_{34}(s)\mathcal{L}_{13}(t)}, \quad \sin\alpha_4 = +\frac{2m_4\sqrt{\Phi}}{\mathcal{L}_{34}(s)\mathcal{L}_{24}(t)},
\end{aligned} \tag{A.323}$$

where the objects Φ and Δ_t were defined (A.239) and (A.240).

Using the crossing relation (A.297), where we set $\phi_2 = \pi$ and $\phi_3 = 0$, and plugging it into (A.319) we get

$$\begin{aligned}
&T_{12\to 34}{}^{\lambda_3,\lambda_4}_{\lambda_1,\lambda_2}(p_1^{\text{com}}, p_2^{\text{com}}, p_3^{\text{com}}, p_4^{\text{com}}) = \epsilon_{23}^{(1)} \sum_{\lambda_i'} e^{i\pi(\lambda_2'+\lambda_3')}\\
&d^{(j_1)}_{\lambda_1'\lambda_1}(\alpha_1) d^{(j_2)}_{\lambda_2'\lambda_2}(\alpha_2) d^{(j_3)}_{\lambda_3'\lambda_3}(\alpha_3) d^{(j_4)}_{\lambda_4'\lambda_4}(\alpha_4)\, T_{1\bar{3}\to\bar{2}4}{}^{\lambda_2',\lambda_4'}_{\lambda_1',\lambda_3'}(\hat{p}_1^{\text{com}}, -\hat{p}_3^{\text{com}}, -\hat{p}_2^{\text{com}}, \hat{p}_4^{\text{com}}).
\end{aligned} \tag{A.324}$$

There is one last important subtlety we need to take into account. Consider the four-momentum of particle 3 in the left- and right-hand side of (A.306). Before the Lorentz transformation the spherical angles of the p_3^{com} are $(\theta_3, \phi_3) = (\theta, 0)$ by definition of the center of mass frame. After the Lorentz transformation the spherical angles of $-\hat{p}_3^{\text{com}}$

[19] The values computed here match precisely the ones of formula (13) in [49]. Notice that our process $12 \to 34$ corresponds to their $ac \to bd$. Thus, in order to see the equivalence one needs to identify the labels as $1 = a$, $2 = c$, $3 = b$ and $4 = d$.

are $(\hat{\theta}_3, \hat{\phi}_3)$.[20] They can take one of the two option

$$(\hat{\theta}, 0) \quad \text{or} \quad (\hat{\theta}, \pi) = (-\hat{\theta}, 0). \tag{A.325}$$

It is hard to see which option is correct from the above arguments. To check this we pick random values of s and t from the domain (A.311). We observe that $\hat{\theta} \in [-\pi, 0]$ which favors the second option in (A.325) is correct. As a result the amplitude in the right-hand side of (A.324) depends on the $-\hat{\theta}$. In order to rewrite it in terms of $+\hat{\theta}$ we use (1.105) and the following properties of the Wigner d-matrix

$$d^{(j)}_{\lambda'\lambda}(-\omega) = (-1)^{\lambda'-\lambda} d^{(j)}_{\lambda'\lambda}(+\omega) \tag{A.326}$$

which lead to

$$T^{\lambda_2',\lambda_4'}_{\lambda_1',\lambda_3'}(S, T(S,-\hat{\theta}), U(S,-\hat{\theta})) = e^{i\pi(\lambda_1'-\lambda_3'-\lambda_2'+\lambda_4')} T^{\lambda_2',\lambda_4'}_{\lambda_1',\lambda_3'}(S, T(S,+\hat{\theta}), U(S,+\hat{\theta})). \tag{A.327}$$

Plugging (A.327) in the right-hand side of (A.324) and using the definition (1.61) we arrive at the final crossing equation

$$\begin{aligned} T_{12\to 34}{}^{\lambda_3,\lambda_4}_{\lambda_1,\lambda_2}(s,t,u) = \epsilon_{23}^{(1)} \sum_{\lambda_i'} & e^{i\pi(\lambda_1'+\lambda_4')} \\ & d^{(j_1)}_{\lambda_1'\lambda_1}(\alpha_1) d^{(j_2)}_{\lambda_2'\lambda_2}(\alpha_2) d^{(j_3)}_{\lambda_3'\lambda_3}(\alpha_3) d^{(j_4)}_{\lambda_4'\lambda_4}(\alpha_4) T_{1\bar{3}\to\bar{2}4}{}^{\lambda_2',\lambda_4'}_{\lambda_1',\lambda_3'}(t,s,u). \end{aligned} \tag{A.328}$$

Focusing on the case of identical particles one can check that applying (A.328) twice gives back the initial process $12 \to 34$. If we chose the other option in (A.325) the resulting crossing equations would not have passed this consistency check.

Analytic continuation 2

For the choice of the analytic continuation (A.256) in the domain (A.311) we have instead

$$\hat{\boldsymbol{p}} = \pm \frac{\mathcal{L}_{13}(t)}{2\sqrt{t}}, \qquad \hat{\boldsymbol{p}}' = \pm \frac{\mathcal{L}_{24}(t)}{2\sqrt{t}}, \tag{A.329}$$

where the minus is taken for the crossed particles 2 and 3, and the plus is taken for the unchanged particles 1 and 4. In other words after the Lorentz transformation (A.306) we get

$$\hat{\boldsymbol{p}}_1 = +\frac{\mathcal{L}_{13}(t)}{2\sqrt{t}}, \quad \hat{\boldsymbol{p}}_2 = -\frac{\mathcal{L}_{24}(t)}{2\sqrt{t}}, \quad \hat{\boldsymbol{p}}_3 = -\frac{\mathcal{L}_{13}(t)}{2\sqrt{t}}, \quad \hat{\boldsymbol{p}}_4 = +\frac{\mathcal{L}_{24}(t)}{2\sqrt{t}}. \tag{A.330}$$

Then the cosine and sine of Wigner angles will be given by (A.322) and (A.323) with an additional overall sign in both sines and cosines for particle 2 and 3. Denoting the

[20] We discuss here $-\hat{p}_3^{\text{com}}$ because it is the quantity which enters the right-hand side of (A.324).

angles for the second analytic continuation by $\alpha_i^{(2)}$ in other words we see that[21]

$$\alpha_1^{(2)} = \alpha_1, \quad \alpha_2^{(2)} = \alpha_2 + \pi, \quad \alpha_3^{(2)} = \alpha_3 + \pi, \quad \alpha_4^{(2)} = \alpha_4. \tag{A.331}$$

Using the crossing relation (A.298) and plugging it into (A.319) we simply get

$$T_{12\to 34}{}^{\lambda_3,\lambda_4}_{\lambda_1,\lambda_2}(p_1^{\text{com}}, p_2^{\text{com}}, p_3^{\text{com}}, p_4^{\text{com}}) = \epsilon_{23}^{(2)} \sum_{\lambda_i'} d^{(j_1)}_{\lambda_1'\lambda_1}(\alpha_1^{(2)}) d^{(j_2)}_{\lambda_2'\lambda_2}(\alpha_2^{(2)}) \\ d^{(j_3)}_{\lambda_3'\lambda_3}(\alpha_3^{(2)}) d^{(j_4)}_{\lambda_4'\lambda_4}(\alpha_4^{(2)}) T_{1\bar{3}\to\bar{2}4}{}^{-\lambda_2',+\lambda_4'}_{+\lambda_1',-\lambda_3'}(\hat{p}_1^{\text{com}}, -\hat{p}_3^{\text{com}}, -\hat{p}_2^{\text{com}}, \hat{p}_4^{\text{com}}). \tag{A.332}$$

Plugging (A.327) and (A.331) in the right-hand side of (A.332) and using the definition (1.61) we arrive at the final equation

$$T_{12\to 34}{}^{\lambda_3,\lambda_4}_{\lambda_1,\lambda_2}(s,t,u) = \epsilon_{23}^{(2)} \sum_{\lambda_i'} e^{i\pi(\lambda_1' - \lambda_3' - \lambda_2' + \lambda_4')} d^{(j_1)}_{\lambda_1'\lambda_1}(\alpha_1) d^{(j_2)}_{\lambda_2'\lambda_2}(\alpha_2 + \pi) \\ d^{(j_3)}_{\lambda_3'\lambda_3}(\alpha_3 + \pi) d^{(j_4)}_{\lambda_4'\lambda_4}(\alpha_4) T_{1\bar{3}\to\bar{2}4}{}^{-\lambda_2',+\lambda_4'}_{+\lambda_1',-\lambda_3'}(t,s,u). \tag{A.333}$$

Renaming the dummy indices $\lambda_2' \to -\lambda_2'$ and $\lambda_3' \to -\lambda_3'$ and using the following property

$$e^{i\pi j} d^{(j)}_{\lambda'\lambda}(\omega) = e^{i\pi\lambda'} d^{(j)}_{-\lambda'\lambda}(\omega + \pi) \tag{A.334}$$

it is straightforward to see that (A.333) is equivalent to (A.328) up to an overall phase.

Concluding remarks

Let us conclude by stressing that Wigner small d-matrices obey the following property

$$d^{(\ell)}_{\lambda'\lambda}(\omega + 2\pi) = e^{2\pi i\,\ell} d^{(\ell)}_{\lambda'\lambda}(\omega). \tag{A.335}$$

This means that for bosonic particles Wigner small d-matrices are 2π periodic instead for fermionic particles they are 4π periodic. As a result the knowledge of (A.322) and (A.323) does not always fix the Wigner angles α_i uniquely since the sine and cosine are 2π periodic functions. This issue appears only for fermionic particles and causes an ambiguity in the overall phase in the crossing equations. Extra input is needed to fix this ambiguity.

[21] Since Wigner d-matrices are 4π periodic we might make an overall sign mistake in the final crossing equation by choosing (A.331).

$s-u$ crossing equation

We now consider the $s-u$ crossing equation due to (2-4) permutation in the center of mass frame. It is given by

$$T_{12\to 34}{}^{\lambda_3,\lambda_4}_{\lambda_1,\lambda_2}(s,t,u) = \epsilon_{24}^{(1)} \sum_{\lambda_i'} e^{i\pi(\lambda_1'+\lambda_3')} \\ d^{(j_1)}_{\lambda_1'\lambda_1}(\beta_1) d^{(j_2)}_{\lambda_2'\lambda_2}(\beta_2) d^{(j_3)}_{\lambda_3'\lambda_3}(\beta_3) d^{(j_4)}_{\lambda_4'\lambda_4}(\beta_4) T_{1\bar{4}\to 3\bar{2}}{}^{\lambda_3',\lambda_2'}_{\lambda_1',\lambda_4'}(u,t,s). \quad \text{(A.336)}$$

The cosines of Wigner angles read as[22]

$$\begin{aligned} \cos\beta_1 &= \frac{+(s+m_1^2-m_2^2)(u+m_1^2-m_4^2)+2m_1^2\,\Delta_u}{\mathcal{L}_{12}(s)\mathcal{L}_{14}(u)}, \\ \cos\beta_2 &= \frac{-(s+m_2^2-m_1^2)(u+m_2^2-m_3^2)+2m_2^2\,\Delta_u}{\mathcal{L}_{12}(s)\mathcal{L}_{23}(u)}, \\ \cos\beta_3 &= \frac{+(s+m_3^2-m_4^2)(u+m_3^2-m_2^2)+2m_3^2\,\Delta_u}{\mathcal{L}_{34}(s)\mathcal{L}_{23}(u)}, \\ \cos\beta_4 &= \frac{-(s+m_4^2-m_3^2)(u+m_4^2-m_1^2)+2m_4^2\,\Delta_u}{\mathcal{L}_{34}(s)\mathcal{L}_{14}(u)}. \end{aligned} \quad \text{(A.337)}$$

The sines of Wigner angles read as

$$\begin{aligned} \sin\beta_1 &= +\frac{2m_1\sqrt{\Phi}}{\mathcal{L}_{12}(s)\mathcal{L}_{14}(u)}, \quad \sin\beta_2 = -\frac{2m_2\sqrt{\Phi}}{\mathcal{L}_{12}(s)\mathcal{L}_{23}(u)}, \\ \sin\beta_3 &= -\frac{2m_3\sqrt{\Phi}}{\mathcal{L}_{34}(s)\mathcal{L}_{23}(u)}, \quad \sin\beta_4 = +\frac{2m_4\sqrt{\Phi}}{\mathcal{L}_{34}(s)\mathcal{L}_{14}(u)}, \end{aligned} \quad \text{(A.338)}$$

where the objects Φ and Δ_u are defined in (A.239) and (A.240).

A.6 Perturbative amplitudes

To complement the discussion of the main text we derive several perturbative results in this section. The computations done in this section closely follow Part II of [97]. Let us start by considering the following free Lagrangian density

$$\mathcal{L}^{\Psi}_{free} \equiv \frac{i}{2}\overline{\Psi}\gamma^{\mu}\partial_{\mu}\Psi - \frac{1}{2}m\overline{\Psi}\Psi, \quad \text{(A.339)}$$

where Ψ is the four component Majorana field. It obeys the Majorana condition

$$\overline{\Psi} = \Psi^T\mathcal{C}, \quad \text{(A.340)}$$

[22]The values computed here match precisely the ones of formula (26) in [49]. Notice that our process $12\to 34$ corresponds to their $ac\to bd$. Thus, in order to see the equivalence one needs to identify the labels as $1=a$, $2=c$, $3=b$ and $4=d$.

where $\mathcal{C}$ is the charge conjugation matrix defined as

$$\mathcal{C} \equiv \begin{pmatrix} 0 & -1 & 0 & 0 \\ +1 & 0 & 0 & 0 \\ 0 & 0 & 0 & +1 \\ 0 & 0 & -1 & 0 \end{pmatrix}. \tag{A.341}$$

When acting on the vacuum Majorana field creates a neutral spin $\frac{1}{2}$ particle. The intrinsic parity, defined in (1.16), for such a particle can only be

$$\eta = \pm i. \tag{A.342}$$

This is the only option compatible with the Majorana condition (A.340).

In what follows we will compute scattering amplitudes of spin $\frac{1}{2}$ particles in Fermi, Yukawa and pseudo-Yukawa theories to the leading order. We will conclude with a brief discussion on counting interaction terms in the effective Lagrangian using scattering amplitudes.

A.6.1 Fermi theory

Consider the Fermi theory defined by the following Lagrangian density

$$\mathcal{L} = \mathcal{L}^{\Psi}_{free} + \frac{\lambda}{8m^2}(\overline{\Psi}\Psi)(\overline{\Psi}\Psi), \tag{A.343}$$

where λ is the coupling known as the Fermi constant. After performing a standard computation one can obtain the following expressions for the scattering amplitudes of Majorana particles to the leading order

$$\begin{aligned} T^{\lambda_3,\lambda_4}_{\lambda_1,\lambda_2}(p_1,p_2,p_3,p_4) = \frac{\lambda}{m^2} \times \Big(& [\bar{u}_{\lambda_3}(p_3)u_{\lambda_1}(p_1)][\bar{u}_{\lambda_4}(p_4)u_{\lambda_2}(p_2)] \\ & - [\bar{u}_{\lambda_4}(p_4)u_{\lambda_1}(p_1)][\bar{u}_{\lambda_3}(p_3)u_{\lambda_2}(p_2)] + [\bar{v}_{\lambda_2}(p_2)u_{\lambda_1}(p_1)][\bar{u}_{\lambda_3}(p_3)v_{\lambda_4}(p_4)] \Big), \end{aligned} \tag{A.344}$$

where u and v are the spinor solutions of the Dirac equation. Their explicit form is given in (2.67). By using the five tensor structures (2.65) and Fierz identities one can bring the result (A.344), as expected from (1.56), to the following form

$$T^{\lambda_3,\lambda_4}_{\lambda_1,\lambda_2}(p_1,p_2,p_3,p_4) = \sum_{I=1}^{5} H_I(s,t,u) \times \mathbb{T}_I{}^{\lambda_3,\lambda_4}_{\lambda_1,\lambda_2}(p_1,p_2,p_3,p_4), \tag{A.345}$$

where the functions H_I (with $I = 1, \ldots, 5$) denoted collectively by $\vec{H}$ read as

$$\vec{H}(s,t,u) = \frac{\lambda}{m^2} \times \begin{pmatrix} 1 \\ 0 \\ 0 \\ 1 \\ -1 \end{pmatrix}. \tag{A.346}$$

A.6.2 Yukawa theory

We consider now the Yukawa theory defined by the following Lagrangian density

$$\mathcal{L} = \mathcal{L}^{\Psi}_{free} - \frac{1}{2}\partial_\mu\varphi\partial^\mu\varphi - \frac{1}{2}M^2\varphi^2 + \frac{1}{2}g\varphi\overline{\Psi}\Psi. \tag{A.347}$$

Due to (A.342) the interaction is parity invariant only if the scalar field has the intrinsic parity

$$\eta_\phi = +1. \tag{A.348}$$

Again performing a standard computation one gets the following scattering amplitude of neutral spin $\frac{1}{2}$ particles to the leading order

$$T^{\lambda_3,\lambda_4}_{\lambda_1,\lambda_2}(p_1,p_2,p_3,p_4) = g^2 \times \left(\frac{[\bar{u}_{\lambda_3}(p_3)u_{\lambda_1}(p_1)][\bar{u}_{\lambda_4}(p_4)u_{\lambda_2}(p_2)]}{-t+M^2} \right.$$
$$\left. - \frac{[\bar{u}_{\lambda_4}(p_4)u_{\lambda_1}(p_1)][\bar{u}_{\lambda_3}(p_3)u_{\lambda_2}(p_2)]}{-u+M^2} + \frac{[\bar{v}_{\lambda_2}(p_2)u_{\lambda_1}(p_1)][\bar{u}_{\lambda_3}(p_3)v_{\lambda_4}(p_4)]}{-s+M^2} \right). \tag{A.349}$$

By using the five tensor structures (2.65) one can bring the above expression to the form (A.345), where

$$\vec{H}(s,t,u) = \frac{g^2}{2} \times \begin{pmatrix} -\frac{4}{s-M^2} + \frac{1}{t-M^2} + \frac{1}{u-M^2} \\ \frac{1}{t-M^2} - \frac{1}{u-M^2} \\ -\frac{1}{t-M^2} + \frac{1}{u-M^2} \\ -\frac{1}{t-M^2} - \frac{1}{u-M^2} \\ \frac{1}{t-M^2} + \frac{1}{u-M^2} \end{pmatrix}. \tag{A.350}$$

A.6.3 Pseudo-Yukawa theory

The pseudo-Yukawa theory is defined by the Lagrangian density

$$\mathcal{L} = \mathcal{L}^{\Psi}_{free} - \frac{1}{2}\partial_\mu\tilde{\varphi}\partial^\mu\tilde{\varphi} - \frac{1}{2}M^2\tilde{\varphi}^2 + \frac{1}{2}\tilde{g}\tilde{\varphi}\overline{\Psi}\gamma^5\Psi. \tag{A.351}$$

Due to (A.342) the interaction is parity invariant only if the scalar field has the intrinsic parity

$$\eta_{\tilde{\phi}} = -1, \tag{A.352}$$

hence we refer to $\tilde{\phi}$ as pseudo-scalar. As before we compute the scattering amplitude to the leading order and obtain

$$T^{\lambda_3,\lambda_4}_{\lambda_1,\lambda_2}(p_1,p_2,p_3,p_4) = \tilde{g}^2 \times \left(\frac{[\bar{u}_{\lambda_3}(p_3)\gamma^5 u_{\lambda_1}(p_1)][\bar{u}_{\lambda_4}(p_4)\gamma^5 u_{\lambda_2}(p_2)]}{-t+M^2} \right.$$
$$\left. - \frac{[\bar{u}_{\lambda_4}(p_4)\gamma^5 u_{\lambda_1}(p_1)][\bar{u}_{\lambda_3}(p_3)\gamma^5 u_{\lambda_2}(p_2)]}{-u+M^2} + \frac{[\bar{v}_{\lambda_2}(p_2)\gamma^5 u_{\lambda_1}(p_1)][\bar{u}_{\lambda_3}(p_3)\gamma^5 v_{\lambda_4}(p_4)]}{-s+M^2} \right). \tag{A.353}$$

Again by using the five tensor structures (2.65) one can bring the above expression to the form (A.345), where

$$\vec{H}(s,t,u) = \frac{\tilde{g}^2}{2} \times \begin{pmatrix} \frac{1}{t-M^2} + \frac{1}{u-M^2} \\ -\frac{1}{t-M^2} + \frac{1}{u-M^2} \\ -\frac{1}{t-M^2} + \frac{1}{u-M^2} \\ \frac{1}{t-M^2} + \frac{1}{u-M^2} \\ -\frac{4}{s-M^2} + \frac{1}{t-M^2} + \frac{1}{u-M^2} \end{pmatrix}. \tag{A.354}$$

A.6.4 Counting couplings at a given order in EFT

Let us consider the effective Lagrangian density of a single Majorana field Ψ describing the two to two scattering process schematically denoted by $\Psi\Psi \to \Psi\Psi$. It reads

$$\mathcal{L} = \mathcal{L}^{\Psi}_{free} + \mathcal{L}_4 + \mathcal{L}_5 + \mathcal{L}_6 + \dots, \tag{A.355}$$

where $\mathcal{L}_n$ with $n = 4, 5, 6$ are the dimension 4, 5 and 6 terms. The question we will address now is how to count the number of linearly independent terms in such an effective Lagrangian density at each order n.

We start with $n = 4$. It is well known that there is only one linearly independent term $(\overline{\Psi}\Psi)(\overline{\Psi}\Psi)$ as was used in (A.343). Naively, one can write however many more terms by appropriately combining

$$\overline{\Psi}\Psi, \quad \overline{\Psi}\gamma^5\Psi, \quad \overline{\Psi}\gamma^\mu\Psi, \quad \overline{\Psi}\gamma^\mu\gamma^5\Psi, \quad \overline{\Psi}\sigma^{\mu\nu}\Psi. \tag{A.356}$$

Let us now rewrite the Majorana field in terms of a two component left-handed Weyl

spinor χ, one has

$$\Psi = \begin{pmatrix} \chi_\alpha \\ \chi^{\dagger\dot{\alpha}} \end{pmatrix}. \tag{A.357}$$

It is then straightforward to show that[23]

$$\begin{aligned} \overline{\Psi}\gamma^\mu\Psi &= \chi^\dagger\sigma^\mu\chi - \chi^\dagger\sigma^\mu\chi = 0, & \text{(A.358)} \\ \frac{i}{2}\overline{\Psi}\sigma^{\mu\nu}\Psi &= \chi\sigma^{\mu\nu}\chi - \chi^\dagger\overline{\sigma}^{\mu\nu}\chi = 0. & \text{(A.359)} \end{aligned}$$

As a result at the $n = 4$ level we can write only four terms

$$\mathcal{L}_4 \ni \left\{(\overline{\Psi}\Psi)(\overline{\Psi}\Psi),\ (\overline{\Psi}\gamma^5\Psi)(\overline{\Psi}\gamma^5\Psi),\ (\overline{\Psi}\gamma^\mu\gamma^5\Psi)(\overline{\Psi}\gamma_\mu\gamma^5\Psi),\ (\overline{\Psi}\Psi)(\overline{\Psi}\gamma^5\Psi)\right\}. \tag{A.360}$$

Rewriting these in terms of the Weyl spinor χ we see see that they are either proportional to each other or vanish

$$\begin{aligned} (\overline{\Psi}\Psi)(\overline{\Psi}\Psi) &= \left(\chi\chi + \chi^\dagger\chi^\dagger\right)^2 = 2(\chi\chi)(\chi^\dagger\chi^\dagger), \\ (\overline{\Psi}\gamma^5\Psi)(\overline{\Psi}\gamma^5\Psi) &= \left(-\chi\chi + \chi^\dagger\chi^\dagger\right)^2 = -2(\chi\chi)(\chi^\dagger\chi^\dagger), \\ (\overline{\Psi}\gamma^\mu\gamma^5\Psi)(\overline{\Psi}\gamma_\mu\gamma^5\Psi) &= \left(-2\chi^\dagger\sigma^\mu\chi\right)\left(-2\chi^\dagger\sigma_\mu\chi\right) = 4(\chi\chi)(\chi^\dagger\chi^\dagger), \\ (\overline{\Psi}\Psi)(\overline{\Psi}\gamma^5\Psi) &= \left(\chi\chi + \chi^\dagger\chi^\dagger\right)\left(-\chi\chi + \chi^\dagger\chi^\dagger\right) = 0. \end{aligned} \tag{A.361}$$

If one is interested in the counting of independent terms only, instead of performing the above algebra one could notice that $\mathcal{L}_4$ terms in the leading order generate the improved scattering amplitudes $\vec{H}(s,t,u)$ at the crossing symmetric point (2.53). Crossing equations severely restrict the form of the improved amplitudes at the crossing symmetric point, see (2.55). The latter contains only one independent parameter. One concludes that there should be only a single parameter in the effective Lagrangian density $\mathcal{L}_4$.

As another example let us consider the $n = 6$ part. One can write

$$\mathcal{L}_6 \ni \left\{(\overline{\Psi}\partial^2\Psi)(\overline{\Psi}\Psi),\ (\overline{\Psi}\partial^\mu\Psi)(\overline{\Psi}\partial_\mu\Psi),\ (\overline{\Psi}\partial^\mu\partial^\nu\Psi)(\overline{\Psi}\gamma_\mu\gamma_\nu\Psi), \ldots\right\}. \tag{A.362}$$

The improved amplitudes generated by such terms at the leading order will have the following most general form

$$\vec{H}(s,t,u) = (s - 4m^2/3) \times \vec{A} + (t - 4m^2/3) \times \vec{B} + (u - 4m^2/3) \times \vec{C}, \tag{A.363}$$

where $\vec{A}$, $\vec{B}$ and $\vec{C}$ are some real constants. They are constrained by the crossing equations

[23] Note that all the Weyl indices here have been contracted appropriately.

(2.27) and (2.28) which require (A.363) to take the following form

$$\vec{H}(s,t,u) = \frac{1}{m^4}\begin{pmatrix} a\times(s-4m^2/3) \\ b\times(s+2t-4m^2) \\ \frac{1}{3}(a+2b)\times(s+2t-4m^2) \\ b\times(s-4m^2/3) \\ (a+4b)\times(s-4m^2/3) \end{pmatrix}, \tag{A.364}$$

where a and b are the undetermined parameters. One concludes that there are only two linearly independent terms in (A.362).

A.7 Bound state close to the two-particle threshold

In section 2.3 we studied the non-perturbative structure of the scattering amplitude of neutral spin $\frac{1}{2}$ particles with mass m in the presence of a scalar particle with mass M. Such a particle can be interpreted as a bound state of two fermions. The structure of the improved scattering amplitude is given by (2.59) and (2.60) for the parity even scalar particle and by (2.61) and (2.62) for parity odd scalar particle. The structure of the center of mass amplitudes is obtained by plugging these into (2.24).

In this appendix we study the behavior of the center of mass amplitudes in the presence of bound states in the limit when $M \to 2m$. We follow the analysis presented in appendix E of [4]. The leading behavior of the COM amplitudes is obtained by taking the following limit

$$M = (2-\epsilon)\,m, \quad s = (2m+E\epsilon)^2, \tag{A.365}$$

where $E \geq 0$ is kept fixed as we take the limit $\epsilon \to 0$. Applying it to (2.24) combined with (2.59) and (2.61) in the leading order in ϵ we get

$$\vec{\Phi}_{\text{scalar}}(E) = \frac{g^2}{4}\frac{E}{E+m}\times\begin{pmatrix}-1\\+1\\0\\0\\0\end{pmatrix}, \quad \vec{\Phi}_{\text{pseudoscalar}}(E) = \frac{\tilde{g}^2}{4}\frac{m}{E+m}\frac{1}{\epsilon}\times\begin{pmatrix}1\\1\\0\\0\\0\end{pmatrix}. \tag{A.366}$$

We see that the amplitude with the scalar particle is completely finite in this limit, however the amplitude with the pseudoscalar particle diverges. The partial amplitudes were defined in (2.44). Plugging there the expressions (A.366), replacing s by M^2 and

only then taking the limit (A.365) we get

$$\begin{aligned}\vec{\Phi}^{\ell=0}_{\text{scalar}}(E) &= \frac{ig^2}{64\pi}\frac{1}{1+m/E}\sqrt{\epsilon}\times\begin{pmatrix}-1\\+1\\0\\0\\0\end{pmatrix},\\ \vec{\Phi}^{\ell=0}_{\text{pseudoscalar}}(E) &= \frac{i\tilde{g}^2}{64\pi}\frac{1}{1+E/m}\frac{1}{\sqrt{\epsilon}}\times\begin{pmatrix}1\\1\\0\\0\\0\end{pmatrix}.\end{aligned} \tag{A.367}$$

Notice that poles coming from scalar particles can appear only in $\ell = 0$ partial amplitudes as is explicitly stated here.

According to (2.58) we can take combination of partial amplitude components to define parity even $\Phi^{\ell}_{+}(s)$ and parity odd $\Phi^{\ell}_{-}(s)$ partial amplitudes. In terms of the objects (2.58) unitarity takes a very simple form

$$|1+i\Phi^{\ell}_{+}(s)| \leq 1, \quad |1+i\Phi^{\ell}_{-}(s)| \leq 1. \tag{A.368}$$

Using (A.367) in our context we can the write

$$\text{scalar exchange:} \qquad \Phi^{\ell=0}_{+}(E) = -\frac{g^2}{32\pi}\frac{1}{1+m/E}\sqrt{\epsilon}, \quad \Phi^{\ell=0}_{-}(E) = 0, \tag{A.369}$$

$$\text{pseudoscalar exchange:} \qquad \Phi^{\ell=0}_{-}(E) = \frac{\tilde{g}^2}{32\pi}\frac{1}{1+E/m}\frac{1}{\sqrt{\epsilon}}, \qquad \Phi^{\ell=0}_{+}(E) = 0. \tag{A.370}$$

In the limit $\epsilon \to 0$ the partial amplitudes (A.369) vanish and we cannot say anything interesting about the coupling g^2. Instead (A.370) diverges. In order to have a partial amplitudes which is able to satisfy unitarity (A.368) we need the scaling

$$\tilde{g}^2 = a\sqrt{\epsilon}, \tag{A.371}$$

with a finite as $\epsilon \to 0$. It is also convenient to make a change of variables from E to z variable which are related via

$$E = -m\,\frac{(z-1)^2}{(z+1)^2}. \tag{A.372}$$

This maps the cut in the E plane to the boundary of the unit disk in z. Plugging the

above into (A.370) we get

$$\Phi_{-}^{\ell=0}(z) = \frac{ia}{128\pi}\frac{(1+z)^2}{z}. \tag{A.373}$$

Using it and taking the leading behavior in small z, the unitarity conditions (A.368) leads to

$$\left|\frac{a}{128\pi}\frac{1}{z}\right| \leq 1, \tag{A.374}$$

which should be satisfied on the boundary of the disc described by $z = e^{i\phi}$, where $\phi \in [0, 2\pi]$. It is then straightforward to see that the maximally allowed value of a which obeys the unitarity condition (A.374) is

$$a = 128\pi. \tag{A.375}$$

Plugging it into (A.371) and expressing ϵ in terms of m and M from (A.365) we get the analytic upper bound

$$\tilde{g}^2 \leq 128\pi\sqrt{\frac{2m-M}{m}}. \tag{A.376}$$

A.8 General spin tensor structures

We have introduced the notion of tensor structures in (1.56). Even though one can completely avoid talking about them, it is sometimes beneficial to know a basis of tensor structures explicitly. In the case of Majorana fermions the detailed discussion of tensor structures was given in section 2.4. In this appendix we will briefly explain how to construct tensor structures for amplitudes with generic spin. There are several possible ways of doing this. One way is to treat particles with generic spin as multi-spinors simply described by tensor products of u and v objects defined in section 2.4. This approach was employed in [28]. Here we describe another approach used in [98]. (In the massless case it reduces to the well known spinor-helicity formalism, see for example [99].) We chose the latter because it closely resembles various approaches used in the CFT literature [50, 100–104].

Index free formalism

In section 1.1, more precisely in equation (1.2), we have chosen the basis of states to be $|c, \vec{p}; \ell, \lambda\rangle$, where $\lambda = -\ell, \ldots, +\ell$ are the helicity labels. It is convenient to move to another basis where instead of helicities λ we use a symmetrized set of indices

$$(a_1 \ldots a_{2\ell}), \tag{A.377}$$

where a_1, a_2, ... are the indices in the fundamental representation of the $SU(2)$ Little group.[24] In other words we can have two equivalent bases

$$|c, \vec{p}; \ell, \lambda\rangle \quad \leftrightarrow \quad |c, \vec{p}; \ell\rangle^{(a_1 \ldots a_{2\ell})}. \tag{A.378}$$

It is then extremely convenient to introduce index free notation by contracting the states with a complex vector (spinor polarization)

$$s^a = \begin{pmatrix} \xi \\ \eta \end{pmatrix}, \tag{A.379}$$

where ξ and η are simply the components of the spinor polarization. With the help of (A.379) one can define the Little group index-free states

$$|c, \vec{p}; \ell\rangle(s) \equiv |c, \vec{p}; \ell\rangle^{(a_1 \ldots a_{2\ell})} \times s_{a_1} \ldots s_{a_{2\ell}}. \tag{A.380}$$

The relation between the two bases (A.378) can be determined by requiring

$$|c, \vec{p}; \ell\rangle(s) = \sum_{\lambda=-\ell}^{\ell} |c, \vec{p}; \ell, \lambda\rangle \times \xi^{\lambda} \eta^{\ell-\lambda}. \tag{A.381}$$

We have defined in (1.47) the interacting part of the scattering amplitude of four particles. In index free notation it reads

$$\begin{aligned}(2\pi)^4 \delta^{(4)}(p_1^\mu + p_2^\mu - p_3^\mu - p_4^\mu) \times T_{12\to 34}(p_i, s_i) \equiv \\ \left((s_3)\langle m_3, \vec{p}_3; \ell_3| \otimes (s_4)\langle m_4, \vec{p}_4; \ell_4| \right) T \left(|m_1, \vec{p}_1; \ell_1\rangle(s_1) \otimes |m_2, \vec{p}_2; \ell_2\rangle(s_2) \right).\end{aligned} \tag{A.382}$$

Analogously to (1.56) we can perform the decomposition of the index free interacting scattering amplitudes

$$T_{12\to 34}(p_i, s_i) = \sum_{I=1}^{(2j_1+1)\ldots(2j_4+1)} T_I(s, t, u)\ \mathbb{T}_I(p_i, s_i), \tag{A.383}$$

where $\mathbb{T}_I(p_i, s_i)$ are the index-free tensor structures.

Auxiliary objects

The index-free tensor structures appearing in (A.383) are kinematic objects constructed from the 4-momenta p_i^μ and the spinor polarizations s_i^a. The former have Lorentz indices

[24] Here we simply use the fact that any generic irreducible representation j of the $SU(2)$ can be represented as $\ell = \left(\frac{1}{2} \otimes \ldots \otimes \frac{1}{2}\right)_{\text{sym}}$.

and the latter have Little group indices. In order to contract them we need to somehow introduce an auxiliary object which has both Lorentz and Little group indices and can be an intermediary in the contraction of the two. In what follows we will define such an auxiliary object.

We use the two-component spinor notation of Wess and Bagger [105]. Given a 4-momentum p^μ one can define the standard $SL(2,C)$ matrices using (A.103),

$$\mathrm{p}_{\alpha\dot{\alpha}} \equiv p \cdot \sigma_{\alpha\dot{\alpha}}, \qquad \bar{\mathrm{p}}^{\dot{\beta}\beta} \equiv p \cdot \bar{\sigma}^{\dot{\beta}\beta}. \tag{A.384}$$

The indices are raised and lowered by the ϵ-symbols $\epsilon_{\alpha\beta}$ and $\epsilon_{\dot{\alpha}\dot{\beta}}$, where $\epsilon^{12} = -\epsilon_{12} = +1$. The representation (A.384) leads to

$$p^2 = -\det \mathrm{p} = -\det \bar{\mathrm{p}}, \tag{A.385}$$

$$p_i \cdot p_j = -\frac{1}{2} \operatorname{tr} [\mathrm{p}_i \bar{\mathrm{p}}_j]. \tag{A.386}$$

One can introduce the following two objects which have one Lorentz index β or $\dot{\beta}$ and one Little group index $b = 1, 2$ (in the fundamental representation)[25]

$$h_\beta{}^b, \quad \bar{h}_b{}^{\dot{\beta}} \tag{A.387}$$

related by hermitian conjugation

$$\left(h_\beta{}^b\right)^\dagger = \bar{h}_{b\dot{\beta}}, \qquad \left(\bar{h}_b{}^{\dot{\beta}}\right)^\dagger = h^{\beta b}. \tag{A.388}$$

The Little group indices are raised and lowered by the ϵ-symbol $\epsilon^{ab} = -\epsilon_{ab}$, where $\epsilon^{12} = +1$. By taking these objects and contracting their Little group indices one can represent the $SL(2,C)$ matrices as

$$\mathrm{p}_{\alpha\dot{\beta}} = h_\alpha{}^b \bar{h}_{b\,\dot{\beta}}, \qquad \bar{\mathrm{p}}^{\dot{\alpha}\beta} = h^{\beta b} \bar{h}_b{}^{\dot{\alpha}}. \tag{A.389}$$

By definition the Little group transformations leave (A.385) invariant. Using the representation (A.389) and this invariance one can compute the actual expressions of h and $\bar{h}$. They read

$$\text{matrix } h_\beta{}^b = \text{matrix } \bar{h}_{b\dot{\beta}} = \frac{1}{\sqrt{2}\sqrt{m+p^0}} \begin{pmatrix} m+p^0+p^3 & p^1 - i\,p^2 \\ p^1 + i\,p^2 & m+p^0-p^3 \end{pmatrix}. \tag{A.390}$$

[25] These "spinor-helicity" variables are denoted by λ and $\tilde{\lambda}$ in [98].

Tensor invariants

We can build tensor structures in (A.383) as products of elementary tensor invariants. These tensor invariants are in turn built out of

$$\mathtt{p}_{i\,\alpha\dot{\beta}}, \quad h_{i\beta}{}^{b}, \quad \bar{h}_{ib}{}^{\dot{\beta}}, \quad s_i^b \tag{A.391}$$

by fully contracting their indices with all possible invariant objects such as the Kronecker and the Levi-Civita symbols. Notice also that one can pair h_i and s_j by contracting their Little group indices only if $i = j$ because each particle has its own little group. For transparency we indicate this contraction by "$\cdot$". Below we make a summary of all the possible invariants.

Type I consists of invariant objects with an even number of 4-momenta

$$\begin{aligned}
\langle \boldsymbol{ij} \rangle &\equiv s_i \cdot h_i^{\alpha}\, \delta_{\alpha}^{\beta}\, h_{j\,\beta} \cdot s_j, \\
\langle \boldsymbol{imnj} \rangle &\equiv s_i \cdot h_i^{\alpha}{}_{\alpha} (\mathtt{p}_m \bar{\mathtt{p}}_n)^{\beta}\, h_{j\,\beta} \cdot s_j, \\
\langle \boldsymbol{imnprj} \rangle &\equiv s_i \cdot h_i^{\alpha}{}_{\alpha} (\mathtt{p}_m \bar{\mathtt{p}}_n \mathtt{p}_p \bar{\mathtt{p}}_r)^{\beta}\, h_{j\,\beta} \cdot s_j, \\
&\cdots\cdots
\end{aligned} \tag{A.392}$$

Type I* consists of structures related by complex conjugation to the ones of type I

$$\begin{aligned}
[\boldsymbol{ij}] &\equiv s_i \cdot \bar{h}_{i\,\dot{\alpha}}\, \delta_{\dot{\beta}}^{\dot{\alpha}}\, \bar{h}_j^{\dot{\beta}} \cdot s_j, \\
[\boldsymbol{imnj}] &\equiv s_i \cdot \bar{h}_{i\,\dot{\alpha}}{}^{\dot{\alpha}} (\bar{\mathtt{p}}_m \mathtt{p}_n)_{\dot{\beta}}\, \bar{h}_j^{\dot{\beta}} \cdot s_j, \\
[\boldsymbol{imnprj}] &\equiv s_i \cdot \bar{h}_{i\,\dot{\alpha}}{}^{\dot{\alpha}} (\bar{\mathtt{p}}_m \mathtt{p}_n \bar{\mathtt{p}}_p \mathtt{p}_r)_{\dot{\beta}}\, \bar{h}_j^{\dot{\beta}} \cdot s_j, \\
&\cdots\cdots
\end{aligned} \tag{A.393}$$

Type II consists of invariant objects with an odd number of 4-momenta

$$\begin{aligned}
\langle \boldsymbol{imj}] &\equiv s_i \cdot h_i^{\alpha}\, \mathtt{p}_{m\,\alpha\dot{\beta}}\, \bar{h}_j^{\dot{\beta}} \cdot s_j, \\
\langle \boldsymbol{imnpj}] &\equiv s_i \cdot h_i^{\alpha}{}_{\alpha} (\mathtt{p}_m \bar{\mathtt{p}}_n \mathtt{p}_p)_{\dot{\beta}}\, \bar{h}_j^{\dot{\beta}} \cdot s_j, \\
&\cdots\cdots
\end{aligned} \tag{A.394}$$

Type II* consists of structures related by complex conjugation to the ones of type II

$$\begin{aligned}
[\boldsymbol{i}m\boldsymbol{j}\rangle &\equiv s_i \cdot \bar{h}_{i\,\dot{\alpha}}\ \bar{\mathtt{p}}_m^{\dot{\alpha}\beta}\ h_{j\,\beta} \cdot s_j,\\
[\boldsymbol{i}mnp\boldsymbol{j}\rangle &\equiv s_i \cdot \bar{h}_{i\,\dot{\alpha}}\ ^{\dot{\alpha}}(\bar{\mathtt{p}}_m \mathtt{p}_n \bar{\mathtt{p}}_p)^{\beta}\ h_{j\,\beta} \cdot s_j,\\
&\ldots\ldots
\end{aligned} \tag{A.395}$$

Type III and III* consists of invariant objects involving the $\epsilon_{\mu\nu\rho\sigma}$ or $\epsilon^{\mu\nu\rho\sigma}$ symbols

$$\begin{aligned}
\langle \boldsymbol{i}\overline{mnp}\boldsymbol{j}] &\equiv s_i \cdot h_i^{\alpha}\ (p_{m\,\mu}\, p_{n\,\nu}\, p_{p\,\rho} \epsilon^{\mu\nu\rho\kappa} \sigma_{\kappa})_{\alpha\dot{\beta}}\ \bar{h}_j^{\dot{\beta}} \cdot s_j,\\
[\boldsymbol{i}\overline{mnp}\boldsymbol{j}\rangle &\equiv s_i \cdot \bar{h}_{i\,\dot{\alpha}}\ (p_{m\,\mu}\, p_{n\,\nu}\, p_{p\,\rho} \epsilon^{\mu\nu\rho\kappa} \bar{\sigma}_{\kappa})^{\dot{\alpha}\beta}\ h_{j\,\beta} \cdot s_j.
\end{aligned} \tag{A.396}$$

Basis of tensor structures

There are a large number of relations among tensor invariants. For instance due to the following properties of σ-matrices

$$\begin{aligned}
\sigma^{\mu}\bar{\sigma}^{\nu}\sigma^{\rho} &= -\eta^{\mu\nu}\sigma^{\rho} + \eta^{\mu\rho}\sigma^{\nu} - \eta^{\nu\rho}\sigma^{\mu} - i\epsilon^{\mu\nu\rho\kappa}\sigma_{\kappa},\\
\bar{\sigma}^{\mu}\sigma^{\nu}\bar{\sigma}^{\rho} &= -\eta^{\mu\nu}\bar{\sigma}^{\rho} + \eta^{\mu\rho}\bar{\sigma}^{\nu} - \eta^{\nu\rho}\bar{\sigma}^{\mu} + i\epsilon^{\mu\nu\rho\kappa}\bar{\sigma}_{\kappa},
\end{aligned} \tag{A.397}$$

see for example [56] for details, any invariant with many products of 4-momenta $(\mathtt{p}_m\, \bar{\mathtt{p}}_n\, \mathtt{p}_p \ldots)$ can be reduced to the ones involving at most two 4-momenta. As a result the most generic tensor structure can be represented by

$$\mathbb{T}_I = \langle \boldsymbol{ij}\rangle^{A_{ij}}\ [\boldsymbol{ij}]^{B_{ij}}\ \langle \boldsymbol{i}m\boldsymbol{j}]^{C_{ij}}\ \langle \boldsymbol{i}mn\boldsymbol{j}\rangle^{D_{ij}}\ [\boldsymbol{i}mn\boldsymbol{j}]^{E_{ij}}\ \langle \boldsymbol{i}\overline{mnp}\boldsymbol{j}]^{F_{ij}}, \tag{A.398}$$

where A, B, C D, E and F are exponents fixed by the requirement[26,27]

$$\mathbb{T}_I \propto s_1^{2\ell_1} s_2^{2\ell_2} s_3^{2\ell_3} s_4^{2\ell_4}. \tag{A.399}$$

The latter is simply the statement that the amplitude must be a polynomial in each s_i with the degree fixed by the spin of the ith particle. This directly follows from the definition of the index-free states (A.380).

Constructing all the possible structures according to (A.398) still gives a set of linearly dependent objects. Eliminating all the dependent structures and forming the basis is the most challenging part of the formalism. It can be done for particles with low spin, but it does not seem to be a viable procedure for higher spin particles. Below we simply give

[26] Notice that the exponent F is either 0 or 1 since any pair of ϵ-symbols can be written in terms of the metric.

[27] Notice also that $\ell_1 + \ell_2 + \ell_3 + \ell_4$ must be even otherwise one will never be able to fully contract all the Little group indices and form tensor invariants. This is a standard selection rule which comes out naturally from this formalism.

a taste of what kind of relations one could expect.

First, one can show that

$$\langle \boldsymbol{i}m\boldsymbol{j}] = +[\boldsymbol{j}m\boldsymbol{i}\rangle, \qquad \langle \boldsymbol{i}\overline{mnp}\boldsymbol{j}] = +[\boldsymbol{j}\overline{mnp}\boldsymbol{i}\rangle. \tag{A.400}$$

This is the reason why type II* and type III* invariants have not being included in (A.398). Second, due to

$$\sigma^\mu\bar{\sigma}^\nu + \sigma^\nu\bar{\sigma}^\mu = 2\eta^{\mu\nu} \tag{A.401}$$

one can show that

$$\begin{aligned} \langle \boldsymbol{ij}\rangle &= -\langle \boldsymbol{ji}\rangle, \quad \langle \boldsymbol{i}mn\boldsymbol{j}\rangle = -\langle \boldsymbol{j}nm\boldsymbol{i}\rangle, \\ [\boldsymbol{ij}] &= -[\boldsymbol{ji}], \quad\ [\boldsymbol{i}mn\boldsymbol{j}] = -[\boldsymbol{j}nm\boldsymbol{i}] \end{aligned} \tag{A.402}$$

together with

$$\begin{aligned} \langle \boldsymbol{i}mn\boldsymbol{j}\rangle + \langle \boldsymbol{i}nm\boldsymbol{j}\rangle &= 2\,(k_m\cdot k_n)\,\langle \boldsymbol{ij}\rangle, \\ [\boldsymbol{i}mn\boldsymbol{j}] + [\boldsymbol{i}nm\boldsymbol{j}] &= 2\,(k_m\cdot k_n)\,[\boldsymbol{ij}]. \end{aligned} \tag{A.403}$$

These relations enforce for instance that type I and I* structures must vanish unless $\boldsymbol{i} \neq \boldsymbol{j}$ and that without loss of generality one can choose $m < n$. Third, one can write a number of Schouten identities. Some of them are

$$\begin{aligned} \langle \boldsymbol{ij}\rangle\langle \boldsymbol{kl}\rangle + \langle \boldsymbol{ik}\rangle\langle \boldsymbol{jl}\rangle + \langle \boldsymbol{il}\rangle\langle \boldsymbol{jk}\rangle &= 0, \\ \langle \boldsymbol{ij}\rangle\langle \boldsymbol{k}l\boldsymbol{m}] + \langle \boldsymbol{ik}\rangle\langle \boldsymbol{j}l\boldsymbol{m}] + \langle \boldsymbol{jl}\rangle\langle \boldsymbol{i}l\boldsymbol{m}] &= 0, \\ \langle \boldsymbol{ijk}]\langle \boldsymbol{l}mn] + \langle \boldsymbol{il}\rangle[\boldsymbol{k}jmn] + \langle \boldsymbol{ljk}]\langle \boldsymbol{i}mn] &= 0. \end{aligned} \tag{A.404}$$

Finally, one should take into account the conservation of 4-momenta

$$p_1^\mu + p_2^\mu = p_3^\mu + p_4^\mu \tag{A.405}$$

and its consequences.

Partial amplitudes

For completeness let us mention that using tensor structures one can also compute partial amplitudes.

In (1.101) we have shown how to decompose the scattering amplitudes into partial amplitudes by injecting a complete set of states. The main objects in this decomposition to be determined is the following matrix element

$$\langle \kappa_1, \kappa_2 | c, \vec{p}, \ell, \lambda\rangle, \tag{A.406}$$

where $|\kappa_1\rangle$ and $|\kappa_2\rangle$ are the 1PS and $|c, \vec{p}, \ell, \lambda\rangle$ is a generic irrep with spin ℓ and helicity λ. The objects (A.406) are the Clebsch-Gordan coefficients of the decomposition. They

were computed in appendix A.1.2 in full generality using group-theoretic arguments. In the COM frame they are basically the Wigner d-matrices.

We can repeat this procedure in the index-free formalism by injecting a complete set of states in the following form

$$\mathbb{I} = \int \frac{d^4p}{(2\pi)^4}\,\theta(p^0)\sum_{\gamma}\sum_{\ell}|c,\vec{p};\ell;\gamma\rangle(s)\times\overset{\leftrightarrow}{D}_s\times(s)\langle c,\vec{p};\ell;\gamma|, \tag{A.407}$$

where γ are all the additional indices characterizing the state and $\overset{\leftrightarrow}{D}_s$ is the "gluing" operator defined as

$$\overset{\leftrightarrow}{D}_s \equiv \frac{1}{(2\ell)!^2}(\overset{\leftarrow a_1}{\partial}_s\ldots\overset{\leftarrow a_{2\ell}}{\partial}_s)(\overset{\rightarrow}{\partial}_{s,a_1}\ldots\overset{\rightarrow}{\partial}_{s,a_{2\ell}}). \tag{A.408}$$

It simply contracts all the Little group indices of two states. The Clebsch-Gordon coefficient (A.406) then becomes

$$C_\ell(s_1,s_2,s) \equiv \Big((s_1)\langle m_1,\vec{p}_1;\ell_1|\otimes(s_2)\langle m_2,\vec{p}_2;\ell_2|\Big)|c,\vec{p},\ell\rangle(s_3). \tag{A.409}$$

One can explicitly construct tensor structures for (A.409). The partial amplitudes is given then by gluing left- and right-hand sides of the amplitudes after the injection of the identity (A.407), namely

$$C_\ell(s_1,s_2,s)\times\overset{\leftrightarrow}{D}_s\times C_\ell(s_3,s_4,s). \tag{A.410}$$

Here we keep the expressions slightly schematic by dropping the dependence of the 4-momenta and focusing only on the spin dependence. The resulting expression (A.410) should encode the Wigner d-matrix. For instance we have explicitly checked that for the scalar particles (when there is no dependence on s_1, s_2, s_3 and s_4) the expression (A.410) is proportional to the Legendre polynomial P_ℓ.

B Appendices to photon bootstrap

B.1 LSZ derivation of crossing equations

The LSZ reduction formula for the scattering process $12 \to 34$ of four spin-1 particles can be written in the following form [97].

$$\begin{aligned} T_{12\to 34}{}^{\lambda_3,\lambda_4}_{\lambda_1,\lambda_2}(p_1,p_2,p_3,p_4) \;=\; & \int d^4x_1\, d^4x_2\, d^4x_3\, d^4x_4 \\ & \times\; e^{-ip_3x_3}\, \epsilon^{\mu_3}_{\lambda_3}(p_3)(-\partial_3^2) \\ & \times\; e^{-ip_4x_4}\, \epsilon^{\mu_4}_{\lambda_4}(p_4)(-\partial_4^2) \\ & \times\; \langle\Omega|T\{A_{\mu_4}(x_4)A_{\mu_3}(x_3)A_{\mu_1}(x_1)A_{\mu_2}(x_2)\}|\Omega\rangle_{connected} \\ & \times\; (-\overleftarrow{\partial_1^2})\epsilon^{\mu_1 *}_{\lambda_1}(p_1)\, e^{ip_1x_1} \\ & \times\; (-\overleftarrow{\partial_2^2})\epsilon^{\mu_2 *}_{\lambda_2}(p_2)\, e^{ip_2x_2}, \end{aligned} \tag{B.1}$$

where $|\Omega\rangle$ denotes the vacuum state and $A_{\mu_i}(x)$ are spin 1 fields (massive or massless). Similarly we can write the LSZ reduction formula for the process $1\bar{3} \to \bar{2}4$

$$\begin{aligned} T_{1\bar{3}\to \bar{2}4}{}^{\lambda_2,\lambda_4}_{\lambda_1,\lambda_3}(p_1,p_3,p_2,p_4) \;=\; & \int d^4x_1\, d^4x_2\, d^4x_3\, d^4x_4 \\ & \times\; e^{-ip_2x_2}\, \epsilon^{\mu_2}_{\lambda_2}(p_2)(-\partial_2^2) \\ & \times\; e^{-ip_4x_4}\, \epsilon^{\mu_4}_{\lambda_4}(p_4)(-\partial_4^2) \\ & \times\; \langle\Omega|T\{A_{\mu_4}(x_4)A_{\mu_2}(x_2)A_{\mu_1}(x_1)A_{\mu_3}(x_3)\}|\Omega\rangle_{connected} \\ & \times\; (-\overleftarrow{\partial_1^2})\epsilon^{\mu_1 *}_{\lambda_1}(p_1)\, e^{ip_1x_1} \\ & \times\; (-\overleftarrow{\partial_3^2})\epsilon^{\mu_3 *}_{\lambda_3}(p_3)\, e^{ip_3x_3}, \end{aligned} \tag{B.2}$$

Note that the amplitudes above are defined for positive energy momenta, namely $p_i^0 > 0$. Crossing symmetry is the statement that the amplitudes for the two processes above are related by analytic continuation. Consider the $1\bar{3} \to 24$ process and analytically

continue the expression (B.2) in p_2 and p_3 to allow for negative energies.

$$\begin{aligned} T_{1\bar{3}\to\bar{2}4}{}^{\lambda_2,\lambda_4}_{\lambda_1,\lambda_3}(p_1,-p_3,-p_2,p_4) \;=\; & \int d^4x_1\, d^4x_2\, d^4x_3\, d^4x_4 \\ & \times \quad e^{ip_2x_2}\,\epsilon^{\mu_2}_{\lambda_2}(-p_2)(-\partial_2^2) \\ & \times \quad e^{-ip_4x_4}\,\epsilon^{\mu_4}_{\lambda_4}(p_4)(-\partial_4^2) \\ & \times \quad \langle\Omega|T\{A_{\mu_4}(x_4)A_{\mu_2}(x_2)A_{\mu_1}(x_1)A_{\mu_3}(x_3)\}|\Omega\rangle_{connected} \\ & \times \quad (-\overleftarrow{\partial_1^2})\epsilon^{\mu_1*}_{\lambda_1}(p_1)\,e^{ip_1x_1} \\ & \times \quad (-\overleftarrow{\partial_3^2})\epsilon^{\mu_3*}_{\lambda_3}(-p_3)\,e^{-ip_3x_3}, \end{aligned} \tag{B.3}$$

We see that the above expression looks very similar to (B.1) except for the correlator and the polarization vectors which are evaluated at negative energies. Using the fact that bosonic operators commute we see that the correlation functions are equal

$$\begin{aligned} &\langle\Omega|T\{A_{\mu_4}(x_4)A_{\mu_3}(x_3)A_{\mu_1}(x_1)A_{\mu_2}(x_2)\}|\Omega\rangle = \\ &\qquad\qquad \langle\Omega|T\{A_{\mu_4}(x_4)A_{\mu_2}(x_2)A_{\mu_1}(x_1)A_{\mu_3}(x_3)\}|\Omega\rangle \end{aligned} \tag{B.4}$$

We now consider the negative energy polarization vectors $\epsilon^{\mu}_{\lambda}(-p)$. They are the analytic continuations of the positive energy polarizations, which were defined in (3.19). Since we deal with massless particles in this work, we choose the following analytic continuation for the momenta

$$p^0 \to -p^0 \quad , \boldsymbol{p} \to -\boldsymbol{p}, \quad \theta \to \theta, \quad \phi \to \phi \tag{B.5}$$

which ensures that $p^\mu \to -p^\mu$. Under this analytic continuation we see from the explicit form (3.19) that

$$\epsilon^{\mu}_{\lambda}(-p) = \epsilon^{\mu}_{\lambda}(p) = \epsilon^{\mu*}_{-\lambda}(p) \tag{B.6}$$

Thus by using (B.6) and (B.4) in (B.3) and then comparing with (B.1) we have

$$T_{12\to34}{}^{\lambda_3,\lambda_4}_{\lambda_1,\lambda_2}(p_1,p_2,p_3,p_4) = T_{1\bar{3}\to\bar{2}4}{}^{-\lambda_2,+\lambda_4}_{+\lambda_1,-\lambda_3}(p_1,-p_3,-p_2,p_4). \tag{B.7}$$

Analogously one derives the other three crossing equations. The complete summary of crossing equations reads

$$\begin{aligned} T_{12\to34}{}^{\lambda_3,\lambda_4}_{\lambda_1,\lambda_2}(p_1,p_2,p_3,p_4) &= T_{\bar{4}2\to3\bar{1}}{}^{+\lambda_3,-\lambda_1}_{-\lambda_4,+\lambda_2}(-p_4,p_2,p_3,-p_1), \\ T_{12\to34}{}^{\lambda_3,\lambda_4}_{\lambda_1,\lambda_2}(p_1,p_2,p_3,p_4) &= T_{1\bar{3}\to\bar{2}4}{}^{-\lambda_2,+\lambda_4}_{+\lambda_1,-\lambda_3}(p_1,-p_3,-p_2,p_4), \\ T_{12\to34}{}^{\lambda_3,\lambda_4}_{\lambda_1,\lambda_2}(p_1,p_2,p_3,p_4) &= T_{\bar{3}2\to\bar{1}4}{}^{-\lambda_1,+\lambda_4}_{-\lambda_3,+\lambda_2}(-p_3,p_2,-p_1,p_4), \\ tT_{12\to34}{}^{\lambda_3,\lambda_4}_{\lambda_1,\lambda_2}(p_1,p_2,p_3,p_4) &= T_{1\bar{4}\to3\bar{2}}{}^{+\lambda_3,-\lambda_2}_{+\lambda_1,-\lambda_4}(p_1,-p_4,p_3,-p_2). \end{aligned} \tag{B.8}$$

B.1.1 All incoming amplitude

Using the LSZ reduction formula (B.1) it is possible to define an unphysical 4 photons to nothing amplitude by analytic continuation:

$$\begin{aligned} T_{\lambda_1,\lambda_2,\lambda_3,\lambda_4}(p_1,p_2,p_3,p_4) &\equiv T^{-\lambda_3,-\lambda_4}_{\lambda_1,\lambda_2}(p_1,p_2,-p_3,-p_4) \qquad \text{(B.9)} \\ &= \int d^4x_1\, d^4x_2\, d^4x_3\, d^4x_4 \\ &\quad \times\ e^{ip_3x_3}\,\epsilon^{\mu_3*}_{\lambda_3}(p_3)(-\partial_3^2) \\ &\quad \times\ e^{ip_4x_4}\,\epsilon^{\mu_4*}_{\lambda_4}(p_4)(-\partial_4^2) \\ &\quad \times\ \langle\Omega|T\{A_{\mu_4}(x_4)A_{\mu_3}(x_3)A_{\mu_1}(x_1)A_{\mu_2}(x_2)\}|\Omega\rangle_{connected} \\ &\quad \times\ (-\overleftarrow{\partial_1^2})\epsilon^{\mu_1*}_{\lambda_1}(p_1)\,e^{ip_1x_1} \\ &\quad \times\ (-\overleftarrow{\partial_2^2})\epsilon^{\mu_2*}_{\lambda_2}(p_2)\,e^{ip_2x_2}, \qquad \text{(B.10)} \end{aligned}$$

where we used (B.6). The benefit of defining this unphysical amplitude is that it is manifestly S_4 permutation invariant.

B.2 Perturbative computations

B.2.1 Tree-level amplitude

In this section, we explicitly compute the tree-level amplitude of the dimension 8 interacting EFT Lagrangian (3.72).
In order to do so, notice that the interpolation of the massless vector field at the origin gives the polarization vector:

$$\langle 0|A_\mu(0)|\vec{p},\lambda\rangle \equiv \epsilon_{\lambda,\mu}(p)\,, \qquad \text{(B.11)}$$

giving at any space-time position:

$$\langle 0|A_\mu(x)|\vec{p},\lambda\rangle = \langle 0|e^{-iP\cdot x}A_\mu(0)e^{iP\cdot x}|\vec{p},\lambda\rangle = \epsilon_{\lambda,\mu}(p)e^{ip\cdot x} \qquad \text{(B.12)}$$

Using this, we can straightforwardly interpolate the electromagnetic tensor (3.70):

$$\langle 0|F_{\mu\nu}(x)|\vec{p},\lambda\rangle = i\left[p_\mu\epsilon_{\lambda,\nu}(p)(p) - p_\nu\epsilon_{\lambda,\mu}(p)(p)\right]e^{ip\cdot x} = iH_{\lambda,\mu\nu}(p)e^{ip\cdot x} \qquad \text{(B.13)}$$

$$\langle\vec{p},\lambda|F_{\mu\nu}(x)|0\rangle = -i\left[H_{\lambda,\mu\nu}(p)\right]^* e^{-ip\cdot x} \equiv -iH^\lambda_{\mu\nu}(p)e^{-ip\cdot x} \qquad \text{(B.14)}$$

Then, the tree-level amplitude is obtained by computing:

$$\left({}_{id}\langle\kappa_3,\kappa_4|\int d^4x\mathcal{L}_8(x)|\kappa_1,\kappa_2\rangle_{id}\right)_{\text{connected}} \qquad \text{(B.15)}$$

Focussing on the first operator gives

$$\left({}_{id}\langle\kappa_3,\kappa_4|\int d^4x c_1 F_{\mu\nu}(x)F^{\nu\nu}(x)F_{\alpha\beta}(x)F^{\beta\alpha}(x)|\kappa_1,\kappa_2\rangle_{id}\right)_{\text{connected}} \tag{B.16}$$

$$= c_1 8(-i)^2 i^2\Big[\operatorname{tr}(H_{\lambda_1}H_{\lambda_2})\operatorname{tr}(H^*_{\lambda_3}H^*_{\lambda_4}) + \operatorname{tr}(H_{\lambda_1}H^*_{\lambda_3})\operatorname{tr}(H_{\lambda_2}H^*_{\lambda_4}) + \operatorname{tr}(H_{\lambda_1}H^*_{\lambda_4})\operatorname{tr}(H_{\lambda_2}H^*_{\lambda_3})\Big]\int d^4x e^{i(p_1+p_2-p_3-p_4)\cdot x} \tag{B.17}$$

$$= 8c_1\Big[\operatorname{tr}(H_{\lambda_1}H_{\lambda_2})\operatorname{tr}(H^{\lambda_3}H^{\lambda_4}) + \operatorname{tr}(H_{\lambda_1}H^{\lambda_3})\operatorname{tr}(H_{\lambda_2}H^{\lambda_4}) + \operatorname{tr}(H_{\lambda_1}H^{\lambda_4})\operatorname{tr}(H_{\lambda_2}H^{\lambda_3})\Big](2\pi)^4\delta^{(4)}(p_1+p_2-p_3-p_4)\,, \tag{B.18}$$

and similarly for the second operator. The tree-level amplitude is therefore

$$\begin{aligned}&\mathcal{T}^{\lambda_3,\lambda_4}_{\lambda_1,\lambda_2}(p_1,p_2,p_3,p_4) = \\ &8c_1\Big[\operatorname{tr}(H_{\lambda_1}H_{\lambda_2})\operatorname{tr}(H^{\lambda_3}H^{\lambda_4}) + \operatorname{tr}(H_{\lambda_1}H^{\lambda_3})\operatorname{tr}(H_{\lambda_2}H^{\lambda_4}) + \operatorname{tr}(H_{\lambda_1}H^{\lambda_4})\operatorname{tr}(H_{\lambda_2}H^{\lambda_3})\Big] \\ +&8c_2\Big[\operatorname{tr}\left(H_{\lambda_1}H^{\lambda_3}H_{\lambda_2}H^{\lambda_4}\right) + \operatorname{tr}\left(H_{\lambda_1}H_{\lambda_2}H^{\lambda_3}H^{\lambda_4}\right) + \operatorname{tr}\left(H_{\lambda_1}H_{\lambda_2}H^{\lambda_4}H^{\lambda_3}\right)\Big].\end{aligned} \tag{B.19}$$

B.3 Asymptotic unitarity constraints

B.3.1 Large spin

In this section we follow the analysis of Appendix D.4 in [4] to estimate the behaviour of partial waves at large spin. The first step is to use the Froissart-Gribov projection and write partial waves as a contour integral in the complex $z = \cos\theta$ plane. To this end we define

$$\begin{aligned}e^{\ell}_{\lambda\mu}(z) = \frac{(-1)^{\lambda-\mu}}{2}\left[\Gamma(\ell+\lambda+1)\Gamma(\ell-\lambda+1)\Gamma(\ell+\mu+1)\Gamma(\ell-\mu+1)\right]^{\frac{1}{2}}\left(\frac{1+z}{2}\right)^{\frac{\lambda+\mu}{2}}\left(\frac{1-z}{2}\right)^{-\frac{\lambda-\mu}{2}} \\ \times\left(\frac{z-1}{2}\right)^{-\ell-\mu-1}\frac{1}{\Gamma(2\ell+2)}{}_2F_1\left(\ell+\lambda+1,\ell+\mu+1,2\ell+2,\frac{2}{1-z}\right)\end{aligned} \tag{B.20}$$

valid for $\lambda+\mu \geq 0$ and $\lambda-\mu \geq 0$. For other ranges of parameters, the function is defined by its symmetry properties

$$e^{\ell}_{\lambda\mu}(z) = (-1)^{\lambda-\mu}e^{\ell}_{\mu\lambda}(z) = (-1)^{\lambda-\mu}e^{\ell}_{-\lambda,-\mu}(z) \tag{B.21}$$

This function has a branch cut in the complex z plane between -1 and 1 and its discontinuity there is the Wigner d function[1]:

$$e^{\ell}_{\lambda\mu}(z+i\epsilon) - e^{\ell}_{\lambda\mu}(z-i\epsilon) = -i\pi d^{\ell}_{\lambda\mu}(z) \tag{B.22}$$

We now recall the definition of partial wave amplitudes

$$T^{\ell\,\lambda_3,\lambda_4}_{\lambda_1,\lambda_2}(s) = \int_{-1}^{+1} dz\; d^{\ell}_{\lambda_{12}\lambda_{34}}(z)\; T^{\lambda_3,\lambda_4}_{\lambda_1,\lambda_2}(s,z) \tag{B.23}$$

At this point we would like to use (B.22) write the above equation as a contour integral. But before we do that we need to first extract the kinematic singularities of the scattering amplitude in the z plane[2]. We therefore write

$$T^{\lambda_3,\lambda_4}_{\lambda_1,\lambda_2}(s,z) = b_{\lambda\mu}(z)\hat{T}^{\lambda_3,\lambda_4}_{\lambda_1,\lambda_2}(s,z) \tag{B.24}$$

where we have defined the b function

$$b_{\lambda\mu}(z) = \left(\frac{1+z}{2}\right)^{\frac{|\lambda+\mu|}{2}} \left(\frac{1-z}{2}\right)^{\frac{|\lambda-\mu|}{2}} \tag{B.25}$$

and the function $\hat{T}$ no longer has any kinematic singularities in the z plane. We can now re-write the partial wave integral as a contour integral

$$T^{\ell\,\lambda_3,\lambda_4}_{\lambda_1,\lambda_2}(s) = \frac{1}{i\pi}\oint_C b_{\lambda_{12}\lambda_{34}}(z) e^{\ell}_{\lambda_{12}\lambda_{34}}(z)\hat{T}^{\lambda_3,\lambda_4}_{\lambda_1,\lambda_2}(s,z) \tag{B.26}$$

with the contour C encircling the line segment $[-1,1]$ anti-clockwise. Opening the contour and dropping the arcs at infinity, which we can do for sufficiently large ℓ[3], we arrive at the (generalized) Froissart-Gribov projection formula

$$\begin{aligned} T^{\ell\,\lambda_3,\lambda_4}_{\lambda_1,\lambda_2}(s) = \frac{1}{i\pi}\Bigg(&\int_{z_t}^{\infty} dz\; b_{\lambda_{12}\lambda_{34}}(z)\, e^{\ell}_{\lambda_{12}\lambda_{34}}(z)\mathrm{Disc}_t\hat{T}^{\lambda_3,\lambda_4}_{\lambda_1,\lambda_2}(s,z) \\ &+ \int_{-z_u}^{-\infty} dz\; b_{\lambda_{12}\lambda_{34}}(z)\, e^{\ell}_{\lambda_{12}\lambda_{34}}(z)\mathrm{Disc}_u\hat{T}^{\lambda_3,\lambda_4}_{\lambda_1,\lambda_2}(s,z)\Bigg) \end{aligned} \tag{B.27}$$

where the 1st term is due to the t channel branch cut from $[z_t,\infty)$ and the 2nd term is due to the u channel branch cut from $(-\infty,-z_u]$[4].

[1] In this respect, its a generalization of the Legendre Q function which obeys an analogous relation to the Legendre P polynomial.

[2] The amplitudes $T(s,z)$ have kinematic branch points at $z=+1$ and $z=-1$:

$$T(s,z) \sim \left(\frac{1+z}{2}\right)^{\frac{|\lambda+\mu|}{2}} \left(\frac{1-z}{2}\right)^{\frac{|\lambda-\mu|}{2}} (regular)$$

.

[3] Note that $e^{\ell} \sim z^{-l}$ for large $|z|$.

[4] Note that we do not consider possible bound state terms in this analysis.

For theories with a mass gap, $z_t = 1 + \frac{2t_0}{s-4m^2} > 1$ and $z_u = 1 + \frac{2u_0}{s-4m^2} > 1$ and due to the exponential decay in spin of the e function, the partial wave amplitudes also have an exponential fall off in spin. For theories with massless particles this is not the case, because $z_t \to 1$ and $z_u \to 1$.

We therefore consider the large ℓ, $z \to 1^+$ limit of the hypergeometric function and find

$$\begin{aligned} {}_2F_1\left(\ell+\lambda+1, \ell+\mu+1, 2\ell+2, \frac{2}{1-z}\right) \approx & \frac{2\,\Gamma(2\ell+2)}{\Gamma(\ell+\mu+1)\Gamma(\ell-\mu+1)} \\ & \times \left(\frac{\ell+\lambda+1}{\ell-\mu}\right)^{\frac{\mu-\lambda}{2}} \left(\frac{z-1}{2}\right)^{\ell+1+\frac{\mu+\lambda}{2}} \\ & \times K_{\lambda-\mu}\left(\sqrt{2(\ell+\lambda+1)(\ell-\mu)(z-1)}\right). \end{aligned} \tag{B.28}$$

Hence we find the approximation for the e function valid for $\ell \gg 1$ and $z \to 1^+$ and $\lambda \ll \ell$, $\mu \ll \ell$

$$e^{\ell}_{\lambda\mu}(z) \approx (-1)^{\lambda-\mu} \left(\frac{1+z}{2}\right)^{\frac{\lambda+\mu}{2}} \left(\frac{1-z}{2}\right)^{-\frac{\lambda-\mu}{2}} \left(\frac{z-1}{2}\right)^{\frac{\lambda-\mu}{2}} K_{\lambda-\mu}\left(\sqrt{2(\ell+\lambda+1)(\ell-\mu)(z-1)}\right). \tag{B.29}$$

For the other limit $\ell \gg 1$ and $z \to -1^-$, we use the relation

$$e^{\ell}_{\lambda\mu}(-z) = (-1)^{l-\lambda+1} e^{\ell}_{\lambda,-\mu}(z) \tag{B.30}$$

The other piece in (B.27) is the discontinuity of the amplitude $\hat{T} \equiv \frac{T}{b}$. In our numerics we parametrize the T amplitude as follows:

$$T = \sum_{abc} \alpha_{abc} \mathfrak{r}^a(s)\mathfrak{r}^b(t)\mathfrak{r}^c(u) \tag{B.31}$$

Therefore the t channel discontinuity comes from

$$\mathfrak{r}(t(s, z+i\epsilon))^b - \mathfrak{r}(t(s, z-i\epsilon))^b = 2ib\sqrt{2s}\sqrt{z-1} \tag{B.32}$$

and the u channel discontinuity comes from

$$\mathfrak{r}(u(s, z-i\epsilon))^c - \mathfrak{r}(u(s, z+i\epsilon))^c = 2ic\sqrt{2s}\sqrt{-z-1} \tag{B.33}$$

By making a change of variable $z \to -z$ for the u channel contribution and using the symmetry properties (B.30) of the e function and the b function

$$b_{\lambda\mu}(-z) = b_{\lambda,-\mu}(z) \tag{B.34}$$

we can reduce all our computations to that of integrals of the following form:

$$\int_1^\infty dz\,(1+z)^m\,(1-z)^n\,\sqrt{z-1}K_a\left(c\sqrt{z-1}\right) \tag{B.35}$$

To perform this integral we make a change of variable $(z-1)=\xi^2$ and then expand in the variable ξ we get the following type of integrals which are easily evaluated

$$\int_0^\infty d\xi\,\xi^b\,K_a\left(c\xi\right)=\frac{2^{b-1}}{c^{b+1}}\Gamma\left(\frac{b-a+1}{2}\right)\Gamma\left(\frac{b+a+1}{2}\right) \tag{B.36}$$

Since $c\sim\ell$, we see that the leading contribution comes from the lowest order term in the ξ expansion. We are now in a position to write the leading large ℓ behaviour of our ansaetze:

$$\begin{aligned}
\Phi_1^\ell\equiv T^{\ell}{}_{+,+}^{+,+}(s)&\approx\frac{1}{\ell^3}\sum_{abc}\alpha_{abc}^{(1)}\left(b\,\mathfrak{r}^c(-s)+(-1)^\ell c\,\mathfrak{r}^b(-s)\right)\sqrt{s}\,\mathfrak{r}^a(s)\\
\Phi_2^\ell\equiv T^{\ell}{}_{+,+}^{-,-}(s)&\approx\frac{1}{\ell^3}\sum_{abc}\alpha_{abc}^{(2)}\left(b\,\mathfrak{r}^c(-s)+(-1)^\ell c\,\mathfrak{r}^b(-s)\right)\sqrt{s}\,\mathfrak{r}^a(s)\\
\Phi_3^\ell\equiv T^{\ell}{}_{+,-}^{+,-}(s)&\approx\frac{1}{\ell^3}\sum_{abc}\alpha_{abc}^{(3)}\left(b\,\mathfrak{r}^c(-s)-(-1)^\ell 15\,c\,\mathfrak{r}^b(-s)\right)\sqrt{s}\,\mathfrak{r}^a(s)\\
\Phi_4^\ell\equiv T^{\ell}{}_{+,-}^{-,+}(s)&\approx\frac{1}{\ell^3}\sum_{abc}\alpha_{abc}^{(4)}\left(-15\,b\,\mathfrak{r}^c(-s)+(-1)^\ell c\,\mathfrak{r}^b(-s)\right)\sqrt{s}\,\mathfrak{r}^a(s)\\
\Phi_5^\ell\equiv T^{\ell}{}_{+,+}^{+,-}(s)&\approx\frac{1}{\ell^3}\sum_{abc}\alpha_{abc}^{(5)}\left(-3\,b\,\mathfrak{r}^c(-s)-(-1)^\ell 3\,c\,\mathfrak{r}^b(-s)\right)\sqrt{s}\,\mathfrak{r}^a(s)
\end{aligned} \tag{B.37}$$

Actually we can simplify the above expressions by noting that

$$\sum_{abc}\alpha_{abc}^{(3)}\,c=0 \tag{B.38}$$

since this combination is the coefficient in front of $\mathfrak{r}(s)^a\mathfrak{r}(t)^b\sqrt{u}$ and we know that the amplitude Φ_3 starts off as u^2 near $u=0$. Similarly, since $\Phi_4\sim t^2$ at $t=0$, we have

$$\sum_{abc}\alpha_{abc}^{(4)}\,b=0 \tag{B.39}$$

and since $\Phi_5\sim t$ at $t=0$ and $\Phi_5\sim u$ at $u=0$

$$\sum_{abc}\alpha_{abc}^{(5)}\,b=\sum_{abc}\alpha_{abc}^{(5)}\,c=0 \tag{B.40}$$

Using these results we can update our large spin approximations for Φ_3, Φ_4 and Φ_5:

$$\begin{aligned}\Phi_3^\ell &\equiv T^{\ell}{}_{+,-}^{+,-}(s) \approx \frac{1}{\ell^3}\sum_{abc}\alpha_{abc}^{(3)}\, b\,\sqrt{s}\,\mathfrak{r}^a(s)\mathfrak{r}^c(-s)\\ \Phi_4^\ell &\equiv T^{\ell}{}_{+,-}^{-,+}(s) \approx \frac{(-1)^\ell}{\ell^3}\sum_{abc}\alpha_{abc}^{(4)} c\,\sqrt{s}\,\mathfrak{r}^a(s)\mathfrak{r}^b(-s)\\ \Phi_5^\ell &\equiv T^{\ell}{}_{+,+}^{+,-}(s) \approx O(\ell^{-4})\end{aligned} \tag{B.41}$$

We can now derive constraints as follows - consider the combination $\Phi_1^\ell - \Phi_2^\ell$ for even ℓ

$$\Phi_1^\ell - \Phi_2^\ell \approx \frac{2}{l^3}\sum_{abc}\left(\alpha_{abc}^{(1)} - \alpha_{abc}^{(2)}\right) b\sqrt{s}\,\mathfrak{r}^a(s)\,\mathfrak{r}^c(-s) \tag{B.42}$$

where we used the fact that Φ_1 and Φ_2 are invariant under $t-u$ crossing which implies that $\alpha_{abc}^{(1)} = \alpha_{acb}^{(1)}$ and $\alpha_{abc}^{(2)} = \alpha_{acb}^{(2)}$. By unitarity $|1 + i(\Phi_1^\ell - \Phi_2^\ell)| \leq 1$, from which we get the condition

$$\boxed{\sum_{abc}\left(\alpha_{abc}^{(1)} - \alpha_{abc}^{(2)}\right) b\sqrt{s}\,\mathrm{Im}(\mathfrak{r}^a(s))\,\mathfrak{r}^c(-s) \geq 0} \tag{B.43}$$

Similarly we get from $|1 + 2i\Phi_3^\ell| \leq 1$ (ℓ odd)

$$\boxed{\sum_{abc}\alpha_{abc}^{(3)} b\sqrt{s}\,\mathrm{Im}(\mathfrak{r}^a(s))\,\mathfrak{r}^c(-s) \geq 0} \tag{B.44}$$

Finally we come to the condition (3.64). Since the off-diagonal term $\Phi_5 \sim O(\ell^{-4})$, at $O(\ell^{-3})$, the condition simplifies to $|1 + i(\Phi_1^\ell + \Phi_2^\ell)| \leq 1$ and we get

$$\boxed{\sum_{abc}\left(\alpha_{abc}^{(1)} + \alpha_{abc}^{(2)}\right) b\sqrt{s}\,\mathrm{Im}(\mathfrak{r}^a(s))\,\mathfrak{r}^c(-s) \geq 0} \tag{B.45}$$

B.3.2 Large energy

In this subsection we are interested in the large energy limit $s \to \infty$. We would like to study what happens to the unitarity constraints in this limit and implement them as additional constraints on our ansatz. Once again the details are dependent on how we parametrize our amplitude. Consider directly writing an ansatz for the scattering amplitude T:

$$T = \sum_{abc}\alpha_{abc}\mathfrak{r}^a(s)\mathfrak{r}^b(t)\mathfrak{r}^c(u) \tag{B.46}$$

We therefore begin by considering the $s \to \infty$ limit of a monomial term in the ansatz:

$$\mathfrak{r}^a(s)\mathfrak{r}^b(t)\mathfrak{r}^c(u) \approx (-1)^{a+b+c}\left[1 - \frac{2}{\sqrt{s}}\left(ia + \frac{\sqrt{2}b}{\sqrt{1-z}} + \frac{\sqrt{2}c}{\sqrt{1+z}}\right) + i\frac{4\sqrt{2}a}{s}\left(\frac{b}{\sqrt{1-z}} + \frac{c}{\sqrt{1+z}}\right) + \frac{1}{s}\left(-2a^2 + \frac{8bc}{\sqrt{1-z}\sqrt{1+z}} + \frac{4b^2}{1-z} + \frac{4c^2}{1+z}\right) + \dots\right] \tag{B.47}$$

Using the expansion above, we can write the $s \to \infty$ expansion of the partial waves

$$\Phi_I^\ell \approx \sum_{abc}(-1)^{a+b+c}\alpha_{abc}\left[\mathscr{I}^{\ell;0,0}_{\lambda_{12},\lambda_{34}} - \frac{2}{\sqrt{s}}\left(ia\,\mathscr{I}^{\ell;0,0}_{\lambda_{12},\lambda_{34}} + \sqrt{2}b\,\mathscr{I}^{\ell;\frac{1}{2},0}_{\lambda_{12},\lambda_{34}} + \sqrt{2}c\,\mathscr{I}^{\ell;0,\frac{1}{2}}_{\lambda_{12},\lambda_{34}}\right) + i\frac{4\sqrt{2}a}{s}\left(b\,\mathscr{I}^{\ell;\frac{1}{2},0}_{\lambda_{12},\lambda_{34}} + c\,\mathscr{I}^{\ell;0,\frac{1}{2}}_{\lambda_{12},\lambda_{34}}\right) + \frac{1}{s}\left(-2a^2\,\mathscr{I}^{\ell;0,0}_{\lambda_{12},\lambda_{34}} + 8bc\,\mathscr{I}^{\ell;\frac{1}{2},\frac{1}{2}}_{\lambda_{12},\lambda_{34}} + 4b^2\,\mathscr{I}^{\ell;1,0}_{\lambda_{12},\lambda_{34}} + 4c^2\,\mathscr{I}^{\ell;0,1}_{\lambda_{12},\lambda_{34}}\right) + \dots\right] \tag{B.48}$$

where we defined the integrals

$$\mathscr{I}^{\ell;m,n}_{\lambda,\mu} \equiv \frac{1}{32\pi}\int_{-1}^{+1}\frac{d^\ell_{\lambda,\mu}(z)}{(1-z)^m(1+z)^n} \tag{B.49}$$

We now analyze the unitarity equations order by order in $\frac{1}{s}$.

O(1):

Consider first the spin 0 partial waves

$$\begin{aligned}\Phi_1^0 + \Phi_2^0 &\approx \frac{1}{32\pi}\sum_{abc}(-1)^{a+b+c}\left(\alpha^{(1)}_{abc} + \alpha^{(2)}_{abc}\right)\left(1 + O\left(\frac{1}{\sqrt{s}}\right)\right)\\ \Phi_1^0 - \Phi_2^0 &\approx \frac{1}{32\pi}\sum_{abc}(-1)^{a+b+c}\left(\alpha^{(1)}_{abc} - \alpha^{(2)}_{abc}\right)\left(1 + O\left(\frac{1}{\sqrt{s}}\right)\right)\end{aligned} \tag{B.50}$$

and thus we get a constraint from $|1 + i(\Phi_1^0 + \Phi_2^0)| \leq 1$:

$$\boxed{\sum_{abc}(-1)^{a+b+c}\left(\alpha^{(1)}_{abc} + \alpha^{(2)}_{abc}\right) = 0} \tag{B.51}$$

and another from $|1 + i(\Phi_1^0 - \Phi_2^0)| \leq 1$:

$$\boxed{\sum_{abc}(-1)^{a+b+c}\left(\alpha_{abc}^{(1)} - \alpha_{abc}^{(2)}\right) = 0} \tag{B.52}$$

Next we consider we consider odd spin ℓ partial waves:

$$\Phi_3^\ell \approx \sum_{abc}(-1)^{a+b+c}\alpha_{abc}^{(3)}\left(\mathscr{I}_{2,2}^{\ell;0,0} + O\left(\frac{1}{\sqrt{s}}\right)\right) \tag{B.53}$$

Hence from $|1 + 2i\Phi_3^\ell| \leq 1$ we conclude

$$\boxed{\sum_{abc}(-1)^{a+b+c}\alpha_{abc}^{(3)} = 0} \tag{B.54}$$

Finally we consider even spin $\ell \geq 2$ partial waves:

$$\Phi_5^\ell \approx \sum_{abc}(-1)^{a+b+c}\alpha_{abc}^{(5)}\left(\mathscr{I}_{2,0}^{\ell;0,0} + O\left(\frac{1}{\sqrt{s}}\right)\right) \tag{B.55}$$

Since Φ_1, Φ_2 and Φ_3 are all 0 at this order due to (B.51), (B.52), (B.54), the unitarity condition (2.47) implies

$$\boxed{\sum_{abc}(-1)^{a+b+c}\alpha_{abc}^{(5)} = 0} \tag{B.56}$$

We now go to the next order in $\frac{1}{s}$ in the unitarity equations.

O($s^{-1/2}$):

Once again we begin by considering the spin 0 partial waves

$$\begin{aligned}
\Phi_1^0 + \Phi_2^0 &\approx \frac{1}{32\pi}\sum_{abc}(-1)^{a+b+c}\left(\alpha_{abc}^{(1)} + \alpha_{abc}^{(2)}\right)\left(-\frac{2}{\sqrt{s}}ia + \frac{\text{real}}{\sqrt{s}} + O\left(\frac{1}{s}\right)\right)\\
\Phi_1^0 - \Phi_2^0 &\approx \frac{1}{32\pi}\sum_{abc}(-1)^{a+b+c}\left(\alpha_{abc}^{(1)} - \alpha_{abc}^{(2)}\right)\left(-\frac{2}{\sqrt{s}}ia + \frac{\text{real}}{\sqrt{s}} + O\left(\frac{1}{s}\right)\right)
\end{aligned} \tag{B.57}$$

Hence from $|1 + i(\Phi_1^0 + \Phi_2^0)| \leq 1$, we have[5]

$$\boxed{\sum_{abc}(-1)^{a+b+c}\left(\alpha_{abc}^{(1)} + \alpha_{abc}^{(2)}\right) a \leq 0} \tag{B.58}$$

and from $|1 + i(\Phi_1^0 - \Phi_2^0)| \leq 1$, we have:

$$\boxed{\sum_{abc}(-1)^{a+b+c}\left(\alpha_{abc}^{(1)} - \alpha_{abc}^{(2)}\right) a \leq 0} \tag{B.59}$$

Next we consider odd spin ℓ partial waves

$$\Phi_3^\ell \approx \sum_{abc}(-1)^{a+b+c}\alpha_{abc}^{(3)}\left(-\frac{2}{\sqrt{s}} ia\, \mathscr{I}_{2,2}^{\ell;0,0} + \frac{\text{real}}{\sqrt{s}} + O\left(\frac{1}{s}\right)\right) \tag{B.60}$$

Using the result

$$\mathscr{I}_{2,2}^{\ell;0,0} \equiv \frac{1}{32\pi}\int dz\, d_{2,2}^\ell(z) < 0 \quad \forall \quad \ell \quad \text{odd} \tag{B.61}$$

we deduce from $|1 + 2i\Phi_3^\ell| \leq 1$ that

$$\sum_{abc}(-1)^{a+b+c}\alpha_{abc}^{(3)}\, a \geq 0 \tag{B.62}$$

Finally we consider even spin $\ell \geq 2$ partial waves:

$$\begin{aligned}
\Phi_1^\ell + \Phi_2^\ell &\approx \frac{1}{32\pi}\sum_{abc}(-1)^{a+b+c}\left(\alpha_{abc}^{(1)} + \alpha_{abc}^{(2)}\right)\left(\frac{\text{real}}{\sqrt{s}} + O\left(\frac{1}{s}\right)\right) \\
\Phi_3^\ell &\approx \sum_{abc}(-1)^{a+b+c}\alpha_{abc}^{(3)}\left(-\frac{2}{\sqrt{s}} ia\, \mathscr{I}_{2,2}^{\ell;0,0} + \frac{\text{real}}{\sqrt{s}} + O\left(\frac{1}{s}\right)\right) \\
\Phi_5^\ell &\approx \sum_{abc}(-1)^{a+b+c}\alpha_{abc}^{(5)}\left(-\frac{2}{\sqrt{s}} ia\, \mathscr{I}_{2,0}^{\ell;0,0} - \frac{4\sqrt{2}}{\sqrt{s}} b\, \mathscr{I}_{2,0}^{\ell;\frac{1}{2},0} + O\left(\frac{1}{s}\right)\right)
\end{aligned} \tag{B.63}$$

where we used the $t-u$ symmetry of the amplitude Φ_5 and also the result $\mathscr{I}_{0,0}^{\ell;0,0} = 0$ for $\ell \neq 0$. In the unitarity condition (3.64), the imaginary parts of $\Phi_1^\ell + \Phi_2^\ell$ and Φ_3^ℓ at $O\left(\frac{1}{\sqrt{s}}\right)$ contribute at $O\left(\frac{1}{\sqrt{s}}\right)$ while their real parts contribute at next order $O\left(\frac{1}{s}\right)$. However note that for the off-diagonal term Φ_5^ℓ, both the real and imaginary part at $O\left(\frac{1}{\sqrt{s}}\right)$ contribute at order $O\left(\frac{1}{\sqrt{s}}\right)$. Studying the eigenvalues of the unitarity matrix in (2.47) at this order,

[5]Note that the real part $\frac{\text{real}}{\sqrt{s}}$ only contributes at next order $O\left(\frac{1}{s}\right)$

we see that imaginary part $\text{Im}(\Phi_5^\ell)$ must be 0:

$$\boxed{\sum_{abc}(-1)^{a+b+c}\alpha^{(5)}_{abc}\,a=0} \tag{B.64}$$

Note that by crossing symmetry this implies that the real part $\text{Re}(\Phi_5^\ell)$ must also be 0 at this order:

$$\sum_{abc}(-1)^{a+b+c}\alpha^{(5)}_{abc}\,b=0 \tag{B.65}$$

In addition because

$$\mathscr{I}_{2,2}^{\ell;0,0}\equiv\frac{1}{32\pi}\int dz\, d^\ell_{2,2}(z)>0\quad\forall\quad\ell\quad\text{even} \tag{B.66}$$

we also see that

$$\sum_{abc}(-1)^{a+b+c}\alpha^{(3)}_{abc}\,a\leq 0 \tag{B.67}$$

Along with (B.62), this leads to

$$\boxed{\sum_{abc}(-1)^{a+b+c}\alpha^{(3)}_{abc}\,a=0} \tag{B.68}$$

Having analyzed at the consequences of unitarity at $O\left(\frac{1}{\sqrt{s}}\right)$, we now delve into the next order.

O(s^{-1}):

Since the spin 0 partial waves can be non-zero at the previous order $O\left(\frac{1}{\sqrt{s}}\right)$, we can not use them to make any further deductions at $O\left(\frac{1}{s}\right)$. We therefore begin with even spin $\ell>2$ partial waves [6]:

$$\Phi_1^\ell-\Phi_2^\ell\approx\sum_{abc}(-1)^{a+b+c}\left(\alpha^{(1)}_{abc}-\alpha^{(2)}_{abc}\right)\left(-\frac{1}{\sqrt{s}}b+i\frac{2}{s}ab\right)4\sqrt{2}\,\mathscr{I}_{0,0}^{\ell;\frac{1}{2},0} \tag{B.69}$$

Hence from $|1+i(\Phi_1^\ell-\Phi_2^\ell)|\leq 1$ we get [7]

$$\boxed{40\pi\sum_{abc}(-1)^{a+b+c}\left(\alpha^{(1)}_{abc}-\alpha^{(2)}_{abc}\right)ab\geq\left(\sum_{abc}(-1)^{a+b+c}\left(\alpha^{(1)}_{abc}-\alpha^{(2)}_{abc}\right)b\right)^2} \tag{B.70}$$

[6] A factor of 2 comes from $t-u$ symmetry of these amplitudes.

[7] Where we used the result that $I_l<I_2=\frac{1}{40\sqrt{2}\pi}$.

This is a quadratic constraint in the parameters α^I_{abc}. To implement it on SDPB, we re-write it as follows:

$$\mathscr{M} \equiv \begin{pmatrix} \mathscr{M}_{11} & \mathscr{M}_{12} \\ \mathscr{M}_{21} & \mathscr{M}_{22} \end{pmatrix} \succeq 0 \tag{B.71}$$

where

$$\begin{aligned} \mathscr{M}_{11} &= 40\pi \sum_{abc} (-1)^{a+b+c} \left(\alpha^{(1)}_{abc} + \alpha^{(2)}_{abc}\right) ab \\ \mathscr{M}_{21} = \mathscr{M}_{12} &= \sum_{abc} (-1)^{a+b+c} \left(\alpha^{(1)}_{abc} + \alpha^{(2)}_{abc}\right) b \\ \mathscr{M}_{22} &= 1 \end{aligned} \tag{B.72}$$

We now consider odd spin ℓ partial waves:

$$\Phi^\ell_3 \approx \sum_{abc} (-1)^{a+b+c} \alpha^{(3)}_{abc} \left[\left(-\frac{1}{\sqrt{s}} b + i \frac{2}{s} ab \right) 2\sqrt{2}\, \mathscr{I}^{\ell;\frac{1}{2},0}_{2,2} + \left(-\frac{1}{\sqrt{s}} c + i \frac{2}{s} ac \right) 2\sqrt{2}\, \mathscr{I}^{\ell;0,\frac{1}{2}}_{2,2} \right] \tag{B.73}$$

Therefore from the unitarity equation $|1 + 2i\Phi^\ell_3| \leq 1$, we have

$$\boxed{\frac{1}{\sqrt{2}} \sum_{abc} (-1)^{a+b+c} \alpha^{(3)}_{abc} \left(ab \mathscr{I}^{\ell;\frac{1}{2},0}_{2,2} + ac \mathscr{I}^{\ell;0,\frac{1}{2}}_{2,2} \right) \geq \left(\sum_{abc} (-1)^{a+b+c} \alpha^{(3)}_{abc} \left(b \mathscr{I}^{\ell;\frac{1}{2},0}_{2,2} + c \mathscr{I}^{\ell;0,\frac{1}{2}}_{2,2} \right) \right)^2} \tag{B.74}$$

As before, to input these constraints into SDPB, we re-write so that it is linear in the parameters. Moreover, we will need to impose the constraints for various values of the spin ℓ:

$$\mathscr{N}^\ell \equiv \begin{pmatrix} \mathscr{N}^\ell_{11} & \mathscr{N}^\ell_{12} \\ \mathscr{N}^\ell_{21} & \mathscr{N}^\ell_{22} \end{pmatrix} \succeq 0 \quad \forall \quad \ell \quad \text{odd} \tag{B.75}$$

where

$$\begin{aligned} \mathscr{N}^\ell_{11} &= \frac{1}{\sqrt{2}} \sum_{abc} (-1)^{a+b+c} \alpha^{(3)}_{abc} \left(ab\, \mathscr{I}^{\ell;\frac{1}{2},0}_{2,2} + ac\, \mathscr{I}^{\ell;0,\frac{1}{2}}_{2,2} \right) \\ \mathscr{N}^\ell_{21} = N^\ell_{12} &= \sum_{abc} (-1)^{a+b+c} \alpha^{(3)}_{abc} \left(b\, \mathscr{I}^{\ell;\frac{1}{2},0}_{2,2} + c\, \mathscr{I}^{\ell;0,\frac{1}{2}}_{2,2} \right) \\ \mathscr{N}^\ell_{22} &= 1 \end{aligned} \tag{B.76}$$

Finally going back to even spin ℓ, we have

$$\Phi^\ell_1 + \Phi^\ell_2 \approx \sum_{abc} (-1)^{a+b+c} \left(\alpha^{(1)}_{abc} + \alpha^{(2)}_{abc}\right) \left(-\frac{1}{\sqrt{s}} b + i \frac{2}{s} ab \right) 4\sqrt{2}\, \mathscr{I}^{\ell;\frac{1}{2},0}_{0,0} \tag{B.77}$$

Φ^ℓ_3 is still given by (B.73) and Φ^ℓ_5 is given by

$$\Phi^\ell_5 \approx \sum_{abc} (-1)^{a+b+c} \alpha^{(5)}_{abc} \left(-\frac{1}{\sqrt{s}} b + i \frac{2}{s} ab \right) 4\sqrt{2}\, \mathscr{I}^{\ell;\frac{1}{2},0}_{2,0} \tag{B.78}$$

The unitarity equation (3.64) then implies the following two conditions:

$$\begin{aligned}(2i_{11}-r_{11}^2)(2i_{22}-r_{22}^2) &\geq 4\, i_{21}^2\\ (2i_{11}-r_{11}^2) &\geq 0\\ (2i_{22}-r_{22}^2) &\geq 0\end{aligned} \tag{B.79}$$

where

$$\begin{aligned}
i_{11} &= 8\sqrt{2}\sum_{abc}(-1)^{a+b+c}\left(\alpha^{(1)}_{abc}-\alpha^{(2)}_{abc}\right) ab\, \mathscr{I}^{\ell;\frac{1}{2},0}_{0,0}\\
r_{11} &= -4\sqrt{2}\sum_{abc}(-1)^{a+b+c}\left(\alpha^{(1)}_{abc}-\alpha^{(2)}_{abc}\right) b\, \mathscr{I}^{\ell;\frac{1}{2},0}_{0,0}\\
i_{21} &= 8\sqrt{2}\sum_{abc}(-1)^{a+b+c}\alpha^{(5)}_{abc}\, ab\, \mathscr{I}^{\ell;\frac{1}{2},0}_{2,0}\\
r_{21} &= 2\sum_{abc}(-1)^{a+b+c}\alpha^{(5)}_{abc}\left(-a^2\, \mathscr{I}^{\ell;0,0}_{2,0}+4bc\, \mathscr{I}^{\ell;\frac{1}{2},\frac{1}{2}}_{2,0}+4b^2\, \mathscr{I}^{\ell;1,0}_{2,0}\right)\\
i_{22} &= 4\sqrt{2}\sum_{abc}(-1)^{a+b+c}\alpha^{(3)}_{abc}\left(ab\, \mathscr{I}^{\ell;\frac{1}{2},0}_{2,2}+ac\, \mathscr{I}^{\ell;0,\frac{1}{2}}_{2,2}\right)\\
r_{22} &= -2\sqrt{2}\sum_{abc}(-1)^{a+b+c}\alpha^{(3)}_{abc}\left(b\, \mathscr{I}^{\ell;\frac{1}{2},0}_{2,2}+c\, \mathscr{I}^{\ell;0,\frac{1}{2}}_{2,2}\right)
\end{aligned} \tag{B.80}$$

We can impose the conditions in (B.79) by adding two extra slack variables β_1 and β_2 and writing the following three conditions:

$$\boxed{\begin{pmatrix}(2i_{11}-\beta_1) & r_{11}\\ r_{11} & 1\end{pmatrix}\succeq 0 \quad \forall \quad \ell\geq 2 \quad \text{even}} \tag{B.81}$$

$$\boxed{\begin{pmatrix}(2i_{22}-\beta_2) & r_{22}\\ r_{22} & 1\end{pmatrix}\succeq 0 \quad \forall \quad \ell\geq 2 \quad \text{even}} \tag{B.82}$$

$$\boxed{\begin{pmatrix}\beta_1 & 2i_{21}\\ 2i_{21} & \beta_2\end{pmatrix}\succeq 0 \quad \forall \quad \ell\geq 2 \quad \text{even}} \tag{B.83}$$

C Appendices to flux-tube bootstrap

C.1 Low energy expansion

Loop diagrams in the branon effective field theory may lead to non-analytic terms of the form $s^p(\log s)^k$ with $p > k > 0$. Thus, we consider the following general low energy expansion

$$\begin{aligned}\sigma_1 &= \sum_{p=1}^{6}\sum_{k=0}^{p-1}(a_{p,k}+ib_{p,k})(is)^p\left[\log(-is)\right]^k\\ \sigma_2 &= 1+\sum_{p=1}^{6}\sum_{k=0}^{p-1}c_{p,k}(is)^p\left[\log(-is)\right]^k\\ \sigma_3 &= \sum_{p=1}^{6}\sum_{k=0}^{p-1}(a_{p,k}-ib_{p,k})(is)^p\left[\log(-is)\right]^k\end{aligned} \tag{C.1}$$

where the coefficients a, b and c are real due to (4.10). Next we impose that $2\delta_{rep} = \frac{s}{4}+O(s^2)$ and

$$\operatorname{Im} 2\delta_{rep} = \eta_{rep}s^6 + O(s^7)\,, \tag{C.2}$$

because particle production starts with $|\mathcal{M}_{2\to4}|^2 \sim l_s^{12}$. In fact, the leading term in the probability of particle production

$$P_{rep\to n\geq 4\,\text{branons}} = 2\eta_{rep}s^6 + O(s^7)\,, \tag{C.3}$$

is universal and can be computed using the leading order expressions for $\mathcal{M}_{2\to4}$ in [74]. Using the ansatz (C.1) in (4.7) and imposing (C.2) we find

$$\begin{aligned}2\delta_{sym} &= \frac{s}{4} + \alpha_2 s^2 + \alpha_3 s^3 + \left(\alpha_4 + \frac{(D-4)\alpha_2^2}{2\pi}\log s\right) s^4 \\ &+ \left(\alpha_5 - \frac{(D-4)\alpha_2\beta_3}{\pi}\log s\right) s^5 \\ &+ \left(i\eta_{sym} + \alpha_6 + \frac{q\log s}{2\pi(D-2)} \right.\\ &\qquad \left. + \frac{(D-4)^2\alpha_2^3}{4\pi^2}\log^2 s\right) s^6 + O\left(s^7\right)\,,\end{aligned} \tag{C.4}$$

$$\begin{aligned}2\delta_{anti} &= \frac{s}{4} - \alpha_2 s^2 + (\alpha_3 + 2\beta_3) s^3 \\ &- \left(\alpha_4 + \frac{(D-4)\alpha_2^2}{2\pi}\log s\right) s^4 \\ &+ \left(\alpha_5 + 2\beta_5 + \frac{D\alpha_2\beta_3}{\pi}\log s\right) s^5 \\ &+ \left(i\eta_{anti} - \alpha_6 + \frac{(D-4)\alpha_2^2}{2} \right.\\ &\qquad \left. - \frac{q\log s}{2\pi(D-2)} - \frac{(D-4)^2\alpha_2^3}{4\pi^2}\log^2 s\right) s^6 + O\left(s^7\right)\,,\end{aligned} \tag{C.5}$$

and

$$\begin{aligned}2\delta_{sing} &= \frac{s}{4} - (D-3)\alpha_2 s^2 + (\alpha_3 - (D-2)\beta_3) s^3 \\ &- (D-3)\left(\alpha_4 + \frac{(D-4)\alpha_2^2}{2\pi}\log s\right) s^4 \\ &+ \left(\alpha_5 - (D-2)\beta_5 - \frac{D(D-3)\alpha_2\beta_3}{\pi}\log s\right) s^5 \\ &+ \left(i\eta_{sing} + \frac{(D-3)\left((D-4)(D-2)\alpha_2^2 - 12\alpha_6\right)}{12} \right.\\ &\left. - \frac{q(D-3)\log s}{2\pi(D-2)} - \frac{(D-4)^2(D-3)\alpha_2^3}{4\pi^2}\log^2 s\right) s^6 + O\left(s^7\right)\,.\end{aligned} \tag{C.6}$$

where $\alpha_2, \alpha_3, \beta_3, \alpha_4, \alpha_5, \beta_5, \alpha_6$ are real parameters and $q \equiv 2\eta_{sing} - D\eta_{sym} + (D-2)(\eta_{anti} + 2(D-4)\alpha_2\alpha_4 + D\beta_3^2)$. Notice that the coefficient of the logs do not involve extra free parameters. The non-linearly realized Poincaré symmetry fixes $\alpha_2 = \frac{D-26}{384\pi}$. On the other hand, $\alpha_3, \beta_3, \alpha_4, \alpha_5, \beta_5, \alpha_6$ are non-universal parameters related to K^4, $\nabla^2 K^4$, $\nabla^4 K^4$ and $\nabla^6 K^4$ terms in the effective action (4.1). The universal coefficient of the $s^4 \log s$ terms agrees with the results of [75]. The terms of order s^5 and s^6 are new. Notice that for $D = 4$ the first non-analytic term is $s^5 \log s$ and it is proportional to the non-universal coefficient β_3.

C.2 Schwarz-Pick

C.2.1 Maximum Modulus Principle

Holomorphic functions are equal to the average of their neighbouring points,

$$f(z) = \oint\limits_{|w-z|=\epsilon} \frac{dw}{2\pi i} \frac{f(w)}{z-w} = \int\limits_0^{2\pi} \frac{d\theta}{2\pi} f(z + \epsilon e^{i\theta}) \,, \tag{C.7}$$

and therefore can not have local maxima or minima inside any domain. All maxima or minima must be at the boundary.

In particular, if a function's modulus is bounded by 1 on a boundary of a connected domain and has no singularities inside that domain then the function's modulus must be bounded by 1 everywhere inside the domain as well. This is known as the maximum modulus principle.

C.2.2 Schwarz-Pick

Schwarz-Pick multi-point lemmas are simple but very powerful extensions of the maximum modulus principle.

Consider a function $f^{(0)}(z)$ regular inside a unit disk and bounded as $|f^{(0)}(z)|_{|z|\leq 1} \leq 1$ everywhere. Out of it construct a new function

$$f^{(1)}(z) := \Delta^{(1)}[f](z|w) \equiv \frac{f^{(0)}(z) - f^{(0)}(w)}{1 - f^{(0)}(z)\overline{f^{(0)}(w)}} \Big/ \frac{z-w}{1-z\overline{w}} \tag{C.8}$$

where $|w| < 1$. Since w is strictly inside the disk, this function has no singularities as can be easily checked. Moreover, it is still bounded along the unit circle: take $z = e^{i\phi}$, then the combination $(z-w)/(1-\bar{w}z)$ in eq. (C.8) can be written as

$$\frac{z-w}{1-\bar{w}z} = \frac{1 - w_r \cos\phi - w_i \sin\phi - i(w_i \cos\phi - w_r \sin\phi)}{1 - w_r \cos\phi - w_i \sin\phi + i(w_i \cos\phi - w_r \sin\phi)}, \tag{C.9}$$

showing that it is a pure phase (the same happens when we replace $f^{(0)}(z)$ with z). As such, by maximum modulus principle, it is bounded everywhere and $|f^{(1)}(z)|_{|z|\leq 1} \leq 1$, just like we had for the original function.

We could now go on constructing a new function $f^{(2)}$ which would depend on a new parameter corresponding to a new point w' strictly inside the unit disk and so on. Each of these new functions would again be bounded everywhere inside the disk. This is the content of the Schwarz-Pick multi-point lemmas [78].

There is a cute relation between these lemmas and some AdS_2 geometry: it is a well established fact in complex analysis that analytic functions are either isometries or contractions of the Poincaré disk

$$d^{(h)}(f(z), f(w)) \leq d^{(h)}(z, w)\,, \tag{C.10}$$

with $d^{(h)}(z,w)=2\tanh^{-1}|(z-w)/(1-z\bar{w})|$ the definition of the hyperbolic distance. Eq. (C.8) is known in the mathematical literature as "hyperbolic quotient" and its infinitesimal form

$$\frac{d_h f}{d_h z} = f'(z)\frac{1-|z|^2}{1-|f(z)|^2}\,, \tag{C.11}$$

is known as the hyperbolic derivative.

The isometries of the disc are given by the single CDD zeros

$$f^{(1)}_{CDD}(z|z_0) = e^{i\alpha}\frac{z-z_0}{1-\bar{z}_0 z}\,, \tag{C.12}$$

and it is easy to check $\Delta^{(1)}[f^{(1)}_{CDD}]$ is a pure phase. If we consider a generic product of CDD zeros

$$f^{(n)}_{CDD}(z|z_0, z_1, \ldots, z_{n-1}) = \prod_{i=0}^{n-1} f^{(1)}_{CDD}(z|z_i)\,, \tag{C.13}$$

then $\Delta^{(1)}[f^{(n)}_{CDD}] \sim f^{(n-1)}_{CDD}$ or equivalently $\Delta^{(n)}[f^{(n)}_{CDD}]$ is a pure phase. Of course, there are functions like $e^{(z-1)/(z+1)}$ that, though saturating unitarity, are not CDDs. Indeed they can be represented as infinite products of CDDs and they satisfy all the finite n Schwarz-Pick inequalities, but we do not know any functional bound saturated by those functions.

C.2.3 Application 1: expansion around the center of the disk

As a first application let us consider a function defined on the unit disk as a Taylor expansion of the form

$$f^{(0)}(z) = \sum_{n=0}^{\infty} a_n z^n, \tag{C.14}$$

and let us assume it is bounded within the unit disc so $|f^{(0)}(z)|_{|z|=1} \leq 1$. The simplest question one could ask is: "what is its maximum/minimum value for $z = 0$?". The answer is given by the maximum modulus principle as explained above and it is $|f^{(0)}| = 1$ or equivalently $|a_0| \leq 1$. A slightly non-trivial question one could then ask is: "given a value of a_0, what are the bounds on the derivative of the function at zero i.e. a_1?" If we construct $\Delta^{(1)}[f^{(0)}]$, or alternatively the hyperbolic derivative and we require its boundeness we readily get that $|a_1| \leq 1-a_0^2$. It is easy to guess that applying $\Delta^{(2)}$ will

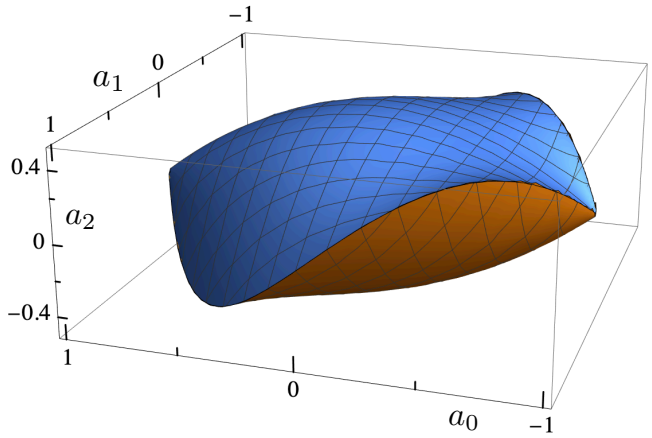

Figure C.1: Allowed space for the first three Taylor coefficients $\{a_0, a_1, a_2\}$ of analytic functions from disk to disk as derived using the Schwarz-Pick lemmas.

give a bound on a_2 as a function of a_0 and a_1

$$|a_2| \leq \frac{(a_0^2-1)^2 + a_1^2(2a_0-1)}{2(a_0^2-1)}\,, \tag{C.15}$$

yielding the nice manifold in figure C.1. We cannot plot the higher order constraints but we can derive them analytically. What we would get is an algebraic manifold contained in the vector space of the Taylor expansion coefficients where all the analytic functions on the unit disc reside. In our language, this is the space of generic massless S-matrices in $1+1$ dimensions.

C.2.4 Application 2: expansion around the threshold

Let us now turn to the application of the above inequalities to $f^{(0)}$ the $D=3$ flux-tube branon S-matrix when $z, w, w', \ldots$ are all close to 1. When translated back to s, this limit corresponds to the very low energy region where we can relate the coefficients of the Taylor expansion of $f^{(0)}$ to the effective field theory parameters. Furthermore, we assume that the threshold is a regular point, which is not the most general behavior for flux tube S-matrices, but, as explained in appendix C.1, it is true up to some high order in s.

For instance, if

$$f^{(0)} = S = e^{i(\gamma_1 s + i\gamma_2 s^2 + \gamma_3 s^3 + i\gamma_4 s^4 + \gamma_5 s^5 + \ldots)}\,, \tag{C.16}$$

and we take $s = \epsilon e^{i\theta}$, with $-\pi \leq \theta \leq \pi$, then the maximum modulus principle implies that

$$|f^{(0)}| = 1 - 2\sin\theta\gamma_1\epsilon + (2\sin^2\theta\gamma_1^2 - 2\cos 2\theta\gamma_2)\epsilon^2 + \mathcal{O}(\epsilon^3) \leq 1. \tag{C.17}$$

For generic θ this condition is equivalent to a positive condition on $\gamma_1 \geq 0$. Since

γ_1 is related to the strength of the tree-level interaction, we notice that in this simple framework the maximum modulus principle is equivalent to the causality bound derived in [20]. Moreover, at $\theta = 0$ we don't get any bound on γ_1, but only on $\gamma_2 \geq 0$. Notice that the maximum modulus principle for $\theta = 0$ is equivalent to unitarity. This is a general feature of the parametrization we chose in eq. (C.16) compatible with crossing and real analyticity: odd powers are pure phases, even powers contribute to inelasticity. Therefore, we could set $\gamma_{2n} = 0$ and focus only on the pure phase coefficients where unitarity has nothing to say about them.

To make contact with flux tube theories (4.11) we set $\gamma_1 = 1/4$. We map the upper half-plane to the unit disk and taking first $z \to w$ and then $1-z = \epsilon e^{i\phi}+\mathcal{O}(\epsilon^2)$ in the Schwarz-Pick lemma we are left with

$$1\geq|f^{(1)}| = 1-16\sec\phi\,\epsilon\gamma_2 + \mathcal{O}(\epsilon^2)+\dots \tag{C.18}$$

If unitarity is saturated the first term vanishes. At the next order

$$|f^{(1)}| = 1 - \frac{1}{12}\epsilon^2\cos^2\phi(1+768\gamma_3) + \mathcal{O}(\epsilon^3)\,, \tag{C.19}$$

the term of $\mathcal{O}(\epsilon^2)$ must be negative leading to

$$\gamma_3 \geq -\frac{1}{768}. \tag{C.20}$$

Combining the constraint above with the one from unitarity $\gamma_4 \geq 0$ at order ϵ^4 we get figure C.2. Assuming unitarity saturation, i.e. $\gamma_{2n} = 0$, we can recursively generate new constraints on the higher derivative coefficients using higher order multi-point lemmas – see also (4.16) and figure 4.1.

If at some order inelasticity kicks in then the Schwarz-Pick inequalities are not saturated and we no longer get any sharp bounds.

As explained in the main text, figure 4.1 represents the space of all integrable S-matrices compatible with the $D = 3$ flux-tube universal low-energy behaviour 4.11. Using the language introduced in this section we would interpret its geometric features saying that the cusp saturates $\Delta^{(1)}$, the red edge $\Delta^{(2)}$ and the surface $\Delta^{(3)}$ Schwarz-Pick constraints. For this reason, it is a theorem that the cusp S-matrix is given by a single CDD, the red edge by products of two CDD and the orange surface by products of three CDD factors

$$S_{\text{surf}} = \frac{(1+3z)(5+z(6+5z))\tilde{\gamma}_3-256(z-1)^3\tilde{\gamma}_3^2+64\tilde{\gamma}_5(z-1)^2(3z+1)}{(z+3)(5+z(6+5z))\tilde{\gamma}_3+256(z-1)^3\tilde{\gamma}_3^2+64\tilde{\gamma}_5(z-1)^2(z+3)} \tag{C.21}$$

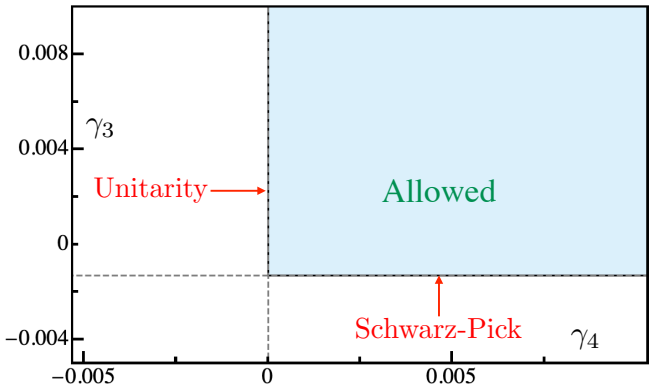

Figure C.2: Allowed region in the $\{\gamma_3, \gamma_4\}$ plane. The unitarity vertical bound is saturated by the integrable S-matrix family in (C.23). The Schwarz-Pick bound would be saturated by theories with a very small amount of particle production localized at threshold for which we don't have an analytic ansatz. The corner at the intersection of the two bounds is saturated by a known integrable theory describing the RG flow from tricritical Ising fixed point to the free fermion.

which for $\tilde{\gamma}_3 = 0$ and $\tilde{\gamma}_5 = 0$ reduces to

$$S_{\text{cusp}} = \frac{1+3z}{z+3}, \tag{C.22}$$

and saturating the second Scwharz-Pick inequality $\tilde{\gamma}_5 = 4\tilde{\gamma}_3^2 - 1/64\tilde{\gamma}_3$ reduces to

$$S_{\text{edge}} = \frac{1+4z+3z^2+128(z-1)^2\tilde{\gamma}_3}{3+4z+z^2+128(z-1)^2\tilde{\gamma}_3}\,. \tag{C.23}$$

whose resonance positions are shown in figure C.3 in the unit disk (to go to the s plane, use $z = \chi(s) = (4+is)/(4-is)$).

Note that these resonances along the red edge of figure 4.1 can be separated into two possibilities – see also figure C.3: they can both be at purely imaginary s (or real χ) or they can be in a pair, symmetric with respect to reflections on the imaginary axis (i.e. given by a complex conjugate pair in χ). These two possibilities are separated by a "collision", represented by the green cross in figure C.3. At that point, the two zeros collide and the S-matrix simply becomes a perfect square with a double zero. This happens at some point along the red edge of the three dimensional figure 4.1.

In the same figure we have the S-matrices on the orange surface, given by (C.21) which have three zeros and again, there is a point on that surface where the three collide. The corresponding S-matrix at that point has a triple zero. Together with the black cusp in figure 4.1 which was given by a single CDD factor, we see that we have a family of three

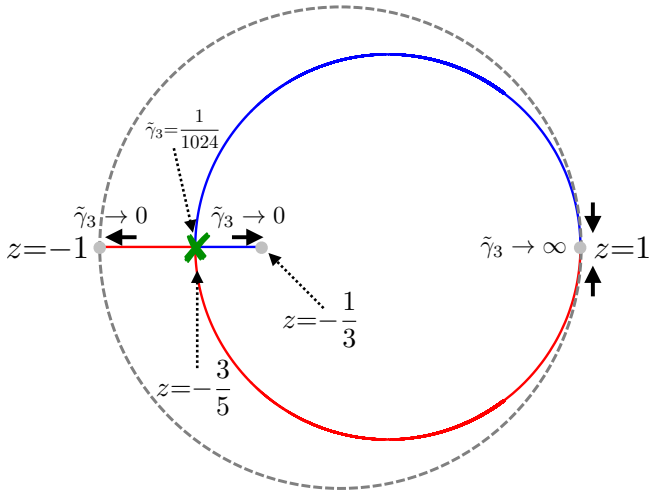

Figure C.3: Resonance positions as we move along the red edge of figure 1: At the cusp we have a virtual state at $\chi = -1/3$ (or $s = 8i$) and the S-matrix can be identified with the goldstino S-matrix of Zamolodchikov [84]. As we move away from the cusp another zero comes in from $i\infty$; eventually the two zeros collide at $s = 16i$ and move away acquiring a real part; in this region they become closer and closer to more conventional sharp resonances until they eventually collide with the $s = t = 0$ threshold.

S-matrices

$$S_n = (-1)^n \left(\frac{s - 8i\,n}{s + 8i\,n}\right)^n \tag{C.24}$$

with $n = 1, 2, 3$ which we can single out as somehow special. We can connect them by a triangle as represented in figure C.4. The region inside the triangle is compact, in contrast to the infinite orange surface in figure 4.1; it is defined by the condition that all zeros there are purely real (in χ). Again, let us stress that $n = 1$ is related to a cusp, $n = 2$ to an edge and $n = 3$ to a face.

There is a clear higher dimensional generalization we could make here if we stick to the family of purely elastic S-matrices that saturate unitarity and therefore have $\gamma_{2n} = 0$. If we further add γ_9 to our analysis, for example, we would now have a four dimensional space and the triangle would be the base of a tetrahedron with the fourth new vertex corresponding to an S-matrix S_4 corresponding to the collision of four zeros. Inside the tetrahedron all zeros would be real (in χ). This is schematically represented in figure C.5. The tetrahedron itself would be the base for a 4 dimensional polyhedra with an extra cusp S_5 (schematically, this is where the dashed purple lines in the figure would meet – of course we can only draw their three-dimensional projections). This would go on thus defining a sequence of S-matrices given by (C.24) for any $n \geq 1$.

So we could ask whether this sequence of vertices in this infinite dimensional space of

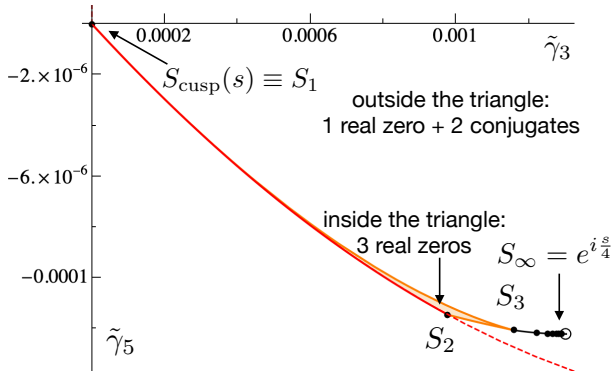

Figure C.4: The triangular area depicted in orange represents the face in the allowed $\{\tilde{\gamma}_3, \tilde{\gamma}_5\}$ region where the three zeros of the S-matrix are real. The three edges of the triangle correspond, respectively, to one single CDD S_1, a double CDD S_2, and a triple CDD zero S_3. The red edge between S_1 and S_2 is the projection of a finite arc of the red edge in fig. 4.1 and correspond to two real distinct CDD zeros. All the S-matrices on the orange edges contain at the same time a double and a single CDD zero. Finally, the interior of the triangle has three CDD zeros all distinct. The unlabeled black dots are the projections of the higher order zeros in (C.24) which converge to $e^{is/4}$.

polyhedra would converge towards anything interesting. Indeed, beautifully, we have

$$\lim_{n\to\infty} S_n = e^{is/4} \tag{C.25}$$

the famous integrable flux tube S-matrix [63, 73]. In practice, already for $n = 3$ on the orange surface we would be very close to $e^{is/4}$ for most values of s. At higher energies we would see deviations. The higher n is in (C.24), the larger is the range in s where the S-matrix is indistinguishable from the integrable flux tube S-matrix.

C.3 Yang-Baxter equation and analytic solution

For massless S-matrices with $O(N)$ symmetry, the Yang-Baxter equation takes the form:

$$S^{cb_2}_{a_2a_3}(\theta_{23}) S^{b_3b_1}_{a_1c}(\theta_{13}) = S^{cb_1}_{a_1a_3}(\theta_{13}) S^{b_3b_2}_{a_2c}(\theta_{23})\,, \tag{C.26}$$

where θ is the rapidity defined by $p_L = -\exp(-\theta)$ for left-movers and $p_R = \exp(\theta)$ for right-movers and $\theta_{ij} \equiv \theta_i - \theta_j$.

In terms of the amplitudes defined by the equation 4.5, this implies the condition $\sigma_1 = \sigma_3 = 0$ for $N > 2$. However for $N = 2$, we have the following relaxed condition:

$$\sigma_3(s) = -\sigma_1(s)\,. \tag{C.27}$$

This is the case for flux tubes in 4 dimensions, where the remnant symmetry of the

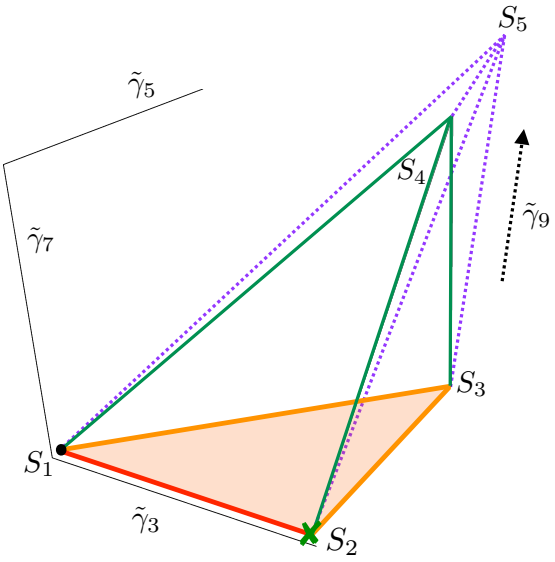

Figure C.5: Schematic representation of the compact region in the allowed $\{\tilde{\gamma}_3, \tilde{\gamma}_5, \tilde{\gamma}_7\}$ space where all the zeros are purely real. In the interior of the tetrahedron there are 4 distinct CDD zeros. As we hit one of the faces two things can happen: two zeros collide becoming a double zero or, as in the case of the orange face (the same shown in figure C.4), one zero goes at infinity. The purple dotted lines are the three-dimensional projections of the edges of the hyper-tetrahedron in the allowed $\{\tilde{\gamma}_3, \tilde{\gamma}_5, \tilde{\gamma}_7, \tilde{\gamma}_9\}$ space: every time we add an extra dimension a higher multiplicity zero cusp appears. Extrapolating to $n \to \infty$ we encounter the $e^{is/4}$ cusp.

goldstone bosons is $O(2)$. In terms of the isospin amplitudes, this implies that $\sigma_{sing} = \sigma_{anti} = \sigma_1 + \sigma_2$ and $\sigma_{sym} = \sigma_2 - \sigma_1$. Moreover, we can make use of the crossing and analyticity relations (4.10) to deduce that

$$\sigma_{sym}(-s^*) = \sigma_{sing}(s)^* = \sigma_{anti}(s)^* \,. \tag{C.28}$$

The symmetric channel S-matrix is bounded by 1 for any $s \in \mathbb{R}$, hence (C.28) now implies that the antisymmetric and the singlet channel amplitudes are also bounded by 1 for $s \in \mathbb{R}$. Under the assumption of integrability, these inequalities are saturated and the isospin amplitudes are a product of CDDs.[1] We therefore consider the following simple ansatz for the solution that satisfies Yang-Baxter:

$$\begin{aligned} \sigma_{sym} &= \frac{(s-a)a^*}{(s-a^*)a} \\ \sigma_{sing} = \sigma_{anti} &= \frac{(s+a^*)a}{(s+a)a^*} \end{aligned} \tag{C.29}$$

where we have used (C.28) to relate the CDD zeroes in the 3 channels. To find the

[1] Any holomorphic function $f(z)$ from the upper half plane $\mathbb{H}$ to the unit disc $\mathbb{D}$ that satisfies $|f(z)| = 1$ for $z \in \mathbb{R}$ must be a product of CDDs.

location of the zero a, we expand the above ansatz at $s = 0$ and match with the low energy expansion (4.2) and we find $a = 8/(32\alpha_2 - i)$. We can also read of the following relation between the α_2 and α_3 coefficients

$$\alpha_3 = -\frac{1}{768} + 4\alpha_2^2 \,. \tag{C.30}$$

Substituting $\alpha_2 = -\frac{22}{384\pi}$, we get $a \approx -3.5 + i6.0$ and

$$\alpha_3 = -\frac{1}{768} + \frac{121}{9216\pi^2} \,, \tag{C.31}$$

which saturates the Schwarz-Pick bound (4.17).

C.4 Numerics

For numerics we parametrize smooth S-matrices as Taylor expansions on the upper half plane or – mapped to the unit disk – as

$$\begin{aligned} \sigma_1(\chi) &= \sum_{n=0}^{N_{max}} (a_n + ib_n)\chi^n \\ \sigma_2(\chi) &= \sum_{n=0}^{N_{max}} c_n\chi^n \\ \sigma_3(\chi) &= \sum_{n=0}^{N_{max}} (a_n - ib_n)\chi^n \end{aligned} \tag{C.32}$$

where real analyticity simply amounts to the statement that the coefficients $\{a_n, b_n, c_n\}$ are real and the χ map was defined in figure 4.2. Given a set $\{a_n, b_n, c_n\}$ we can simply expand the amplitudes close to $s = 0$ (or $\chi = 1$) to read off the threshold parameters (4.2).

As mentioned in the main text, the isospin amplitudes diagonalise unitarity constraints and in the χ disc we have:

$$|\sigma_{rep}(e^{i\theta})| \leq 1 \,, \quad \forall\, \theta \in [0, \pi] \,. \tag{C.33}$$

This is easily imposed as a semi definite constraint: We first divide the range of θ into a grid, and then for a given point on the grid and for each one of the isospin amplitudes, eq. (C.33) is the same as the condition

$$\mathcal{U} \equiv \begin{pmatrix} 1 + \mathcal{R} & \mathcal{I} \\ \mathcal{I} & 1 - \mathcal{R} \end{pmatrix} \succeq 0 \,. \tag{C.34}$$

where $\mathcal{R} = \mathrm{Re}(\sigma_{rep}(e^{i\theta}))$ and $\mathcal{I} = \mathrm{Im}(\sigma_{rep}(e^{i\theta}))$.

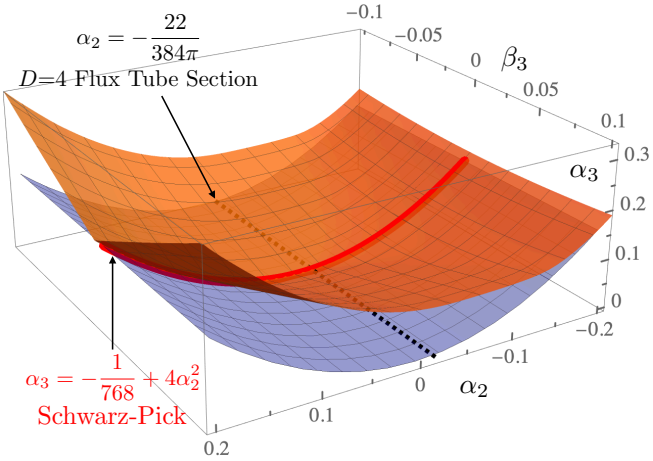

Figure C.6: Allowed region in the generic $\{\alpha_2, \beta_3, \alpha_3\}$ parameter space compatible with $D = 4$ flux tube S-matrices. The light blue surface is given by the Schwarz-Pick bound in the symmetric channel; the orange surface by the numerics. They are tangent along the line $\beta_3 = 0$ (in red) where the S-matrix satisfy Yang-Baxter and is given in appendix C.3. The black dashed line denotes the flux-tube α_2 as predicted by the 1-loop universal $2 \to 2$ scattering.

Experimentally, we find that a Chebyshev grid of points gives the best results and a grid size of around 200 points is sufficient for N_{max} all the way up to 100.

C.4.1 The space of S-matrices compatible with $D = 4$ flux tubes universality

In section 4.2.3 we fixed α_2 to be the universal value predicted by non-linearly realized Poincaré as for flux tube theories. From a general S-matrix perspective it is a legitimate question to first ask about the allowed space of $\{\alpha_2, \beta_3, \alpha_3\}$ parameters and look for any structure pointing to the physical section at fixed α_2. So, the question we ask is: "what is the minimum of α_3 at fixed α_2 and β_3?"

The answer is shown in figure C.6. The orange surface is the numerical minimum bound, the blue surface is the Schwarz-Pick analytic bound (C.30) and the red line is their intersection. The black dashed line denotes the physical section at fixed $\alpha_2 = -\frac{22}{384\pi}$. There is no sign along this general boundary that any value of α_2 plays a special role, except perhaps, $\alpha_2 = 0$: it seems that at fixed $\alpha_2 > 0$ there is a cusp for $\beta_3 = 0$ that becomes smooth as we go to $\alpha_2 < 0$. We do not know the reason for this, since we did not fully explore the features of the S-matrices saturating this minimal surface in general. It would be nice to perform a detailed analysis in the future.

The red line at $\beta_3 = 0$, as explained in Appendix C.3, is saturated by S-matrices satisfying Yang-Baxter and we have analytic solutions for them, see eq. (C.29).

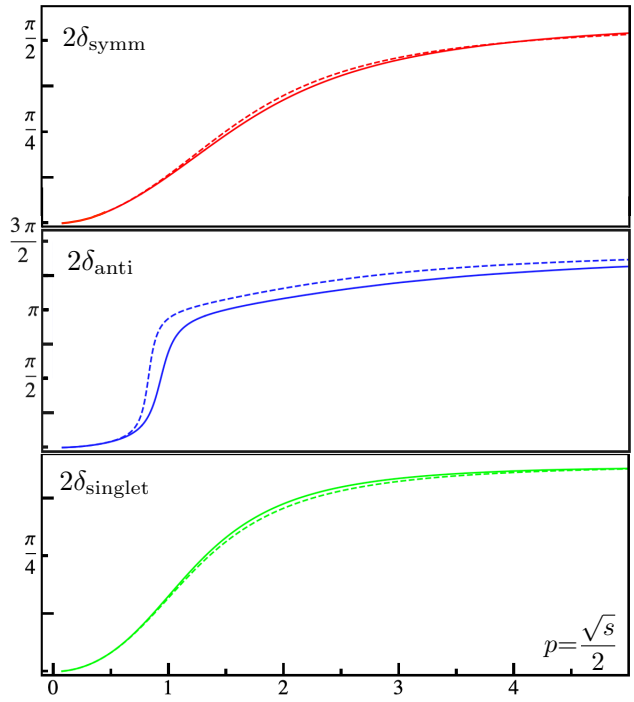

Figure C.7: The phase shifts respectively in the symmetric, antisymmetric and singlet channel at the $SU(3)$ point (solid line) and $SU(5)$ point (dashed line).

C.4.2 Resonances along the boundary at the physical values of α_2.

In figure C.7 we plot the phase of each irrep channel as a function of the momenta – in solid/dashed the $SU(3)/SU(5)$ point S-matrix. These graphs show nice phase-shifts that are characteristic of resonance behaviour. Such phase-shifts are generated by zeros in the complex s-plane, see ref. [5] for a discussion. Measuring zeros in the complex energy plane from experimental or lattice MC data is not an easy task and in general one needs to use dispersive methods to analytically continue the real data to the complex plane; a procedure often plagued by numerical instabilities. Fortunately, we have the full S-matrix in the physical upper half s-plane (or the χ unit disk) and thus we can easily identify the zeros corresponding to the phase-shifts of figure C.7.

For the flux tube value $\alpha_2 = -\frac{22}{384\pi}$, there is a unique S-matrix at each boundary point of the $\{\beta_3, \alpha_3\}$ space shown in figure 4.3. In figure C.8 we show the position of the resonances for the S-matrices in a section of the boundary. The $SU(3)/SU(5)$ benchmark points in the table of sec. 4.4 are denoted with a circle/diamond. The triangle signals the resonances at the integrable point $\beta_3 = 0$. Note that the symmetry $\beta_3 \leftrightarrow -\beta_3$ of the crossing equations introduced in the main text is now visible in the symmetric positions of the resonances in the singlet and antisymmetric channels. The symmetron resonance is invariant under $\beta_3 \leftrightarrow -\beta_3$, hence we only show $\beta_3 > 0$.

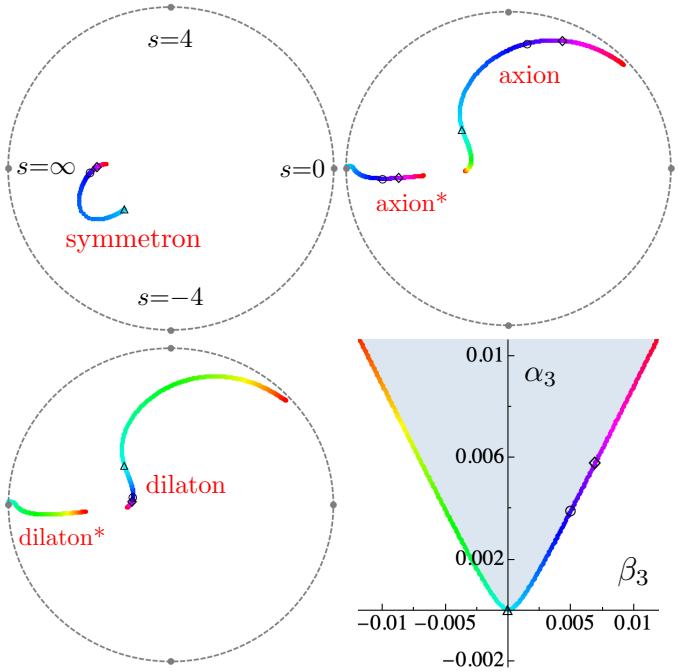

Figure C.8: Zeros trajectory in the unit disk as we move along the boundary of the allowed region in the $\{\alpha_3, \beta_3\}$ space (bottom-right) plot. In each channel we mark with an upper-triangle the zeros at the integrable point, with a circle those at the $SU(3)$ point and with a diamond at the $SU(5)$ point.

C.4.3 Exploring the boundary and the spectrum fixing the axion

The last numerical problem we address in this section is what happens to the spectrum if we fix the experimentally observed world-sheet axion. For instance, we can minimize the value of α_3 at any fixed β_3 and look at the S-matrix optimizing the bound, given the additional condition that $S(s_{\text{axion}}) = 0$. The result when we fix the axion at the $SU(3)$ value is shown in figure C.9.

As we might expect, imposing an additional condition shrinks the allowed space of parameters, but interestingly, while the previous bound was smooth, now there is a kink. Moreover, the resonance spectrum is somehow stable: for any value of β_3 we find an axion*, a dilaton and a symmetron and for the range of β_3 we scanned their position does not vary much. Another game one could play is to fix β_3, α_3 and the axion at the experimentally estimated values and repeat the analysis of the spectrum varying some other higher order parameter or bounding it. We leave this interesting analysis to future explorations.

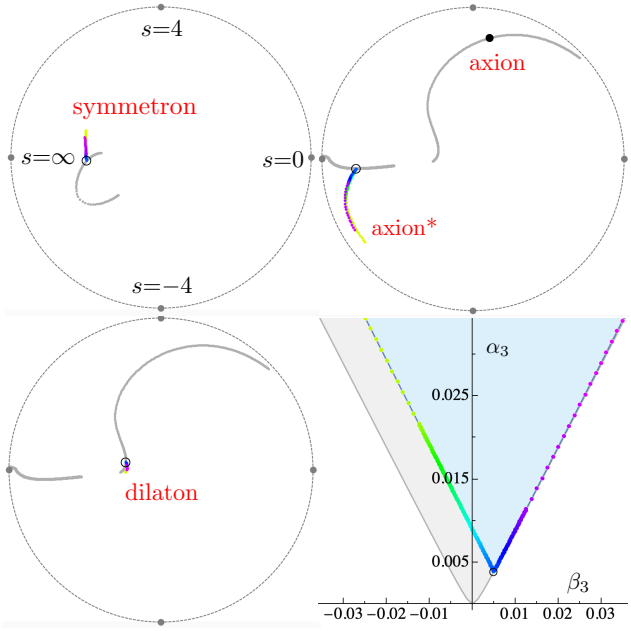

Figure C.9: Zeros trajectory in the unit disk of each irrep S-matrix as we move along the boundary of the allowed region in $\{\beta_3, \alpha_3\}$ parameter space (bottom-right) *at fixed* $SU(3)$ axion as given in tab. 4.4. In gray are the old resonance trajectories without the axion imposed. In the bound figure (bottom-right) we show in gray shades the old smooth boundary: the presence of a fixed resonance sharply cut the allowed region giving rise to a kink at the point where the optimal bound allows to emerge the resonance we fix.

C.4.4 Coupling Q

When a resonance is close to the real energy axis, the phase of the S-matrix jumps by π as it passes close to it. A neat example is given in figure C.7 where there is a clear jump in the phase of the antisymmetric channel when evaluated close to the resonance. To estimate the coupling to the sharp axion resonance we do a "narrow width" approximation

$$S(s)\Big|_{s\sim m_{\rm res}^2} = -\frac{s+s_m-is_\Gamma/2}{s-s_m+is_\Gamma/2} = e^{2i\delta_{\rm res}(s)}\,, \tag{C.35}$$

where the unitarity cuts are neglected and $s_\Gamma = m_{\rm res}\Gamma$. Therefore,

$$\frac{1}{\Gamma} = \sqrt{s}\,\frac{\partial\delta_{\rm res}(s)}{\partial s}\bigg|_{s=m_{\rm res}^2}\,, \tag{C.36}$$

up to terms of $\mathcal{O}(s_\Gamma/s_m)$. From equation (C.36) and the parametrisation of the phase as a function of Q $2\delta_{\rm res}(s)|=\arctan\frac{Q^2s^3}{8(m^2-s)}$ [67,83], we have $\Gamma = m^5Q^2/8$. which is used in section **??**.

C.5 Integrability computations

C.5.1 TBA

When expanding the TBA equation at large radius as discussed in the text we end up with simple integrals to evaluate. In fact, all we need is

$$\int \frac{x^n}{e^x-1} = n!\,\zeta_{n+1} \equiv I_n\,, \tag{C.37}$$

plus two other integrals obtained from this one by integrating by parts:

$$\int x^n \log(1-e^{-x}) = -\frac{I_{n+1}}{n+1}\,,\quad \int \frac{x^n}{(e^x-1)^2} = -nI_{n-1}-I_n\,.$$

Only even zeta's are generated leading to all the π's in the final result (4.26). Expanding to higher orders we find

$$\begin{aligned} E_0 &= \sqrt{R^2-\tfrac{\pi}{3}} - \frac{32\pi^6\gamma_3}{225R^7} - \frac{64\pi^7\gamma_3}{675R^9} - \frac{\frac{2\pi^8\gamma_3}{45}+\frac{32768\pi^{10}\gamma_5}{3969}}{R^{11}} \\ &- \frac{\frac{16384\pi^{11}\gamma_3^2}{4725}+\frac{22\pi^9\gamma_3}{1215}+\frac{32768\pi^{11}\gamma_5}{3969}}{R^{13}} \\ &- \frac{\frac{208384\pi^{12}\gamma_3^2}{50625}+\frac{1001\pi^{10}\gamma_3}{145800}+\frac{26624\pi^{12}\gamma_5}{5103}+\frac{524288\pi^{14}\gamma_7}{225}}{R^{15}} \\ &+ O(R^{-17})\,. \end{aligned} \tag{C.38}$$

For $D=4$ we have two goldstone particles and hence two pseudo-energies and thus a priori, we have two coupled differential equations to solve. Nicely, for the ground state energy they can be reduced to a single equation [67] which differs from the $D=3$ equations (4.24), (4.23) in a few factors of 2 only, precisely stemming from the fact that we have now twice as many goldstone particles:

$$E_0(R) = R + \frac{2}{\pi R}\int_0^\infty dx\, \log(1-e^{-\varepsilon(x)}) \tag{C.39}$$

$$\varepsilon(x) = x + \frac{1}{2\pi}\int_0^\infty \frac{dx'}{x'}\mathcal{K}\log(1-e^{-\varepsilon(x')}), \tag{C.40}$$

$$\mathcal{K} = x'\frac{\partial(\delta_{sym}+\delta_{anti})}{\partial x'} = 2\left(\frac{xx'}{R^2}+3\alpha_3\left(\frac{4xx'}{R^2}\right)^3+\dots\right).$$

Expanding again as in (4.25) and using again the integrals (C.37) leads to an expansion

$$E_0 = R - \frac{\pi}{3R} - \frac{\pi^2}{18R^3} - \frac{\pi^3}{54R^5} - \frac{5\pi^4}{648R^7} - \frac{128\pi^6\alpha_3}{225R^7} + \dots \tag{C.41}$$

perfectly reproducing (4.3) and (4.22).

C.5.2 Level Splitting

Another quantity which is very sensitive to the deviation from universality of the S-matrix low energy parameters is the level splitting between various excited energy levels of the flux tube. In three dimensions, for example, their degeneracy is broken precisely by the non-universal parameter γ_3 so we can translate the bound $\gamma_3 > -1/768$ directly into a bound on how much the levels can split. This is simplest to do in the integrability context where those energy levels are given by a TBA generalization valid for the excited states [106].

Here they simplify quite a lot due to the bosonic nature of the particles (very rare in integrable models) which allows for particles to have the same momenta and also because of the absence of LL and RR scattering in this spontaneous symmetry breaking setup. If we consider N right movers with the same mode number n and N left movers with the same mode number $-n$ then each quanta will have the same momentum $+p/-p$ for right/left movers respectively where p is quantized through a souped up set of Bethe ansatz equations which include finite size corrections and which also yield the ($D = 3$) exited state energy as

$$\begin{aligned} E &= R + 2Np + \int_0^\infty \frac{dx}{\pi R} \log(1 - e^{-\varepsilon(x)}) \\ 2\pi n &= pR + 2N\delta\left(\frac{4p^2}{R^2}\right) + \int_0^\infty \frac{dx}{2\pi x} \mathcal{K}\left(\frac{4px}{R^2}\right) \log(1 - e^{-\varepsilon(x)}), \\ \varepsilon(x) &= x + 2N\delta\left(\frac{4xp}{R^2}\right) + \int_0^\infty \frac{dx'}{2\pi x'} \mathcal{K}\left(\frac{4xx'}{R^2}\right) \log(1 - e^{-\varepsilon(x')}), \end{aligned} \tag{C.42}$$

which can be solved using the ansatz in (4.25) for the pseudo-energy and an ansatz of the form

$$p = \frac{2\pi n}{R} + \frac{p_1}{R^3} + \frac{p_2}{R^5} + \frac{p_3}{R^7} + \mathcal{O}\left(\frac{1}{R^8}\right). \tag{C.43}$$

for the momentum. Note, without the need for any computation, that if the phase shift is linear $\delta(x) \sim x$, as it is for the first few universal terms, then we can rescale p and the corresponding mode number to absorb N completely leading to the above mentioned degeneracy: the energy only depends on $N \times n$ in this case. The breaking of the degeneracy will thus be directly proportional to the first non-universal deviation from the e^{is} S-matrix. The simplest example is (4.27) which upon using our bound implies the upper bound

$$E_{N=2,n=2} - E_{N=4,n=1} \leq \frac{9592\,\pi^6}{15R^7} + O(R^{-9}), \tag{C.44}$$

on the degeneracy of the first two degenerate states.

While a small degeneracy is indeed nicely measured in the lattice, it is unfortunately quite challenging to compare it with this analytic bound. In short, because of all the π's in the expressions above, we need a radius of about $R \sim 10\,\ell_s$ to be able to properly order the terms in the low energy expansion while most lattice data is given up to $R \sim 6\,\ell_s$. It would be very nice to produce larger radius data.

C.6 Perturbative Flux Tube Computations

As explained in 4.3 the strategy that we follow to compute (4.3) consists in organizing the calculation by dividing the action (4.1) into two pieces

$$A = A_{\text{int}} + A_{\not{int}}\,. \tag{C.45}$$

A_{int} produces an integrable S-matrix up to $O(s^3)$. This S-matrix is fed into the TBA, which returns the universal part of $E_0(R)$. The piece $A_{\not{int}}$ consists of the leading order breaking of integrability. In particular, this invovles the leading non-universal operators – see below for a clarification. We work at leading order in perturbation theory with the integrability breaking piece $A_{\not{int}}$. Thus, the leading order non-universal contribution to the vacuum energy density is


$$= \frac{32\pi^6(2-D)((D-2)\alpha_3+(D-4)\beta_3)}{225R^8}\,, \tag{C.46}$$

after regularizing out the zero mode.

Before closing this section we must explain two effects that we have glossed over. First, recall that the low energy universality of the NG theory implies that all the one-loop leading order scattering amplitudes are universal. In particular, the one-loop $2 \to 4$ processes are non-zero away from $D = 3, 26$. Interestingly, this implies that, in the absence of further massless degrees of freedom, the NG theory is not integrable away from $D = 3, 26$ [74]. These one-loop six-point amplitudes can be reproduced with the following local operator

$$(\partial_\mu\partial_\nu X^i)^2\left[(\partial_\rho X^j)^4 - \frac{1}{2}\partial_\rho X^j\partial_\sigma X^j\partial^\rho X^k\partial_\sigma X^k\right], \tag{C.47}$$

where the overall normalization is unimportant for our purposes. Generically, (C.47) implies $O(1/R^7)$ deviations from the finite volume spectrum associated to the integrable S-matrix in appendix C.5.1. Indeed, (C.47) is added in A_{int} and subtracted in $A_{\not{int}}$. For the vacuum energy density, we must compute a single insertion of (C.47)

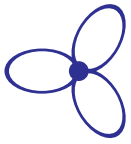
$$= \partial_\nu\partial_\alpha\partial_\beta\Delta_R(0)\,\partial_\nu\partial_\gamma\partial_\beta\Delta_R(0)\,\partial_\alpha\partial_\gamma\Delta_R(0) = 0\,,$$

where we omitted the symmetry factor. Given that the latter diagram vanishes, we conclude that at $O(1/R^7)$ the vacuum energy is insensitive to (C.47) and therefore the unique deviation from the square root formula at $O(1/R^7)$ is given by (C.46).

In $D = 3$, the presence of the leading non-universal operator induces $2 \to 4$ particle production at $O(\ell_s^8 s^5)$ in the M-matrix element [76]. Therefore, one could expect an $O(1/R^9)$ contribution to the vacuum energy from this process. However, similarly to (C.47), this process can be reproduced by a local operator $(\partial_\mu \partial_\nu X)^2 (\partial_\rho X)^2$ that has a vanishing vacuum expectation value at finite volume.

The second effect is about the Einstein-Hilbert operator $\mathcal{R}$ introduced in **??**. It is an evanescent operator, i.e. its contribution to the tree-level S-matrix vanishes for $d = 2$ world-sheet spacetime dimensions; but, when dressed with virtual corrections in dimensional regularization, gives a non-zero contribution to the S-matrix. Its presence is needed for a consistent one-loop renormalization of the NG theory. Thus $\mathcal{R}$ appears as a $1/\epsilon + \omega_3$ counter-term in dimensional regularization [63], where ω_3 is a finite non-universal choice for the counter-term. At $O(s^3)$ the $2 \to 2$ S-matrix of the renormalized NG theory involves two-loop Feynman diagrams from the NG vertices $\sqrt{-\det \partial_\alpha X^\mu \partial_\beta X_\mu}$ and one loop diagrams with a single insertion of the $\mathcal{R}$ and NG vertices. A priori, one could expect that ω_3 together with the constants α_3 and β_3 in (4.19) make up a triad of possible non-universal deformations at $O(s^3)$. However, the $O(s^3)$ contribution of ω_3 is analytic and thus can be absorbed in the $K^4 = O(\partial^8 X^4)$ operators, i.e. in a shift of the $\{\alpha_3, \beta_3\}$ parameters [75].

C.7 Axionic String Ansatz: no resonances

Here we elaborate further on the analysis of 4.2.2, by assuming that there are no resonances on the $D = 3$ flux tube, namely the Axionic String Ansatz (ASA) [83]. If there are no resonances, then the phase shift $\delta(s) = \frac{1}{2i} \log S(s)$ is analytic in the upper half plane. Let us derive a dispersion relation for the phase shift. We start from the identity

$$\frac{2\delta(s) - \frac{s}{4}}{s^2} = \oint_s \frac{dz}{2\pi i} \left[\frac{1}{z - s} - \frac{1}{z + s} \right] \frac{2\delta(z) - \frac{z}{4}}{z^2} \tag{C.48}$$

where the contour goes around s in the upper half plane. Assuming that $\delta(s)/s^3 \to 0$ for $|s| \to \infty$ in the upper half plane, we can open the contour to the real axis to obtain

$$2\delta(s) = \frac{s}{4} + \frac{2s^3}{\pi} \int_{-\infty}^{\infty} dz \frac{\mathrm{Im}\, \delta(z)}{z^2 (z^2 - s^2)} \tag{C.49}$$

This gives

$$\gamma_3/\gamma_7 = \langle z^4 \rangle \,, \quad \gamma_5/\gamma_7 = \langle z^2 \rangle \tag{C.50}$$

with

$$\langle z^n \rangle = \int_{-\infty}^{\infty} dz\, \rho(z) z^n\,, \qquad \rho(z) = \frac{2}{\pi\gamma_7} \frac{\operatorname{Im}\delta(z)}{z^8}\,. \tag{C.51}$$

Notice that $\rho(z) = \rho(-z)$ is a non-negative normalized distribution $\int dz\, \rho(z) = 1$. Therefore, we conclude the

$$\gamma_3, \gamma_5, \gamma_7 \geq 0\,. \tag{C.52}$$

Furthermore the large s behavior of the phase shift is given by

$$2\delta(s) = \left(\frac{1}{4} - \gamma_7 \langle z^6 \rangle\right) s + \dots \tag{C.53}$$

Causality allows for a time-delay but not a time advance. This implies that the coefficient of the linear term in s at high energies must be positive [73, 107]. In other words,

$$\ell_{UV}^2 = \ell_s^2 \left(1 - 4\gamma_7 \langle z^6 \rangle\right) > 0\,. \tag{C.54}$$

We can derive more inequalities. Firstly,

$$\left\langle \left(z^2 - \langle z^2 \rangle\right)^2 \right\rangle \geq 0 \Rightarrow \gamma_3\gamma_7 \geq \gamma_5^2 \tag{C.55}$$

Secondly,

$$\left\langle z^2 \left(z^2 - \langle z^2 \rangle\right)^2 \right\rangle \geq 0 \Rightarrow \langle z^6 \rangle \geq 2\langle z^4 \rangle \langle z^2 \rangle - \langle z^2 \rangle^3 \tag{C.56}$$

together with $\langle z^6 \rangle \leq \frac{1}{4\gamma_7}$, leads to

$$\gamma_7^2 \geq 4\gamma_5(2\gamma_3\gamma_7 - \gamma_5^2)\,. \tag{C.57}$$

These give an upper and lower bound on γ_3,

$$\frac{\gamma_5^2}{\gamma_7} \leq \gamma_3 \leq \frac{\gamma_7^2 + 4\gamma_5^3}{8\gamma_5\gamma_7}\,. \tag{C.58}$$

This must fit inside the allowed region in figure 4.1. Notice that the new region has an edge where the upper and lower bounds coincide,

$$\gamma_7^2 = 4\gamma_5^3 = 4\gamma_3\gamma_5\gamma_7\,. \tag{C.59}$$

At this edge, $\ell_{UV} = 0$ because

$$\int_{-\infty}^{\infty} dz \frac{\operatorname{Im}\delta(z)}{z^2} = \frac{\pi}{8} \tag{C.60}$$

and the distribution is delta-function type,

$$\rho(z) = \frac{1}{2}\delta(z - z_0) + \frac{1}{2}\delta(z + z_0)$$

where $4\gamma_7 z_0^6 = 1$.

Can we confirm or disprove the ASA? In principle, the ASA can be disproved if one measures low energy constants $\gamma_3, \gamma_5, \ldots$ incompatible with the constraints (C.52) or (C.58). Currently, the available estimate $\gamma_3 \approx 3 \times 10^{-4}$ (from lattice data for $SU(6)$ YM [67,76,77]) is compatible with the ASA.

D Appendices to glueball-branon bootstrap

D.1 Derivation of the unitarity equations

D.1.1 Phase space integrals

We will first compute two phase space integrals: two branon phase space $\rho_{bb}(s)$ and the one glueball phase space $\rho_g(s)$.

Two branon phase-space

$$\rho_{bb}(s) = \int \frac{1}{2}\frac{dp_5}{2|p_5|}\frac{dp_6}{2|p_6|}\delta^{(2)}(\mathcal{P}^a - p_5^a - p_6^a) \tag{D.1}$$

Note that $\mathcal{P}$ is the total momentum. Due to Lorentz invariance, the above integral only depends on $s = \mathcal{P}^2$. Therefore, to evaluate the integral, we choose to go to the center of mass frame where $\mathcal{P} = (\sqrt{s}, 0)$, which gives the integral:

$$\begin{aligned}\rho_{bb}(s) &= \int \frac{1}{2}\frac{dp_5}{2|p_5|}\frac{dp_6}{2|p_6|}\delta(p_5 - p_6)\delta(\sqrt{s} - |p_5| - |p_6|) \\ &= \int \frac{1}{2}\frac{dp_6}{(2|p_6|)^2}\delta(\sqrt{s} - 2|p_6|)\end{aligned} \tag{D.2}$$

There are two solutions: $p_6 = \pm\frac{\sqrt{s}}{2}$ and we also get a factor of $\frac{1}{2}$ since $\delta(\lambda x) = \frac{\delta(x)}{\lambda}$. Thus we get our result:

$$\rho_{bb}(s) = \frac{1}{2s} \tag{D.3}$$

One glueball phase-space

$$\rho_g(s) = \int \frac{dp_5 dq_5}{2(p_5^2 + q_5^2 + m^2)^{1/2}}\delta^{(2)}(\mathcal{P}^a - p_5^a) \tag{D.4}$$

where once again, Lorentz invariance implies that it is just a function of $s = \mathcal{P}^2$. We go to the center of mass frame $\mathcal{P} = (\sqrt{s}, 0)$, which gives the integral:

$$\begin{aligned}\rho_g(s) &= \int \frac{dp_5 dq_5}{2(p_5^2+q_5^2+m^2)^{1/2}}\delta(p_5)\delta\left(\sqrt{s}-\sqrt{p_5^2+q_5^2+m^2}\right)\\ &= \int \frac{dq_5}{2(q_5^2+m^2)^{1/2}}\delta\left(\sqrt{s}-\sqrt{q_5^2+m^2}\right)\end{aligned} \tag{D.5}$$

In this case $q_5 \geq 0$ and hence there is only one solution $q_5 = \sqrt{s-m^2}$ and since $\delta(f(x)) = \sum_i \frac{\delta(x-x_i)}{f'(x_i)}$ (where x_i are the zeroes of f), we have

$$\rho_g(s) = \frac{1}{2\sqrt{s-m^2}} \tag{D.6}$$

D.1.2 Unitarity equation for branon-branon scattering

We begin with the equation $-i(T - T^\dagger) = T^\dagger T$, and taking matrix elements between two particle branon states:

$$-i\langle p_3, p_4|T - T^\dagger|p_1, p_2\rangle = \langle p_3, p_4|T^\dagger T|p_1, p_2\rangle \tag{D.7}$$

Using the definition 5.6, we see that left hand side is proportional to Im $M(s)$:

$$-i\langle p_3, p_4|T - T^\dagger|p_1, p_2\rangle = (2\pi)^2\delta^{(2)}(p_1^a + p_2^a - p_3^a - p_4^a)\ 2\ \text{Im}\ M(s) \tag{D.8}$$

while on the right hand side we plug in a complete set of states to get:

$$\begin{aligned}\langle p_3, p_4|T^\dagger T|p_1, p_2\rangle &= \int d\Pi_{bb}\langle p_3, p_4|T^\dagger|p_5, p_6\rangle\langle p_5, p_6|T|p_1, p_2\rangle\\ &+ \Theta(s-m^2)\int d\Pi_g\langle p_3, p_4|T^\dagger|m, p_5, q_5, +\rangle\langle m, p_5, q_5, +|T|p_1, p_2\rangle\\ &+ \text{contributions from other states}\end{aligned} \tag{D.9}$$

where $d\Pi_{bb} = \frac{1}{2}\frac{dp_5}{(2\pi)2|p_5|}\frac{dp_6}{(2\pi)2|p_6|}$ and $d\Pi_g = \frac{dp_5 dq_5}{(2\pi)^2 2(p_5^2+q_5^2+M^2)^{1/2}}$. Note that q_5 only runs from 0 to ∞. The Θ function appears because glueball intermediate states are only possible for $s \geq m^2$.

Consider the first term, due to momentum conservation we get the delta function factors $\delta^{(2)}(p_1^a + p_2^a - p_5^a - p_6^a) \times \delta^{(2)}(p_3^a + p_4^a - p_5^a - p_6^a)$. On the support of these delta functions, we can replace them with $\delta^{(2)}(p_1^a + p_2^a - p_5^a - p_6^a) \times \delta^{(2)}(p_1^a + p_2^a - p_3^a - p_4^a)$. Moreover, in $2D$, momentum conservation implies that p_5^a and p_6^a are permutations of p_1^a and p_2^a, hence we also get $[M(s)]^* M(s)$. The remaining integral gives $\rho_{bb}(s)$. Putting these together,

we may write the first term as:

$$\int d\Pi_{bb}\langle p_3, p_4|T^\dagger|p_5, p_6\rangle\langle p_5, p_6|T|p_1, p_2\rangle = (2\pi)^2\delta^{(2)}(p_1^a + p_2^a - p_3^a - p_4^a) \times\rho_{bb}(s)[M(s)]^* M(s) \quad \text{(D.10)}$$

We now go back to the second term in equation D.9, once again by momentum conservation, we can pull out a factor $\delta^{(2)}(p_1^a + p_2^a - p_3^a - p_4^a)$, the remaining integral gives $\rho_g(s)$ and hence we have:

$$\int d\Pi_g\langle p_3, p_4|T^\dagger|m, p_5, q_5\rangle\langle m, p_5, q_5|T|p_1, p_2\rangle = (2\pi)^2\delta^{(2)}(p_1^a + p_2^a - p_3^a - p_4^a) \times\rho_g(s)[F(s)]^* F(s) \quad \text{(D.11)}$$

Thus by putting all these together,

$$2 \text{ Im } M(s) = \frac{1}{2s}|M(s)|^2 + \frac{1}{2\sqrt{s-m^2}}|F(s)|^2\Theta(s-m^2) + ... \quad \text{(D.12)}$$

D.1.3 Unitarity equation for glueball-glueball scattering

Once again we begin with the equation $-i(T - T^\dagger) = T^\dagger T$, but this time we take matrix elements between two 1-particle glueball states:

$$-i\langle m, p_2, q_2, +|T - T^\dagger|m, p_1, q_1, +\rangle = \langle m, p_2, q_2, +|T^\dagger T|m, p_1, q_1, +\rangle \quad \text{(D.13)}$$

Using equation 5.7, we can write the left hand side as:

$$-i\langle m, p_2, q_2, +|T - T^\dagger|m, p_1, q_1, +\rangle = (2\pi)^2\delta^{(2)}(p_1^a - p_2^a)\ 2 \text{ Im } G(s) \quad \text{(D.14)}$$

To evaluate the right hand side, we plug in a complete set of states to get:

$$\begin{aligned}\langle m, p_2, q_2, +|T^\dagger T|m, p_1, q_1, +\rangle &= \int d\Pi_{bb}\langle m, p_2, q_2, +|T^\dagger|p_5, p_6\rangle\langle p_5, p_6|T|m, p_1, q_1, +\rangle \\ &+ \Theta(s-m^2)\int d\Pi_g\langle m, p_2, q_2, +|T^\dagger|m, p_5, q_5, +\rangle \\ &\qquad \times\langle m, p_5, q_5, +|T|m, p_1, q_1, +\rangle \\ &+ \text{contributions from other states} \quad \text{(D.15)}\end{aligned}$$

Consider the first term, momentum conservation leads to $\delta^{(2)}(p_1^a - p_5^a - p_6^a) \times \delta^{(2)}(p_2^a - p_5^a - p_6^a)$ which can be rewritten as $\delta^{(2)}(p_1^a - p_2^a) \times \delta^{(2)}(p_1^a - p_5^a - p_6^a)$. The remaining

integral is precisely $\rho_{bb}(s)$ and we have:

$$\int d\Pi_{bb}\langle m,p_2,q_2,+|T^\dagger|p_5,p_6\rangle\langle p_5,p_6|T|m,p_1,q_1,+\rangle = (2\pi)^2\delta^{(2)}(p_1^a-p_2^a) \times\rho_{bb}(s)[F(s)]^*F(s) \quad \text{(D.16)}$$

Similarly, upon considering the second term, momentum conservation leads to a $\delta^{(2)}(p_1^a-p_2^a)$ factor, while the remaining integral gives $\rho_g(s)$ and hence we have:

$$\int d\Pi_g\langle m,p_2,q_2,+|T^\dagger|m,p_5,q_5,+\rangle\langle m,p_5,q_5,+|T|m,p_1,q_1,+\rangle = (2\pi)^2\delta^{(2)}(p_1^a-p_2^a) \times\rho_g(s)[G(s)]^*G(s) \quad \text{(D.17)}$$

Putting all the pieces together, we have:

$$2\ \text{Im}\ G(s) = \frac{1}{2\sqrt{s-m^2}}|G(s)|^2\Theta(s-m^2)+\frac{1}{2s}|F(s)|^2+... \quad \text{(D.18)}$$

D.1.4 Unitarity equation for glueball-branon scattering

Once again we begin with the equation $-i(T-T^\dagger)=T^\dagger T$, and take matrix elements between two particle branon state and a glueball state:

$$-i\langle m,p_3,q_3,+|T-T^\dagger|p_1,p_2\rangle = \langle m,p_3,q_3,+|T^\dagger T|p_1,p_2\rangle \quad \text{(D.19)}$$

Using equations 5.8 and 5.9, the left hand side becomes:

$$-i\langle m,p_3,q_3,+|T-T^\dagger|p_1,p_2\rangle = (2\pi)^2\delta^{(2)}(p_1^a+p_2^a-p_3^a)\ 2\ \text{Im}\ F(s) \quad \text{(D.20)}$$

To evaluate the right hand side, we plug in a complete set of states to get:

$$\begin{aligned}\langle m,p_3,q_3,+|T^\dagger T|p_1,p_2\rangle &= \int d\Pi_{bb}\langle m,p_3,q_3,+|T^\dagger|p_5,p_6\rangle\langle p_5,p_6|T|p_1,p_2\rangle \\ &+ \Theta(s-m^2)\int d\Pi_g\langle m,p_3,q_3,+|T^\dagger|m,p_5,q_5,+\rangle \\ &\qquad\times\langle m,p_5,q_5,+|T|p_1,p_2\rangle \\ &+ \text{contributions from other states} \quad \text{(D.21)}\end{aligned}$$

Following the same procedure as before, for each term we can pull out a momentum preserving delta function and the remaining part becomes the respective phase space integral. In other words we have

$$\int d\Pi_{bb}\langle m,p_3,q_3,+|T^\dagger|p_5,p_6\rangle\langle p_5,p_6|T|p_1,p_2\rangle = (2\pi)^2\delta^{(2)}(p_1^a+p_2^a-p_3^a) \times\rho_{bb}(s)[F(s)]^*M(s) \quad \text{(D.22)}$$

and

$$\int d\Pi_g \langle m, p_3, q_3, +|T^\dagger|m, p_5, q_5, +\rangle \langle m, p_5, q_5, +|T|p_1, p_2\rangle = (2\pi)^2 \delta^{(2)}(p_1^a + p_2^a - p_3^a) \times \rho_g(s)[G(s)]^* F(s) \tag{D.23}$$

Therefore we have

$$2 \text{ Im } F(s) = \frac{1}{2\sqrt{s-m^2}} G^*(s) F(s) \Theta(s-m^2) + \frac{1}{2s} F^*(s) M(s) + ... \tag{D.24}$$

D.2 Perturbative amplitudes

Consider the following Action

$$\mathcal{S} = \frac{1}{2}\int d^3x \left[(\nabla\phi)^2 - m^2\right] + \frac{1}{2}\int d^2x (\partial\pi)^2 + \frac{\lambda}{2\sqrt{m}}\int d^2x \phi (\partial\pi)^2 \tag{D.25}$$

where ϕ is the glueball field in 3D and π is the branon field on the flux tube. We couple the two via the term proportional to λ. Our objective here is to only derive tree level amplitudes and try to get a feel for the $s = 0$ expansion of the amplitudes. The Feynman rules are:

- Glueball propagator: $\frac{i}{p^2+q^2-m^2}$
- Branon progator: $\frac{i}{p^2}$
- Vertex: $i\frac{\lambda}{\sqrt{m}} p_1.p_2$, (here p_1 and p_2 are momenta of the branon)

We can now compute the branon-branon amplitude M, the glueball-glueball amplitude G and the glueball-branon amplitude F. We get at leading order

$$M(s) = \frac{\lambda^2}{16m\sqrt{s-m^2}} s^2 \tag{D.26}$$

$$F(s) = \frac{\lambda}{2\sqrt{m}} s \tag{D.27}$$

$$G(s) = -\frac{\lambda^2}{16\pi m} s \left(\frac{8}{3} - \log s\right) \tag{D.28}$$

Of course the Lagrangian was not reparametrization invariant. It would be interesting to start with a reparametrization invariant coupling say $\sqrt{g}\phi$ and compute the amplitudes to leading order in perturbation theory.

Bibliography

[1] R. J. Eden, P. V. Landshoff, D. I. Olive and J. C. Polkinghorne, *The analytic S-matrix*. Cambridge Univ. Press, Cambridge, 1966.

[2] M. F. Paulos, J. Penedones, J. Toledo, B. C. van Rees and P. Vieira, *The S-matrix bootstrap. Part I: QFT in AdS*, *JHEP* **11** (2017) 133, [1607.06109].

[3] M. F. Paulos, J. Penedones, J. Toledo, B. C. van Rees and P. Vieira, *The S-matrix bootstrap II: two dimensional amplitudes*, *JHEP* **11** (2017) 143, [1607.06110].

[4] M. F. Paulos, J. Penedones, J. Toledo, B. C. van Rees and P. Vieira, *The S-matrix Bootstrap III: Higher Dimensional Amplitudes*, 1708.06765.

[5] N. Doroud and J. Elias Miró, *S-matrix bootstrap for resonances*, *JHEP* **09** (2018) 052, [1804.04376].

[6] Y. He, A. Irrgang and M. Kruczenski, *A note on the S-matrix bootstrap for the 2d O(N) bosonic model*, *JHEP* **11** (2018) 093, [1805.02812].

[7] L. Córdova and P. Vieira, *Adding flavour to the S-matrix bootstrap*, *JHEP* **12** (2018) 063, [1805.11143].

[8] A. L. Guerrieri, J. Penedones and P. Vieira, *Bootstrapping QCD Using Pion Scattering Amplitudes*, *Phys. Rev. Lett.* **122** (2019) 241604, [1810.12849].

[9] A. Homrich, J. a. Penedones, J. Toledo, B. C. van Rees and P. Vieira, *The S-matrix Bootstrap IV: Multiple Amplitudes*, *JHEP* **11** (2019) 076, [1905.06905].

[10] J. Elias Miró, A. L. Guerrieri, A. Hebbar, J. a. Penedones and P. Vieira, *Flux Tube S-matrix Bootstrap*, *Phys. Rev. Lett.* **123** (2019) 221602, [1906.08098].

[11] L. Córdova, Y. He, M. Kruczenski and P. Vieira, *The O(N) S-matrix Monolith*, *JHEP* **04** (2020) 142, [1909.06495].

[12] C. Bercini, M. Fabri, A. Homrich and P. Vieira, *S-matrix bootstrap: Supersymmetry, Z_2, and Z_4 symmetry*, *Phys. Rev. D* **101** (2020) 045022, [1909.06453].

[13] D. Karateev, S. Kuhn and J. a. Penedones, *Bootstrapping Massive Quantum Field Theories*, *JHEP* **07** (2020) 035, [1912.08940].

[14] M. Correia, A. Sever and A. Zhiboedov, *An Analytical Toolkit for the S-matrix Bootstrap*, 2006.08221.

[15] A. Bose, P. Haldar, A. Sinha, P. Sinha and S. S. Tiwari, *Relative entropy in scattering and the S-matrix bootstrap*, 2006.12213.

[16] H. Lehmann, K. Symanzik and W. Zimmermann, *On the formulation of quantized field theories*, *Nuovo Cim.* **1** (1955) 205–225.

[17] S. Weinberg, *The Quantum theory of fields. Vol. 1: Foundations*. Cambridge University Press, 2005.

[18] F. Kos, D. Poland, D. Simmons-Duffin and A. Vichi, *Precision Islands in the Ising and $O(N)$ Models*, *JHEP* **08** (2016) 036, [1603.04436].

[19] D. Poland, S. Rychkov and A. Vichi, *The Conformal Bootstrap: Theory, Numerical Techniques, and Applications*, *Rev. Mod. Phys.* **91** (2019) 015002, [1805.04405].

[20] A. Adams, N. Arkani-Hamed, S. Dubovsky, A. Nicolis and R. Rattazzi, *Causality, analyticity and an IR obstruction to UV completion*, *JHEP* **10** (2006) 014, [hep-th/0602178].

[21] L. Vecchi, *Causal versus analytic constraints on anomalous quartic gauge couplings*, *JHEP* **11** (2007) 054, [0704.1900].

[22] A. V. Manohar and V. Mateu, *Dispersion Relation Bounds for pi pi Scattering*, *Phys. Rev. D* **77** (2008) 094019, [0801.3222].

[23] A. Nicolis, R. Rattazzi and E. Trincherini, *Energy's and amplitudes' positivity*, *JHEP* **05** (2010) 095, [0912.4258].

[24] B. Bellazzini, C. Cheung and G. N. Remmen, *Quantum Gravity Constraints from Unitarity and Analyticity*, *Phys. Rev. D* **93** (2016) 064076, [1509.00851].

[25] C. Cheung and G. N. Remmen, *Positive Signs in Massive Gravity*, *JHEP* **04** (2016) 002, [1601.04068].

[26] B. Bellazzini, *Softness and amplitudes' positivity for spinning particles*, *JHEP* **02** (2017) 034, [1605.06111].

[27] C. de Rham, S. Melville, A. J. Tolley and S.-Y. Zhou, *Positivity bounds for scalar field theories*, *Phys. Rev. D* **96** (2017) 081702, [1702.06134].

[28] C. de Rham, S. Melville, A. J. Tolley and S.-Y. Zhou, *UV complete me: Positivity Bounds for Particles with Spin*, *JHEP* **03** (2018) 011, [1706.02712].

[29] C. de Rham, S. Melville, A. J. Tolley and S.-Y. Zhou, *Positivity Bounds for Massive Spin-1 and Spin-2 Fields*, *JHEP* **03** (2019) 182, [1804.10624].

[30] N. Arkani-Hamed, *Lectures at the CERN Winter School on Supergravity, Strings and Gauge Theory 2019*, .

[31] B. Bellazzini, J. Elias Miró, R. Rattazzi, M. Riembau and F. Riva, *Positive Moments for Scattering Amplitudes*, 2011.00037.

[32] A. J. Tolley, Z.-Y. Wang and S.-Y. Zhou, *New positivity bounds from full crossing symmetry*, 2011.02400.

[33] S. Caron-Huot and V. Van Duong, *Extremal Effective Field Theories*, 2011.02957.

[34] S. Hellerman and I. Swanson, *String Theory of the Regge Intercept*, *Phys. Rev. Lett.* **114** (2015) 111601, [1312.0999].

[35] A. Sever and A. Zhiboedov, *On Fine Structure of Strings: The Universal Correction to the Veneziano Amplitude*, *JHEP* **06** (2018) 054, [1707.05270].

[36] J. Bros, H. Epstein and V. Glaser, *A proof of the crossing property for two-particle amplitudes in general quantum field theory*, *Commun. Math. Phys.* **1** (1965) 240–264.

[37] S. Mizera, *Crossing Symmetry in the Planar Limit*, 2104.12776.

[38] G. Sommer, *Present state of rigorous analytic properties of scattering amplitudes*, *Fortsch. Phys.* **18** (1970) 577–688.

[39] H. Lehmann, *Analytic properties of scattering amplitudes as functions of momentum transfer*, *Nuovo Cim.* **10** (1958) 579–589.

[40] J. Bros, H. Epstein and V. J. Glaser, *Some rigorous analyticity properties of the four-point function in momentum space*, *Nuovo Cim.* **31** (1964) 1265–1302.

[41] S. Mandelstam, *Some rigorous analytic properties of transition amplitudes*, *Il Nuovo Cimento* **15** 658—-685.

[42] A. Martin, *Extension of the axiomatic analyticity domain of scattering amplitudes by unitarity. 1.*, *Nuovo Cim. A* **42** (1965) 930–953.

[43] D. Simmons-Duffin, *A Semidefinite Program Solver for the Conformal Bootstrap*, *JHEP* **06** (2015) 174, [1502.02033].

[44] A. D. Martin and T. D. Spearman, *Elementary-particle theory*. North-Holland, Amsterdam, 1970.

[45] E. Majorana, *Teoria simmetrica dell'elettrone e del positrone*, *Nuovo Cim.* **14** (1937) 171–184.

[46] W. K. Tung, *Group Theory in Physics*. 1985.

[47] T. Trueman and G. Wick, *Crossing Relations for Helicity Amplitudes for Helicity Amplitudes*, *Annals Phys.* **26** (1964) 332.

[48] Y. Hara, *On crossing relations for helicity amplitudes*, *J. Math. Phys.* **11** (1970) 253–257.

[49] Y. Hara, *Crossing relations for helicity amplitudes*, *Prog. Theor. Phys.* **45** (1971) 584–595.

[50] M. S. Costa, J. Penedones, D. Poland and S. Rychkov, *Spinning Conformal Correlators*, *JHEP* **11** (2011) 071, [1107.3554].

[51] P. Kravchuk and D. Simmons-Duffin, *Counting Conformal Correlators*, *JHEP* **02** (2018) 096, [1612.08987].

[52] A. Dymarsky, *On the four-point function of the stress-energy tensors in a CFT*, *JHEP* **10** (2015) 075, [1311.4546].

[53] D. Karateev, P. Kravchuk, M. Serone and A. Vichi, *Fermion Conformal Bootstrap in 4d*, *JHEP* **06** (2019) 088, [1902.05969].

[54] A. Edmonds, *Angular momentum in quantum mechanics*, .

[55] V. Gribov and D. Volkov, *Regge poles in the amplitudes of nucleon-nucleon and nucleon-antinucleon scattering*, *Sov. Phys. JETP* **17** (1963) 720–725.

[56] H. K. Dreiner, H. E. Haber and S. P. Martin, *Two-component spinor techniques and Feynman rules for quantum field theory and supersymmetry*, *Phys. Rept.* **494** (2010) 1–196, [0812.1594].

[57] S. Mandelstam, *Analytic properties of transition amplitudes in perturbation theory*, *Phys. Rev.* **115** (1959) 1741–1751.

[58] W. Landry and D. Simmons-Duffin, *Scaling the semidefinite program solver SDPB*, 1909.09745.

[59] A. Manohar and H. Georgi, *Chiral Quarks and the Nonrelativistic Quark Model*, *Nucl. Phys. B* **234** (1984) 189–212.

[60] E. E. Jenkins, A. V. Manohar and M. Trott, *Naive Dimensional Analysis Counting of Gauge Theory Amplitudes and Anomalous Dimensions*, *Phys. Lett. B* **726** (2013) 697–702, [1309.0819].

[61] C. Itzykson and J. B. Zuber, *Quantum Field Theory*. International Series In Pure and Applied Physics. McGraw-Hill, New York, 1980.

[62] C. Cheung and G. N. Remmen, *Infrared Consistency and the Weak Gravity Conjecture*, *JHEP* **12** (2014) 087, [1407.7865].

[63] S. Dubovsky, R. Flauger and V. Gorbenko, *Effective String Theory Revisited*, *JHEP* **09** (2012) 044, [1203.1054].

[64] O. Aharony and Z. Komargodski, *The Effective Theory of Long Strings*, *JHEP* **05** (2013) 118, [1302.6257].

[65] M. Luscher and P. Weisz, *String excitation energies in SU(N) gauge theories beyond the free-string approximation*, *JHEP* **07** (2004) 014, [hep-th/0406205].

[66] S. Dubovsky, R. Flauger and V. Gorbenko, *Evidence from Lattice Data for a New Particle on the Worldsheet of the QCD Flux Tube*, *Phys. Rev. Lett.* **111** (2013) 062006, [1301.2325].

[67] S. Dubovsky, R. Flauger and V. Gorbenko, *Flux Tube Spectra from Approximate Integrability at Low Energies*, *J. Exp. Theor. Phys.* **120** (2015) 399–422, [1404.0037].

[68] M. Teper, *Large N and confining flux tubes as strings - a view from the lattice*, *Acta Phys. Polon.* **B40** (2009) 3249–3320, [0912.3339].

[69] A. Athenodorou and M. Teper, *Closed flux tubes in D = 2 + 1 SU(N) gauge theories: dynamics and effective string description*, *JHEP* **10** (2016) 093, [1602.07634].

[70] A. Athenodorou, B. Bringoltz and M. Teper, *Closed flux tubes and their string description in D=3+1 SU(N) gauge theories*, *JHEP* **02** (2011) 030, [1007.4720].

[71] A. Athenodorou and M. Teper, *On the mass of the world-sheet 'axion' in $SU(N)$ gauge theories in 3+1 dimensions*, *Phys. Lett.* **B771** (2017) 408–414, [1702.03717].

[72] P. Fendley, H. Saleur and A. B. Zamolodchikov, *Massless flows, 2. The Exact S matrix approach*, *Int. J. Mod. Phys.* **A8** (1993) 5751–5778, [hep-th/9304051].

[73] S. Dubovsky, R. Flauger and V. Gorbenko, *Solving the Simplest Theory of Quantum Gravity*, *JHEP* **09** (2012) 133, [1205.6805].

[74] P. Cooper, S. Dubovsky, V. Gorbenko, A. Mohsen and S. Storace, *Looking for Integrability on the Worldsheet of Confining Strings*, *JHEP* **04** (2015) 127, [1411.0703].

[75] P. Conkey and S. Dubovsky, *Four Loop Scattering in the Nambu-Goto Theory*, *JHEP* **05** (2016) 071, [1603.00719].

[76] C. Chen, P. Conkey, S. Dubovsky and G. Hernandez-Chifflet, *Undressing Confining Flux Tubes with $T\bar{T}$*, *Phys. Rev.* **D98** (2018) 114024, [1808.01339].

[77] A. Athenodorou, B. Bringoltz and M. Teper, *Closed flux tubes and their string description in D=2+1 SU(N) gauge theories*, *JHEP* **05** (2011) 042, [1103.5854].

[78] A. F. Beardon and D. Minda, *A multi-point Schwarz-Pick Lemma*, *J. Anal. Math* **92** (2004) 81–104.

[79] M. Luscher, *Two particle states on a torus and their relation to the scattering matrix*, *Nucl. Phys.* **B354** (1991) 531–578.

[80] R. A. Briceno, M. T. Hansen and S. R. Sharpe, *Relating the finite-volume spectrum and the two-and-three-particle S matrix for relativistic systems of identical scalar particles*, *Phys. Rev.* **D95** (2017) 074510, [1701.07465].

[81] I. Kostov, D. Serban and D.-L. Vu, *TBA and tree expansion*, *Springer Proc. Math. Stat.* **255** (2017) 77–98, [1805.02591].

[82] R. Dashen, S.-K. Ma and H. J. Bernstein, *S Matrix formulation of statistical mechanics*, *Phys. Rev.* **187** (1969) 345–370.

[83] S. Dubovsky and V. Gorbenko, *Towards a Theory of the QCD String*, *JHEP* **02** (2016) 022, [1511.01908].

[84] A. B. Zamolodchikov, *From tricritical Ising to critical Ising by thermodynamic Bethe ansatz*, *Nucl. Phys.* **B358** (1991) 524–546.

[85] A. L. Guerrieri, A. Homrich and P. Vieira, *Dual S-matrix bootstrap. Part I. 2D theory*, *JHEP* **11** (2020) 084, [2008.02770].

[86] D. Volkov and V. Akulov, *Is the Neutrino a Goldstone Particle?*, *Phys. Lett. B* **46** (1973) 109–110.

[87] Z. Komargodski and N. Seiberg, *From Linear SUSY to Constrained Superfields*, *JHEP* **09** (2009) 066, [0907.2441].

[88] Y. He and M. Kruczenski, *S-matrix bootstrap in 3+1 dimensions: regularization and dual convex problem*, 2103.11484.

[89] V. N. Gribov, *The theory of complex angular momenta: Gribov lectures on theoretical physics*. Cambridge Monographs on Mathematical Physics. Cambridge University Press, 6, 2007, 10.1017/CBO9780511534959.

[90] P. P. Kulish and L. D. Faddeev, *Asymptotic conditions and infrared divergences in quantum electrodynamics*, *Theor. Math. Phys.* **4** (1970) 745.

[91] N. Arkani-Hamed, M. Pate, A.-M. Raclariu and A. Strominger, *Celestial Amplitudes from UV to IR*, 2012.04208.

[92] F. Wilczek, *Quantum Mechanics of Fractional Spin Particles*, *Phys. Rev. Lett.* **49** (1982) 957–959.

[93] S. Jain, M. Mandlik, S. Minwalla, T. Takimi, S. R. Wadia and S. Yokoyama, *Unitarity, Crossing Symmetry and Duality of the S-matrix in large N Chern-Simons theories with fundamental matter*, *JHEP* **04** (2015) 129, [1404.6373].

[94] A. Kitaev, *Fault tolerant quantum computation by anyons*, *Annals Phys.* **303** (2003) 2–30, [quant-ph/9707021].

[95] S. Komatsu, M. F. Paulos, B. C. Van Rees and X. Zhao, *Landau diagrams in AdS and S-matrices from conformal correlators*, *JHEP* **11** (2020) 046, [2007.13745].

[96] R. F. Streater and A. S. Wightman, *PCT, spin and statistics, and all that*. 1989.

[97] M. Srednicki, *Quantum field theory*. Cambridge University Press, 1, 2007.

[98] N. Arkani-Hamed, T.-C. Huang and Y.-t. Huang, *Scattering Amplitudes For All Masses and Spins*, 1709.04891.

[99] C. Cheung, *TASI Lectures on Scattering Amplitudes*. 1708.03872.

[100] M. S. Costa, J. Penedones, D. Poland and S. Rychkov, *Spinning Conformal Blocks*, *JHEP* **11** (2011) 154, [1109.6321].

[101] L. Iliesiu, F. Kos, D. Poland, S. S. Pufu, D. Simmons-Duffin and R. Yacoby, *Bootstrapping 3D Fermions*, *JHEP* **03** (2016) 120, [1508.00012].

[102] D. Simmons-Duffin, *Projectors, Shadows, and Conformal Blocks*, *JHEP* **04** (2014) 146, [1204.3894].

[103] E. Elkhidir, D. Karateev and M. Serone, *General Three-Point Functions in 4D CFT*, *JHEP* **01** (2015) 133, [1412.1796].

[104] G. F. Cuomo, D. Karateev and P. Kravchuk, *General Bootstrap Equations in 4D CFTs*, *JHEP* **01** (2018) 130, [1705.05401].

[105] J. Wess and J. Bagger, *Supersymmetry and supergravity*. Princeton University Press, Princeton, NJ, USA, 1992.

[106] P. Dorey and R. Tateo, *Excited states by analytic continuation of TBA equations*, *Nucl. Phys.* **B482** (1996) 639–659, [hep-th/9607167].

[107] X. O. Camanho, J. D. Edelstein, J. Maldacena and A. Zhiboedov, *Causality Constraints on Corrections to the Graviton Three-Point Coupling*, *JHEP* **02** (2016) 020, [1407.5597].

Aditya Hebbar | Curriculum Vitae

Chemin de la Foret 22, Ecublens 1024, Switzerland
(+41) 78 736 5060 • aditmh@gmail.com

Education

- **Ecole Polytechnique Federale de Lausanne (EPFL), Switzerland**
  Ph.D. in Physics, ongoing [2017-Present]

- **University of Delaware, USA**
  Master of Science in Physics
  GPA of 4.0 out of 4.0 [2015-2017]

- **Indian Institute of Science (IISc)**
  Bachelor of Science with Physics major and Mathematics minor.
  Cumulative GPA of 7.5 out of 8 [2011-2015]

- **Kumarans (SKCH), Bangalore, India**
  Graduated Senior Secondary School/+2 with 95.6% marks, CBSE [2009-2011]

Scholastic Achievements

- Received the **IISc Institute Gold Medal** for highest GPA among Physics majors. [2015]
- Perfect scores in both **General** (340/340) and **Physics** (990/990) **GRE**. [2014]
- One of the two undergraduates nominated by IISc to visit **Japan** as part of the **JENESYS 2.0** program. [2014]
- Recipient of the Kishore Vaigyanik Protsahan Yojana (**KVPY**) fellowship from the Government of India. [2011-2015]

Publications

- A. Hebbar, D. Karateev, J. Penedones, "Spinning S-matrix Bootstrap in 4d", arXiv:2011.11708 [hep-th]
- J.E. Miro, A.L. Guerrieri, A. Hebbar, J. Penedones, P. Vieira, "Flux Tube S-matrix Bootstrap", Phys. Rev. Lett. 123 (2019) no.22, 221602, arXiv:1906.08098 [hep-th]
- A. Hebbar, G. Lazarides, Q. Shafi, "Light sterile neutrinos, dark matter, and new resonances in a U(1) extension of the MSSM", Phys.Rev. D96 (2017) no.5, 055026, arXiv:1706.09630
- A. Hebbar, Q. Shafi, C.S. Un, "Light Higgsinos, Heavy Gluino and b-τ Quasi-Yukawa Unification: Will the LHC find the Gluino?", Phys.Rev. D95 (2017) no.11, 115026, arXiv: 1702.05431
- B. Ananthanarayan, J. Bijnens, S. Ghosh, A. Hebbar, "An Analytic Approach to Sunset Diagrams in Chiral Perturbation Theory: Theory and Practice", Eur.Phys.J. A (2016) 52: 374, arXiv:1608.02386
- A. Hebbar, G. Leontaris, Q. Shafi, "Masses of Third Family Vector-like Quarks and Leptons in Yukawa-Unified E_6", Phys.Rev. D93 (2016) no.11, 111701, arXiv:1604.08328

Talks

- "Spinning S-matrix Bootstrap in 4d", Simons Bootstrap Collaboration Seminar Series, online, Dec 2nd, 2020
- "Supersymmetry and Yukawa Unification", Mid-Atlantic APS meeting, University of Delaware, Oct 15th, 2016

Technical skills

PROGRAMMING LANGUAGES: C, C++

SCIENTIFIC SOFTWARE/PACKAGES: MATHEMATICA, MATLAB, SDPB, SARAH, ISAJET

Coursework

PHYSICS: Conformal Field Theory, Gauge Theories and Standard Model, Quantum Field Theory, General Relativity, Advanced Math Methods (Lie Groups and Lie Algebras), Quantum Computation, Quantum Mechanics I and II, Statistical Mechanics, Electromagnetic Theory, Classical Mechanics, Astrophysics, Math Methods

MATHEMATICS: Real Analysis, Algebra, Linear Algebra, Combinatorics

Positions of Responsibility

CORE TEAM MEMBER-PRAVEGA 2014 [Jan 2012– Feb 2014]
Sci-Tech festival

- Part of the main organising committee that managed a team of over 100 members and a budget of Rs 3,000,000 to have a science festival at IISc.
- Was a key member in interactions and discussions with sponsors such as **Mercedes Benz**, **Carl-Zeiss** and **Bosch**.

Languages

Kannada: Native language

English: Fluent

Hindi: Intermediate

French: Intermediate (reading), basic (speaking, writing)

Interests

- Football (Soccer)
- Hiking/Trekking
- Chess

Ce document a été imprimé au Centre d’impression EPFL,
imprimerie climatiquement neutre, certifiée myClimate.